



**T.C.  
ISTANBUL UNIVERSITY-CERRAHPASA  
INSTITUTE OF GRADUATE STUDIES**



**Ph.D. THESIS**

**SYNTHESIS AND CHARACTERIZATION OF SOME TRANSITION  
METAL COMPLEXES OF SUBSTITUTED SCHIFF BASES AND  
BENZIMIDAZOLES CONTAINING FERROCENE AND PHENOL**

**ELHAM AHMED S. ABDULMALEK ALTERHONI**

**SUPERVISOR  
Prof. Dr. Aydın TAVMAN**

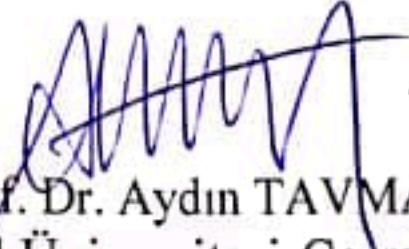
**Department of Chemistry**

**Chemistry Programme**

**ISTANBUL- March, 2019**

Bu çalışma 25.03.2019 Tarihinde aşağıdaki jüri tarafından  
Kimya Anabilim Dalı, Kimya Programı Doktora Tezi olarak kabul edilmiştir.

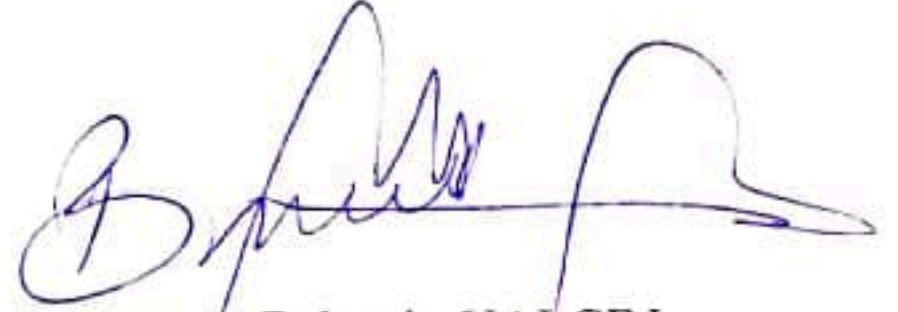
TEZ JÜRİSİ



Prof. Dr. Aydın TAVMAN  
İstanbul Üniversitesi-Cerrahpaşa  
Mühendislik Fakültesi – Kimya Bölümü



Prof. Dr. İrfan KIZILCIKLI  
İstanbul Üniversitesi-Cerrahpaşa  
Mühendislik Fakültesi – Kimya Bölümü



Prof. Dr. Bahattin YALÇIN  
Marmara Üniversitesi  
Fen-Edebiyat Fakültesi – Kimya Bölümü



Prof. Dr. Ayşe ERÇAĞ  
İstanbul Üniversitesi-Cerrahpaşa  
Mühendislik Fakültesi – Kimya Bölümü



Prof. Dr. Şaziye ABDURRAHMANOĞLU  
Marmara Üniversitesi  
Fen-Edebiyat Fakültesi – Kimya Bölümü



As required by the 9/2 and 22/2 articles of the Graduate Education Regulation which was published in the Official Gazette on 20.04.2016, this graduate thesis is reported as in accordance with criteria determined by the Institute of Graduate Studies by using the plagiarism software to which Istanbul University-Cerrahpasa is a subscriber.

This thesis is supported by the project numbered FDK-2017-23684 of Istanbul University-Cerrahpaşa Scientific Research Projects Executive Secretariat.

## **FOREWORD**

First and foremost, I would like to thank Allah Almighty for granting me the force, ability, knowledge and opportunity to proceed this research study and complete it.

I deepest thanks my thesis supervisor Prof. Dr Aydin Tavman for the guidance, advice, patience and support during the research study and writing of my thesis.

I would like to thank to Assoc. Prof. Dr. Onur Şahin from Sinop University, for his useful comments on X-ray single data and Assoc. Prof. Dr. Ayşe Seher BIRTEKSOZ TAN from Istanbul University for antimicrobial activity tests.

I feel debited to my country which offered me the financial resources to pursue my study abroad.

Finally, very big thanks go to my parents, also, my husband, sisters, brothers, children, and friends for giving me permanent support and encouragement during my study. This success would not have been done without all of them.

March 2019

ELHAM AHMED S. ABDULMALEK  
ALTERHONI

# TABLE OF CONTENTS

|  | Page         |
|--|--------------|
| <b>FOREWORD</b> .....  | <b>iv</b>    |
| <b>TABLE OF CONTENTS</b> .....   | <b>v</b>     |
| <b>LIST OF FIGURES</b> .....   | <b>viii</b>  |
| <b>LIST OF TABLES</b> .....  | <b>xv</b>    |
| <b>LIST OF SYMBOLS AND ABBREVIATIONS</b> .....                                   | <b>xvii</b>  |
| <b>ÖZET</b> .....  | <b>xviii</b> |
| <b>SUMMARY</b> .....   | <b>xx</b>    |
| <b>1. INTRODUCTION</b> .....   | <b>1</b>     |
| 1.1. <b>SCHIFF BASES AND THEIR COMPLEXES AS BIOLOGICALLY ACTIVE AGENTS</b> ..... | <b>4</b>     |
| 1.2. <b>BENZIMIDAZOLES AND THEIR COMPLEXES</b> .....                             | <b>6</b>     |
| 1.3. <b>BIOLOGICAL ACTIVITIES OF BENZIMIDAZOLE DERIVATIVES</b> .....             | <b>7</b>     |
| 1.3.1.  Antibacterial effects.....   | 8            |
| 1.3.2.  Anti-viral effect .....  | 8            |
| 1.3.3.  Anti-parasitic effect .....  | 8            |
| 1.3.4.  Antiprotozoal activity .....   | 9            |
| 1.3.5.  Androgen receptor antagonist.....  | 10           |
| 1.3.6.  HIV inhibitors.....  | 10           |
| 1.3.7.  Anti-hypertensive Agents .....   | 10           |
| 1.3.8.  Anti-ulcer Activity.....   | 10           |
| 1.3.9.  Anti-proliferative activity .....  | 11           |
| 1.3.10.  Anti-cancer activity .....  | 11           |
| 1.3.11.  Antioxidant activity .....  | 11           |
| 1.4. <b>CYCLOPENTADIENYL TRANSITION METAL COMPOUNDS</b> .....                    | <b>12</b>    |
| 1.5. <b>METALLOCENES</b> .....   | <b>14</b>    |
| 1.6. <b>FERROCENE BASED LIGANDS AND THEIR METAL COMPLEXES</b> .....              | <b>15</b>    |
| 1.7. <b>MEDICINAL CHEMISTRY OF FERROCENYL COMPOUNDS</b> .....                    | <b>16</b>    |
| 1.8. <b>COORDINATION CHEMISTRY OF SOME TRANSITION METAL</b> .....                | <b>19</b>    |
| 1.8.1.  Cobalt .....   | 19           |
| 1.8.2.  Nickel .....   | 20           |

|  |           |
|--|-----------|
| 1.8.3. Copper .....  | 21        |
| 1.8.4. Zinc .....  | 22        |
| 1.8.5. Platinum (II) and Palladium (II) .....  | 23        |
| <b>2. MATERIALS AND METHODS .....</b>  | <b>26</b> |
| 2.1. CHEMICALS AND REAGENTS .....  | 26        |
| 2.2. PREPARATION OF SCHIFF BASE LIGAND .....   | 27        |
| 2.2.1. Synthesis of Schiff base using glacial acetic acid as catalyst.....   | 27        |
| 2.2.1.1. Synthesis of Schiff base 2-(Ferrocen-1-yl-methyliden)amino-4-methylphenol ( <b>HL<sub>1</sub></b> ) .....                                   | 27        |
| 2.2.1.2. Synthesis of Schiff base 2-(Ferrocen-1-yl-methyliden)amino-4-chloro-5-nitrophenol ( <b>HL<sub>2</sub></b> ) .....                           | 28        |
| 2.2.2. Synthesis of Schiff base without catalyst .....   | 29        |
| 2.2.2.1. Synthesis of Schiff base (E)-4-chloro-2-((2-hydroxy-5-methylphenyl)imino) methyl phenol ( <b>H<sub>2</sub>L<sub>3</sub></b> ).....          | 29        |
| 2.2.2.2. Synthesis of Schiff base (E)-4-chloro-2-((5-chloro-2-hydroxy-4-nitrophenyl) imino) methyl phenol ( <b>H<sub>2</sub>L<sub>4</sub></b> )..... | 29        |
| 2.3. SYNTHESIS OF BENZIMIDAZOL DERIVATIVES .....   | 30        |
| 2.3.1. Synthesis of 2-(Ferrocen-1-yl)-5-methyl-1H-benzimidazole ( <b>L<sub>5</sub></b> ) .....   | 30        |
| 2.3.2. Synthesis of 2-(Ferrocen-1-yl)-5,6-dimethyl-1H benzimidazole ( <b>L<sub>6</sub></b> ) .....   | 31        |
| 2.3.3. Synthesis of 2-(Ferrocen-1-yl)-5-chloro-6-nitro-1H-benzimidazole ( <b>L<sub>7</sub></b> ).....  | 31        |
| 2.3.4. Synthesis of 4-Chloro-2-(5-methyl-1H-benzimidazol-2-yl) phenol ( <b>HL<sub>8</sub></b> ).....   | 32        |
| 2.3.5. Synthesis of 4-Chloro-2-(5,6-dimethyl-1H-benzimidazol-2-yl) phenol ( <b>HL<sub>9</sub></b> ).....   | 33        |
| 2.3.6. Synthesis of 4-Chloro-2-(5-chloro-6-nitro-1H-benzimidazol-2-yl)phenol ( <b>HL<sub>10</sub></b> ).....   | 34        |
| 2.4. PREPARATION OF METAL COMPLEXES: GENERAL PROCEDURE.....  | 34        |
| 2.5. SINGLE CRYSTAL STUDIES.....   | 35        |
| 2.6. ANALYTICAL TECHNIQUES AND INSTRUMENTATION .....   | 35        |
| 2.6.1. Melting points.....   | 35        |
| 2.6.2. FTIR .....  | 35        |
| 2.6.3. UV Visible spectra .....  | 35        |
| 2.6.4. Elemental analysis .....  | 35        |
| 2.6.5. Molar conductivity .....  | 36        |
| 2.6.6. <sup>1</sup> H- and <sup>13</sup> C-NMR spectra.....  | 36        |
| 2.6.7. Magnetic moment measurement.....  | 36        |
| 2.6.8. Mass spectrometer .....   | 36        |
| 2.6.9. XRD single crystal .....  | 36        |

|   |            |
|---|------------|
| 2.6.10. Cyclic voltammetry .....  | 37         |
| 2.6.11. Thermo gravimetric Analysis (TGA) .....   | 37         |
| 2.6.12. Determination of antimicrobial activity .....                                     | 37         |
| <b>3. RESULTS .....</b>   | <b>39</b>  |
| 3.1. CHARACTERIZATIONS OF THE LIGANDS .....   | 39         |
| 3.1.1. The physical properties of the ligands .....                                       | 39         |
| 3.1.2. Mass spectra .....   | 40         |
| 3.1.3. Infrared spectra .....   | 46         |
| 3.1.4. NMR spectra.....   | 52         |
| 3.1.5. UV-Visible Spectroscopy .....  | 63         |
| 3.2. CHARACTERIZATIONS OF THE METAL COMPLEXES .....                                       | 66         |
| 3.2.1. Elemental analysis .....   | 66         |
| 3.2.2. Magnetic moment, conductivity measurements and electronic spectra .....            | 70         |
| 3.2.3. Infrared spectra of ligands and the metal complexes .....                          | 80         |
| 3.2.4. NMR data of diamagnetic metal complex ( $Zn^{2+}$ , $Pd^{2+}$ and $Pt^{2+}$ )..... | 85         |
| 3.3. CRYSTAL STRUCTURE DETERMINATION .....  | 111        |
| 3.4. CYCLIC VOLTAMMETRY .....   | 119        |
| 3.5. THERMO GRAVIMETRIC ANALYSIS (TGA) .....  | 127        |
| 3.6. SUGGESTED STRUCTURES FOR THE METAL COMPLEXES.....                                    | 130        |
| 3.7. ANTIMICROBIAL ACTIVITY OF THE COMPOUNDS.....   | 135        |
| <b>4. DISCUSSION .....</b>  | <b>136</b> |
| 4.1. GENERAL PROPERTIES .....   | 136        |
| 4.2. FTIR SPECTROSCOPY .....  | 139        |
| 4.3. NMR SPECTROSCOPY .....   | 141        |
| 4.4. MAGNETIC MOMENT AND MOLAR CONDUCTIVITY<br>MEASUREMENTS .....                         | 144        |
| 4.5. X-RAY CRYSTAL STRUCTURE .....  | 144        |
| 4.6. UV-VISIBLE SPECTROSCOPY.....   | 146        |
| 4.7. CYCLIC VOLTAMMETRY .....   | 147        |
| 4.8. THERMO GRAVIMETRIC ANALYSIS (TGA) .....  | 147        |
| 4.9. ANTIMICROBIAL ACTIVITY.....  | 148        |
| <b>5. CONCLUSION AND RECOMMENDATIONS.....</b>   | <b>149</b> |
| <b>REFERENCES .....</b>   | <b>152</b> |
| <b>CURRICULUM VITAE .....</b>   | <b>170</b> |

## LIST OF FIGURES

|   | Page |
|---|------|
| <b>Figure 1.1:</b> Ligand coordination to metal ion.....  | 1    |
| <b>Figure 1.2:</b> Factors effecting on stability of complexes.....                                       | 2    |
| <b>Figure 1.3:</b> Scheme of Synthesis Schiff base.....   | 4    |
| <b>Figure 1.4:</b> Examples of bioactive Schiff bases .....   | 5    |
| <b>Figure 1.5:</b> General structure of benzimidazole.....  | 6    |
| <b>Figure 1.6:</b> General structure of vitamin B12 .....   | 6    |
| <b>Figure 1.7:</b> Example benzimidazole containing drugs .....   | 7    |
| <b>Figure 1.8:</b> Structure of mebendazole (MBZ) and albendazole (ABZ).....                              | 9    |
| <b>Figure 1.9:</b> Structure of omeprazole.....   | 11   |
| <b>Figure 1.10:</b> Structure of ferrocene .....  | 12   |
| <b>Figure 1.11:</b> Example of metallocenes (M: Fe, Ti, Zn, Ni, and Cr).....                              | 14   |
| <b>Figure 1.12:</b> Tamoxifen (2-[4-[(Z)-1, 2-diphenylbut-1-enyl] phenoxy]-N, N-dimethylethanamine) ..... | 17   |
| <b>Figure 1.13:</b> Ferrocenyl derivative of tamoxifen .....  | 17   |
| <b>Figure 1.14:</b> Structure of Ferroquine .....   | 18   |
| <b>Figure 1.15:</b> Herbicidal active compounds (Fc = Ferrocene) .....                                    | 18   |
| <b>Figure 1.16:</b> Structure of cisplatin .....  | 24   |
| <b>Figure 1.17:</b> Structures of carboplatin and oxaliplatin .....                                       | 24   |
| <b>Figure 1.18:</b> Structures of satraplatin .....   | 24   |
| <b>Figure 1.19:</b> Activation step of cisplatin formation .....  | 25   |
| <b>Figure 2.1:</b> Scheme of preparation of <b>HL</b> <sub>1</sub> .....                                  | 28   |
| <b>Figure 2.2:</b> Scheme of preparation of <b>HL</b> <sub>2</sub> .....                                  | 28   |
| <b>Figure 2.3:</b> Scheme of preparation of <b>H</b> <sub>2</sub> <b>L</b> <sub>3</sub> .....             | 29   |



|   |    |
|---|----|
| <b>Figure 2.4:</b> Scheme of preparation of <b>H<sub>2</sub>L<sub>4</sub></b> ..... | 30 |
| <b>Figure 2.5:</b> Scheme of preparation of <b>L<sub>5</sub></b> .....              | 31 |
| <b>Figure 2.6:</b> Scheme of preparation of <b>L<sub>6</sub></b> .....              | 31 |
| <b>Figure 2.7:</b> Scheme of preparation of <b>L<sub>7</sub></b> .....              | 32 |
| <b>Figure 2.8:</b> Scheme of preparation of <b>HL<sub>8</sub></b> .....             | 33 |
| <b>Figure 2.9:</b> Scheme of preparation of <b>HL<sub>9</sub></b> .....             | 33 |
| <b>Figure 2.10:</b> Scheme of preparation of <b>HL<sub>10</sub></b> .....           | 34 |
| <b>Figure 3.1:</b> Mass spectra of <b>HL<sub>1</sub></b> .....                      | 41 |
| <b>Figure 3.2:</b> Mass spectra of <b>HL<sub>2</sub></b> .....                      | 41 |
| <b>Figure 3.3:</b> Mass spectra of <b>H<sub>2</sub>L<sub>3</sub></b> .....          | 42 |
| <b>Figure 3.4:</b> Mass spectra of <b>H<sub>2</sub>L<sub>4</sub></b> .....          | 42 |
| <b>Figure 3.5:</b> Mass spectra of <b>L<sub>5</sub></b> .....                       | 43 |
| <b>Figure 3.6:</b> Mass spectra of <b>L<sub>6</sub></b> .....                       | 43 |
| <b>Figure 3.7:</b> Mass spectra of <b>L<sub>7</sub></b> .....                       | 44 |
| <b>Figure 3.8:</b> Mass spectra of <b>HL<sub>8</sub></b> .....                      | 44 |
| <b>Figure 3.9:</b> Mass spectra of <b>HL<sub>9</sub></b> .....                      | 45 |
| <b>Figure 3.10:</b> Mass spectra of <b>HL<sub>10</sub></b> .....                    | 45 |
| <b>Figure 3.11:</b> IR spectrum of <b>HL<sub>1</sub></b> .....                      | 47 |
| <b>Figure 3.12:</b> IR spectrum of <b>HL<sub>2</sub></b> .....                      | 47 |
| <b>Figure 3.13:</b> IR spectrum of <b>H<sub>2</sub>L<sub>3</sub></b> .....          | 48 |
| <b>Figure 3.14:</b> IR spectrum of <b>H<sub>2</sub>L<sub>4</sub></b> .....          | 48 |
| <b>Figure 3.15:</b> IR spectrum of <b>L<sub>5</sub></b> .....                       | 49 |
| <b>Figure 3.16:</b> IR spectrum of <b>L<sub>6</sub></b> .....                       | 49 |
| <b>Figure 3.17:</b> IR spectrum of <b>L<sub>7</sub></b> .....                       | 50 |
| <b>Figure 3.18:</b> IR spectrum of <b>HL<sub>8</sub></b> .....                      | 50 |
| <b>Figure 3.19:</b> IR of spectrum of <b>HL<sub>9</sub></b> .....                   | 51 |
| <b>Figure 3.20:</b> IR spectrum of <b>HL<sub>10</sub></b> .....                     | 51 |

|   |    |
|---|----|
| <b>Figure 3.21:</b> $^1\text{H-NMR}$ spectrum of <b>HL</b> <sub>1</sub> .   | 54 |
| <b>Figure 3.22:</b> $^{13}\text{C-NMR}$ spectrum of <b>HL</b> <sub>1</sub> .  | 54 |
| <b>Figure 3.23:</b> $^1\text{H-NMR}$ spectrum of <b>HL</b> <sub>2</sub> .   | 55 |
| <b>Figure 3.24:</b> $^{13}\text{C-NMR}$ spectrum of <b>HL</b> <sub>2</sub> .  | 55 |
| <b>Figure 3.25:</b> $^1\text{H-NMR}$ spectrum of <b>H</b> <sub>2</sub> <b>L</b> <sub>3</sub> .                          | 56 |
| <b>Figure 3.26:</b> $^{13}\text{C-NMR}$ spectrum of <b>H</b> <sub>2</sub> <b>L</b> <sub>3</sub> .                       | 56 |
| <b>Figure 3.27:</b> $^1\text{H-NMR}$ spectrum of <b>H</b> <sub>2</sub> <b>L</b> <sub>4</sub> .                          | 57 |
| <b>Figure 3.28:</b> $^{13}\text{C-NMR}$ spectrum of <b>H</b> <sub>2</sub> <b>L</b> <sub>4</sub> .                       | 57 |
| <b>Figure 3.29:</b> $^1\text{H-NMR}$ ( $\text{D}_2\text{O}$ ) spectrum of <b>H</b> <sub>2</sub> <b>L</b> <sub>4</sub> . | 58 |
| <b>Figure 3.30:</b> $^1\text{H-NMR}$ spectrum of <b>L</b> <sub>5</sub> .  | 58 |
| <b>Figure 3.31:</b> $^1\text{H-NMR}$ spectrum of <b>L</b> <sub>6</sub> .  | 59 |
| <b>Figure 3.32:</b> $^1\text{H-NMR}$ spectrum of <b>L</b> <sub>7</sub> .  | 59 |
| <b>Figure 3.33:</b> $^1\text{H-NMR}$ spectrum of <b>HL</b> <sub>8</sub> .   | 60 |
| <b>Figure 3.34:</b> $^1\text{H-NMR}$ spectrum of <b>HL</b> <sub>9</sub> .   | 60 |
| <b>Figure 3.35:</b> $^{13}\text{C-NMR}$ spectrum of <b>HL</b> <sub>9</sub> .  | 61 |
| <b>Figure 3.36:</b> $^1\text{H-NMR}$ spectrum of <b>HL</b> <sub>10</sub> .  | 61 |
| <b>Figure 3.37:</b> $^{13}\text{C-NMR}$ spectrum of <b>HL</b> <sub>10</sub> .   | 62 |
| <b>Figure 3.38:</b> Electronic spectra of the ligands.  | 64 |
| <b>Figure 3.39:</b> Structure of the ligands.   | 65 |
| <b>Figure 3.40:</b> Electronic spectra of the <b>HL</b> <sub>1</sub> complexes.   | 74 |
| <b>Figure 3.41:</b> Electronic spectra of the <b>HL</b> <sub>2</sub> complexes.   | 74 |
| <b>Figure 3.42:</b> Electronic spectra of the <b>H</b> <sub>2</sub> <b>L</b> <sub>3</sub> complexes.                    | 75 |
| <b>Figure 3.43:</b> Electronic spectra of the <b>H</b> <sub>2</sub> <b>L</b> <sub>4</sub> complexes.                    | 75 |
| <b>Figure 3.44:</b> Electronic spectra of the <b>L</b> <sub>5</sub> complexes.  | 76 |
| <b>Figure 3.45:</b> Electronic spectra of the <b>L</b> <sub>6</sub> complexes.  | 77 |
| <b>Figure 3.46:</b> Electronic spectra of the <b>L</b> <sub>7</sub> complexes.  | 78 |
| <b>Figure 3.47:</b> Electronic spectra of the <b>HL</b> <sub>8</sub> complexes.   | 78 |

|   |    |
|---|----|
| <b>Figure 3.48:</b> Electronic spectra of the <b>HL<sub>9</sub></b> complexes.....                            | 79 |
| <b>Figure 3.49:</b> Electronic spectra of the <b>HL<sub>10</sub></b> complexes. ....                          | 79 |
| <b>Figure 3.50:</b> Comparison of the IR spectra of <b>HL<sub>1</sub></b> and its complexes. ....             | 80 |
| <b>Figure 3.51:</b> Comparison of the IR spectra of <b>HL<sub>2</sub></b> and its complexes. ....             | 80 |
| <b>Figure 3.52:</b> Comparison of the IR spectra of <b>H<sub>2</sub>L<sub>3</sub></b> and its complexes. .... | 81 |
| <b>Figure 3.53:</b> Comparison of the IR spectra of <b>H<sub>2</sub>L<sub>4</sub></b> and its complexes. .... | 81 |
| <b>Figure 3.54:</b> Comparison of the IR spectra of <b>L<sub>5</sub></b> and its complexes. ....              | 82 |
| <b>Figure 3.55:</b> Comparison of the IR spectra of <b>L<sub>6</sub></b> and its complexes. ....              | 82 |
| <b>Figure 3.56:</b> Comparison of the IR spectra of <b>L<sub>7</sub></b> and its complexes. ....              | 83 |
| <b>Figure 3.57:</b> Comparison of the IR spectra of <b>HL<sub>8</sub></b> and its complexes.....              | 83 |
| <b>Figure 3.58:</b> Comparison of the IR spectra of <b>HL<sub>9</sub></b> and its complexes.....              | 84 |
| <b>Figure 3.59:</b> Comparison of the IR spectra of <b>HL<sub>10</sub></b> and its complexes. ....            | 84 |
| <b>Figure 3.60:</b> <sup>1</sup> H-NMR spectrum of <b>HL<sub>1</sub>+Zn</b> complex. ....                     | 88 |
| <b>Figure 3.61:</b> <sup>13</sup> C-NMR spectrum of <b>HL<sub>1</sub>+Zn</b> complex. ....                    | 88 |
| <b>Figure 3.62:</b> <sup>1</sup> H-NMR spectrum of <b>HL<sub>1</sub>+Pd</b> Complex.....                      | 89 |
| <b>Figure 3.63:</b> <sup>13</sup> C- NMR spectrum of <b>HL<sub>1</sub>+Pd</b> Complex. ....                   | 89 |
| <b>Figure 3.64:</b> <sup>1</sup> H-NMR spectrum of <b>HL<sub>2</sub>+Zn</b> complex. ....                     | 90 |
| <b>Figure 3.65:</b> <sup>13</sup> C-NMR spectrum of <b>HL<sub>2</sub>+Zn</b> complex. ....                    | 90 |
| <b>Figure 3.66:</b> <sup>1</sup> H-NMR spectrum of <b>HL<sub>2</sub>+Pd</b> complex. ....                     | 91 |
| <b>Figure 3.67:</b> <sup>13</sup> C-NMR spectrum of <b>HL<sub>2</sub>+Pd</b> complex. ....                    | 91 |
| <b>Figure 3.68:</b> <sup>1</sup> H-NMR spectrum of <b>H<sub>2</sub>L<sub>3</sub>+ Zn</b> complex.....         | 92 |
| <b>Figure 3.69:</b> <sup>13</sup> C-NMR spectrum of <b>H<sub>2</sub>L<sub>3</sub>+ Zn</b> complex.....        | 92 |
| <b>Figure 3.70:</b> <sup>1</sup> H-NMR spectrum of <b>H<sub>2</sub>L<sub>3</sub>+Pd</b> complex. ....         | 93 |
| <b>Figure 3.71:</b> <sup>13</sup> C-NMR spectrum of <b>H<sub>2</sub>L<sub>3</sub>+Pd</b> complex.....         | 93 |
| <b>Figure 3.72:</b> <sup>1</sup> H-NMR spectrum of <b>H<sub>2</sub>L<sub>3</sub>+Pt</b> complex. ....         | 94 |
| <b>Figure 3.73:</b> <sup>13</sup> C-NMR spectrum of <b>H<sub>2</sub>L<sub>3</sub>+Pt</b> complex.....         | 94 |
| <b>Figure 3.74:</b> <sup>1</sup> H-NMR spectrum of <b>H<sub>2</sub>L<sub>4</sub>+Zn</b> complex.....          | 95 |

|  |     |
|--|-----|
| <b>Figure 3.75:</b> $^{13}\text{C}$ -NMR spectrum of $\text{H}_2\text{L}_4+\text{Zn}$ complex..... | 95  |
| <b>Figure 3.76:</b> $^1\text{H}$ -NMR spectrum of $\text{H}_2\text{L}_4+\text{Pd}$ complex.....    | 96  |
| <b>Figure 3.77:</b> $^{13}\text{C}$ -NMR spectrum of $\text{H}_2\text{L}_4+\text{Pd}$ complex..... | 96  |
| <b>Figure 3.78:</b> $^1\text{H}$ -NMR spectrum of $\text{L}_5+\text{Zn}$ complex. ....             | 97  |
| <b>Figure 3.79:</b> $^{13}\text{C}$ -NMR spectrum of $\text{L}_5+\text{Zn}$ complex. ....          | 97  |
| <b>Figure 3.80:</b> $^1\text{H}$ -NMR spectrum of $\text{L}_5+\text{Pd}$ complex.....              | 98  |
| <b>Figure 3.81:</b> $^{13}\text{C}$ -NMR spectrum of $\text{L}_5+\text{Pd}$ complex. ....          | 98  |
| <b>Figure 3.82:</b> $^1\text{H}$ -NMR spectrum of $\text{L}_5+\text{Pt}$ complex.....              | 99  |
| <b>Figure 3.83:</b> $^{13}\text{C}$ -NMR spectrum of $\text{L}_5+\text{Pt}$ complex. ....          | 99  |
| <b>Figure 3.84:</b> $^1\text{H}$ -NMR spectrum of $\text{L}_6+\text{Zn}$ complex. ....             | 100 |
| <b>Figure 3.85:</b> $^{13}\text{C}$ -NMR spectrum of $\text{L}_6+\text{Zn}$ complex. ....          | 100 |
| <b>Figure 3.86:</b> $^1\text{H}$ -NMR spectrum of $\text{L}_6+\text{Pd}$ complex.....              | 101 |
| <b>Figure 3.87:</b> $^{13}\text{C}$ -NMR spectrum of $\text{L}_6+\text{Pd}$ complex.....           | 101 |
| <b>Figure 3.88:</b> $^1\text{H}$ -NMR spectrum of $\text{L}_6+\text{Pt}$ complex.....              | 102 |
| <b>Figure 3.89:</b> $^{13}\text{C}$ -NMR spectrum of $\text{L}_6+\text{Pt}$ complex. ....          | 102 |
| <b>Figure 3.90:</b> $^1\text{H}$ -NMR spectrum of $\text{L}_7+\text{Zn}$ complex. ....             | 103 |
| <b>Figure 3.91:</b> $^{13}\text{C}$ -NMR spectrum of $\text{L}_7+\text{Zn}$ complex. ....          | 103 |
| <b>Figure 3.92:</b> $^1\text{H}$ -NMR spectrum of $\text{L}_7+\text{Pd}$ complex.....              | 104 |
| <b>Figure 3.93:</b> $^{13}\text{C}$ - NMR spectrum of $\text{L}_7+\text{Pd}$ complex. ....         | 104 |
| <b>Figure 3.94:</b> $^1\text{H}$ -NMR spectrum of $\text{HL}_8+\text{Zn}$ complex. ....            | 105 |
| <b>Figure 3.95:</b> $^{13}\text{C}$ -NMR spectrum of $\text{HL}_8+\text{Zn}$ complex. ....         | 105 |
| <b>Figure 3.96:</b> $^1\text{H}$ -NMR spectrum of $\text{HL}_8+\text{Pd}$ complex. ....            | 106 |
| <b>Figure 3.97:</b> $^1\text{H}$ -NMR spectrum of $\text{HL}_9+\text{Zn}$ complex. ....            | 106 |
| <b>Figure 3.98:</b> $^{13}\text{C}$ -NMR spectrum of $\text{HL}_9+\text{Zn}$ complex. ....         | 107 |
| <b>Figure 3.99:</b> $^1\text{H}$ -NMR spectrum of $\text{HL}_9+\text{Pd}$ complex. ....            | 107 |
| <b>Figure 3.100:</b> $^{13}\text{C}$ -NMR spectrum of $\text{HL}_9+\text{Pd}$ complex. ....        | 108 |
| <b>Figure 3.101:</b> $^1\text{H}$ -NMR spectrum of $\text{HL}_{10}+\text{Zn}$ complex.....         | 108 |

|  |     |
|--|-----|
| <b>Figure 3.102:</b> $^{13}\text{C}$ -NMR spectrum of $\text{HL}_{10}+\text{Zn}$ complex.....  | 109 |
| <b>Figure 3.103:</b> $^1\text{H}$ -NMR spectrum of $\text{HL}_{10}+\text{Pd}$ complex.....   | 109 |
| <b>Figure 3.104:</b> $^{13}\text{C}$ -NMR spectrum of $\text{HL}_{10}+\text{Pd}$ complex.....  | 110 |
| <b>Figure 3.105:</b> The molecular structure of $\text{H}_2\text{L}_3$ showing the atom numbering scheme.....  | 113 |
| <b>Figure 3.106:</b> Unit cell packing diagram for $\text{H}_2\text{L}_3$ ; molecular overlap view from the b-axis. ....   | 113 |
| <b>Figure 3.107:</b> The molecular structure of $[\text{Pd}(\text{L}_3)\text{CH}_3\text{CN}]\cdot\text{H}_2\text{O}$ complex showing the atom numbering scheme. ....         | 115 |
| <b>Figure 3.108:</b> Unit cell packing diagram for $[\text{Pd}(\text{L}_3)\text{CH}_3\text{CN}]\cdot\text{H}_2\text{O}$ complex; molecular overlap view from the b-axis..... | 117 |
| <b>Figure 3.109:</b> Unit cell packing diagram for $[\text{Pd}(\text{L}_3)\text{CH}_3\text{CN}]\cdot\text{H}_2\text{O}$ complex; molecular overlap view from the c-axis..... | 118 |
| <b>Figure 3.110:</b> Cyclic voltammograms of $\text{HL}_1$ at GCE at different scan rates.....   | 119 |
| <b>Figure 3.111:</b> Cyclic voltammograms of $\text{Co}(\text{II}) + \text{HL}_1$ at GCE at different scan rates . ....  | 120 |
| <b>Figure 3.112:</b> Cyclic voltammograms of $\text{HL}_1$ and $\text{Co}(\text{II}) +\text{HL}_1$ at GCE at scan rates $100 \text{ mVs}^{-1}$ . ....                        | 120 |
| <b>Figure 3.113:</b> Cyclic voltammograms of $\text{HL}_2$ at GCE at different scan rates. ....  | 121 |
| <b>Figure 3.114:</b> Cyclic voltammograms of $\text{Co}(\text{II})+\text{HL}_2$ at GCE at different scan rates. ....   | 121 |
| <b>Figure 3.115:</b> Cyclic voltammograms of $\text{HL}_2$ and $\text{Co}(\text{II}) +\text{HL}_2$ at GCE at scan rates $100 \text{ mVs}^{-1}$ . ....                        | 122 |
| <b>Figure 3.116:</b> Cyclic voltammograms of $\text{L}_5$ at GCE at different scan rates.....  | 122 |
| <b>Figure 3.117:</b> Cyclic voltammograms of $\text{Co}(\text{II}) +\text{L}_5$ at GCE at different scan rates. ....   | 123 |
| <b>Figure 3.118:</b> Cyclic voltammograms of $\text{L}_5$ and $\text{Co}(\text{II}) +\text{L}_5$ at GCE at scan rates $100 \text{ mVs}^{-1}$ .....                           | 123 |
| <b>Figure 3.119:</b> Cyclic voltammograms of $\text{L}_6$ at GCE at different scan rates. ....   | 124 |
| <b>Figure 3.120:</b> Cyclic voltammograms of $\text{Co}(\text{II}) + \text{L}_6$ at GCE at different scan rates. ....  | 124 |
| <b>Figure 3.121:</b> Cyclic voltammograms of $\text{L}_6$ and $\text{Co}(\text{II}) +\text{L}_6$ at GCE at scan rates $100 \text{ mVs}^{-1}$ .....                           | 125 |

|   |     |
|---|-----|
| <b>Figure 3.122:</b> Cyclic voltammograms of <b>L<sub>7</sub></b> at GCE at different scan rates.....   | 125 |
| <b>Figure 3.123:</b> Cyclic voltammograms of Co(II) + <b>L<sub>7</sub></b> at GCE at different scan rates. ....   | 126 |
| <b>Figure 3.124:</b> Cyclic voltammograms of <b>L<sub>7</sub></b> and Co(II) + <b>L<sub>7</sub></b> at GCE at scan rates 100 mVs <sup>-1</sup> .....      | 126 |
| <b>Figure 3.125:</b> TGA spectrum of Pd + <b>L<sub>6</sub></b> .....  | 127 |
| <b>Figure 3.126:</b> TGA spectrum of Cu+ <b>HL<sub>10</sub></b> .....   | 127 |
| <b>Figure 3.127:</b> TGA spectrum of Pd + <b>L<sub>7</sub></b> .....  | 128 |
| <b>Figure 3.128:</b> TGA spectrum of Zn + <b>H<sub>2</sub>L<sub>4</sub></b> .....   | 128 |
| <b>Figure 3.129:</b> TGA spectrum of Zn + <b>L<sub>9</sub></b> .....  | 129 |
| <b>Figure 3.130:</b> Proposed structures for the Co(II) complexes. ....   | 130 |
| <b>Figure 3.131:</b> Proposed structures for the Cu(II) complexes. ....   | 131 |
| <b>Figure 3.132:</b> Proposed structures for the Zn(II) complexes.....  | 132 |
| <b>Figure 3.133:</b> Proposed structures for the Pd(II) complexes.....  | 133 |
| <b>Figure 3.134:</b> Proposed structures for the Pt(II) complexes.....  | 134 |
| <b>Figure 4.1:</b> <b>HL<sub>2</sub></b> isomeric structure.....  | 137 |
| <b>Figure 4.2:</b> Intra-molecular hydrogen bonding in <b>H<sub>2</sub>L<sub>4</sub></b> .....  | 137 |
| <b>Figure 4.3:</b> Intra-molecular hydrogen bonding in <b>H<sub>2</sub>L<sub>3</sub></b> .....  | 138 |
| <b>Figure 4.4:</b> Tautomer structure (keto-enol) of the compound <b>H<sub>2</sub>L<sub>3</sub></b> .....   | 138 |
| <b>Figure 4.5:</b> Keto-enol tautomerism of the compound <b>H<sub>2</sub>L<sub>4</sub></b> .....  | 138 |
| <b>Figure 4.6:</b> Intramolecular hydrogen bonding in <b>H<sub>2</sub>L<sub>3</sub></b> (left) and <b>H<sub>2</sub>L<sub>4</sub></b> ligands (right)..... | 142 |
| <b>Figure 4.7:</b> The keto-enol isomeric structures of the <b>H<sub>2</sub>L<sub>4</sub></b> .....   | 142 |
| <b>Figure 4.8:</b> The isomeric structures of the <b>HL<sub>10</sub></b> . ....   | 143 |
| <b>Figure 4.9:</b> The structure of the Pd+ <b>H<sub>2</sub>L<sub>3</sub></b> . ....  | 145 |

## LIST OF TABLES

|  | Page |
|--|------|
| <b>Table 1.1:</b> Coordination number and shape of complexes .....   | 3    |
| <b>Table 3.1:</b> Some physical data of the ligands. ....  | 39   |
| <b>Table 3.2:</b> Mass spectral data of the ligands.....   | 40   |
| <b>Table 3.3:</b> Infrared spectral data of the ligands (cm <sup>-1</sup> ).....   | 46   |
| <b>Table 3.4:</b> <sup>1</sup> H-NMR and <sup>13</sup> C-NMR spectral data of the ligands. ....                                  | 52   |
| <b>Table 3.5:</b> Electronic spectral data of the ligands.....   | 63   |
| <b>Table 3.6:</b> Analytical data and physical properties of the Co(II) complexes. ....  | 66   |
| <b>Table 3.7:</b> Analytical data and physical properties of the Cu(II) complexes. ....  | 67   |
| <b>Table 3.8:</b> Analytical data and physical properties of the Pd(II) complexes.....   | 68   |
| <b>Table 3.9:</b> Analytical data and physical properties of the Zn(II) complexes.....   | 69   |
| <b>Table 3.10:</b> Analytical data and physical properties of the Pt(II) complexes.....  | 69   |
| <b>Table 3.11:</b> Magnetic moment, molar conductivity measurements and<br>electronic spectra data of the Co(II) complexes.....  | 70   |
| <b>Table 3.12:</b> Magnetic moment, molar conductivity measurements and<br>electronic spectra data of the Cu(II) complexes.....  | 71   |
| <b>Table 3.13:</b> Magnetic moment, molar conductivity measurements and<br>electronic spectral data of the Pd(II) complexes..... | 72   |
| <b>Table 3.14:</b> Magnetic moment, molar conductivity measurements and<br>electronic spectra data of the Zn(II) complexes.....  | 73   |
| <b>Table 3.15:</b> Magnetic moment, molar conductivity measurements and<br>electronic spectra data of the Pt(II) complexes.....  | 73   |
| <b>Table 3.16:</b> <sup>1</sup> H -NMR and <sup>13</sup> C- NMR spectral data of the diamagnetic metal<br>complex.....           | 85   |
| <b>Table 3.17:</b> X-Ray crystallographic data for <b>H<sub>2</sub>L<sub>3</sub></b> .....                                       | 111  |
| <b>Table 3.18:</b> Selected bond distances and angles for <b>H<sub>2</sub>L<sub>3</sub></b> (Å, °).....                          | 112  |
| <b>Table 3.19:</b> Hydrogen bond parameters for <b>H<sub>2</sub>L<sub>3</sub></b> (Å, °).....                                    | 112  |

|   |     |
|---|-----|
| <b>Table 3.20:</b> Selected torsion angles for <b>H<sub>2</sub>L<sub>3</sub></b> (°).....   | 112 |
| <b>Table 3.21:</b> X-Ray crystallographic data for [Pd( <b>L<sub>3</sub></b> )CH <sub>3</sub> CN]·H <sub>2</sub> O complex.....   | 114 |
| <b>Table 3.22:</b> Hydrogen bond parameters for [Pd( <b>L<sub>3</sub></b> )CH <sub>3</sub> CN]·H <sub>2</sub> O complex<br>(Å, °).....  | 115 |
| <b>Table 3.23:</b> Selected bond distances and angles for [Pd( <b>L<sub>3</sub></b> )CH <sub>3</sub> CN]·H <sub>2</sub> O<br>complex (Å, °). .....  | 116 |
| <b>Table 3.24:</b> Selected torsion angles for [Pd( <b>L<sub>3</sub></b> )CH <sub>3</sub> CN]·H <sub>2</sub> O complex (°).....   | 117 |
| <b>Table 3.25:</b> Electrochemical parameter of the ligands including ferrocene<br>groups ( <b>HL<sub>1</sub></b> , <b>HL<sub>2</sub></b> , <b>L<sub>5</sub></b> , <b>L<sub>6</sub></b> and <b>L<sub>7</sub></b> ) and their Co <sup>2+</sup> complexes on<br>GCE electrode vs. Ag/AgCl in methanol solution inclosing<br>0.1M TBAP as supporting electrolyte at 100 m Vs <sup>-1</sup> scan rate at<br>25°C..... | 119 |
| <b>Table 3.26:</b> <i>In vitro</i> antimicrobial activity of the compounds and the standard<br>reagents (MIC, µg mL <sup>-1</sup> ).....  | 135 |



## LIST OF SYMBOLS AND ABBREVIATIONS

### Abbreviation Explanation

**EAN:** Effective Atomic Number

**VBT:** Valence Bond Theory

**MOT:** Molecular Orbital Theory

**AOM:** Angular Overlap Model

**MBZ:** Mebendazole

**ABZ:** Albendazole

**ER  $\alpha$ :** Estrogen Receptore subtype alpha

**TLC:** ThinLayer Chromatography

**FTIR:** Fourier Transform Infrared Spectroscopy

**XRD:** X-Ray Diffraction Spectroscopy

**UV/Vis:** Ultraviolet-Visible Spectrophotometry

**CV:** Cyclic Voltammetry

**Mp:** Melting Point

**DMSO:** Dimethylsulfoxide

**DMF:** Dimethylformamide

**NMR:** Nuclear Magnetic Resonance.

## ÖZET

# FERROSEN VE FENOL İÇEREN SÜBSTİTÜE SCHIFF BAZI VE BENZİMİDAZOLLERİN BAZI GEÇİŞ METAL KOMPLEKSLERİNİN SENTEZİ VE KARAKTERİZASYONU

## DOKTORA TEZİ

ELHAM AHMED S. ABDULMALEK ALTERHONI

İstanbul Üniversitesi-Cerrahpasa

Lisansüstü Eğitim Enstitüsü

Kimya Anabilim Dalı

Danışman : Prof. Dr.Aydin TAVMAN

Schiff bazları ve benzimidazol türevleri, başta tıbbi kimya ve ilaç uygulamaları olmak üzere pek çok alanda uygulama imkânı olan bileşik gruplarıdır. Ferrosen grubu içeren moleküller, kararlı oluşları, organik sentez çalışmalarında kullanılmaları, biyolojik aktivitelere sahip olmaları gibi özelliklerinden dolayı ilgi çeken bileşikler olmuşlardır. Bu doktora tezinde, ferrosen ve fenol gruplarını içeren dört tane Schiff bazı bileşiği (**HL<sub>1</sub>**, **HL<sub>2</sub>**, **H<sub>2</sub>L<sub>3</sub>** ve **H<sub>2</sub>L<sub>4</sub>**) ve altı tane benzimidazol bileşiği (**L<sub>5</sub>**, **L<sub>6</sub>**, **L<sub>7</sub>**, **HL<sub>8</sub>**, **HL<sub>9</sub>** ve **HL<sub>10</sub>**) olmak üzere iki farklı ligand grubu olacak şekilde toplam 10 adet ligand sentez edildi. Bu ligandlardan beş tanesi **HL<sub>1</sub>**, **HL<sub>2</sub>**, **L<sub>5</sub>**, **L<sub>6</sub>** ve **L<sub>7</sub>** ferrosen grubu, diğer beş tanesi **H<sub>2</sub>L<sub>3</sub>**, **H<sub>2</sub>L<sub>4</sub>**, **HL<sub>8</sub>**, **HL<sub>9</sub>** ve **HL<sub>10</sub>** ise fenol grubu içermektedir. Ligandların CoCl<sub>2</sub>, CuCl<sub>2</sub>, K<sub>2</sub>PdCl<sub>4</sub>, K<sub>2</sub>PtCl<sub>4</sub> ve ZnCl<sub>2</sub> ile kompleks bileşikleri elde edildi. Elde edilen bileşiklerin elementel analiz, FTIR, <sup>1</sup>H- ve <sup>13</sup>C-NMR, UV-visible, kütle spektrometri (MS) ve siklik voltametri analizleri yapıldı. Kompleks bileşikler için ayrıca molar iletkenlik ve manyetik moment ölçümleri yapıldı. Ayrıca, **H<sub>2</sub>L<sub>3</sub>** ligandı ile bunun Pd(II) kompleksinin ([Pd(L<sub>3</sub>)CH<sub>3</sub>CN]·H<sub>2</sub>O) X-ışını tek kristal analizleri de gerçekleştirildi. Ligandlardan **L<sub>5</sub>**, **L<sub>6</sub>** ve **L<sub>7</sub>**'nin tek dişli (monodentat), **HL<sub>1</sub>**, **HL<sub>2</sub>**, **HL<sub>8</sub>**, **HL<sub>9</sub>** ve **HL<sub>10</sub>**'un iki dişli (bidentat), **H<sub>2</sub>L<sub>3</sub>** ve **H<sub>2</sub>L<sub>4</sub>**'ün ise üç dişli (tridentat) olarak davrandığı gözlenmiştir. Ferrosen grubu içeren ligandların komplekslerinde iki farklı metal iyonunun bulunması bu bileşiklere heterobinükleer özellik kazandırmış ve bileşikleri ilginç hale getirmiştir. Ligandların oluşup oluşmadıkları ince tabaka kromatografisi (TLC) ile takip edildi ve MS analizleri ile molekül ağırlıkları doğrulandı. İnfrared spektrumlarında gerek Schiff

bazılarının ve gerekse benzimidazol türevlerinin C=N bağlarına ait gerilme titreşimleri 1600 – 1650 cm<sup>-1</sup> arasında; aromatik yapılara ve ferrosen kısmındaki siklopentadienil (Cp) grubuna ait C=C bağlarının gerilme titreşimleri ise 1550 – 1600 cm<sup>-1</sup> arasında tespit edildi. 1200 – 1300 cm<sup>-1</sup> bölgesinde fenolik C–O bağlarına ait titreşimler belirlendi. Kompleks oluşumuyla birlikte bu bandlarda kayda değer değişimlerin olduğu gözlemlendi. Diyamanyetik bileşiklerin NMR spektrumlarında, kompleks oluşumuyla birlikte, beklendiği gibi tüm ligandlarda fenolik OH protonlarında ve bağlı buldukları karbon atomlarında önemli değişimler ortaya çıkmış, Schiff bazı komplekslerinde ise OH protonlarının yanında azometin gruplarının (N=CH) protonlarında ve karbon atomlarının sinyallerinde de kayda değer kaymalar gözlenmiştir. **H<sub>2</sub>L<sub>3</sub>**'ün X-ray analizinde ligandın katı halde keto formunda olduğu görülmektedir. **H<sub>2</sub>L<sub>4</sub>**'ün <sup>1</sup>H-NMR spektrumunda da keto-enol tautomer yapısının karışımı bir yapı karşımıza çıkmaktadır. [Pd(**L<sub>3</sub>**)CH<sub>3</sub>CN]·H<sub>2</sub>O kompleksinin X-ışını verileri Pd(II) iyonunun bir kare düzlem geometride bulunduğunu göstermektedir. Molar iletkenlik ölçüm sonuçlarına göre [Cu(**H<sub>2</sub>L<sub>3</sub>**)Cl]Cl·3H<sub>2</sub>O, [Pd(**H<sub>2</sub>L<sub>4</sub>**)Cl]Cl·H<sub>2</sub>O ve [Pt(**HL<sub>3</sub>**)(EtOH)]·Cl kompleksleri hariç (bu üç kompleks 1:1 elektrolit özelliğe sahip olup molar iletkenlik değerleri sırasıyla 42.6, 59.3 ve 40.3 Scm<sup>2</sup>mol<sup>-1</sup>'dir) diğer tüm kompleksler iyonik olmayan (non-iyonik) karaktere sahiptir. Manyetik moment ölçüm sonuçları da kompleks bileşiklerin geometrileri ve yapısal özellikleri ile ilgili katkı sağlamıştır. Örneğin Co<sup>2+</sup> komplekslerinde 4.31–5.82 BM arasında bulunan manyetik moment değerleri, bu komplekslerde Co<sup>2+</sup> iyonunun yüksek spin yapısında olduğunu, kompleks geometrisinin ise tetrahedral ya da oktahedral olduğunu göstermektedir. Yine bazı Cu<sup>2+</sup> komplekslerinde 1.70–2.20 BM arasında bulunan manyetik moment değerleri de beklenti dâhilinde olup, yine komplekslerin oktahedral ya da tetrahedral olduğuna dair ipuçları vermektedir. Bunun yanında ferrosen grubu içeren pek çok paramanyetik olarak beklenen kompleks bileşikte manyetik moment değerinin beklenenden yüksek olduğu, bazı diyamanyetik olması beklenen komplekslerde ise (Zn<sup>2+</sup>, Pd<sup>2+</sup>, Pt<sup>2+</sup> kompleksleri) paramanyetik özelliğin ortaya çıktığı görülmektedir. Bu durum ferrosen grubunda bulunan Fe<sup>2+</sup> iyonunun diyamanyetik özelliğinin ortadan kalkması ve molekülün manyetik moment değerine yaklaşık iki adet eşleşmemiş elektron ile katkı yaptığını göstermektedir. UV-visible spektroskopi verileri, ligandlarda molekülicü yük transfer geçişleri, komplekslerde ise ligandan metale yük transfer (LMCT) geçişlerinin yoğun şekilde etkili olduğunu göstermektedir. Yoğun yük geçişleri nedeniyle komplekslerde görünür bölge d-d geçişlerine ait soğurmalar tespit edilememiş olup, dolayısıyla komplekslerin yapıları ile ilgili fazla bilgi elde edilememiştir. Ferrosen grubu içeren ligandlar (**HL<sub>1</sub>**, **HL<sub>2</sub>**, **L<sub>5</sub>**, **L<sub>6</sub>**, **L<sub>7</sub>**) ve bunların Co<sup>2+</sup> komplekslerinin elektrokimyasal davranışları siklik voltametri ile incelendi. Elde edilen veriler ligand ve komplekslerde anot ve katot potansiyel fark değerleri (ΔE<sub>p</sub>) bir adet elektronun transferine karşılık gelmektedir. Ligandlarda en iyi ΔE<sub>p</sub> değeri 0.07 V ile **HL<sub>2</sub>**'ye aittir. Ligandlara göre komplekslerde ΔE<sub>p</sub> değerlerinde gözlenen küçük azalmalar (mesela ΔE<sub>p</sub> değeri **HL<sub>1</sub>** için 0.13 V, Co<sup>2+</sup> kompleksinde 0.09 V), kompleks oluşumu ile birlikte elektron transferinin hızlandığını göstermektedir. Ancak 0.79 E<sub>p</sub>a değerine sahip **HL<sub>2</sub>**'de nitro grubunun etkisiyle yükseltgenmenin daha zor olduğu gözlenmiştir. Son olarak, bileşiklerin bazı bakteri ve mantarlara karşı antimikrobiyal aktiviteleri de test edildi. Pek çok bileşiğin zayıftan orta dereceye kadar antifungal ve antibakteriyel etki gösterdiği gözlemlendi. [Co(**L<sub>5</sub>**)Cl<sub>2</sub>(H<sub>2</sub>O)<sub>3</sub>] kompleksinin, *C. albicans*, *C. parapsilosis* ve *C. tropicalis* mantarlarına karşı, diğer bileşiklere göre daha geniş bir yelpazede aktivite gösterdiği tespit edildi.

Mart 2019, 191 sayfa.

**Anahtar kelimeler:** Schiff bazı, benzimidazol, fenol, ferrosen, kompleks, spektral karakterizasyon, antimikrobiyal aktivite

## SUMMARY

### SYNTHESIS AND CHARACTERIZATION OF SOME TRANSITION METAL COMPLEXES OF SUBSTITUTED SCHIFF BASES AND BENZIMIDAZOLES CONTAINING FERROCENE AND PHENOL

#### Ph.D. THESIS

ELHAM AHMED S. ABDULMALEK ALTERHONI

Istanbul University-Cerrahpasa

Institute of Graduate Studies

Department of Chemistry

Supervisor : Prof. Dr. Aydin TAVMAN

Schiff bases and benzimidazole derivatives are groups of compounds which can be applied in many fields, particularly in medical chemistry and drug applications. Ferrocene group-containing compounds are of interest because of their stability, uses in organic synthesis studies, their biological activities, etc. In this dissertation, two different ligand groups were prepared including ferrocene and phenol groups: four of them are Schiff base type ligands (**HL**<sub>1</sub>, **HL**<sub>2</sub>, **H**<sub>2</sub>**L**<sub>3</sub> and **H**<sub>2</sub>**L**<sub>4</sub>) and six of them benzimidazole derivatives (**L**<sub>5</sub>, **L**<sub>6</sub>, **L**<sub>7</sub>, **HL**<sub>8</sub>, **HL**<sub>9</sub> and **HL**<sub>10</sub>), totally ten ligands were synthesized. **HL**<sub>1</sub>, **HL**<sub>2</sub>, **L**<sub>5</sub>, **L**<sub>6</sub> and **L**<sub>7</sub> contain the ferrocene group whereas the other five, **H**<sub>2</sub>**L**<sub>3</sub>, **H**<sub>2</sub>**L**<sub>4</sub>, **HL**<sub>8</sub>, **HL**<sub>9</sub> and **HL**<sub>10</sub>, have phenol group. The complexes of the ligands with CoCl<sub>2</sub>, CuCl<sub>2</sub>, K<sub>2</sub>PdCl<sub>4</sub>, K<sub>2</sub>PtCl<sub>4</sub> and ZnCl<sub>2</sub> were obtained. Elemental analysis, FTIR, <sup>1</sup>H- and <sup>13</sup>C-NMR, UV-visible, mass spectrometry (MS) and cyclic voltammetry analysis were performed. The ligands were monitored by thin layer chromatography (TLC) and their molecular weights were verified by MS analysis. Molar conductivity and magnetic moment were also measured for the complexes. Furthermore, X-ray single crystal analyses of the **H**<sub>2</sub>**L**<sub>3</sub> ligand and its Pd(II) complex, ([Pd(**L**<sub>3</sub>)CH<sub>3</sub>CN]·H<sub>2</sub>O), were also performed. Ligands **L**<sub>5</sub>, **L**<sub>6</sub> and **L**<sub>7</sub> are monodentate, **HL**<sub>1</sub>, **HL**<sub>2</sub>, **HL**<sub>8</sub>, **HL**<sub>9</sub> and **HL**<sub>10</sub> bidentate, **H**<sub>2</sub>**L**<sub>3</sub> and **H**<sub>2</sub>**L**<sub>4</sub> were observed to act as tridentate. The presence of two different metal ions in the complexes of the ferrocene group containing ligands gives heterobinuclear

properties to these compounds and thus these compounds have become more interesting. In the infrared spectra, the stretching vibrations of both Schiff bases and benzimidazole derivatives of the C=N bonds are between 1600-1650  $\text{cm}^{-1}$ , stretching vibrations of C=C bonds belonging to the aromatic structures and the cyclopentadienyl (Cp) group in the ferrocene section were determined between 1550-1600  $\text{cm}^{-1}$ . Stretching vibrations of phenolic C–O bonds were determined in 1200-1300  $\text{cm}^{-1}$  region. Significant changes were observed in these bands with complex formation. In the NMR spectra of the diamagnetic complexes, significant changes were observed in phenolic OH protons and NH protons of benzimidazole derivatives. In the Schiff base complexes, significant shifts were observed in proton of azomethine groups (N=CH) and in carbon atoms signals. X-ray analysis of  $\mathbf{H}_2\mathbf{L}_3$  shows that the ligand is in solid state keto form. In the  $^1\text{H-NMR}$  spectrum of  $\mathbf{H}_2\mathbf{L}_4$ , a mixture of keto-enol tautomeric structure appears. The X-ray analysis data of  $[\text{Pd}(\mathbf{L}_3)\text{CH}_3\text{CN}]\cdot\text{H}_2\text{O}$  complex approve a square planar geometry for this complex. According to the results of molar conductivity measurements, the complexes have non-ionic character except  $[\text{Cu}(\mathbf{H}_2\mathbf{L}_3)\text{Cl}]\text{Cl}\cdot 3\text{H}_2\text{O}$ ,  $[\text{Pd}(\mathbf{H}_2\mathbf{L}_4)\text{Cl}]\text{Cl}\cdot\text{H}_2\text{O}$  and  $[\text{Pt}(\mathbf{HL}_3)(\text{EtOH})]\cdot\text{Cl}$  (these three complexes have 1:1 electrolyte character and their molar conductivity values are 42.6, 59.3 and 40.3  $\text{Scm}^2\text{mol}^{-1}$ , respectively). The magnetic moment measurement results also contributed to the geometry and structural properties of the complex compounds. For example, in the  $\text{Co}^{2+}$  complexes, the magnetic moment values between 4.31-5.82 BM indicate that the  $\text{Co}^{2+}$  ion in these complexes has a high spin structure and the complex geometry is tetrahedral or octahedral. Also, in some  $\text{Cu}^{2+}$  complexes, the magnetic moment values between 1.70-2.20 BM are also in the expectation and give clues about the complexes being octahedral or tetrahedral. In addition, in many paramagnetic complexes containing ferrocene group, the magnetic moment value is higher than expected and also in some complexes expected to be diamagnetic ( $\text{Zn}^{2+}$ ,  $\text{Pd}^{2+}$ ,  $\text{Pt}^{2+}$  complexes) paramagnetic character is observed. This unexpected case shows that the diamagnetic character of the  $\text{Fe}^{2+}$  of ferrocene group is eliminated and the magnetic moment value of the molecule is contributed by approximately two non-paired electrons by ferrocene group. UV-visible data shows that there are intense intramolecular charge transfers in the ligands and ligand to metal charge transfer (LMCT) transitions in the complexes. Because of the intense LMCT transitions in the complexes, adequate information about the d-d transitions in the metal ions could not obtained. The electrochemical behaviors of ferrocene group containing ligands ( $\mathbf{HL}_1$ ,  $\mathbf{HL}_2$ ,  $\mathbf{L}_5$ ,  $\mathbf{L}_6$  and  $\mathbf{L}_7$ ) and their  $\text{Co}^{2+}$  complexes were measured by cyclic voltammetry. The obtained data corresponds to the transfer of one electron that arise from anode and cathode potential difference values ( $\Delta\text{Ep}$ ) in the ligands and complexes. The best ( $\Delta\text{Ep}$ ) value in ligands belongs to  $\mathbf{HL}_2$  with 0.07 V. Minor differences in the ( $\Delta\text{Ep}$ ) values of complexes compared to ligands (eg, the values 0.13 V and 0.09 V were measured for  $\mathbf{HL}_1$  and its  $\text{Co}^{2+}$  complex, respectively) show that the electron transfer is accelerated by the complex formation, the nitro group in  $\mathbf{HL}_2$  makes the oxidation difficult by increasing  $\text{Epa}$  0.79. Finally, the antimicrobial activities of the compounds against some bacteria and fungi were also tested. It was observed that many compounds exhibited antifungal and antibacterial effects from weak to medium.  $[\text{Co}(\mathbf{L}_5)\text{Cl}_2(\text{H}_2\text{O})_3]$  complex showed broader activity than the other compounds towards *C. albicans*, *C. parapsilosis* and *C. tropicalis* fungi.

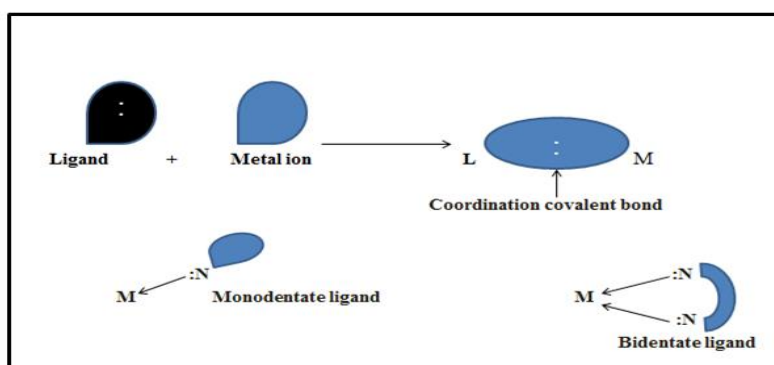
March 2019, 191 pages.

**Keywords:** Schiff base, benzimidazole, phenol, ferrocene, complex, spectral characterization, antimicrobial activity

## 1. INTRODUCTION

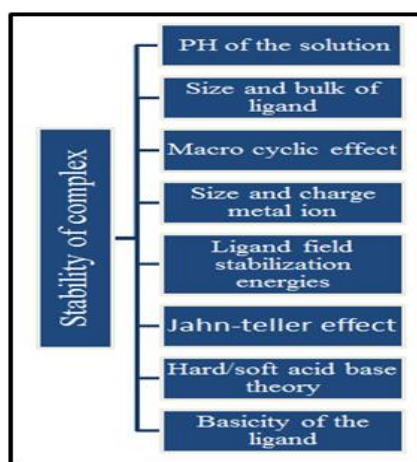
Modern development in inorganic chemistry is carried around the creation of a miscellaneous metal complexes production from different organic donor ligands for several applications. In modern sciences coordination chemistry heart of inorganic chemistry, 19th century Alfred Werner first man gained Nobel Prize in 1913 due to study and exploration of coordinated metal complexes. The coordination chemistry received a lot of consideration and provided successful results an extremely attractive area of science research. The majority in coordination chemistry is central metal atom surrounded by groups of molecules called ligands be capable to give pair of electron to the central metal atom as Lewis bases (Figure 1.1). If the several ligand molecules introduces into the central metal atom called polydentate, binary system a consist metal atom and single ligand compound, otherwise if the ligands different on the same metal called mixed ligand complexes [1].

Recently, coordination chemistry is energetic and progressive study areas, the major goal of coordination chemistry understanding the synthesis procedure and predicting the result reaction of transition metals with suitable ligand to form anionic, cationic, or neutral complexes. These complexes play important role in life, for example some of complexes have pharmaceutical activities as anticancer drugs, antimicrobial, and catalysis activity.... etc. These activities depend on several features such as photochemical behavior, coordination geometry, magnetic properties, electronic properties and oxidation state [2].



**Figure 1.1:** Ligand coordination to metal ion.


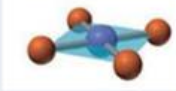

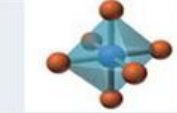
On the other hand, the metal atoms play a main significant function in biological systems. So it would not be overstatement the metal complexes make critical function role in the modern science for example nutrition plant, medicine, organism's biological action, industry addition to agriculture. Metal is not synthesized in the body, for normal health and normal growth should be accurate amount of metals, if the excess or insufficiency of metals lead to many health disorder, for example metabolic disorders, metal poisoning, and skeletal abnormalities [3]. The coordination compounds have major important role in nature, it's very common used some of metals in therapeutic area example gold in the teeth, silver in the hair, and lead in the bones and other, these three metals, gold, silver and lead be able to have several influence toward living organisms, metal ion be there electrophiles own charged positively, lead to charge transfer interaction. The metal ions are very essential to keep human homeostasis furthermore show vital roles in numerous biological developments through acting as cofactors in the proteins function thereby causing in the regulation, stabilization and completion courses of cellular functions [4]. Several ligands action surrounding the metal atom at the same time due to metal ions have more than one positive charge and contain a larger ionic volume. The coordination compounds character is based on several factor as the metal-ligand interaction, donor atom, ligand structure, metal ion as well stability of complex depends on several factors (Figure1.2). The major play problem in coordination chemistry is strength and nature bond within metal and ligand, usually metal ion bond between diverse donor atoms not appearance identical strength. Also a donor atom bonds not appearance similar strength among dissimilar metal ions [5].



**Figure 1.2:** Factors effecting on stability of complexes.

Wonderful development of coordination chemistry in various areas leads to intense academic researcher towards synthesis, because numerous physicochemical instruments accessible for instance IR,  $^1\text{H}$ NMR, UV-VIS, Mass spectra, ESR, X-ray... etc. These big assist intended for determination and study metal complex constructions. Also thermal performances for example DTA, TG and DSC are used supportive study complex structure, broad uses coordination compound guide researchers towards manner study activities [6]. Sedgwick in 1927 suggested Effective Atomic Number (EAN) pair of electron bond directed ligands are donating electron pairs toward metal ions, so creating coordinated bond. Valence bond theory (VBT) bonding metal and ligand studied by Pauling [7]. The vast popularity of VBT between 1930 and 1940, after that crystal field theory (CFT) supplemented in 1950. In 1929 the crystal field theory was diverse by Bethe [8]. In 1940 ligand field theory (LFT) and developed crystal field theory by the physicists Vanvlenck. Crystal field theory takes several consideration d-orbital metal ions. Whereas molecular orbital theory (MOT) creates explanation ligand orbital, similarly angular overlap model (AOM) [9]. The characterization of several transition metals is depending on several factors such as by their capability of metals to appearance a broad variety for instant tetrahedral, square-planar, square-pyramidal in addition to octahedral. A number of transition metals complexes as  $\text{Zn}^{2+}$ ,  $\text{Ni}^{2+}$ ,  $\text{Cd}^{2+}$ ,  $\text{Cu}^{2+}$ ,  $\text{Hg}^{2+}$  and  $\text{Co}^{2+}$  are recognized (Table 1.1) [10].

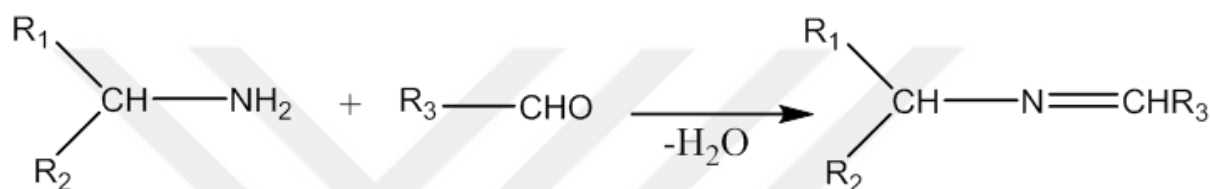
**Table 1.1:** Coordination number and shape of complexes [10].

| Coordination number | Shape         |   |
|---------------------|---------------|---|
| 2                   | linear        |  |
| 4                   | Square planer |  |
| 4                   | Tetrahedral   |  |
| 6                   | Octahedral    |  |



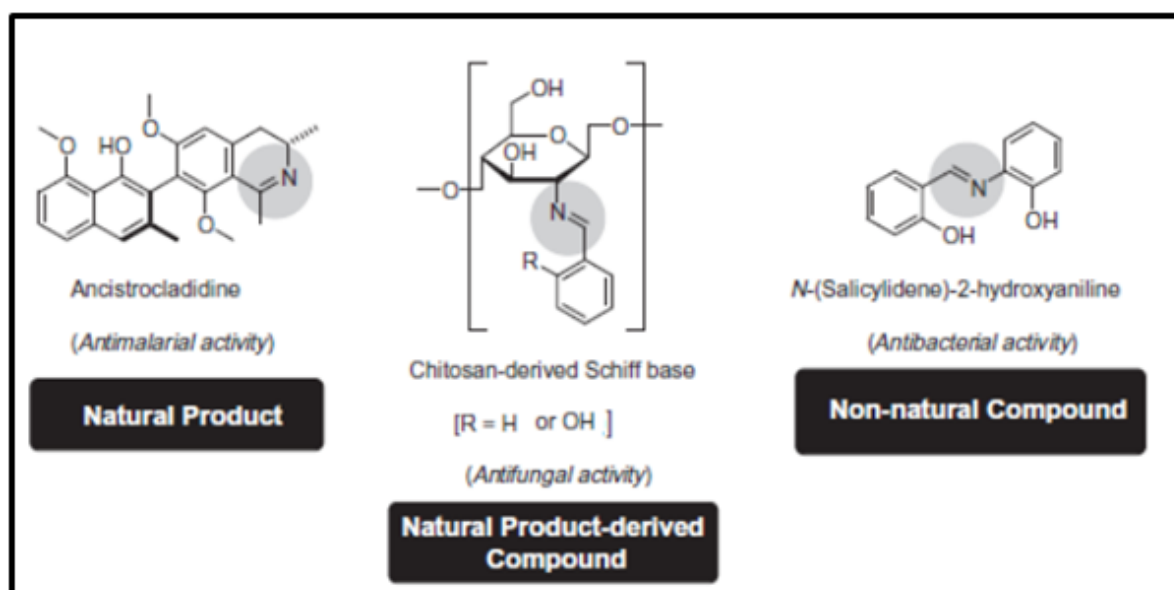
## 1.1. SCHIFF BASES AND THEIR COMPLEXES AS BIOLOGICALLY ACTIVE AGENTS

First man reported and described of Schiff base in 1864 is Hugo Schiff. Schiff base also called azomethine, considering major functional group in compounds that are enclosed a carbon and nitrogen double bond in addition nitrogen atom linked to group aryl or otherwise alkyl. Synthesized via nucleophilic addition reaction amine aliphatic or aromatic with a carbonyl compound to creating hemiaminal, after that a dehydration to create an imine (Figure 1.3) [11].



**Figure 1.3:** Scheme of Synthesis Schiff base.

Numerous applications of Schiff bases for example rubber accelerators, perfume bases, chemical intermediates, liquid crystals for electronics dyes.....etc. Recently, there are several considerations around Schiff bases used as ligand in chemistry of the metal complexes due to containing nitrogen and extra donors lead to stabilize them in different oxidation states [12]. Also if administered drug as metal complexes have greater action than free ligands [13]. Cu(II) complex of salicylaldehyde benzoylhydrazone as instance have a potent inhibitor of cell growth and DNA synthesis[14]. Antimicrobial activities also are examination such as benzene sulfanohydrazone and their complexes[15]. Depending on previous study on numerous Schiff bases ligands and their complexes showed most have biological activity as antibacterial, antiviral, antimalarial and anti-proliferative activities (Figure 1.4) [16,17].



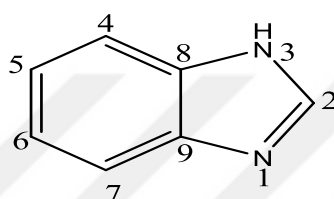
**Figure 1.4:** Examples of bioactive Schiff bases [18].

Various reactions to increase their yield and product selectivity used catalyst. The transition metal Schiff base complexes exhibit great catalytic activity, Because of the Schiff base ligands suitable method of preparation and thermal stability, metal complexes for their potential applications in catalysis. The activity catalytic of metal complexes has been informed in several reactions such as polymerization reaction, reduction of thionyl chloride, aldol reaction, epoxidation of alkenes, reduction reaction of ketones, oxidation of organic compounds and Henry reaction [18].

Various publications and research are concentrated on Schiff bases because structural differences, synthesis method simple, inexpensive, stability and broad applications [19,20]. General synthesis of Schiff base ligand employments by using volatile organic solvent have high boiling point [21,22]. Schiff base ligands coordinate with metals by the imine nitrogen and alternative group and stabilized in many oxidation states [23].

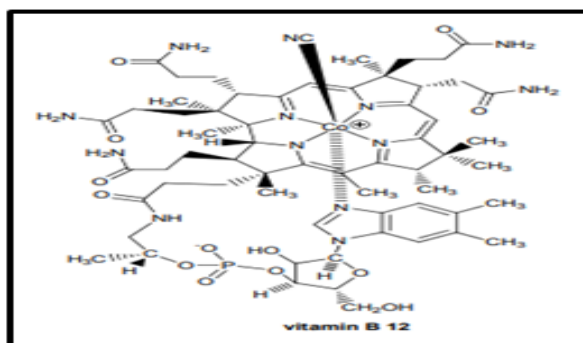
## 1.2. BENZIMIDAZOLES AND THEIR COMPLEXES

Fused a phenyl ring with 4,5-positions of imidazole ring formed heterocyclic aromatic organic compound are called Benzimidazole (Figure 1.5). In 1859 the Debus discovered imidazole nucleus reaction of glyoxal and ammonia, Debus is suggested the term glyoxaline. Imidazole compound because of Hantzsch implies are heterocyclic ring five membered structures possessed imino group and a tertiary nitrogen atom, situated at the locations 1 and 3 respectively [24].



**Figure 1.5:** General structure of benzimidazole.

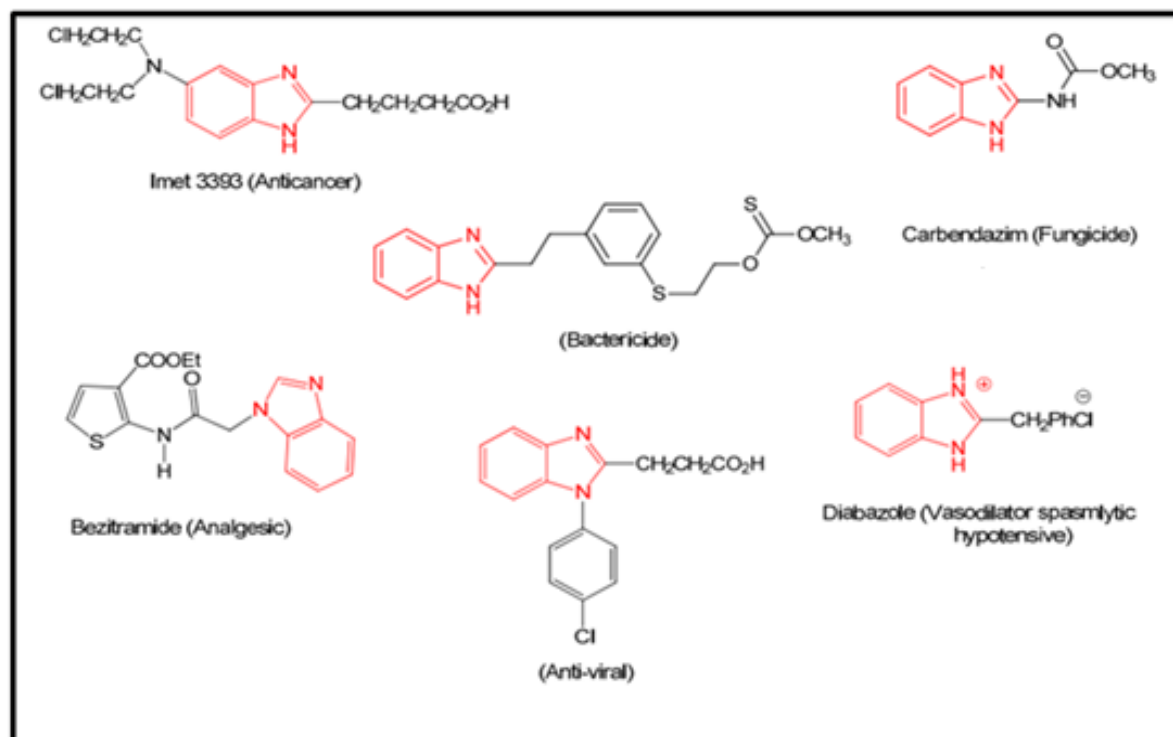
Benzimidazole and substituted benzimidazole derivatives are create miscellaneous therapeutic applications and pharmaceutical industries for instance antibacterial, antiviral, antifungal, antiulcer, antihistaminic, anticancer, anti-hypertensive in addition analgesic activities [25]. Instead, heterocyclic group as thiadiazole, pyrazole, triazole, 2-azetidinone moieties and coumarin fused with benzimidazole derivatives are exposed different pharmacological activities [26]. In 1889, Fischer discovered the biological effect of the parental benzimidazole compound as bacteriostatic and fungicidal properties[27]. In 1984 discovered benzimidazole ring in structure of vitamin B12 (Figure 1.6) [28].



**Figure 1.6:** General structure of vitamin B12 [28].

### 1.3. BIOLOGICAL ACTIVITIES OF BENZIMIDAZOLE DERIVATIVES

The benzimidazole and its derivatives important pharmacophore in medicinal chemistry due to create high activity in the treatment of numerous of diseases, have been found to be active against several categories of microorganisms, based on their biochemical and pharmacological properties of benzimidazoles. So, several consideration has been progressively given to the production of benzimidazole derivatives because own lesser toxicities besides powerful pharmacological action. Recently several investigators have been concerned for scheming and design high powerful benzimidazole derivatives with various of biological activity (Figure1.7) [29].



**Figure 1.7:** Example benzimidazole containing drugs [28].

### 1.3.1. Antibacterial effects

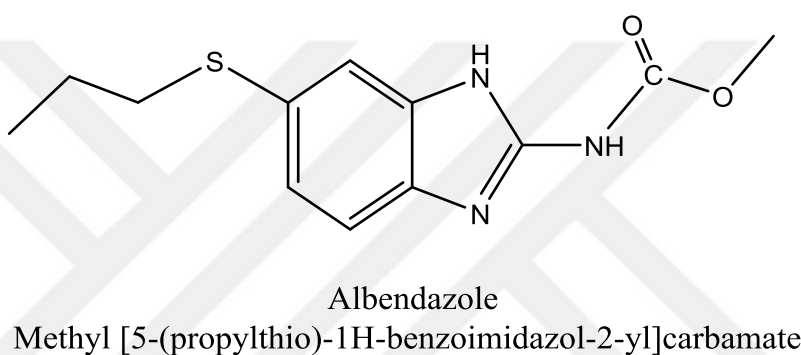
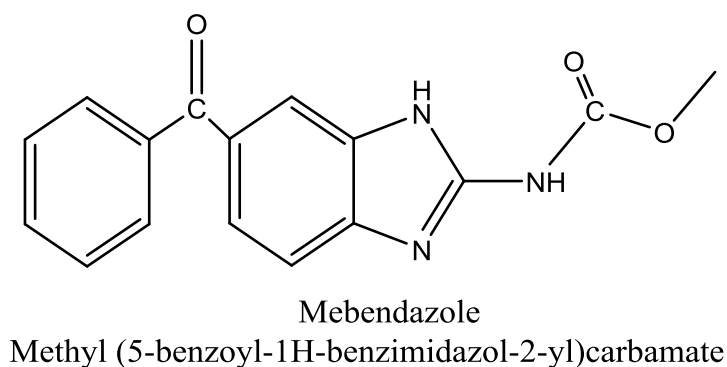
Recently, several antibacterial drugs contain benzimidazole group for example furacilin, ftivazide and furazolidone [30]. Also hydrazones reported various studies due to possess chemotherapeutic value [31, 32]. Several studies try to synthesis actual effective against *S. aureus* and methicillin resistant *S. aureus* microorganism such as sequence 1,2-disubstituted-1H-benzimidazole-N alkylated 5-carboxamide derivatives by values MIC low around 0.78 - 0.39  $\mu\text{g/mL}$  produce best activity [33]. Also substituted dichloro and chloro benzimidazole have board antibacterial activities [34].

### 1.3.2. Anti-viral effect

The virus gene is development for this reason several research intensive for preparation new medication, benzimidazoles they are play remarkably role as anti-viral against different kinds of virus as picornavirus, poliovirus, enterovirus [35, 36]. Tobacco mosaic virus causes infection of plant, appearance research N-substituted in addition 2- substituted benzimidazoles possess action strong against tobacco mosaic virus [37]. Furthermore informed series research against categories of enteroviruses as Coxsackie virus A16, B3, B6 as well as Enteroviruses71 in VERO cells. Antiviral potency in height ( $\text{IC}_{50} = 1.76 \mu\text{g/mL}$ ) besides significant selectivity index of compound (L)-2-(pyridin-2-yl)-N-(2-(4-nitrophenyl)pentan-3-yl)-1H-benzimidazole-4-carboxamide [38].

### 1.3.3. Anti-parasitic effect

Several types of benzimidazole such as 2-(trifluoromethyl)-1H-benzimidazole derivatives exposed the greatest desired anti-parasitic effect in vitro against series of *Entamoeba histolytica*, *Giardia intestinalis*, *Trichinella spiralis* and *Trichomonas vaginalis* [39]. Mebendazole (MBZ) and albendazole (ABZ) are anthelmintic medications are used mostly to treatment endo parasitic disease in animals and humans, its create from benzimidazole-2-carbamates, these compounds are possessing a low toxicity and high therapeutic index, but is finding poor solubility and absorption problems causes tissue-dwelling parasites (Figure1.8) [40].



**Figure 1.8:** Structure of mebendazole (MBZ) and albendazole (ABZ).

#### 1.3.4. Antiprotozoal activity

The compounds 5,6-dinitro and thioalkyl/thioaryl substituted benzimidazole derivatives, possess strong activity against strain of *stentrophomonas malthophilia*. It is board activity linked to metronidazole against both bacteria (gram negative and gram positive bacteria). Also research reported substituted 2-trifluorobenzimidazoles have same activity, anti-giardia activity it has informed [41,42]. Furthermore, the sequence 2-(trifluoromethyl)-1H-benzimidazole derivatives synthesis via Phillips cyclo condensation of a substituted 1,2-phenylenediamine and trifluoroacetic acid [43,44], then estimated against numerous protozoan parasites as *leishmania Mexicana*, *giardia intestinalis*, *entamoeba histolytica*, and *trichomonas vaginalis*, also some of the above mentioned protozoa has showed nano molar activities against these compound [39].

### 1.3.5. Androgen receptor antagonist

Non-steroidal antiandrogen naming bicalutamide used for treatment prostate cancer due to possess antiandrogen for the treatment of androgen dependant [45]. However, 5,6-dichlorobenzimidazole derivative possess activity as androgen receptor antagonist [46].

### 1.3.6. HIV inhibitors

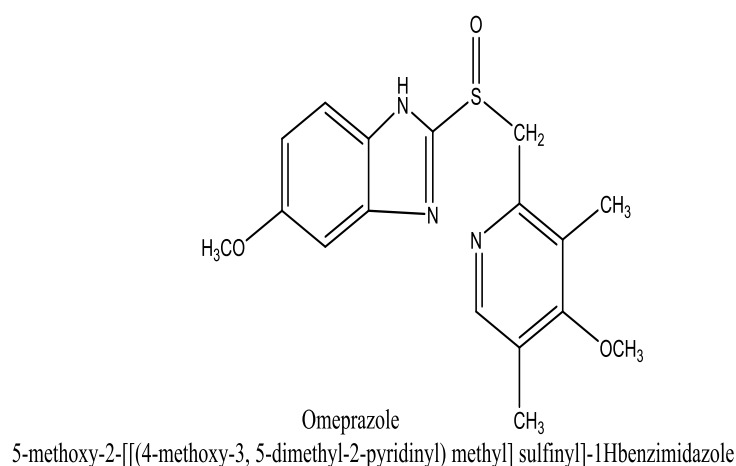
Reported some of benzimidazole as a non-competitive non nucleotide antiretroviral drug as tetrahydro-imidazole[4,5,ljk][1,4]-benzodiazepin-2(1H)-one (TIBO), specific binding to HIV-1 RT. It is possess highly selective, high significant potent and only HIV-1 inhibitors duplication. TIBO compounds inhibited reverse transcriptase (RT) of HIV-1, but not HIV-2. However, recently numerous new benzimidazole derivatives compounds other than TIBO were informed HIV-1 replication inhibit. a several studied novel benzimidazole derivatives compounds, bearing similarity to TIBO to evaluated for inhibit HIV-1 replication [47].

### 1.3.7. Anti-hypertensive Agents

Potent antihypertensive action of biphenyl benzimidazoles at two-position be there important for the best effective, these compounds oral administration give excellent bioavailability [48]. Also reported the 5-substituted aryl/alkyl-caboxamido derivatives own Angiotensin-II AT1 receptor antagonistic activity lead to use best anti-hypertensive agents [49].

### 1.3.8. Anti-ulcer Activity

The affectivity response substituted benzimidazoles increase activity blocking gastric acid excretion due to possess powerful inhibitors board parietal cell proton pump, H<sup>+</sup>/K<sup>+</sup> ATPase. The methylene and sulfoxide group with heterocycles enhance activity [50]. Recently, new substituted benzimidazol such as Omeprazole that inhibitor proton pump lead to inhibits gastric acid secretion (Figure1.9) [51].



**Figure 1.9:** Structure of omeprazole.

### 1.3.9. Anti-proliferative activity

2-aminobenzimidazole as well as substituted aromatic aldehydes derivatives refluxing in ethanol and benzene then reduced by  $\text{NaBH}_4$  to produced 2-benzylaminobenzimidazoles then acylated via cinnamoyl chloride donate good anti-proliferative activity compound in vitro naming 2-(orto-bromobenzylamino)-1-cinnamoylbenzimidazole [38,52].

### 1.3.10. Anti-cancer activity

Some benzimidazoles have been reported as anti-cancer as nitro-benzimidazoles is used for treatment breast cancer due to own cytotoxic activity against cancer cells [53]. Also reported anticancer activities of 1,3-diarylpyrazinobenzimidazole derivatives compounds, however, imidazoles, triazines, thiadiazole and tetrazole drugs similarly have the same activity [54]. methyl-1-(4-methoxyphenethyl)-2-(4-fluoro-3-nitrophenyl)-1H-benzimidazole-5-carboxylate compound encouraged extreme death cell happening leukemic cells a IC (50) of 3 micro M [55].

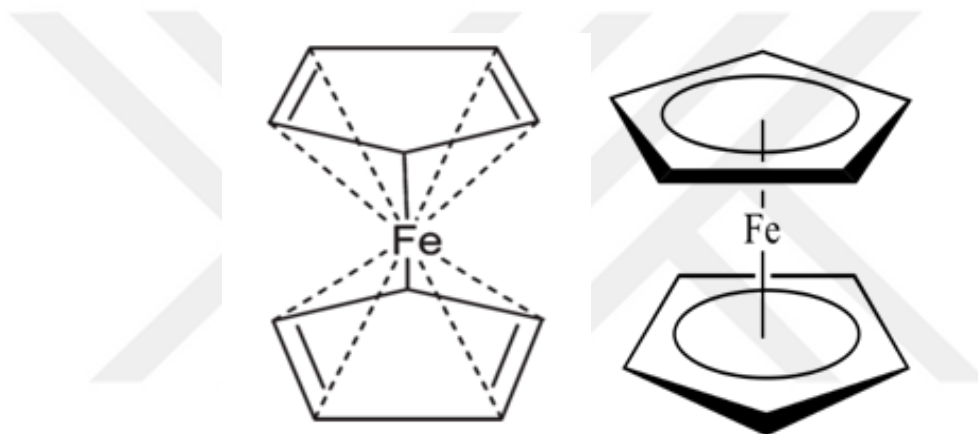
### 1.3.11. Antioxidant activity

Some dihydrochlorides compounds owning antioxidant activity, it is formed as salts have best platelet and erythrocyte antiaggregant action [56]. Benzimidazole with trimethyl group possess best inhibitory action of 5-lipoxygenase used as anti-oxidative activity [57].



#### 1.4. CYCLOPENTADIENYL TRANSITION METAL COMPOUNDS

In the recent years, several research concentrated on new field bio-organ metallic chemistry is reported cyclopentadiene ligated transition metal compounds. These compounds used in several areas as biology, molecular biotechnology and medicine [58-61]. One of cyclopentadienyl is ferrocene compound it is major interest because have greatly resonance stabilized activities and unique redox properties. Ferrocene compound formed two cyclopentadienyl rings pi-coordinated to ferrous ion Fe(II) atom to form unique structure sandwich through d-orbitals on  $\text{Fe}^{2+}$  are coordinated into the  $\pi$  orbitals on the two cyclopentadienyl radicals (Figure 1.10) [62].



**Figure 1.10:** Structure of ferrocene [63].

Several research groups and scientists international interest of study and ferrocenyl derivatives due to uses in many fields of science and asymmetric synthesis. In 1951 discovered sandwich  $\text{Cp}_2\text{Fe}$  structure was by Geoffrey Wilkinson, Robert Woodward [64,65]. In 1973 Nobel Prize gave for Wilkinson and Fischer because suggested the successive production of ferrocene and extra complexes, also they are proposed structure a “double cone” by all five carbon atom of a cyclopentadienyl ligand co-operating with the centre metal atom. Non-linear optical materials of ferrocene compounds be able to performance as undergoes oxidation and electron donor to the ferrocenium ion [66-68].

Ferrocene compounds derivatives are strong connection with biomolecules by covalently bonded creating the bio conjugates, the biomolecules such as peptides, proteins, amino acids, nucleic acid (DNA, RNA), hormones and carbohydrates [69].

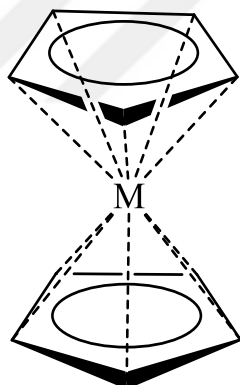
A Ferrocene compound is kind of a stable organometallic compound possess resistant towards of the acids and alkalis action, however it undergoes several reactions; simplifying preparation typical substituted derivatives [70].

Also the most research of Schiff base ligands concentrating on their biological activity as mutable bonding and strong inhibitors [71]. Recently, several pharmaceutical companies are concentrated synthesis new medication based on ferrocene Schiff base, benzimidazole ligands. These compounds are interesting material for advance research. Generally most ferrocene Schiff base ligands were prepared addition-elimination reaction [72- 74].

## 1.5. METALLOCENES

The organometallic compounds as metallocenes are made by inserted metal atom in the oxidation state II between two planar cyclopentadienyl anions rings are designation and naming “sandwich compounds” they are aromatically stabilized. The cyclopentadienyl ligand ( $C_5H_5$ ) is play major factor in the progress and growth organometallic chemistry, Cp ring is used in different field of technology and chemistry (Figure 1.11) [75-77].

Most of compounds oligomeric metallocene exposing multielectron redox chemistry has greatly attracted consideration as electrochemical, magnetic and electronic properties [78]. There are various studies concentrated on bridged biferrocenyl structures due to redox chemistry of ferrocene such as a powerful electrochemical to explore ground state electronic link through bonds ferrocene. Ferrocene compounds are considered safer than other metallocene for mammalian species [79]. The complexes containing two different types of metal are naming biheterometallocene. [80-82].



**Figure 1.11:** Example of metallocenes (M: Fe, Ti, Zn, Ni, and Cr).

## 1.6. FERROCENE BASED LIGANDS AND THEIR METAL COMPLEXES

In 1951 the Peter L. Pauson discovered ferrocene or di( $\eta^5$ -cyclopentadienyl) iron(II). In recent years, organometallic complexes of ferrocene and substituted ferrocenes coordination with different types of transition metal complexes that used in number of applications research area such as nonlinear optics semi conductivity and cooperative magnetics, having several advantages as unique optical, magnetic and electrical properties. Ferrocene is a diamagnetic solid and special crystalline orange colour; possess special properties as reversible redox and high stability characteristics, used as starting materials in the synthesis of numerous ferrocenyl derivatives. Ferrocene has 18 valence electrons, is considering one in the metallocene sequence with the better stable than other metallocene. Ferrocene stimulated to electrophilic reactions, acts in many compliments like an aromatic electron-rich organic compound exactly like phenyl, major treated similar phenyl group as mercuration, Vilsmeier formylation, Friedel-Crafts acylation and alkylation. Asymmetric substituents of ferrocene derivatives compounds ligands used for asymmetric hydrogenation catalysts [62, 83, 84].

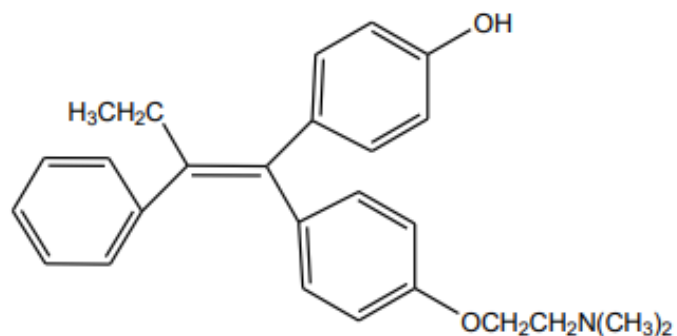
However, the most of scientists concerned ferrocenyl Schiff base and benzimidazole ligands and their metal complexes, in 1954 was synthesized N-(benzylidene)-4-ferrocenyl aniline Schiff base containing phenylferrocene by the condensation of 4-ferrocenyl aniline with benzaldehyde [85]. Also used 4-Ferrocenyl aniline synthesis a number of ferrocenyl Schiff bases through reaction diverse aromatic aldehydes with 4-ferrocenyl aniline [86].

It is try to understand and investigate their board biological activity for instance anti-microbial as antibacterial, anti-fungal, anti-viral and anti-cancer. However, ferrocenyl Schiff base with lanthanide ion complexes ligands recognised in photobiology area [43].

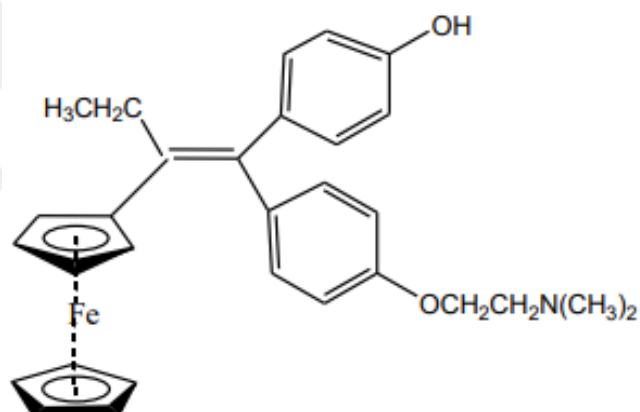
## 1.7. MEDICINAL CHEMISTRY OF FERROCENYL COMPOUNDS

Nowadays, researches are successful on to design interesting novel compounds containing ferrocene and metal complexes possess redox and photo-reactive metal centres coupling electronically by unsaturated bridging ligand. Ferrocenes are recognised strong biological activity as antitumor, DNA cleaving activities, antimalarial, anti-fungal with fewer side effects. It is having best properties as neutral chemically, stable, non-toxic molecule and good redox properties. The vital role in ferrocenium compounds for the inhibition of the tumour cell growth. Ferrocene is not water soluble, some of literature solved this problem for example generate a salt form on the organic residue of ferrocene moiety and create salt through oxidation of central iron atom [87, 88].

Antitumor activity of ferrocene derivatives due to oxidation state of the central iron atom of the ferrocene moiety, research showed salts of ferrocenium have best antitumor inhibitor if only central iron atoms as oxidation state +3 [89]. There are several of literatures citing the usage of ferrocene in medicine design approaches. Tamoxifen is the drug used against breast cancer cells that are mediated by estrogen receptore subtype alpha ( $ER\alpha$ ) receptors [90]. Breast cancer cells divided two types one are mediated by estrogen receptore subtype alpha ( $ER\alpha$ ) and the other mediated by estrogen receptore subtype beta ( $ER\beta$ ). If Tamoxifen mediated by  $ER\beta$  estrogen receptors is not active against breast cancer cells, in 2002 Jaouen and co-workers, inspected and proposed the analogs of Tamoxifen that possess an organometallic moiety via changing the phenyl group by ferrocenyl group to formed compounding naming ferrocifen anticancer drug are mediated by both  $ER\alpha$  and  $ER\beta$  estrogen receptors for give great influence against breast cancer cells (Figures 1.12-1.13) [91].



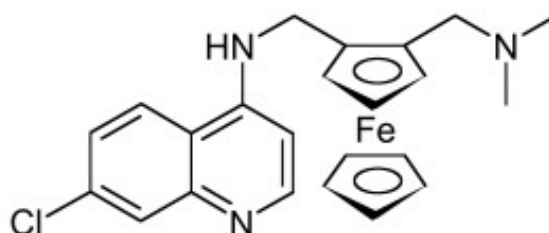
**Figure 1.12:** Tamoxifen (2-[4-[(Z)-1, 2-diphenylbut-1-enyl] phenoxy]-N, N-dimethylethanamine) [91].



**Figure 1.13:** Ferrocenyl derivative of tamoxifen [91].

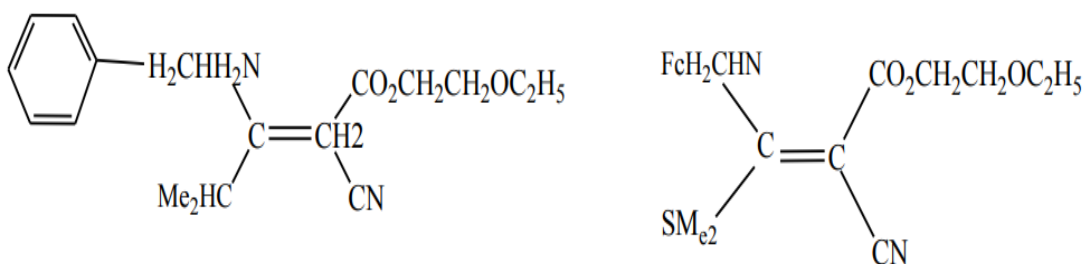
Ferrocene derivatives are stable, small molecule exposed anti-tumor influence by a distinct mechanism in mice bearing recognized lung metastases of B-16 melanoma, anti-tumour achievement refereed by immune stimulation dosage form between 0.05– 0.2 mg/kg for maximal anti-tumor effect but lower or higher dosage form are not active by intraperitoneal injection and oral administration [92].

Ferroquine it is one of ferrocenyl compound it is considering analogue compound of chloroquine have best biologically active. Chloroquinines are used against malaria parasite. Brocard and co-workers reported a ferrocenyl group introduced into the side chain of the chloroquine create ferroquine compound for obtained further advantages effective and harmless in mice non-mutagenic (Figure 1.14) [93].



**Figure 1.14:** Structure of Ferroquine [93].

The past decades, cyanoacrylates representative compounds is powerful attention because have herbicides activity via photosynthetic electron transport disrupting. Cyanoacrylates are known as (Z)-ethoxyethyl-2-cyano-3-(4-chlorophenyl) methylamino-3-isopropylacrylate (Figure 1.15). The synthesize a novel compound by Qingmin and co-workers through exchanging phenyl group with ferrocenyl moiety the result obtained ferrocenyl cyanoacrylates that also having very excellent herbicidal actions [94].



**Figure 1.15:** Herbicidal active compounds (Fc = Ferrocene) [94].

## 1.8. COORDINATION CHEMISTRY OF SOME TRANSITION METAL

### 1.8.1. Cobalt

Cobalt is one of the least abundant of the first row transition metals, element of set nine classified periodic table, also electronic configurations own is  $[\text{Ar}] 4s^2 3d^7$ . Cobalt is one of transition metal possess ranging oxidation states between +1 into +5, but is best record oxidation state common is +2(cobaltous) and +3(cobaltic) with different coordination number, stability, geometry [95]. The Co(IV) as well Co(V) exist uncommon. The electronic configuration of Co(II) ion is  $d^7$ , has single unpaired electrons lead to paramagnetic effect. Several literature survey exposes that Co(II) possess different type of stereo chemical configurations for instance tetrahedral, octahedral and square planar, Co(II) ion various coordination numbers are starting two into eight, Conversely, huge numeral coordination geometries ranging linear to octahedral, complexes Co(II) possess coordination numbers ranging from 6 or 4 coordinate. Maximum magnetic moments of are high spin existence greater than spin only value. General, Co(II) high spin own octahedral geometry with magnetic moment complexes between of 4.3-5.2 BM, although tetrahedral species between 4.2-4.8 BM [96].

Additionally, greatest catalytic activities intended for complexes Co(II) ion Schiff bases example epoxidation, catalyzed on oxidative carbonylation of amines [97,98], as well Co(II) complexes show greater play role in biochemistry [99]. Zahid H. Chohan M. Praveen reported biological activity of cobalt compounds, indicated some effect against diverse serious types bacterial as *Staphylococcus aureus*, *Escherichia coli*, *Klebsiella pneumoniae* and *Pseudomonas aeruginosa*. In comparison with the ligands, the cobalt metal complexes were found to be more biologically active than the ligands [100].



### 1.8.2. Nickel

Nickel is one main atom in transition metal, be located ten set in periodic table, a late first row, 2 electronic configurations possess identical in energy  $[\text{Ar}] 3d^8 4s^2$  or  $3d^9 4s^1$  [96]. Nickel metal shows most oxidation states +1 to +4, but the greatest oxidation state is +2. Ni (IV) as well Ni (III) identified the same potent oxidants. For formation Ni(IV) needs very strong oxidants, e.g.  $\text{K}_2[\text{NiF}_6]$ , and as well consider Ni(III) perfect oxidizing agent, however, become constant via  $\sigma$ -donor ligands for example phosphines and thiols [101].

Complexes formation with Nickel (II) demonstration a number of geometry square-planar and octahedralis influenced by number of factors as temperature, nature of the solvent and concentration [95].

Ni(II) compounds common anions consist of sulfide, sulfate, hydroxide, carbonate, halides, and carboxylates. A Ni(II) complexes has extensive range of coordination geometries via own coordination numbers 4 to 6 for instance square and octahedral very common, however geometries as tetrahedral, trigonal bipyramidal in addition square-based pyramidal uncommon[102]. For corresponding geometries of Ni(II) complexes used the magnetic moments, both octahedral and tetrahedral geometries of Ni(II) complexes are paramagnetic, but diamagnetic effect of square planar, however, magnetic moment of octahedral complexes usually exist near spin only value of 2.84 BM with  $d^8$  configuration lead to paramagnetic complexes, and magnetic moments of tetrahedral complexes 4.5 BM [103,104].

Organisms are need nickel necessary for increase effective of various enzymes for example peptidase, arginase, decarboxylase acid, phosphatase, and deoxyribonuclease[105,106].

### 1.8.3. Copper

Copper is one main atom in transition metal, be located group eleven in periodic table, a late first row, possess  $[\text{Ar}] 3d^{10}4s^1$  electronic configurations, shows +1, +2 and +3 oxidation states, +2, +1, named cupric and cuprous, respectively, but general oxidation state +2 is very common. However, also, Cu(I) is approve oxidation state +1, electronic configuration  $d^{10}$  which funds the complexes exist colourless in addition to diamagnetic, Cu(I) are oxidized readily into Cu(II) but is more difficult further oxidation into Cu (III), also Cu(III) and Cu(IV) are detected comparatively uncommon [107,108].

Copper possesses single electron external shell for the completed 3d,  $3d^9$  configuration styles effect on its stereochemistry of Cu(II) created octahedral or tetrahedral, Cu(II) complex structures of are create as of tetragonal distortion because of Jahn Teller distortion [109,110]. Cu(II) ion has a  $d^9$  configuration lead to paramagnetic as a result of possess lone unpaired electron, as well shows configuration  $d^9$ , also appearance effect to Jahn-Teller distortions exposure happening an octahedral otherwise tetrahedral environment, due to influence indicates requirement molecules into implement geometries that do not produce degeneracy happening valence level orbitals. Instance, six coordinated mostly detected octahedral geometry contains 4 short copper ligand bonds in addition 2 long trans bonds.

Cu(II) complex coordination number subject four, five and six, such as octahedral are greatest public in which record axial groups are coordinating counter ions otherwise solvents. Informed Cu(II) Schiff base complexes containing pentadentate  $N_3O_2$  own geometry a trigonal bipyramidal. Anuradha and coworkers Cu(II) complex established a four coordinate square planar geometry of new macrocyclic binuclear [108,111,112].

Several copper compounds have uses in branch organic chemistry as halogenations, coupling and oxidations reactions; the most oxidation phenol via copper amine complexes is responsible intended for classic phenol-oxidizing enzymes. However, display majors an important role in biological processes as anti-bacterial, anti-fungi, also it is having high activity against different types of cancers and improves the life span in the degree of 20 to 30% [113]. As well-known enormous applications Schiff base complexes by Cu(II) and salicylaldehyde sciences literature, are extensively used as catalysts and for their biological application for instance antimicrobial activities. In 2013 reported by Ourari and co-workers Cu(II) Schiff base complex using pyrrole rings [114].

#### 1.8.4. Zinc

Zinc has an electronic configuration of  $[\text{Ar}] 3d^{10} 4s^2$ , also, main element in periodic table set twelve. The most oxidation state is +2. Diamagnetic Zn(II) complexes are caused by full  $d^{10}$  electronic configuration. The filled d orbitals indicate diamagnetic complexes are generally absent colour. In coordination chemistry the Zn(II) complexes from Schiff base great common, but not in reported same huge quantity of derivatives nickel and copper [108]. Coordination numbers are 4, 5 and 6. Zinc just created tetrahedral complexes by coordination number 4, but by coordination number 5 formed square pyramidal or trigonal bipyramidal, and octahedral of Zn(II) complexes possess coordination number is 6, numerous application of the zinc as used in synthesis alloy to prepare containers due to very low toxicity [115].

In 2006 informed sun and co-workers recognized Schiff base Zn(II) complex pentadentate the 7 coordinate with a pentadentate  $\text{N}_3\text{O}_2$  ligand plus 2 residual coordination site full via solvent donor molecules. However, Chisholm, M.H and co-workers in 2001 synthesized Schiff base Zn(II) a 3 coordinate complex [116]. Also, a 6 coordinated Zn(II) complex definite by Yang, J and co-workers in 2009 through two N,N, O-tridentate resulting octahedral coordination [117].

The Zn(II) Schiff bases complexes expression less catalytic less significant than other transition metal as Mn, Ni, Cu and Co complexes [118]. Zinc has several biological activities for example the insufficiency of zinc in animals lead to disorder as male sexual immaturity and inhibited growth. Besides commonly used as antimicrobial as Zn salts and primarily zinc citrate against oral streptococci and streptococcus mutans. It is very beneficial activity supplement zinc for increases resistance against diseases as diarrheal, besides recover mucosal innate immunity by generation from intestinal epithelial cells the antimicrobial peptide excretion [119].

Kumaran and coworkers reported the important interface between DNA plus complex Schiff base Zn(II), studied using silico techniques besides recommended possess great influence agonist microorganism like bacterial and fungal [120].

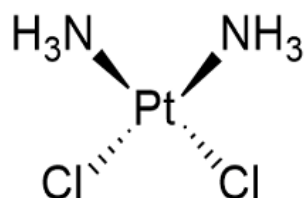
#### **1.8.5. Platinum (II) and Palladium (II)**

Generally palladium desires low oxidation states, the most stable organopalladium compounds with this +4 recognized oxidation state. But, an organopalladium compound with a oxidation state above +4 has never been identified. Instead, highly electronegative fluorine ligands apparently can create +5 and +6 oxidation states, but this species are unstable and have not been fine characterized. Other hand, oxidation state is palladium(0) also know, Pd(IV) and palladium(III) compounds are less common for instance is sodium hexachloropalladate(IV) [121-122]. In 2002 palladium(VI) is detected [123]. The several biological activity platinum(II) complexes have strong cytotoxicity[124].

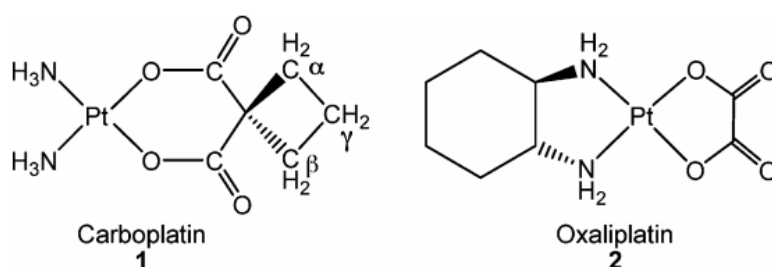
The platinum recorded oxidation states +2 and +4, but fewer common oxidation states are +1 and +3. Tetra coordinate platinum(II) complexes estimated square planar geometries accept 16-electron [125]. Drug compound cisplatin or cis-diamminedichloroplatinum(II) (Figure1.16), reflect actual active cytotoxicity on cancer start used at 1978 [126]. It's given to synthesis another tow medicines such as carboplatin as well as oxaliplatin (Figure1.17), above 3 platinum(II) complexes are working via an analogous mechanism, cisplatin by chloride , oxalate intended for oxaliplatin, carboxylate used for carboplatin, creates inhibition of DNA replication and transcription through react with purine nucleobases in DNA [127].

Distortions the structural of DNA made by platinum binding generate several cellular responses eventually destroyed cell, the best clinical dosage form of these compounds must

intravenous administration to reduce side effect. The 4+ oxidation states of platinum anticancer complexes are shown significant potential together for administration oral and systematic toxicity decline [127-130].

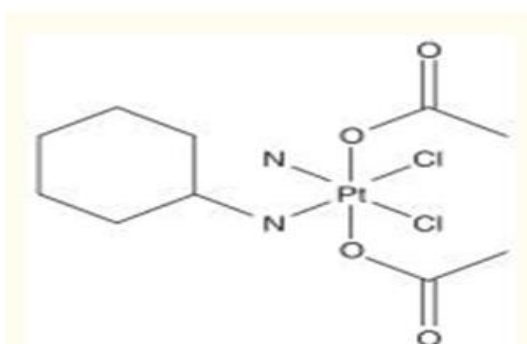


**Figure 1.16:** Structure of cisplatin [131].



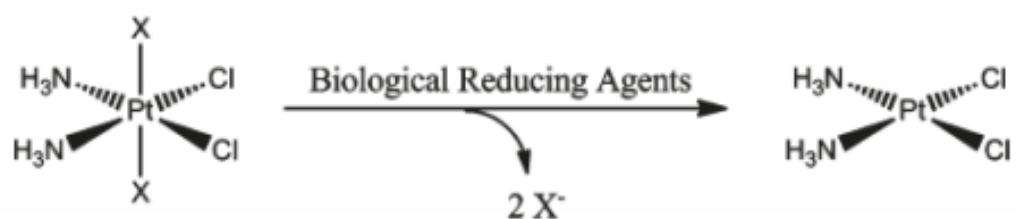
**Figure 1.17:** Structures of carboplatin and oxaliplatin [132].

The administered orally of platinum(IV) satraplatin complex in advanced clinical trials, have more advantages than cisplatin/carboplatin as enhanced toxicity profiles, in addition to reduced cross-resistance toward cisplatin (Figure 1.18) [133].



**Figure 1.18:** Structures of satraplatin [133].

Mechanism similar work of Pt(II) analogues first and second generation. The stimulation stage first reduction Pt(IV) into Pt(II) happen prior binding DNA (Figure 1.19) [131].



**Figure 1.19:** Activation step of cisplatin formation [131].

The development of organometallic chemistry platinum metal played major roles, the several scientist concentrated on development several platinum complexes formulate for biological application [134].

In research work synthesize a new Schiff base and benzimidazole compounds containing ferrocene group and phenol, first to reveal its structural properties, to examine its physical and chemical properties, then to prepare some transition metal compounds and metal complexes of these compounds and to elucidate their structure. In the complex compounds to be obtained, besides the iron atom in the ferrocene group, the complex compounds to be obtained are expected to have significant potential, especially in terms of antimicrobial activity.

## 2. MATERIALS AND METHODS

In this chapter explained the general materials are used, also analytical procedures like preparation of ligands, preparation of metal complexes and experimental instrumentation used for their characterization.

### 2.1. CHEMICALS AND REAGENTS

All chemicals in this study were obtained from (Sigma-Aldrich) used as received without further purification. Ligands and complexes were synthesized by direct reaction of the reactants. The chemicals used as 5-chlorosalicylaldehyde, ferrocene carboxaldehyde, 2-amino-4-methylphenol, 2-amino-4-chloro-5-nitrophenol, 4-methyl-1,2-phenyldiamine, 4,5-dimethyl-1,2-phenyldiamine, 4-chloro-5-nitro-1,2-phenyldiamine. Metal salts as  $\text{CoCl}_2 \cdot 6\text{H}_2\text{O}$ ,  $\text{CuCl}_2 \cdot 2\text{H}_2\text{O}$ ,  $\text{K}_2\text{PtCl}_4$  and  $\text{ZnCl}_2 \cdot 6\text{H}_2\text{O}$  will be used for complex preparation in the study.  $\text{K}_2\text{PdCl}_4$  is prepared as following: 2 mmol KCl was dissolved in distilled water (2 mL) and  $\text{PdCl}_2$  was dissolved in ethanol (5 mL). Then these two solutions were mixed. Common solvents are used puriss quality (for synthesis) like ethanol (technic and puriss), methanol, acetone, chloroform, dichloromethane, hexane, ethyl acetate, DMSO, DMF.

In this study, totally 10 different ligands (nine of them are new, only **HL**<sub>1</sub> is reported in literature: References 135 and 137) and 43 complex compounds are synthesized, the complex compounds to be obtained are expected to have significant potential, especially in terms of antimicrobial activity.

## 2.2. PREPARATION OF SCHIFF BASE LIGAND

Four Schiff bases were prepared. The compounds synthesized were crystalline, precipitate, colored, non-hygroscopic, and insoluble in water, but soluble in ethanol, acetone, chloroform, ethyl acetate, DMF and DMSO.

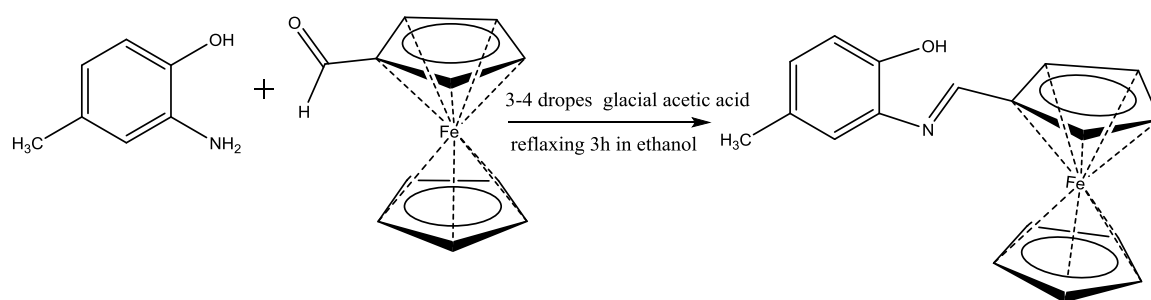
### 2.2.1. Synthesis of Schiff base using glacial acetic acid as catalyst

Synthesis of organometallic compounds was prepared by amine with ferrocene carboxaldehyde, these compounds were separately dissolved in absolute ethanol 15ml, stirred on magnetic hot plate for 45 minutes and refluxed using water condenser for 3 hour. During refluxing 3-4drops of acetic acid was added. After complete refluxing the reaction mixture is cooled at room temperature, kept overnight in dark place, completion of the reaction was checked by TLC. Acetic acid it makes the carbonyl carbon more electrophilic by protonation of oxygen of carbonyl group [135,137].

#### 2.2.1.1. Synthesis of Schiff base 2-(Ferrocen-1-yl-methyliden)amino-4-methylphenol ( $HL_1$ )

Ferrocene carboxaldehyde (1 mmol, 214.0 mg) and 2-amino-4-methylphenol (1 mmol, 123.1 mg) were taken up in a beaker. Ethanol (15 mL) was used as the solvent, stirred on hot magnetic plate for 45 minutes and refluxed using water condenser for 3 hours. During refluxing 3-4 drops of acetic acid was added. After complete refluxing the reaction mixture is cooled at room temperature, completion of the reaction was checked by TLC, kept overnight in dark place, to form a black solid. The solid formed was filtered, the solid obtained was allowed to dry and after drying 0.224g of ligand was obtained in 70% yield. The melting point of the resulting ligand is 187 °C (Figure 2.1).

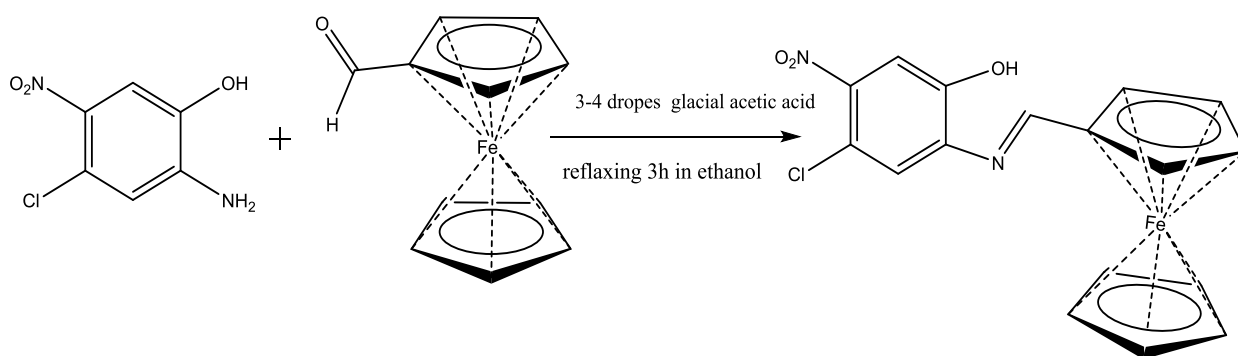




**Figure 2.1:** Scheme of preparation of **HL<sub>1</sub>**.

### 2.2.1.2. Synthesis of Schiff base 2-(Ferrocen-1-yl-methyliden)amino-4-chloro-5-nitrophenol (**HL<sub>2</sub>**)

Ferrocene carboxaldehyde (1 mmol, 214.0 mg) and 2-amino-4-chloro-5-nitrophenol (1 mmol, 188.5 mg) were taken up in a beaker. Ethanol (15 mL) was used as the solvent, stirred on hot magnetic plate for 45 minutes and refluxed using water condenser for 3 hours. During refluxing 3-4 drops of acetic acid was added. After complete refluxing the reaction mixture is cooled at room temperature, completion of the reaction was checked by TLC, kept overnight in dark place, to form a black solid, The solid formed was filtered, the solid obtained was allowed to dry and after drying 0.230 g of ligand was obtained in 66% yield. The melting point of the resulting ligand is 189 °C (Figure 2.2).



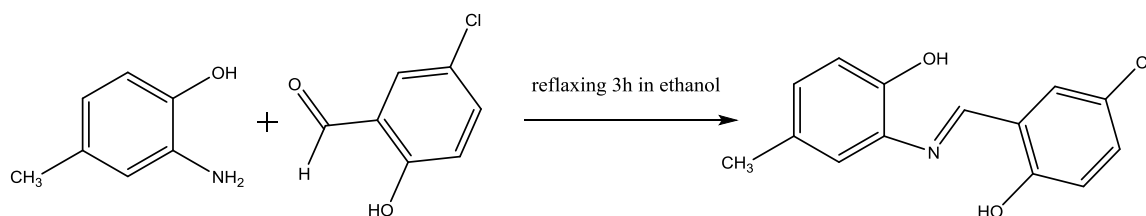
**Figure 2.2:** Scheme of preparation of **HL<sub>2</sub>**.

## 2.2.2. Synthesis of Schiff base without catalyst

Synthesis of organometallic compounds was prepared by amine with 5-chlorosalicylaldehyde, these compounds were separately dissolved in absolute ethanol 25 mL, stirred on magnetic hot plate for 45 minutes and refluxed using water condenser for 3 hour. After complete reaction the reaction mixture is cooled at room temperature, then the solution was checked by TLC. After keeping overnight the crystals are formed [138].

### 2.2.2.1. Synthesis of Schiff base (*E*)-4-chloro-2-(((2-hydroxy-5methylphenyl)imino) methyl) phenol ( $H_2L_3$ )

5-chlorosalicylaldehyde (1 mmol, 156.5 mg) and 2-amino-4-methylphenol (1 mmol, 123.1 mg) were taken up in a beaker. Ethanol (25 mL) was used as the solvent, stirred on hot magnetic plate for 45 minutes and refluxed using water condenser for 3 hours. After complete refluxing the reaction was checked by TLC, and cooled at room temperature to form an orange crystal, the crystal formed was filtered and allowed to dry and after drying 0.211 g of ligand was obtained in 81% yield. The melting point of the resulting ligand is 184 °C (Figure 2.3).

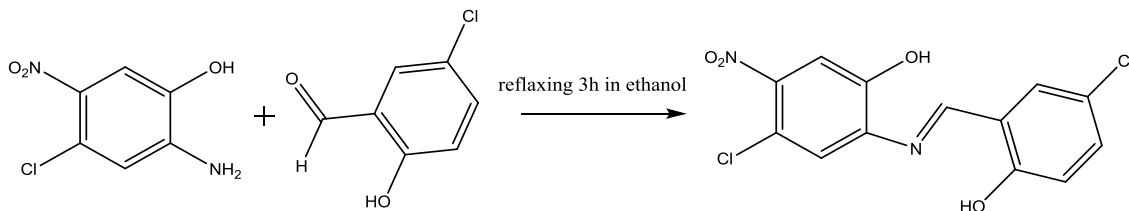


**Figure 2.3:** Scheme of preparation of  $H_2L_3$ .

### 2.2.2.2. Synthesis of Schiff base (*E*)-4-chloro-2-(((5-chloro-2-hydroxy-4-nitrophenyl)imino) methyl) phenol ( $H_2L_4$ )

5-chlorosalicylaldehyde (1 mmol, 156.5 mg) and 2-amino-4-chloro-5-nitrophenol (1 mmol, 188.5 mg) were taken up in a beaker. Ethanol (25 mL) was used as the solvent, stirred on hot magnetic plate for 45 minutes and refluxed using water condenser for 3 hours. After complete refluxation the reaction mixture was checked by TLC, and cooled at room temperature to form a yellowish crystal, the crystal formed was filtered and allowed to dry and after drying

0.256g of ligand was obtained in 78% yield. The melting point of the resulting ligand is 219 °C (Figure 2.4).



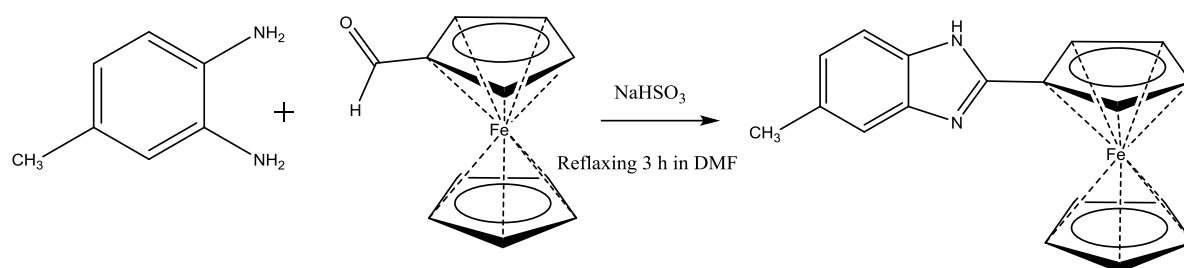
**Figure 2.4:** Scheme of preparation of **H<sub>2</sub>L<sub>4</sub>**.

### 2.3. SYNTHESIS OF BENZIMIDAZOL DERIVATIVES

The benzimidazole derivative ligands were prepared according to literature procedures by used NaHSO<sub>3</sub> as catalyst [139-141].

#### 2.3.1. Synthesis of 2-(Ferrocen-1-yl)-5-methyl-1H-benzimidazole (L<sub>5</sub>)

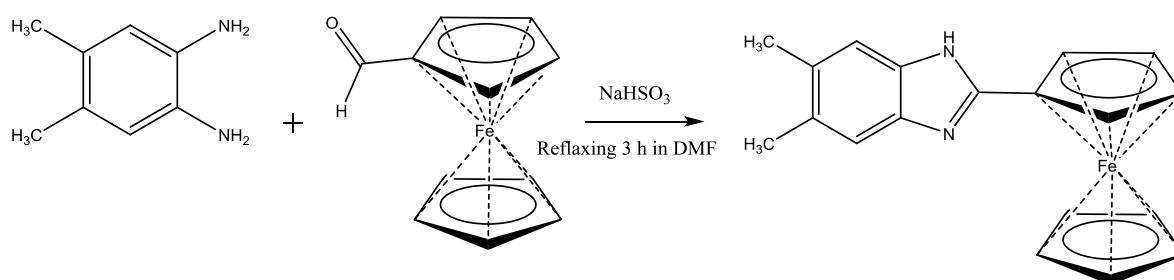
Ferrocene carboxaldehyde (1 mmol, 214.0 mg) and sodium hydrogensulfite (1 mmol, 104.0 mg) as catalyst with ethanol (20 mL) and water (2 mL) was used as the solvent were taken up in a beaker. The mixture was stirred for three hours at room temperature until no more insoluble material was present in the bottom. A cloud white mixture was obtained. To the resulting mixture was added 20 mL of N,N-dimethylformamide (DMF). 4-methyl-1,2-phenyldiamine (1 mmol, 122.2 mg) was then added to the reaction vessel. The reaction mixture was then stirred for about 3 hours, depending on the heater and the reflux. At the end of the reaction, the solution was removed from the heater and allowed to stand at room temperature, and then the brownish precipitate was formed by distilled water and filtered off. The brownish solid obtained was allowed to dry and after drying 0.246 mg of ligand was obtained in 78 % yield. The melting point of the resulting ligand is 172 °C (Figure 2.5).



**Figure 2.5:** Scheme of preparation of L<sub>5</sub>.

### 2.3.2. Synthesis of 2-(Ferrocen-1-yl)-5,6-dimethyl-1H benzimidazole (L<sub>6</sub>)

Ferrocene carboxaldehyde (1 mmol, 214.0 mg) and sodium hydrogensulfite (1 mmol, 104.0 mg) as catalyst with ethanol (20 mL) and water (2 mL) was used as the solvent were taken up in a beaker. The mixture was stirred for three hours at room temperature until no more insoluble material was present in the bottom. A cloud white mixture was obtained. To the resulting mixture was added 20 mL of N, N-dimethylformamide (DMF). 4,5-dimethyl-1,2-phenyldiamine (1 mmol, 136.2 mg) was then added to the reaction vessel. The reaction mixture was then stirred for about 3 hours, depending on the heater and the reflux. At the end of the reaction, the solution was removed from the heater and allowed to stand at room temperature, and then the brownish precipitate was formed by distilled water and filtered off. The brownish solid obtained was allowed to dry and after drying 0.263 mg of ligand was obtained in 80 % yield. The melting point of the resulting ligand is 178 °C (Figure 2.6).

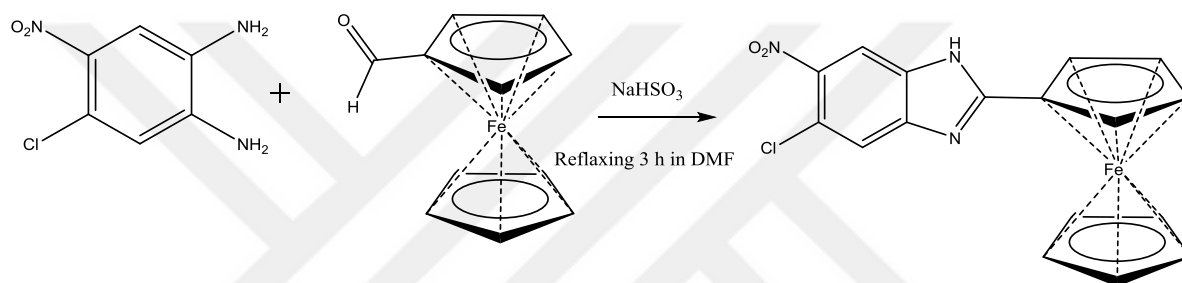


**Figure 2.6:** Scheme of preparation of L<sub>6</sub>.

### 2.3.3. Synthesis of 2-(Ferrocen-1-yl)-5-chloro-6-nitro-1H-benzimidazole (L<sub>7</sub>)

Ferrocene carboxaldehyde (1 mmol, 214.0 mg) and sodium hydrogensulfite (1 mmol, 104.0 mg) as catalyst with ethanol (20 mL) and water (2 mL) was used as the solvent were taken up

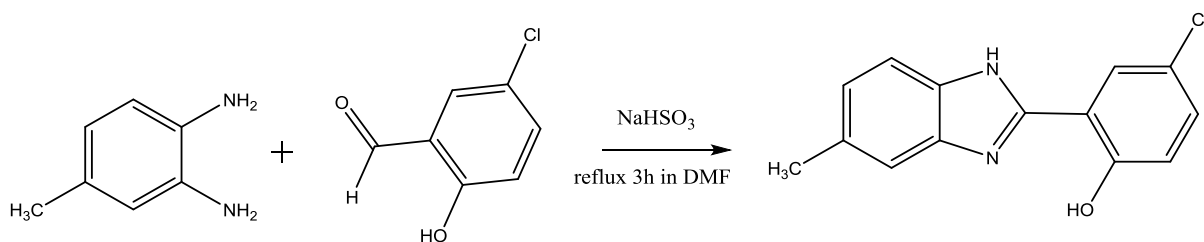
in a beaker. The mixture was stirred for three hour at room temperature until no more insoluble material was present in the bottom. A cloud white mixture was obtained. To the resulting mixture was added 20 mL of N, N-dimethylformamide (DMF), 4-chloro-5-nitro-1,2-phenyldiamine (1 mmol, 187.5 mg) was then added to the reaction vessel. The reaction mixture was then stirred for about 3 hours, depending on the heater and the reflux. At the end of the reaction, the solution was removed from the heater and allowed to stand at room temperature, and then the brownish precipitate was formed by distilled water and filtered off. The brownish solid obtained was allowed to dry and after drying 0.287 mg of ligand was obtained in 75 % yield. The melting point of the resulting ligand is 224 °C (Figure 2.7).



**Figure 2.7:** Scheme of preparation of **L<sub>7</sub>**.

#### 2.3.4. Synthesis of 4-Chloro-2-(5-methyl-1H-benzimidazol-2-yl) phenol (**HL<sub>8</sub>**)

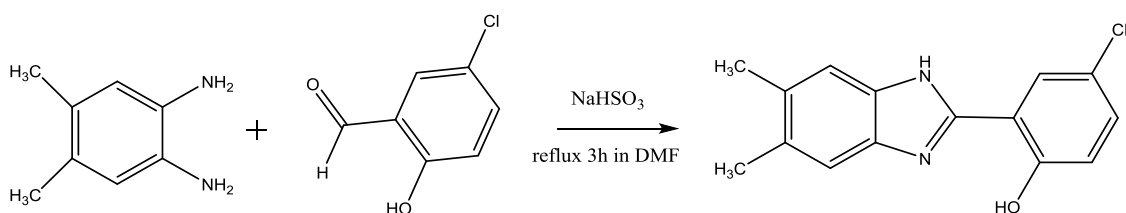
5-chlorosalicylaldehyde (1mmol, 156.5 mg) and sodium hydrogensulfite (1mmol, 104.0 mg) as catalyst with ethanol (20 mL) and water (2 mL) was used as the solvent were taken up in a beaker. The mixture was stirred for three hour at room temperature until no more insoluble material was present in the bottom. A cloud white mixture was obtained. To the resulting mixture was added 20 mL of N, N-dimethylformamide (DMF). 4-methyl-1,2-phenyldiamine (1 mmol, 122.2 mg) was then added to the reaction vessel. The reaction mixture was then stirred for about 3 hours, depending on the heater and the reflux. At the end of the reaction, the solution was removed from the heater and allowed to stand at room temperature, and then the brownish precipitate was formed by distilled water and filtered off. The brownish solid obtained was allowed to dry and after drying 0.221 mg of ligand was obtained in 86 % yield. The melting point of the resulting ligand is 146 °C (Figure 2.8).



**Figure 2.8:** Scheme of preparation of **HL<sub>8</sub>**.

### 2.3.5. Synthesis of 4-Chloro-2-(5,6-dimethyl-1H-benzimidazol-2-yl) phenol (**HL<sub>9</sub>**)

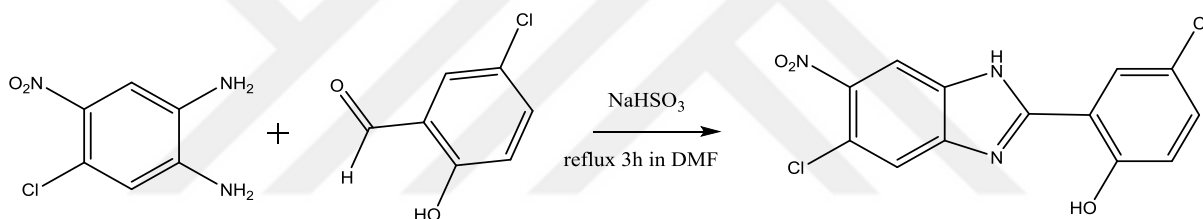
5-chlorosalicylaldehyde (1 mmol, 156.5 mg) and sodium hydrogensulfite (1mmol, 104.0 mg) as catalyst with ethanol (20 mL) and water (2 mL) was used as the solvent were taken up in a beaker. The mixture was stirred for three hours at room temperature until no more insoluble material was present in the bottom. A cloud white mixture was obtained. To the resulting mixture was added 20ml of N,N-dimethylformamide (DMF), 4,5-dimethyl-1,2-phenyldiamine (1 mmol, 136.2 mg) was then added to the reaction vessel. The reaction mixture was then stirred for about 3 hours, depending on the heater and the reflux. At the end of the reaction, the solution was removed from the heater and allowed to stand at room temperature, and then the brownish precipitate was formed by distilled water and filtered off. The brownish solid obtained was allowed to dry and after drying 0.210 mg of ligand was obtained in 77 % yield. The melting point of the resulting ligand is 158 °C (Figure 2.9).



**Figure 2.9:** Scheme of preparation of **HL<sub>9</sub>**.

### 2.3.6. Synthesis of 4-Chloro-2-(5-chloro-6-nitro-1H-benzimidazol-2-yl)phenol (HL<sub>10</sub>)

5-chlorosalicylaldehyde (1mmol, 156.5 mg) and sodium hydrogensulfite (1 mmol, 104.0 mg) as catalyst with ethanol (20 mL) and water (2 mL) was used as the solvent were taken up in a beaker. The mixture was stirred for three hours at room temperature until no more insoluble material was present in the bottom. A cloud white mixture was obtained. To the resulting mixture was added 20 mL of N, N-dimethylformamide (DMF), 4-chloro-5-nitro-1, 2-phenyldiamine (1mmol, 187.5 mg) was then added to the reaction vessel. The reaction mixture was then stirred for about 3 hours, depending on the heater and the reflux. At the end of the reaction, the solution was removed from the heater and allowed to stand at room temperature, and then the brownish precipitate was formed by distilled water and filtered off. The brownish solid obtained was allowed to dry and after drying 0.241 mg of ligand was obtained in 74 % yield. The melting point of the resulting ligand is 230 °C (Figure 2.10).



**Figure 2.10:** Scheme of preparation of HL<sub>10</sub>.

### 2.4. PREPARATION OF METAL COMPLEXES: GENERAL PROCEDURE

Ligand (e.g. HL<sub>1</sub>, 1 mmol, 319.2 mg) and equivalent amounts of metal salts (e.g. ZnCl<sub>2</sub>, 1 mmol, 136.28 mg) were dissolved in 20 mL of ethanol and the mixture was stirred and refluxed for 3h. The solution allowed to stand at room temperature for a few days, the resulting precipitate formed was filtered and washed with ethanol (2 mL), dried at room temperature and weighed. The other complexes were obtained similarly, the salts used for synthesis of the complexes are: as CoCl<sub>2</sub>·6H<sub>2</sub>O, CuCl<sub>2</sub>·2H<sub>2</sub>O, K<sub>2</sub>PdCl<sub>4</sub>, K<sub>2</sub>PtCl<sub>4</sub> and ZnCl<sub>2</sub>·6H<sub>2</sub>O [141, 142].

## 2.5. SINGLE CRYSTAL STUDIES

**H<sub>2</sub>L<sub>3</sub>:** H<sub>2</sub>L<sub>3</sub> was dissolved in methanol, filtered and kept at room temperature. After six days some crystals suitable for X-ray single crystal study were formed. The crystals were collected and dried at room temperature.

[Pd(L<sub>3</sub>)CH<sub>3</sub>CN]·H<sub>2</sub>O, 4-Chloro-2-[(5-methyl-2-oxidophenyl)imino]methyl phenolate (acetonitrile-κN) palladium(II): The complex [Pd(L<sub>3</sub>)H<sub>2</sub>O]·3H<sub>2</sub>O was dissolved in methanol+acetonitrile (1:10) mixture by refluxing. After cooling to room temperature the solution was filtered and kept at room temperature. After 2 weeks, the single crystals were formed. The crystals were collected and dried at room temperature.

## 2.6. ANALYTICAL TECHNIQUES AND INSTRUMENTATION

### 2.6.1. Melting points

Determined the melting point was using an Electro thermal melting-point apparatus. Melting point determined by taking little quantity of the ligands and their metal complexes in a capillary tube closed at one end then employed in the melting point apparatus and the temperature degree of compounds which melts (decomposes) were well-known.

### 2.6.2. FTIR

FT-IR spectra were recorded on a Bruker optics vertex 70 spectrometer using ATR (Attenuated Total Reflection) techniques between 400 and 4000 cm<sup>-1</sup>.

### 2.6.3. UV Visible spectra

UV-Visible spectra was performed on a Perkin Elmer Lambda 25 UV/Visible Spectrometer in methanol.

### 2.6.4. Elemental analysis

C, H, N content was determined on a Thermo Finnigan Flash EA 1112 analyzer.



### 2.6.5. Molar conductivity

Molar conductivity of the complexes was measured on a WTW Cond315i conductivity meter in DMF at  $25 \pm 1^\circ\text{C}$ .

### 2.6.6. $^1\text{H}$ - and $^{13}\text{C}$ -NMR spectra

$^1\text{H}$ -NMR spectra were run on a Varian Unity Inova 500 NMR spectrometer.  $^{13}\text{C}$ -NMR spectra were recorded as attached proton test (APT). The residual DMSO-d<sub>6</sub> signal was used as an internal reference.

### 2.6.7. Magnetic moment measurement

Magnetic measurements of the paramagnetic complexes were carried out on MK1 Sherwood Scientific apparatus at room temperature by Gouy's method.

### 2.6.8. Mass spectrometer

The Electron Spray Ionization-Mass Spectrometry (ESI-MS) analysis was carried out in positive ion modes using a Thermo Finnigan LCQ Advantage MAX LC/MS/MS.

### 2.6.9. XRD single crystal

Suitable crystals were selected for data collection which was performed on a D8-QUEST diffractometer equipped with a graphite-monochromatic Mo-K $\alpha$  radiation at 296 K. The structure was solved by direct methods using SHELXS-2013 [143] and refined by full-matrix least-squares methods on F<sup>2</sup> using SHELXL-2013 [144]. All non-hydrogen atoms were refined with anisotropic parameters. The H atoms of C atoms were located from difference maps and then treated as riding atoms with C–H distance of 0.93–0.97 Å. The other H atoms were located in a difference map refined freely. The following procedures were implemented in our analysis: data collection: Bruker APEX2 [145]; program used for molecular graphics were as follow: MERCURY programs [146]; software used to prepare material for publication: WinGX [147]. Details of data collection and crystal structure determinations of  $\text{H}_2\text{L}_3$  and  $[\text{Pd}(\text{L}_3)\text{CH}_3\text{CN}] \cdot \text{H}_2\text{O}$  are given in Tables 3.17–3.24 and Figures 3.105–3.108.

### 2.6.10. Cyclic voltammetry

The electrochemical performance by used bipotentiostat Gamry Instruments (Reference 3000) (USA) with electrochemical cell, three electrodes was used platinum wire electrode were used as counter electrodes, GCE as working electrode and Ag/AgCl as the reference electrode, were run in methanol solution 0.1 M and 0.1M TBAP as a supporting electrolyte was examined on the surface of GCE at potential scan rate of 100, 50, 20, 10 and 5 mVs<sup>-1</sup> at 25°C, Potential range of 0 to 1.

### 2.6.11. Thermo gravimetric Analysis (TGA)

Thermo gravimetric studies were made on a TG-60WS Shimadzu, with a heating rate of 10 °C/min and air flowing at the rate of 50 mL/min.

### 2.6.12. Determination of antimicrobial activity

Antimicrobial activity against *Staphylococcus aureus* ATCC 29213, *Staphylococcus epidermidis* ATCC 12228, *Escherichia coli* ATCC 25922, *Klebsiella pneumoniae* ATCC 4352, *Pseudomonas aeruginosa* ATCC 27853, *Proteus mirabilis* ATCC 14153 (bacteria) and *Candida albicans* ATCC 10231, *Candida parapsilosis* ATCC 22019 and *Candida tropicalis* ATCC 750 (fungi) were determined by the microbroth dilutions technique following the Clinical and Laboratory Standards Institute (CLSI) recommendations [166, 167]. Mueller-Hinton broth (MHB) (Difco, Detroit, MI, USA) for bacteria, RPMI-1640 medium buffered to pH 7.0 with MOPS (Sigma, St. Louis, MO, USA) for yeast strain was used as the test medium. Serial two-fold dilutions ranging from 5000 µg/mL to 2.4 µg/mL were prepared in MHB. The inoculum was prepared using a 4–6 h broth culture of each bacteria and 24 culture of yeast strains adjusted to a turbidity equivalent to a 0.5 McFarland standard, diluted in broth media to give a final concentration of 5×10<sup>5</sup> cfu/mL for bacteria and 0.5×10<sup>3</sup> to 2.5×10<sup>3</sup> cfu/mL for yeast in the test tray. The trays were covered and placed in plastic bags to prevent evaporation. The trays containing MHB were incubated at 35°C for 18–20 h and the trays containing RPMI-1640 medium were incubated at 35°C for 46–50 h. The minimum inhibitory concentrations (MIC) were defined as the lowest concentration of compound giving complete inhibition of visible growth. As control, antimicrobial effects of dimetil sulfoxid (DMSO) were investigated against test microorganisms. Ciprofloxacin and Amphotericin B

were used to verify the standardization of the microdilution test procedure as reference antimicrobials for bacteria and yeast, respectively. According to values of the controls, the results were evaluated. The MIC values of the Ciprofloxacin and Fluconazole were within the accuracy range in CLSI throughout the study [168]. The experiments were performed in duplicate.



### 3. RESULTS

The synthesized compounds Schiff bases, benzimidazole derivatives and their metal complexes with  $\text{Pd}^{2+}$ ,  $\text{Zn}^{2+}$ ,  $\text{Cu}^{2+}$ ,  $\text{Pt}^{2+}$  and  $\text{Co}^{2+}$  characterized by melting point, elemental analysis, IR, UV-Vis, mass spectra,  $^{13}\text{C}$ - and  $^1\text{H}$ -NMR spectra, cyclic voltammetry, molar conductivity, magnetic moment and single crystal XRD.

#### 3.1. CHARACTERIZATIONS OF THE LIGANDS

##### 3.1.1. The physical properties of the ligands

The some physical properties of the ligands are summarized in the Table 3.1.

**Table 3.1:** Some physical data of the ligands.

| Compounds ID                  | Empirical formula  | Formula weight(g/mol) | M.P* °C | Colour    | Yield % |
|-------------------------------|--|-----------------------|---------|-----------|---------|
| HL <sub>1</sub>               | C <sub>18</sub> H <sub>17</sub> NOFe   | 319.20                | 187     | black     | 70      |
| HL <sub>2</sub>               | C <sub>17</sub> H <sub>13</sub> N <sub>2</sub> O <sub>3</sub> Fe             | 384.60                | 189     | black     | 66      |
| H <sub>2</sub> L <sub>3</sub> | C <sub>14</sub> H <sub>12</sub> ClNO <sub>2</sub>                            | 261.70                | 184     | orange    | 81      |
| H <sub>2</sub> L <sub>4</sub> | C <sub>13</sub> H <sub>7</sub> C <sub>12</sub> N <sub>3</sub> O <sub>3</sub> | 327.12                | 219     | yellowish | 78      |
| L <sub>5</sub>                | C <sub>18</sub> H <sub>16</sub> N <sub>2</sub> Fe                            | 316.20                | 172     | brownish  | 78      |
| L <sub>6</sub>                | C <sub>19</sub> H <sub>18</sub> N <sub>2</sub> Fe                            | 330.20                | 178     | brownish  | 80      |
| L <sub>7</sub>                | C <sub>17</sub> H <sub>12</sub> ClN <sub>3</sub> O <sub>2</sub> Fe           | 381.59                | 224     | brownish  | 75      |
| HL <sub>8</sub>               | C <sub>14</sub> H <sub>11</sub> ClN <sub>2</sub> O                           | 258.70                | 146     | brownish  | 86      |
| HL <sub>9</sub>               | C <sub>15</sub> H <sub>13</sub> ClN <sub>2</sub> O                           | 272.73                | 158     | brownish  | 77      |
| HL <sub>10</sub>              | C <sub>13</sub> H <sub>7</sub> C <sub>12</sub> N <sub>3</sub> O <sub>3</sub> | 324.12                | 230     | brownish  | 74      |

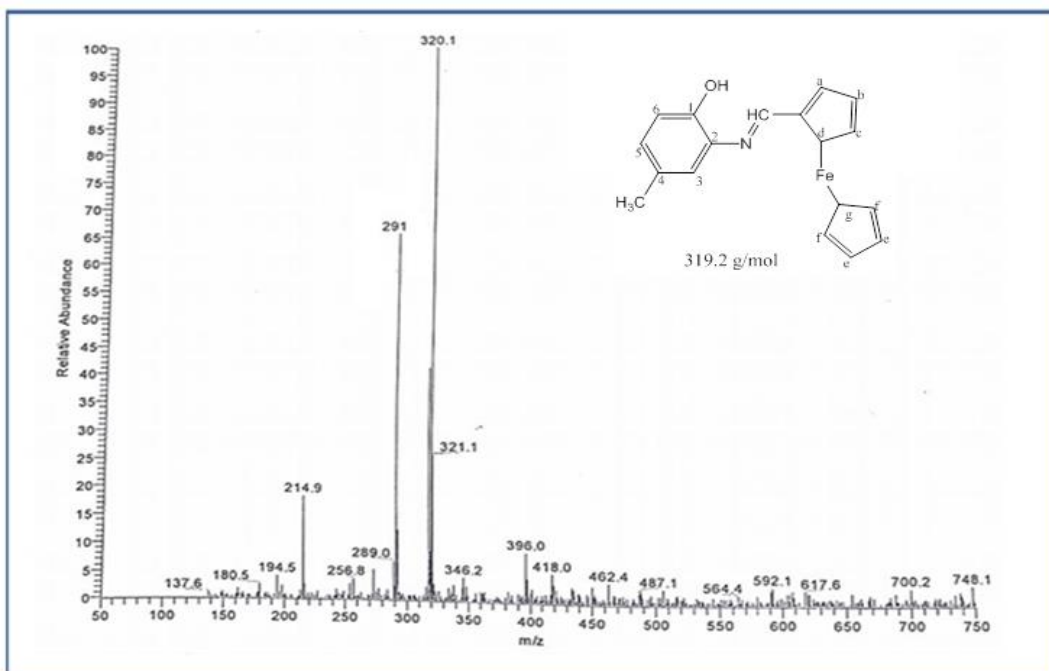
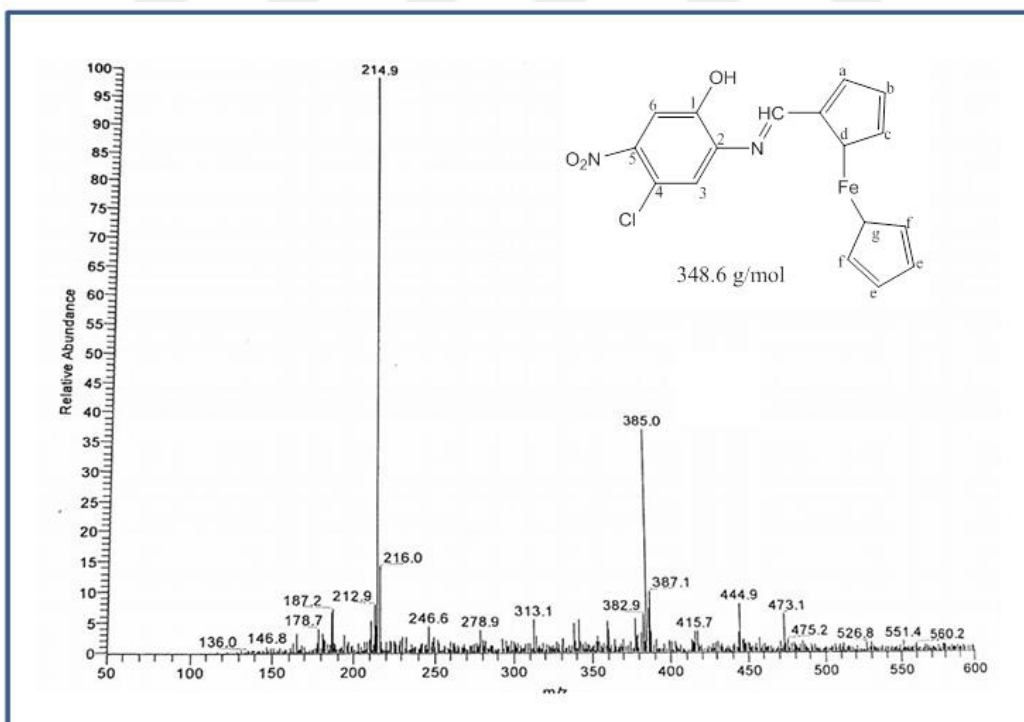
\*M.p (decomposition)

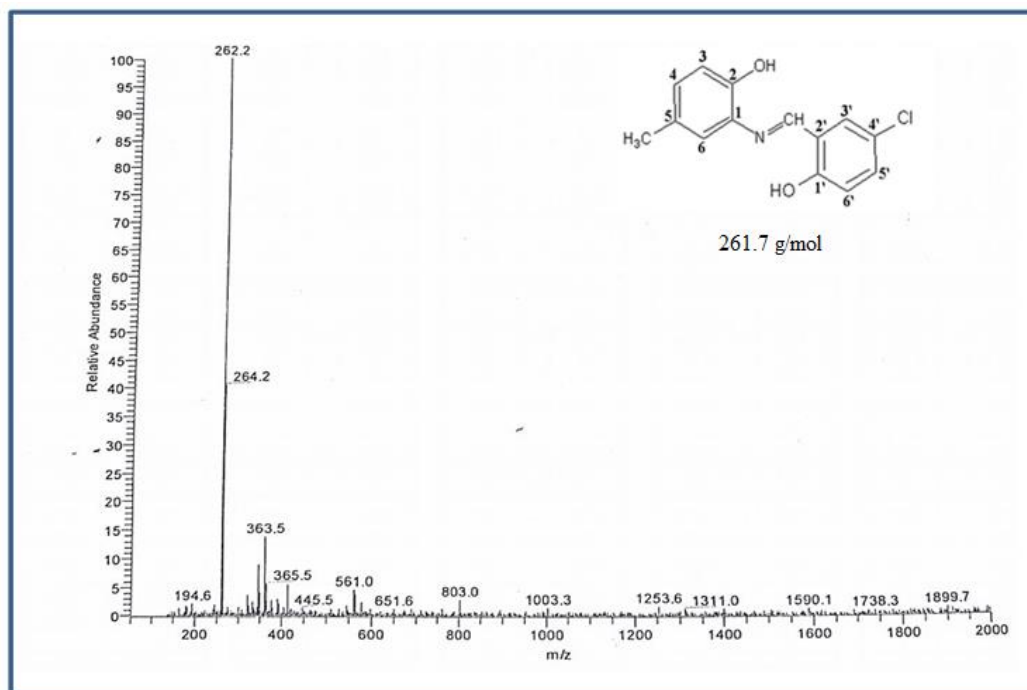
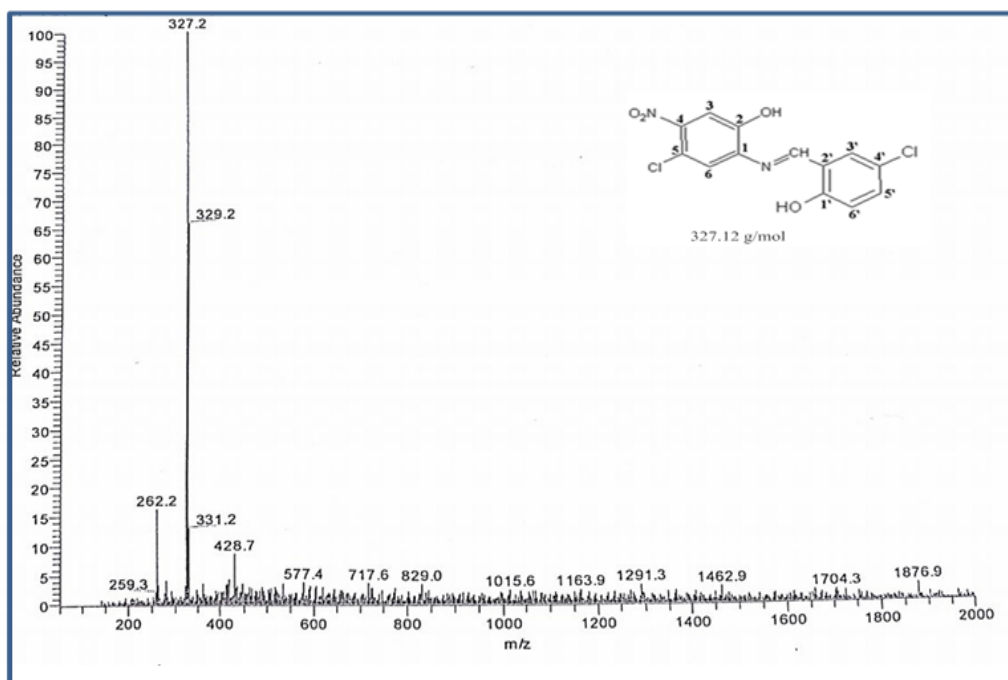
### 3.1.2. Mass spectra

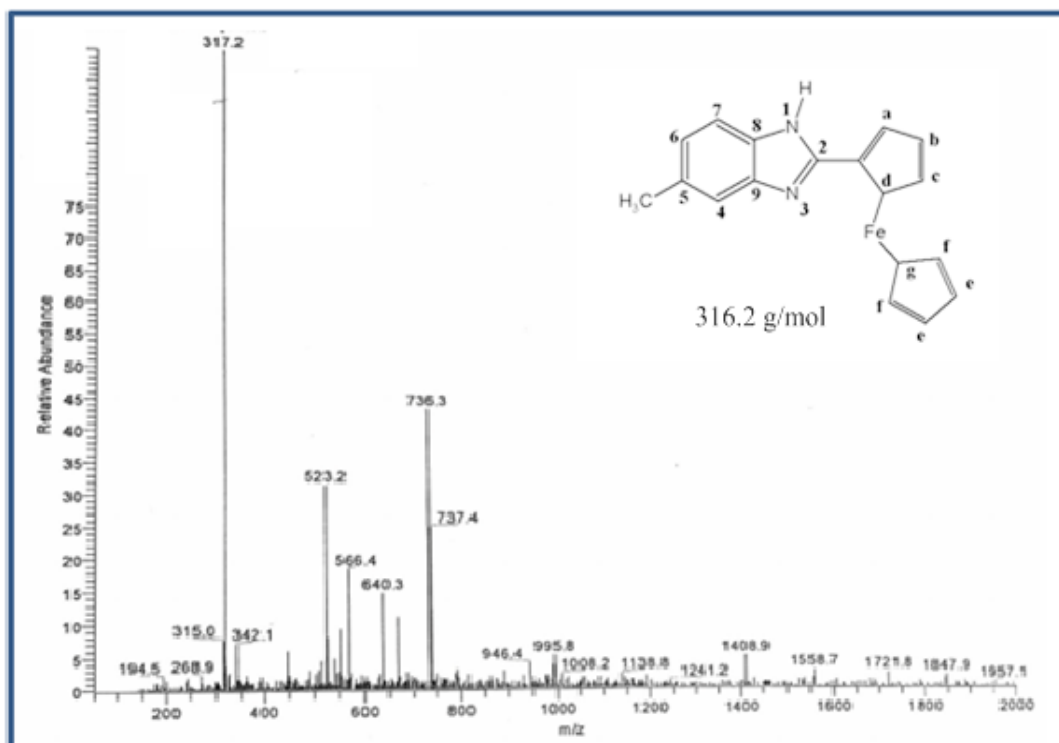
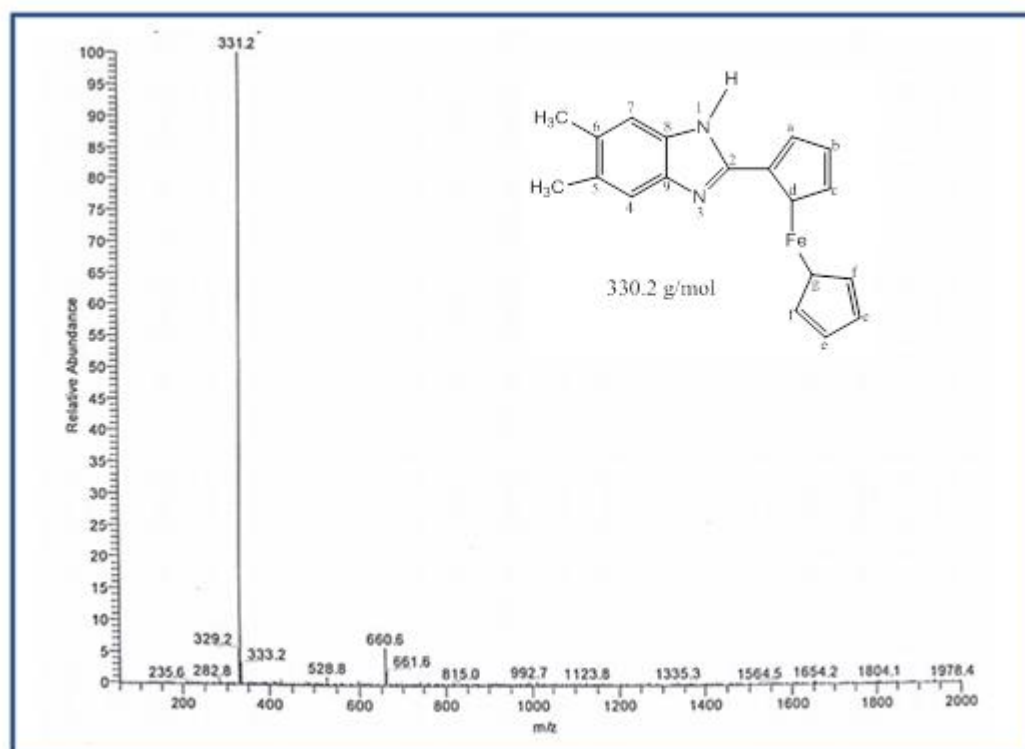
The mass spectral data of the ligands are given in Table 3.2 and Figures 3.1-3.10.

**Table 3.2:** Mass spectral data of the ligands.

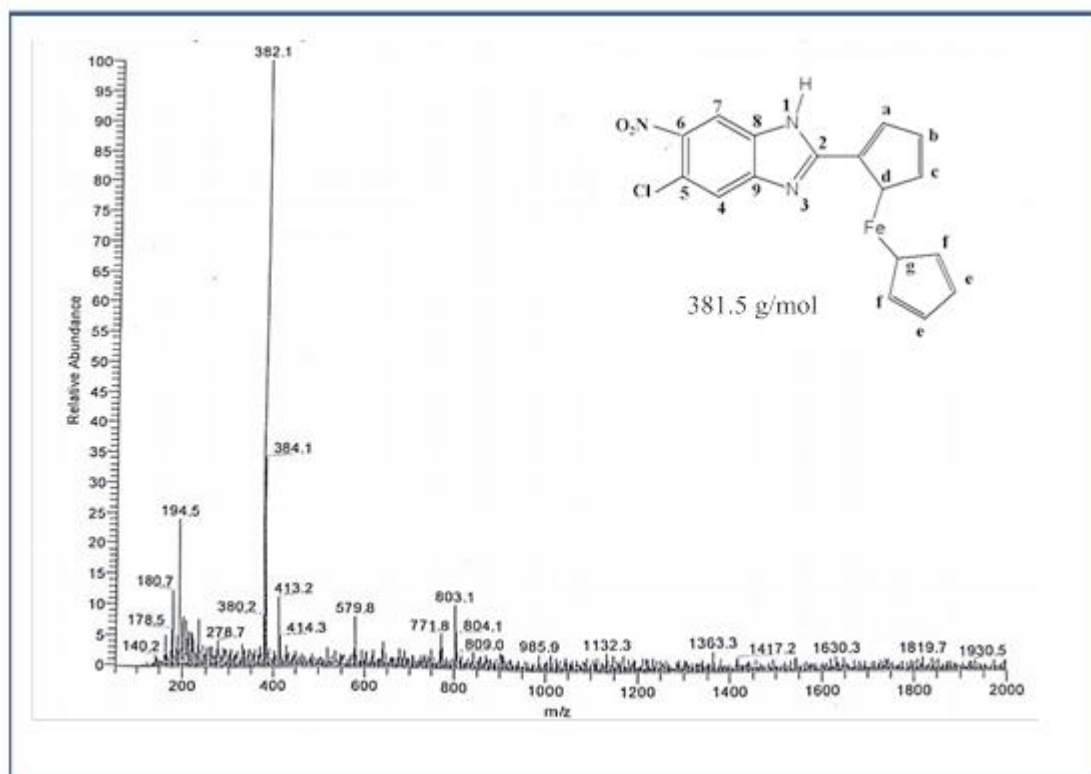
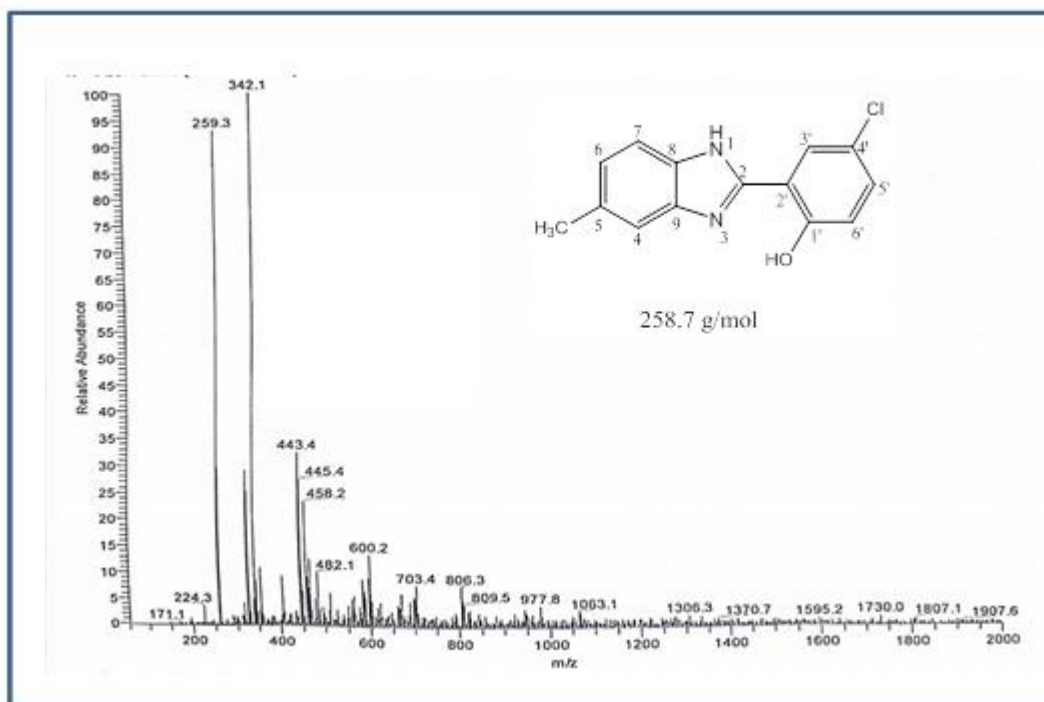
| Compounds (ID)                | Formula weigh (g/mol) | Molecular ion peak (m/z)             |
|-------------------------------|-----------------------|--------------------------------------|
| HL <sub>1</sub>               | 319.2                 | 320.1 [((M <sup>+</sup> ), 100 %)]   |
| HL <sub>2</sub>               | 384.6                 | 385.0 [((M), 38.02 %)]               |
| H <sub>2</sub> L <sub>3</sub> | 261.7                 | 262.2 [((M <sup>+</sup> ), 100 %)]   |
| H <sub>2</sub> L <sub>4</sub> | 327.12                | 327.2 [((M), 100 %)]                 |
| L <sub>5</sub>                | 316.2                 | 317.2 [((M <sup>+</sup> ), 100 %)]   |
| L <sub>6</sub>                | 330.2                 | 331.2 [((M <sup>+</sup> ), 100 %)]   |
| L <sub>7</sub>                | 381.59                | 382.1 [((M <sup>+</sup> ), 100 %)]   |
| HL <sub>8</sub>               | 258.70                | 259.3 [((M <sup>+</sup> ), 92.83 %)] |
| HL <sub>9</sub>               | 272.73                | 273.3 [((M <sup>+</sup> ), 100 %)]   |
| HL <sub>10</sub>              | 324.12                | 324.4 [((M), 100 %)]                 |

Figure 3.1: Mass spectra of HL<sub>1</sub>.Figure 3.2: Mass spectra of HL<sub>2</sub>.

Figure 3.3: Mass spectra of  $H_2L_3$ .Figure 3.4: Mass spectra of  $H_2L_4$ .

Figure 3.5: Mass spectra of L<sub>5</sub>.Figure 3.6: Mass spectra of L<sub>6</sub>.



Figure 3.7: Mass spectra of **L<sub>7</sub>**.Figure 3.8: Mass spectra of **HL<sub>8</sub>**.

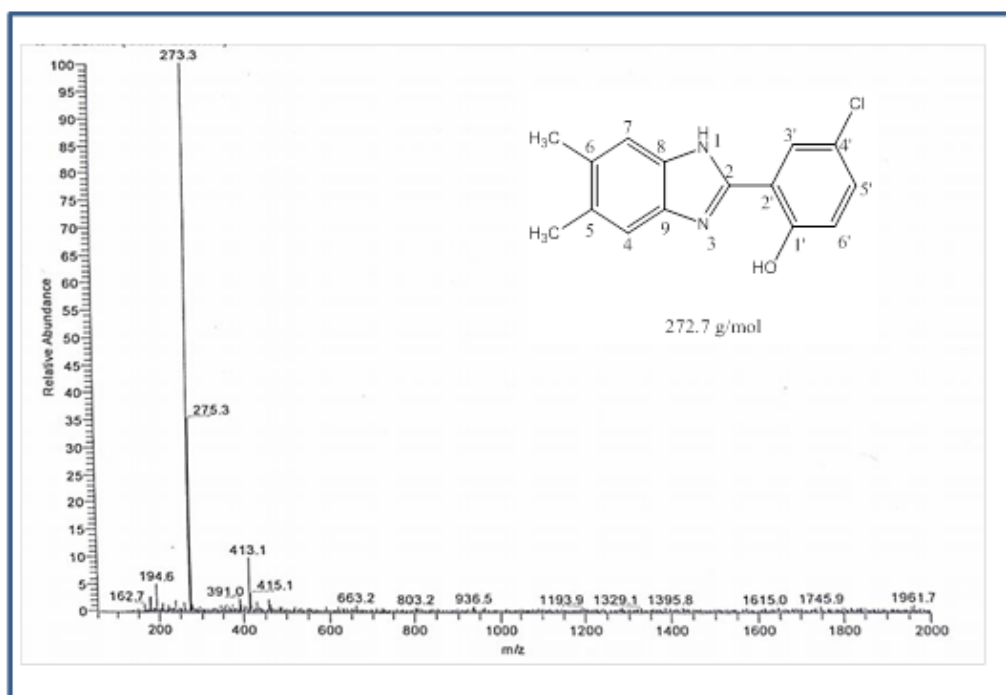


Figure 3.9: Mass spectra of HL<sub>9</sub>.

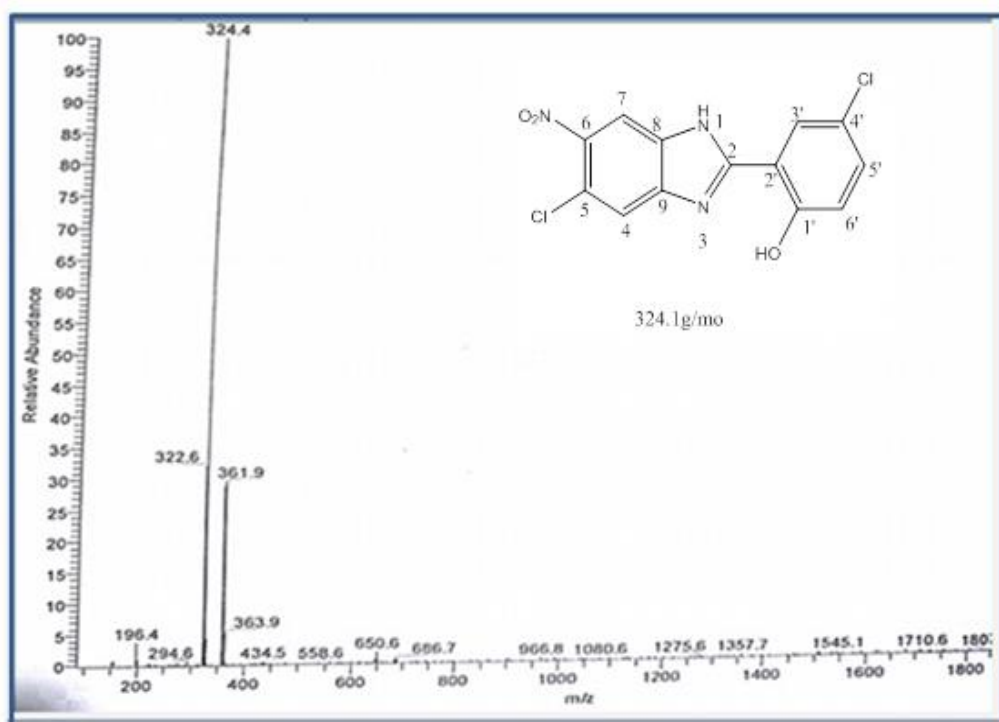


Figure 3.10: Mass spectra of HL<sub>10</sub>.

### 3.1.3. Infrared spectra

FTIR spectral data of the ligands were summarized in Table 3.3. As well, hydrogen bonding presence information of (**HL<sub>1</sub>**-**HL<sub>10</sub>**) obtainable and corresponding spectra are given in (Figures 3.11 - 3.20).

**Table 3.3:** Infrared spectral data of the ligands (cm<sup>-1</sup>).

| Compound ID                       | $\nu(\text{OH})$ | $\nu(\text{NH})$ | $\nu(\text{C}=\text{N})$ | $\nu(\text{C}=\text{C})$<br>(Cp) | $\nu(\text{C}=\text{C})$<br>(aromatic) | $\nu(\text{C}-\text{O})$ | $\nu(\text{Fe}-\text{Cp})$ | $\nu(\text{NO}_2)$ | H-bonding<br>in the IR<br>spectra |
|-----------------------------------|------------------|------------------|--------------------------|----------------------------------|--|--------------------------|----------------------------|--------------------|-----------------------------------|
| <b>HL<sub>1</sub></b>             | 3400-2500m, br   | -                | 1640 m                   | 1577 m                           | 1500 m                                 | 1300 m                   | 510 m                      | -                  | Considerable H bonding            |
| <b>HL<sub>2</sub></b>             | 3400 m, br       | -                | 1643 m                   | 1580 m                           | 1500 m                                 | 1350 m                   | 495 m                      | 1480 m, 1332 m     | Considerable H bonding            |
| <b>H<sub>2</sub>L<sub>3</sub></b> | 3200-2500, m, br | -                | 1650 m                   | -                                | 1510 m                                 | 1320 m                   | -                          | -                  | Considerable H bonding            |
| <b>H<sub>2</sub>L<sub>4</sub></b> | 3500m, br        | -                | 1655 m                   | -                                | 1520 s                                 | 1300 m                   | -                          | 1549 m, 1332 m     | Considerable H bonding            |
| <b>L<sub>5</sub></b>              | -                | 3300m, br        | 1620m                    | 1560 m                           | 1470m                                  | -                        | 511 m                      | -                  | -                                 |
| <b>L<sub>6</sub></b>              | -                | 3200 m, br       | 1600 m                   | 1500 m                           | 1450 m                                 | -                        | 500 m                      | -                  | -                                 |
| <b>L<sub>7</sub></b>              | -                | 3400 m, br       | 1615m                    | 1580 m                           | 1500m                                  | -                        | 500 m                      | 1480 m, 1350 m     | -                                 |
| <b>HL<sub>8</sub></b>             | 3200-2500w, br   | 3300 s           | 1612 m                   | -                                | 1500 m                                 | 1310 m                   | -                          | -                  | Considerable H bonding            |
| <b>HL<sub>9</sub></b>             | 3200-2500w, br   | 3300 s           | 1600 m                   | -                                | 1580 m                                 | 1300 m                   | -                          | -                  | Considerable H bonding            |
| <b>HL<sub>10</sub></b>            | 3300m, br        | 3500 m           | 1610 m                   | -                                | 1560 m                                 | 1315 m                   | -                          | 1480 m, 1350 m     | Considerable H bonding            |

s = sharp, w = weak, m = medium, br = broad.

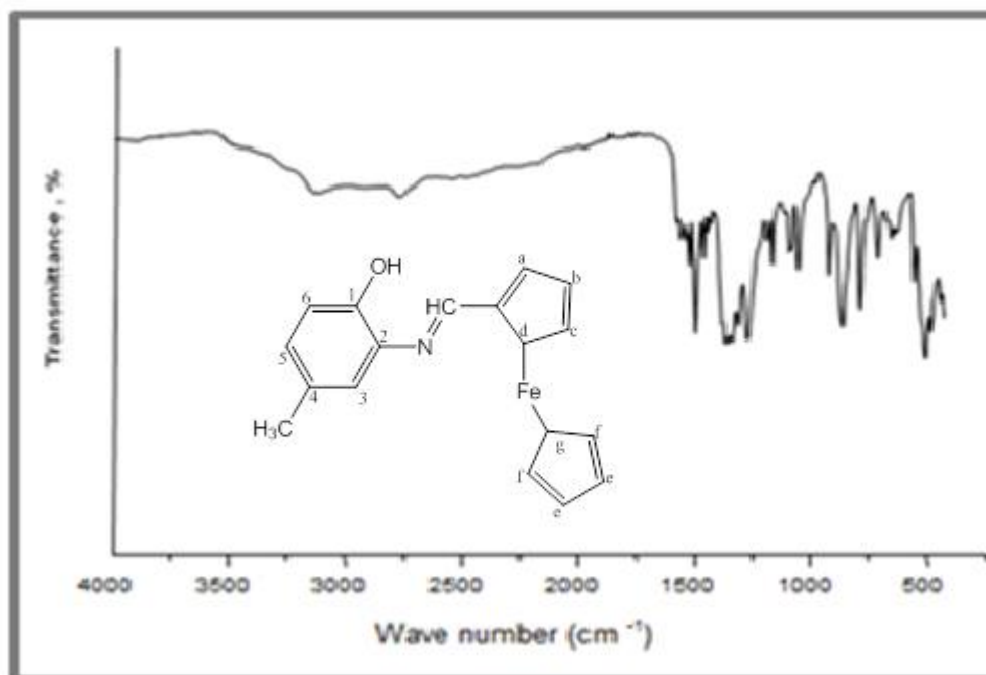


Figure 3.11: IR spectrum of HL<sub>1</sub>.

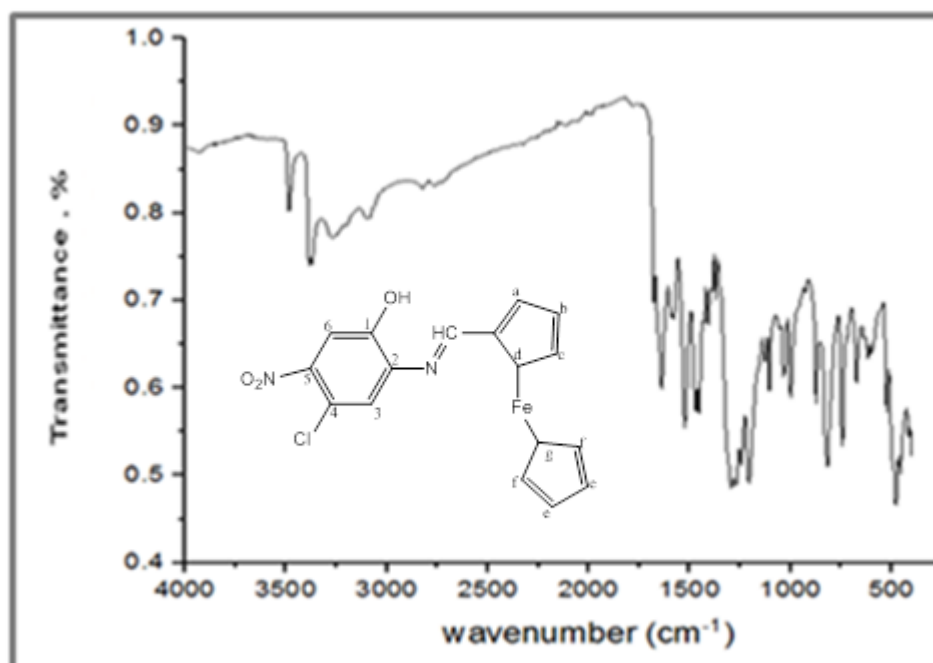


Figure 3.12: IR spectrum of HL<sub>2</sub>.

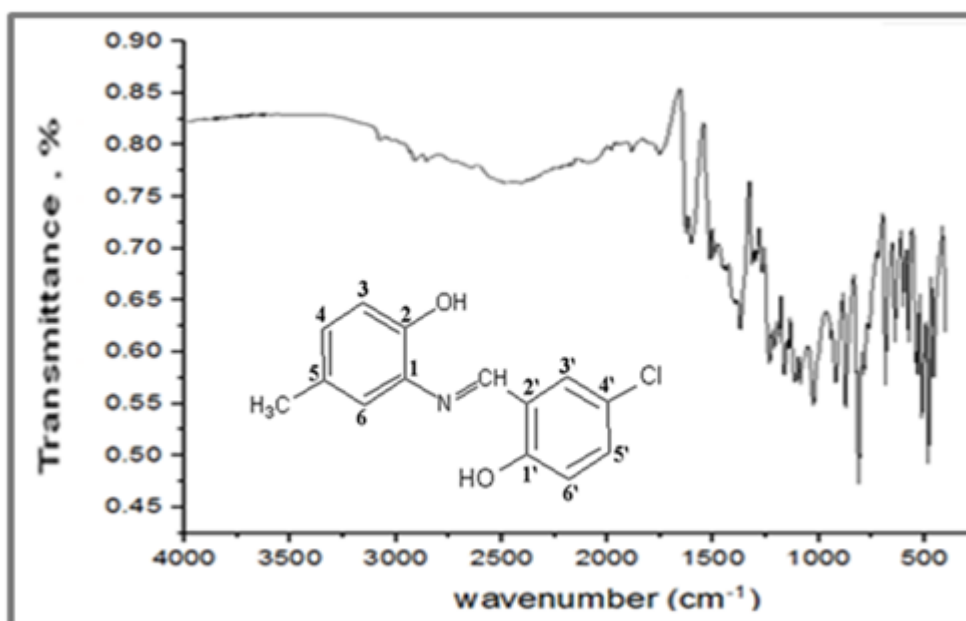


Figure 3.13: IR spectrum of  $H_2L_3$ .

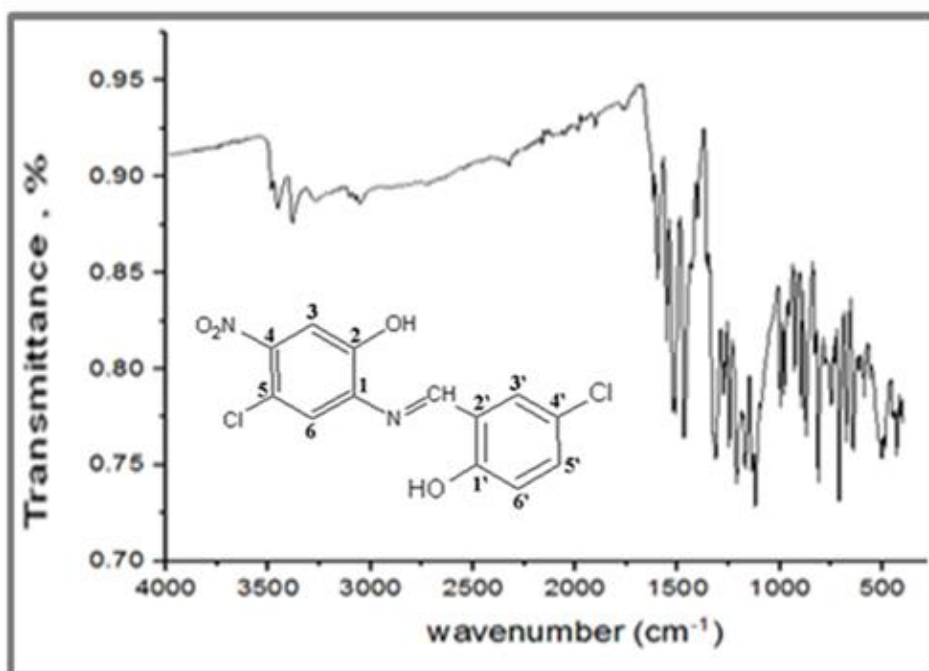


Figure 3.14: IR spectrum of  $H_2L_4$ .

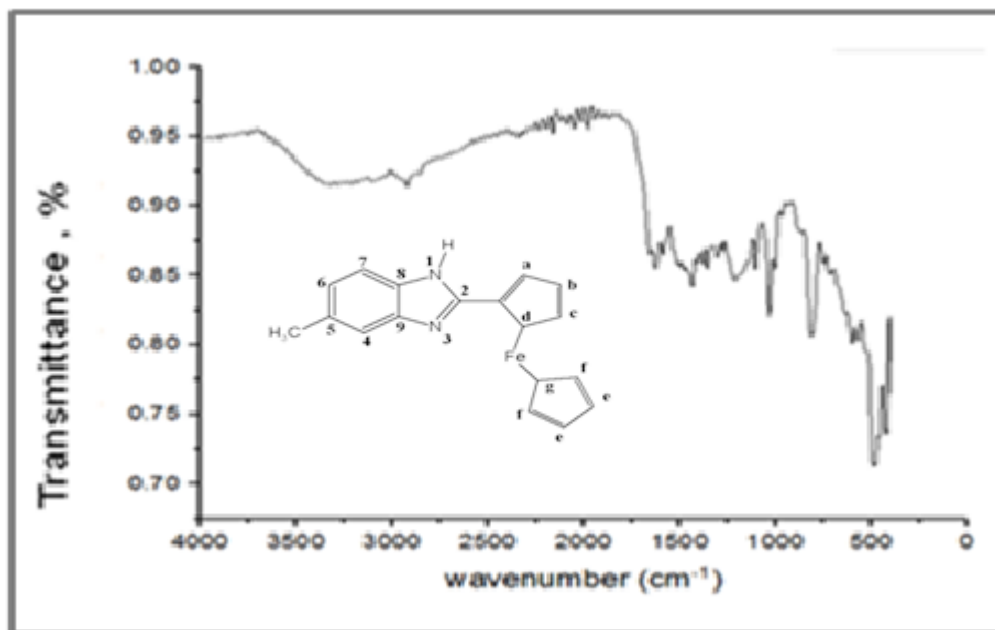


Figure 3.15: IR spectrum of L<sub>5</sub>.

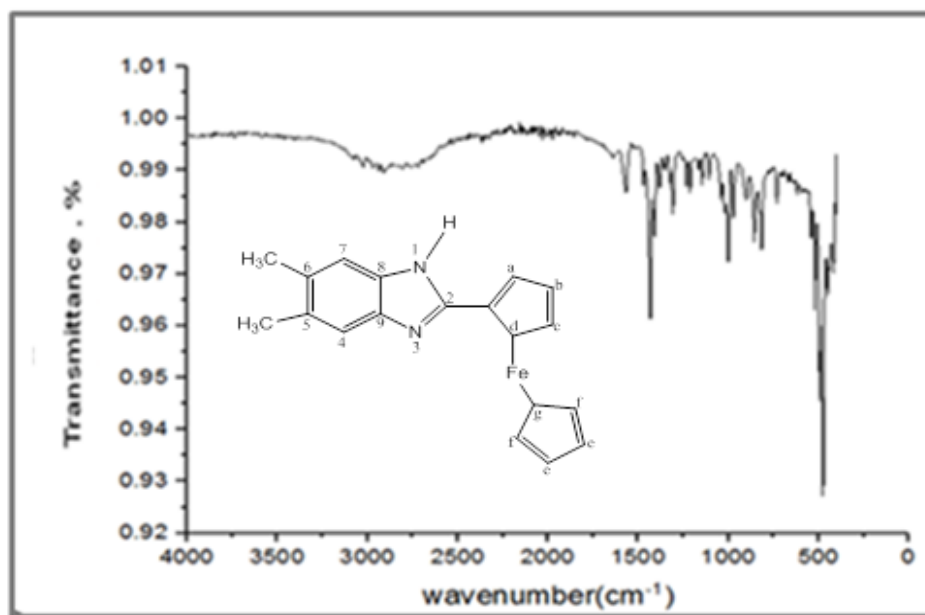


Figure 3.16: IR spectrum of L<sub>6</sub>.

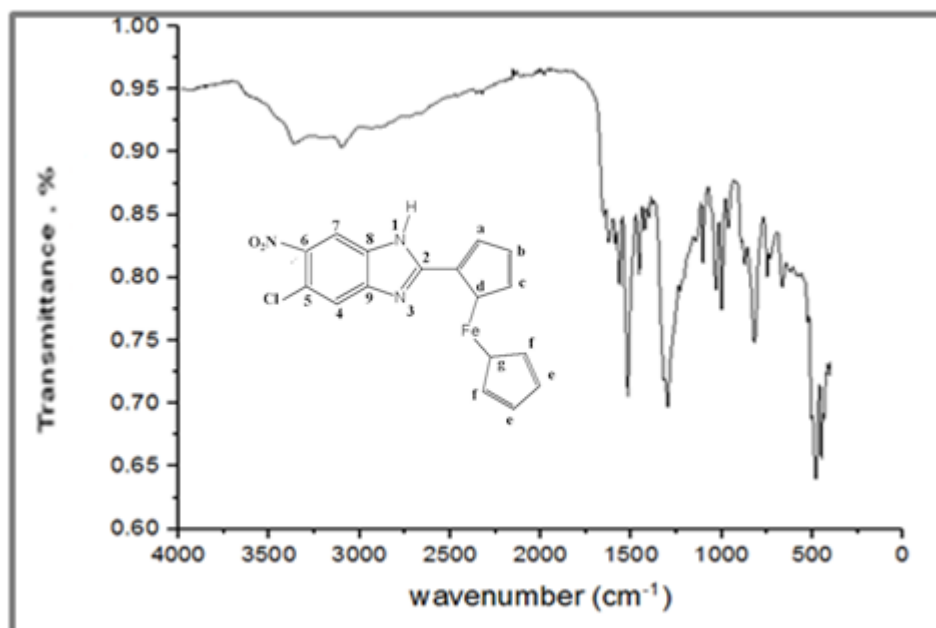


Figure 3.17: IR spectrum of L<sub>7</sub>.

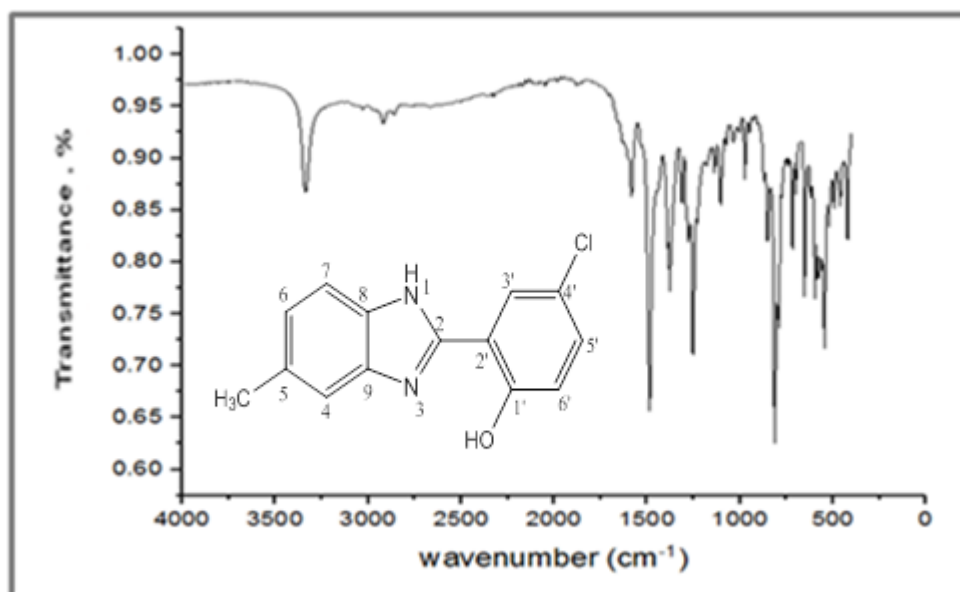


Figure 3.18: IR spectrum of HL<sub>8</sub>.

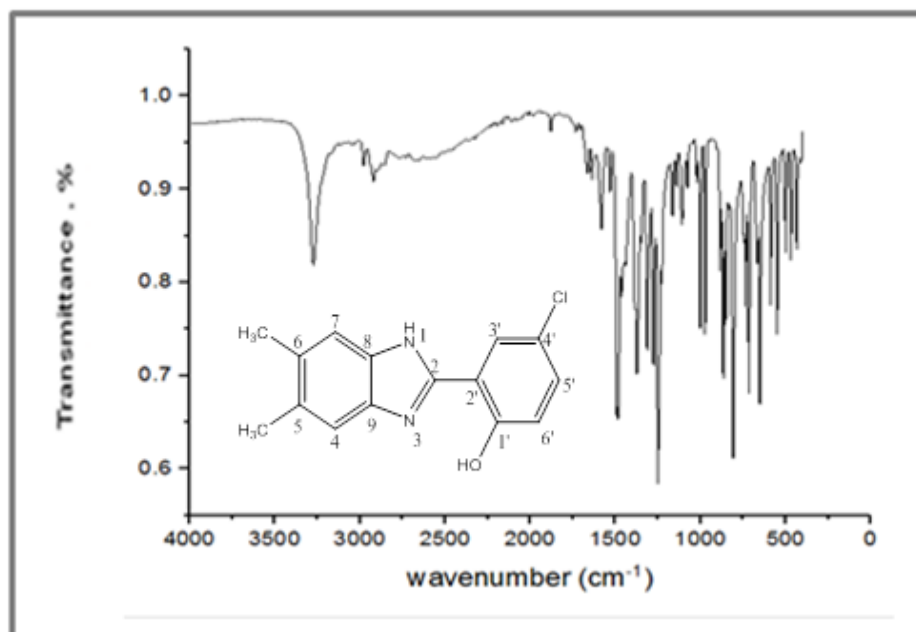


Figure 3.19: IR of spectrum of HL<sub>9</sub>.

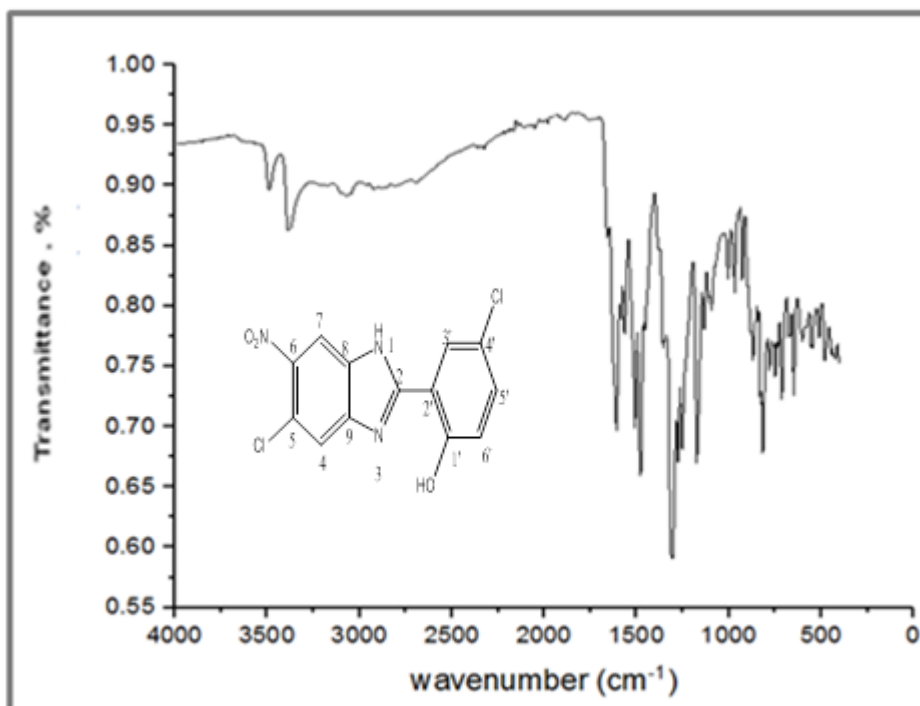


Figure 3.20: IR spectrum of HL<sub>10</sub>.



### 3.1.4. NMR spectra

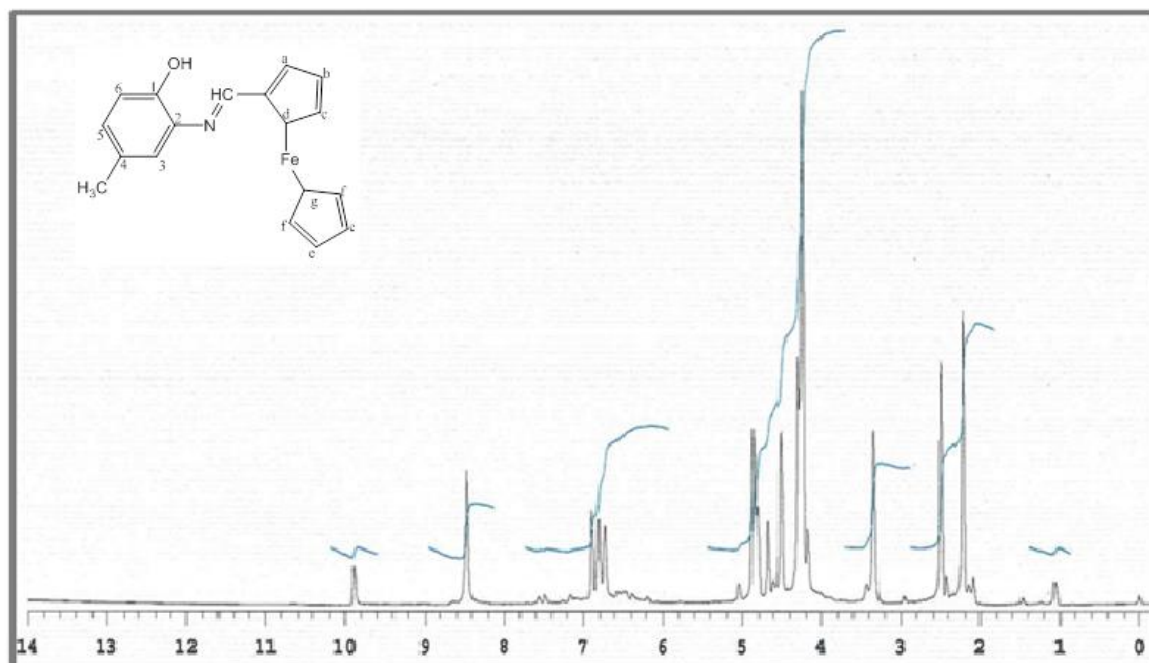
The NMR spectra carried out in DMSO-d<sub>6</sub>. The information is presented in Table 3.4 and corresponding spectra are given in Figures 3.21 - 3.37.

**Table 3.4:** <sup>1</sup>H-NMR and <sup>13</sup>C-NMR spectral data of the ligands.

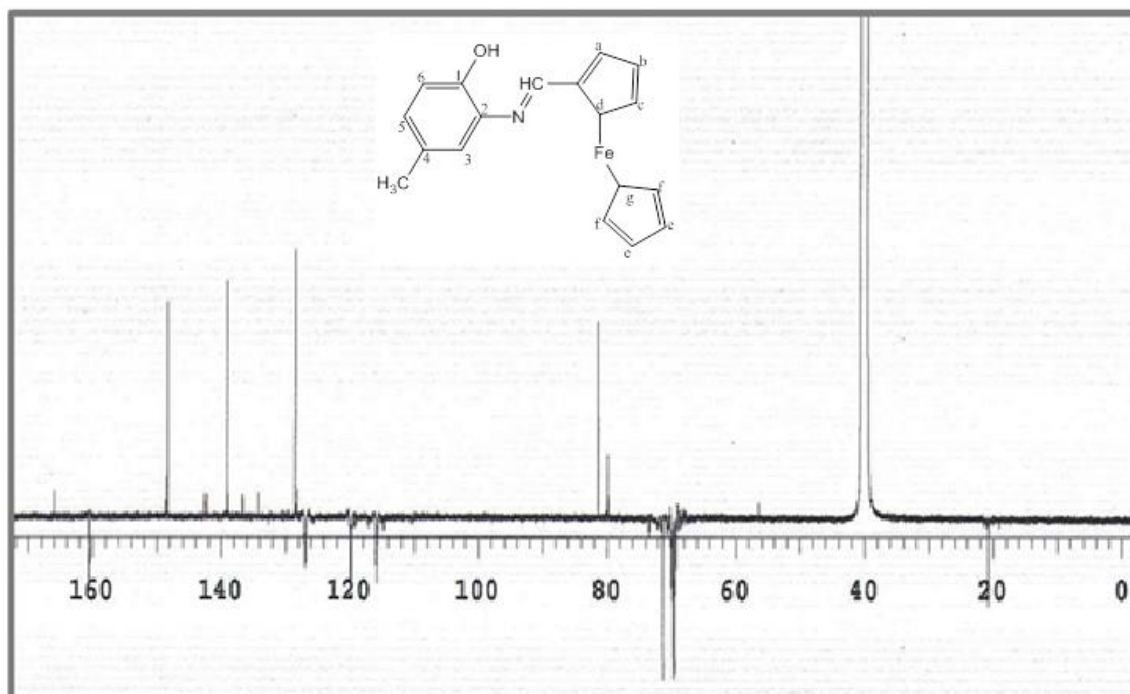
| Compounds ID                      | Assignments   |
|-----------------------------------|---|
| <b>HL1</b>                        | <p><b><sup>1</sup>H-NMR:</b> 9.90 (s, br, 1H, OH), 8.47 (s, br, 1H, N=CH), 6.90 (s, 1H, H3), 6.81 (s, 1H, H6), 6.73 (s, 1H, H5), 4.86 (s, 2H, H<sub>a</sub>+H<sub>b</sub>), 4.43 (s, 2H, H<sub>c</sub>+H<sub>d</sub>), 4.30 (s, 5H, 2xH<sub>e</sub>+2xH<sub>f</sub>+H<sub>g</sub>) 2.23 (s, 3H, CH<sub>3</sub>).</p> <p><b><sup>13</sup>C-NMR:</b> 20.74 (CH<sub>3</sub>), 70.17 (2xC<sub>e</sub>), 70.24 (2xC<sub>f</sub>), 70.66 (C<sub>g</sub>), 71.36 (C<sub>b</sub>), 71.53(C<sub>c</sub>), 79.89 (C<sub>d</sub>), 80.13 (C<sub>h</sub>), 81.37 (C<sub>a</sub>), 115.88 (C5), 119.93 (C3), 127.30 (C6), 128.49 (C4), 139.07 (C2), 148.72 (C1), 160.38 (N=CH).</p>  |
| <b>HL2</b>                        | <p><b><sup>1</sup>H-NMR: Isomer A:</b> 9.88 (s, 1H, OH), 7.47(s, 1H, CH=N), 6.28 (s, 2H, H6+H3) 4.80 (s, 2H, H<sub>a</sub>+H<sub>b</sub>), 4.29 (s, 2H, H<sub>c</sub>+H<sub>d</sub>), 3.39 (s, 5H, 2xH<sub>e</sub>+2xH<sub>f</sub>+H<sub>g</sub>).</p> <p><b>Isomer B:</b> 10.2 (s, 1H, NH), 9.88(s, 1H, OH), 6.67(s, 1H, CH=C), 6.28 (s, 2H, H6+H3) 4.80 (s, 2H, H<sub>a</sub>+H<sub>b</sub>), 4.29 (s, 2H, H<sub>c</sub>+H<sub>d</sub>), 3.39 (s, 5H, 2xH<sub>e</sub>+2xH<sub>f</sub>+H<sub>g</sub>).</p> <p><b><sup>13</sup>C-NMR:</b> 68.25 (2xC<sub>e</sub>), 69.67 (2xC<sub>f</sub>), 69.67 (C<sub>g</sub>), 69.79 (C<sub>b</sub>), 69.93 (C<sub>c</sub>), 70.11 (C<sub>d</sub>), 73.45(C<sub>h</sub>), 79.88 (C<sub>a</sub>), 111.73 (C3), 113.63 (C6), 120.76 (C4), 133.16 (C5), 142.07 (C1), 145.44 (C2), 193.85 (N=CH).</p>   |
| <b>H<sub>2</sub>L<sub>3</sub></b> | <p><b><sup>1</sup>H-NMR:</b> 13.9 (s, br 1H, H1' (OH) ), 9.6 (s, 1H, H2 (OH)), 9.0 (s,1H, N=CH), 7.71 (d,1H, J=2.4, H3'), 7.40 (d, 1H, J=8.8, H5'), 7.39 (d ,1H, J=8.8, H6'), 7.17 (s, 1H, H6), 6.96 (d, J=9.25, 1H, H3) 6.84 (d, J=8.8, 1H, H4), 2.40 (s, 3H, CH<sub>3</sub>).</p> <p><b><sup>13</sup>C-NMR:</b> 20.64 (CH<sub>3</sub>), 116.90 (C4) 119. 18 (C5), 119.24 (C3), 120.09 (C6), 121.17 (C1), 122.48 (C2), 131.31 (C5'), 132.68 (C6'), 132.76(C4'), 134.41(C2'), 149.50(C3'), 160.07 (C1'), 160.11 (N=CH).</p>   |
| <b>H<sub>2</sub>L<sub>4</sub></b> | <p><b><sup>1</sup>H-NMR: Enol isomer (ratio 2/3):</b> 12.62 (s, 1H, OH1'), 10.28 (s,br, 1H, OH1), 8.98 (s, 1H, N=CH), 7.66 (s, 1H, H3'), 7.54 (d, 1H, J=2.9, H6), 7.52 (d, 1H, J=2.9, H3), 7.47 (d, 1H, J=8.8, H6'), 7.02 (dd, 1H, J=8.8 2.0, H5').<b><sup>13</sup>C-NMR:</b> 111.63 (C4), 113. 61(C6), 116.22 (C3), 119.27 (C2), 119.97 (C1), 122.77 (C5), 131.29 (C5'), 133.19 (C6'), 136.12 (C4'), 145.34 (C2'), 150.67(C3'), 159.91 (C1'), 190.15 (N=CH).</p> <p><b><sup>1</sup>H-NMR: Keto isomer (ratio: 1/3):</b> 10.89 (s,br, 1H, OH1), 10.22 (s, 1H, NH), 7.79 (d, 1H, N-CH, J=2.9), 7.59 (s, 1H, H6), 7.58 (d, 1H, J=2.9, H3), 7.46 (1H, d, J=8.8, H6'), 7.02 (dd, 1H, J=8.8 2.0, H5'), 6.69 (s,1H, H3'). <b><sup>13</sup>C-NMR:</b> 111.69 (C4), 113.67 (C6), 116.22(C3), 119.33(C2), 120.70 (C1), 122.81 (C5), 133.19 (C5'), 134.03(C6'), 136.17 (C4'), 145.42 (C2'), 159.54 (C3'), 164.19 (C1'), 190.21 (N=CH). <b>After D<sub>2</sub>O exchange:</b> 9.85 s,br (NH, keto form), 8.61 s,br (CH, enol form). The signals at 12.62, 10.89, 10.28 ppm are removed. The all aromatic protons</p> |

|                        |  |
|------------------------|--|
|                        | change to broad signals.   |
| <b>L<sub>5</sub></b>   | <b><sup>1</sup>H-NMR:</b> 12.18 (s, br, 1H, NH), 7.32 (s, br, 1H, H <sub>4</sub> ), 7.22 (s, br, 1H, H <sub>7</sub> ), 6.94 (s, br, 1H, H <sub>6</sub> ), 5.00 (s, 1H, H <sub>a</sub> ), 4.44 (s, 1H, H <sub>b</sub> ), 4.29 (s, 1H, H <sub>c</sub> ), 4.22 (s, 1H, H <sub>d</sub> ), 4.08 (s, 5H, 2xH <sub>e</sub> +2xH <sub>f</sub> +H <sub>g</sub> ), 2.39 (s, 3H, CH <sub>3</sub> ).   |
| <b>L<sub>6</sub></b>   | <b><sup>1</sup>H-NMR:</b> 12.08 (s, br, 1H, NH), 7.25 (s, 2H, H <sub>4</sub> +H <sub>7</sub> ), 4.99 (s, 2H, H <sub>a</sub> +H <sub>d</sub> ), 4.43 (s, 2H, H <sub>b</sub> +H <sub>c</sub> ), 4.07 (s, 5H, 2H <sub>e</sub> +2H <sub>f</sub> +H <sub>g</sub> ), 2.29 (s, 6H, 2xCH <sub>3</sub> ).   |
| <b>L<sub>7</sub></b>   | <b><sup>1</sup>H-NMR:</b> 13.34 (s, br, 1H, NH), 8.18 (s, 1H, H <sub>7</sub> ), 7.73 (s, 1H, H <sub>4</sub> ), 6.56 (s, 1H, H <sub>d</sub> ), 5.10 (s, 1H, H <sub>a</sub> ), 4.57 (s, 1H, H <sub>c</sub> ), 4.13 (s, 6H, 2H <sub>e</sub> +2H <sub>f</sub> +1H <sub>g</sub> +H <sub>b</sub> ).  |
| <b>HL<sub>8</sub></b>  | <b><sup>1</sup>H-NMR:</b> 13.2(s, br, 1H, NH), 10.22(s, 1H, (OH)), 8.12(s, 1H, H <sub>3'</sub> ), 7.58(d, 1H, J=8.3, H <sub>5'</sub> ), 7.4(s, 1H, H <sub>4</sub> ), 7.30 (d, 1H, J=8.8, H <sub>6'</sub> ), 7.19 (d, 1H, J=7.8, H <sub>6</sub> ), 7.14(d, J=8.8, 1H, H <sub>7</sub> ), 2.46(s, 3H, CH <sub>3</sub> ).<br><b><sup>13</sup>C-NMR:</b> 157.01 (C <sub>2</sub> ), 150.38 (C <sub>1'</sub> ), 131.54 (C <sub>5</sub> ), 131.44 (C <sub>8</sub> +C <sub>9</sub> ), 125.87 (C <sub>5'</sub> ), 125.83 (C <sub>3'</sub> ), 125.06 (C <sub>4'</sub> ), 123.14 (C <sub>6</sub> ), 119.45 (C <sub>2'</sub> ), 119.38 (C <sub>6'</sub> ), 114.50 (C <sub>4</sub> +C <sub>7</sub> ), 21.75 (CH <sub>3</sub> ).  |
| <b>HL<sub>9</sub></b>  | <b><sup>1</sup>H-NMR:</b> 13.36 (s, br, 1H, NH), 13.04 (s, br, 1H, (OH)), 8.12 (d, 1H, J=2.4, H <sub>3'</sub> ), 7.39 (d, 1H, J=8.3, H <sub>5'</sub> ), 7.36 (1H, d, J=8.8, H <sub>6'</sub> ), 7.05 (s, 1H, H <sub>4</sub> ), 7.03 (s, 1H, H <sub>7</sub> ), 2.49 (s, 6H, 2xCH <sub>3</sub> ).<br><b><sup>13</sup>C-NMR:</b> 20.42 (2xCH <sub>3</sub> ), 114.65 (C <sub>4</sub> +C <sub>7</sub> ), 119.36 (C <sub>6'</sub> ), 119.43 (C <sub>2'</sub> ), 123.09 (C <sub>4'</sub> ), 125.65 (C <sub>3'</sub> ), 125.69 (C <sub>5</sub> +C <sub>6</sub> ), 131.25 (C <sub>5'</sub> ), 131.30 (C <sub>8</sub> +C <sub>9</sub> ), 149.92 (C <sub>1'</sub> ), 157.06 (C <sub>2</sub> ).   |
| <b>HL<sub>10</sub></b> | <b>Isomer A (ratio: 2/3):</b> 12.20 (s, br, 1H, NH), 10.94 (s, br, 1H, OH), 8.87 (s, 1H, H <sub>7</sub> ), 8.09 (s, 1H, H <sub>4</sub> ), 7.91 (s, 1H, H <sub>3'</sub> ), 7.38 (d, 1H, J=8.8, H <sub>5'</sub> ), 6.97 (d, 1H, J=8.8, H <sub>6'</sub> ).<br><b>Isomer B (ratio: 1/3):</b> 11.40 (s, 1H, NH), 10.20 (s, 1H, OH), 8.32 (s, 1H, H <sub>7</sub> ), 7.94 (s, 1H, H <sub>4</sub> ), 7.86 (s, 1H, H <sub>3'</sub> ), 7.04 (d, 1H, J=8.3, H <sub>5'</sub> ), 6.84 (d, br, 1H, H <sub>6'</sub> ).<br><b><sup>13</sup>C-NMR:</b> 159.65 (C <sub>2</sub> , isomer A), 159.52 (C <sub>2</sub> , isomer B), 158.32 (C <sub>1'</sub> , isomer A), 156.63 (C <sub>1'</sub> , isomer B), 153.90, 149.77, 143.31, 143.02, 140.13, 134.33, 133.71, 132.27, 129.86, 127.42, 127.29, 123.61, 122.48, 119.77, 119.31, 117.52, 115.24, 114.50, 113.86 |

s, singlet; br, broad; dd, doublet of doublet.



**Figure 3.21:**  $^1\text{H-NMR}$  spectrum of **HL**<sub>1</sub>.



**Figure 3.22:**  $^{13}\text{C-NMR}$  spectrum of **HL**<sub>1</sub>.

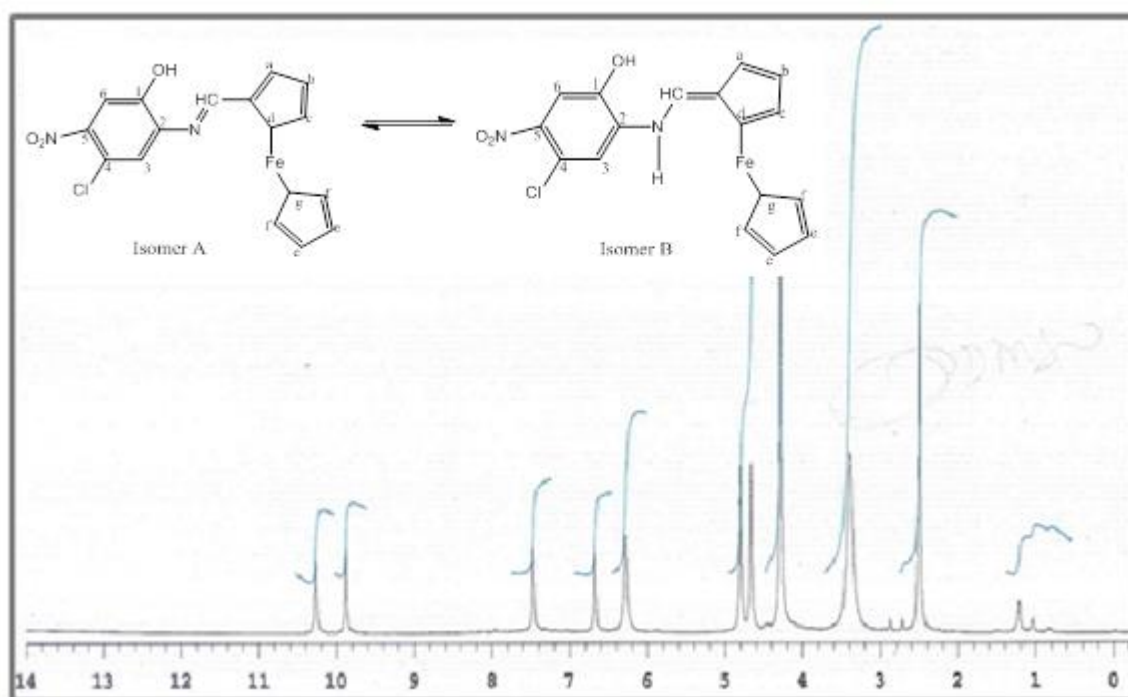


Figure 3.23:  $^1\text{H-NMR}$  spectrum of  $\text{HL}_2$ .

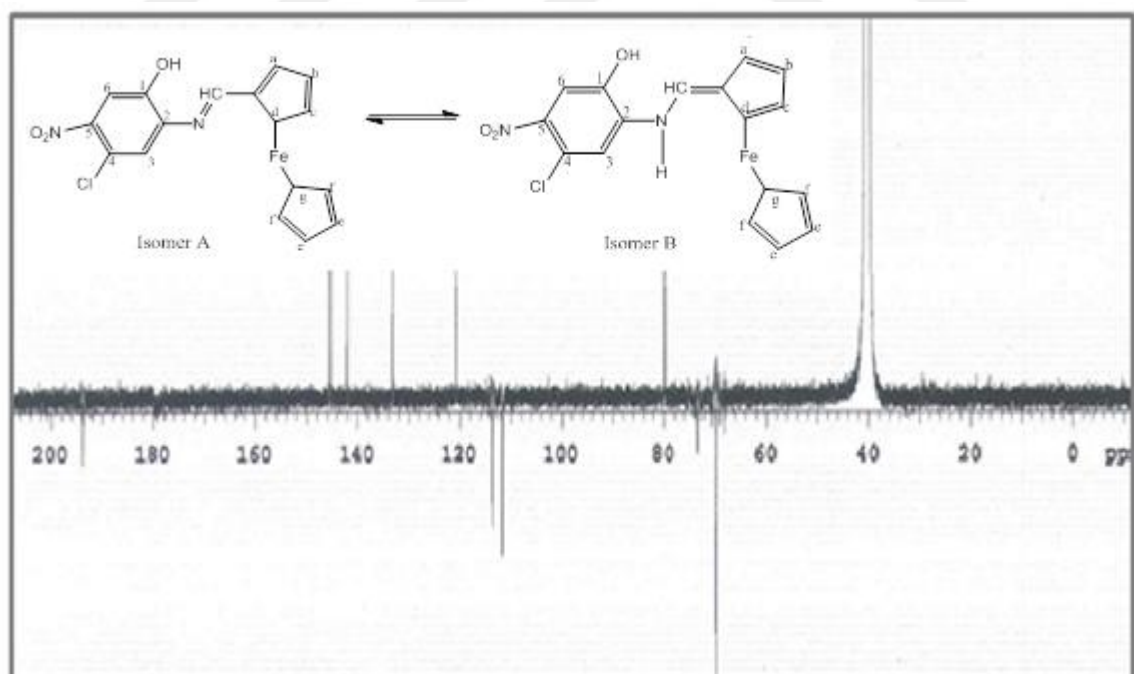


Figure 3.24:  $^{13}\text{C-NMR}$  spectrum of  $\text{HL}_2$ .

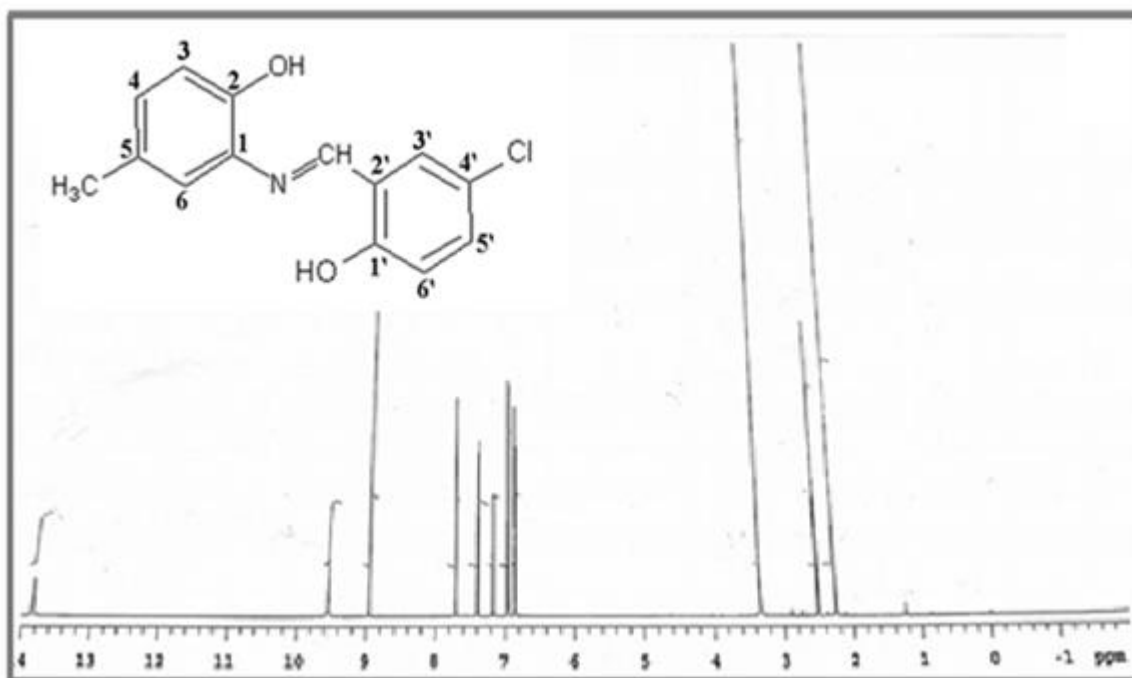


Figure 3.25:  $^1H$ -NMR spectrum of  $H_2L_3$ .

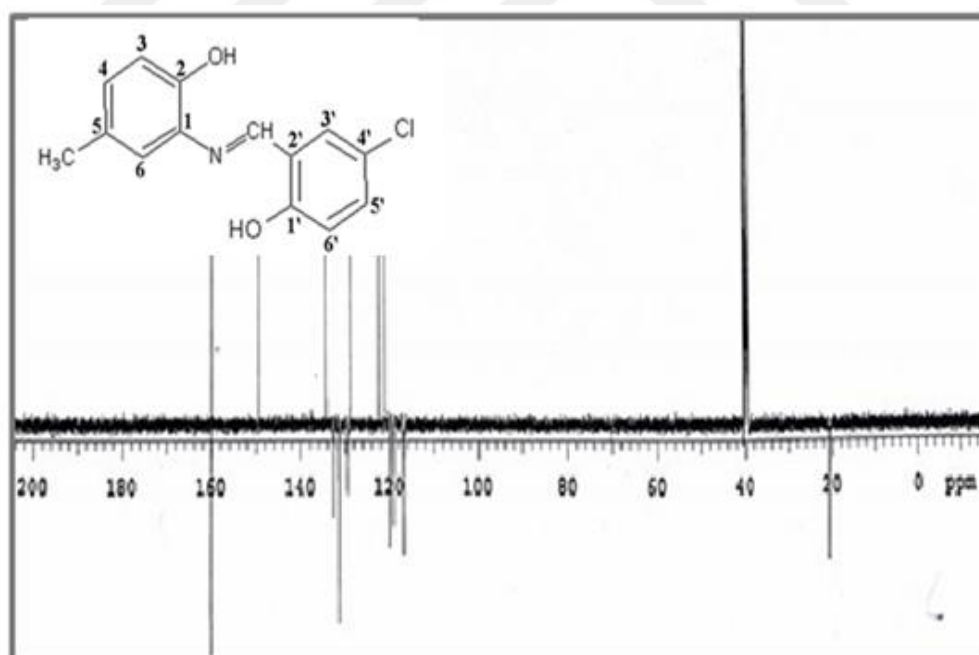


Figure 3.26:  $^{13}C$ -NMR spectrum of  $H_2L_3$ .

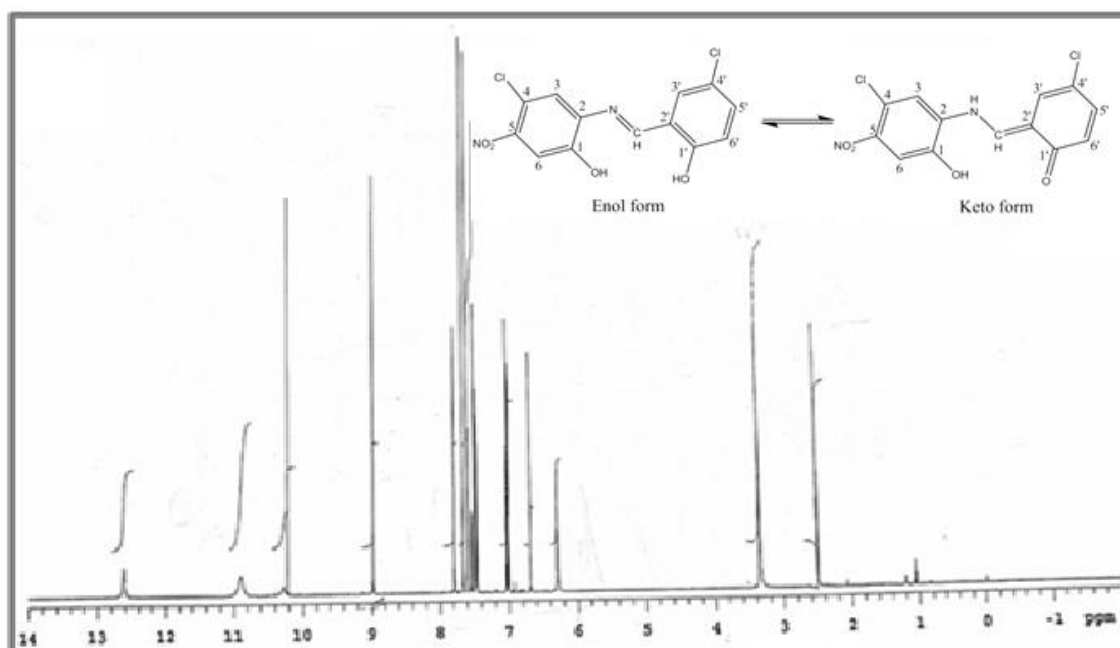


Figure 3.27:  $^1\text{H-NMR}$  spectrum of  $\text{H}_2\text{L}_4$ .

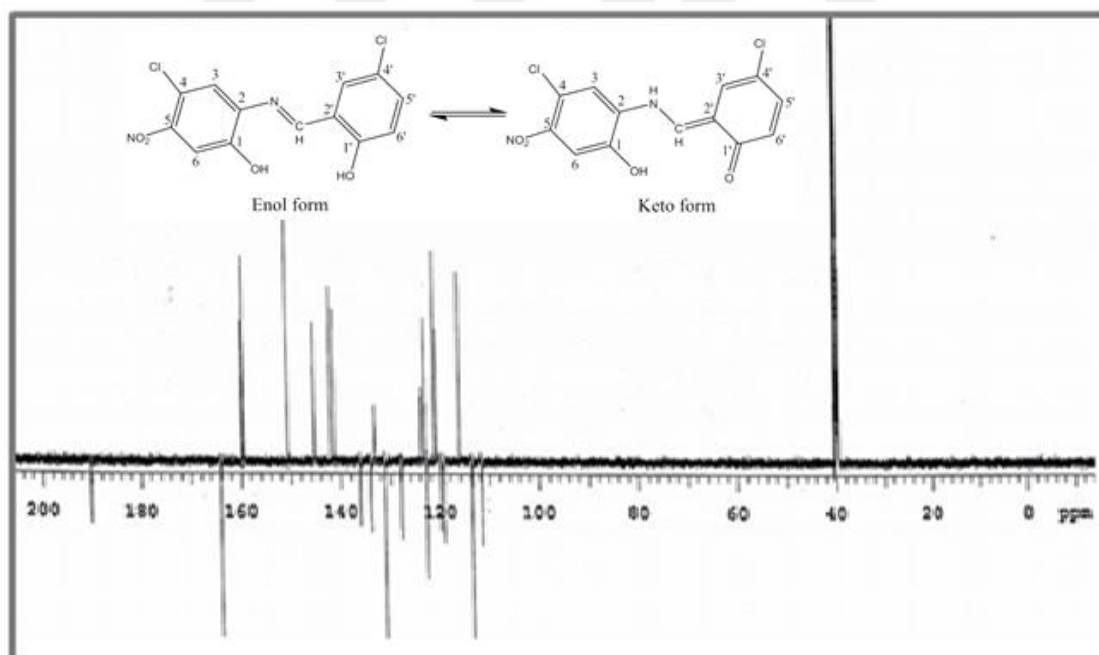


Figure 3.28:  $^{13}\text{C-NMR}$  spectrum of  $\text{H}_2\text{L}_4$ .

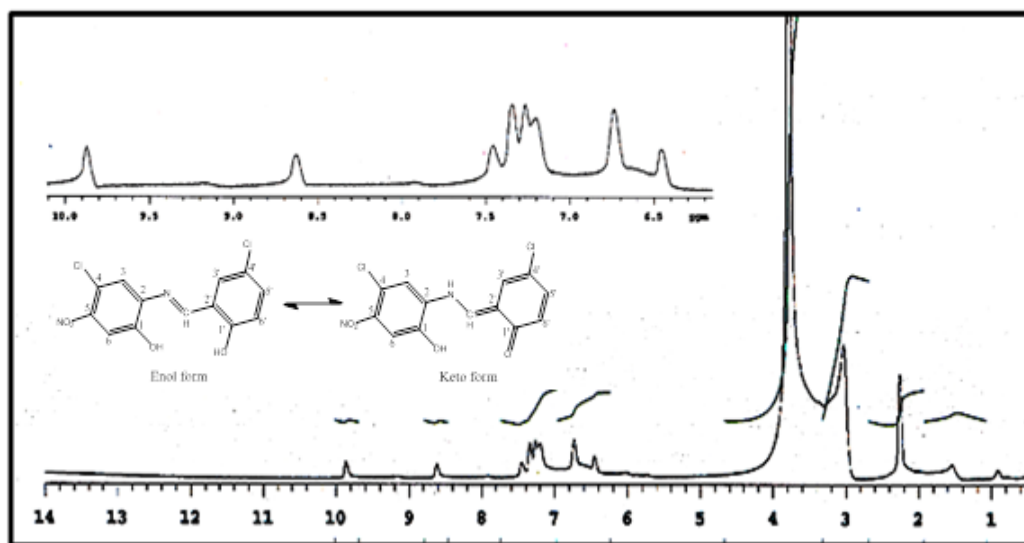


Figure 3.29:  $^1\text{H-NMR}$  ( $\text{D}_2\text{O}$ ) spectrum of  $\text{H}_2\text{L}_4$ .

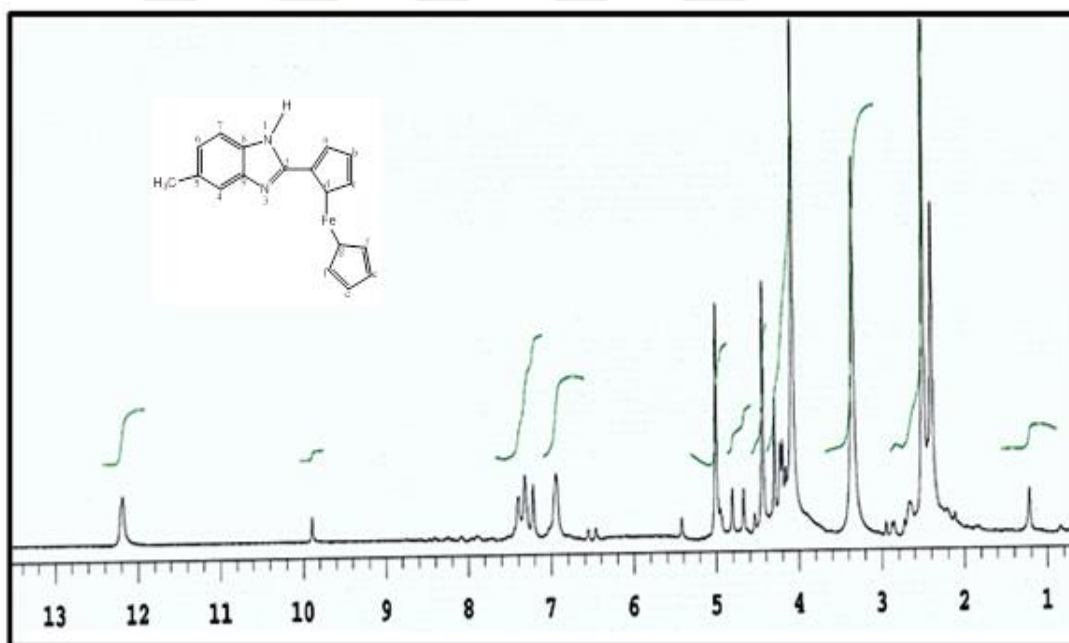


Figure 3.30:  $^1\text{H-NMR}$  spectrum of  $\text{L}_5$ .

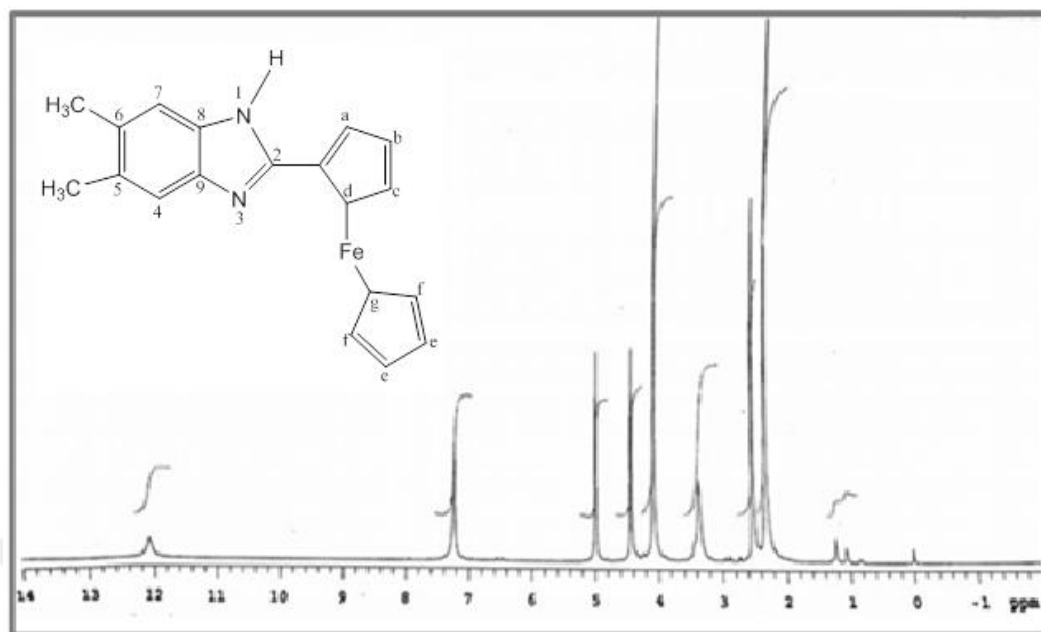


Figure 3.31: <sup>1</sup>H-NMR spectrum of L<sub>6</sub>.

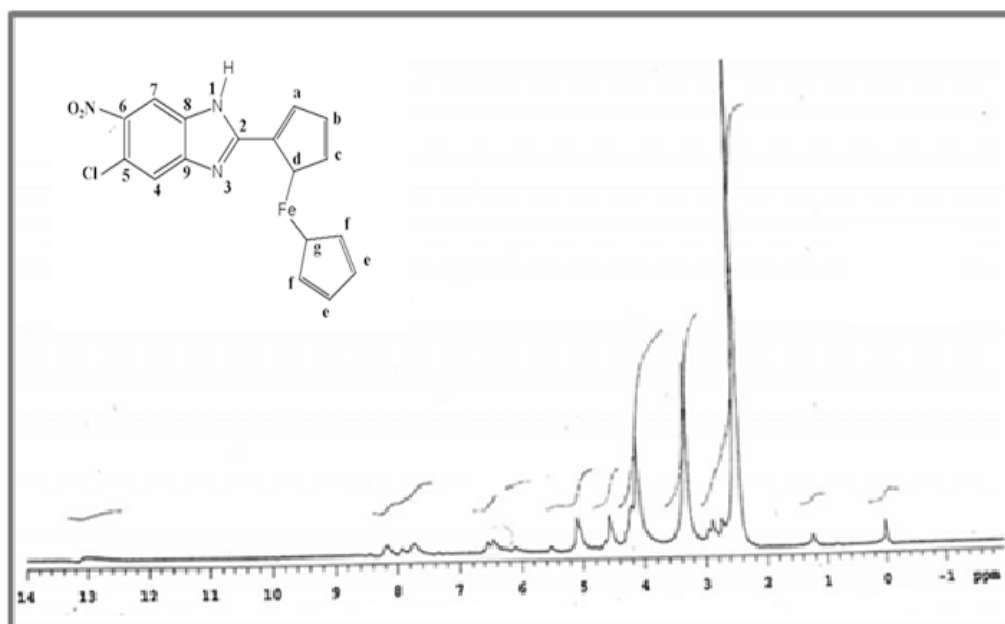


Figure 3.32: <sup>1</sup>H-NMR spectrum of L<sub>7</sub>.



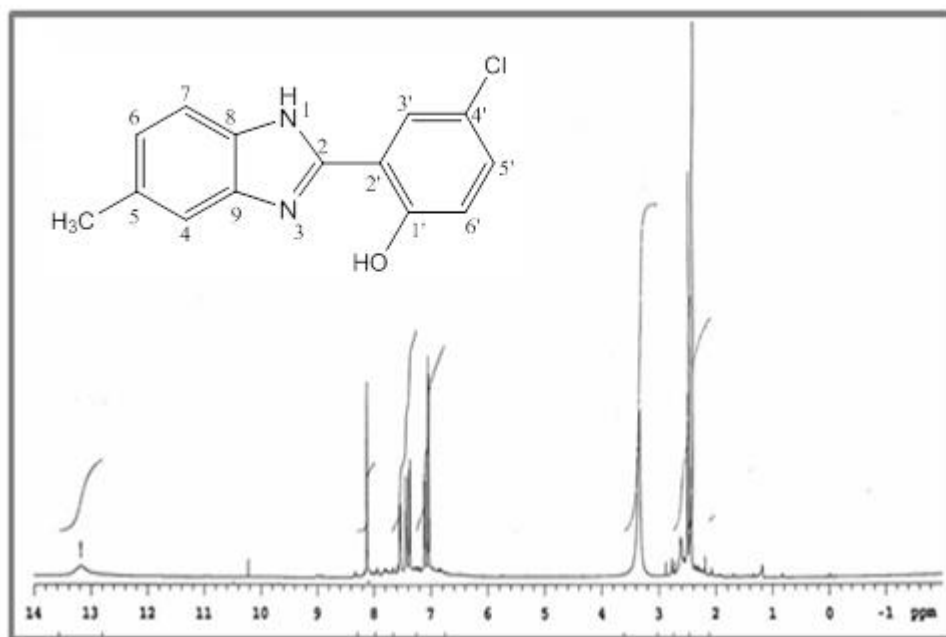


Figure 3.33: <sup>1</sup>H-NMR spectrum of **HL<sub>8</sub>**.

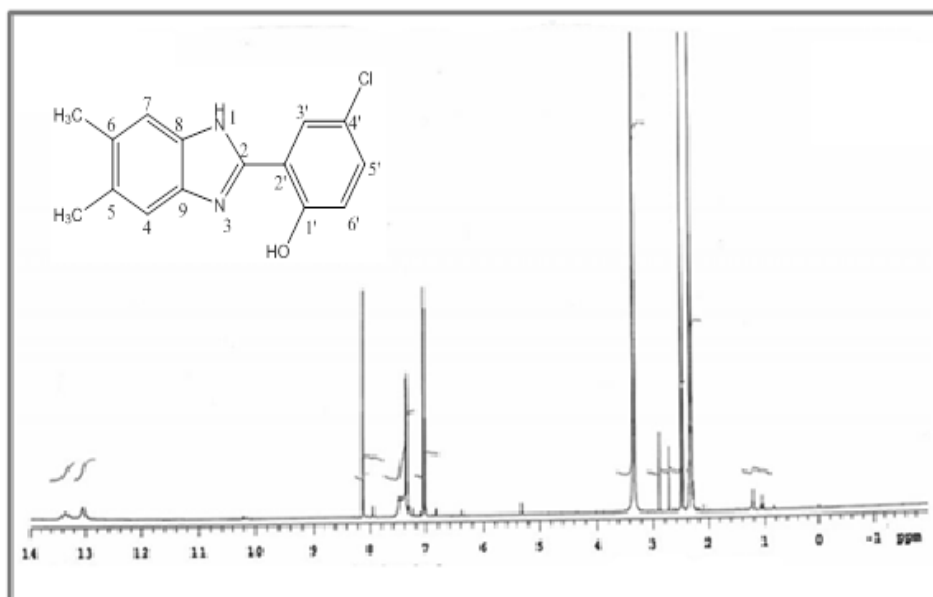


Figure 3.34: <sup>1</sup>H-NMR spectrum of **HL<sub>9</sub>**.

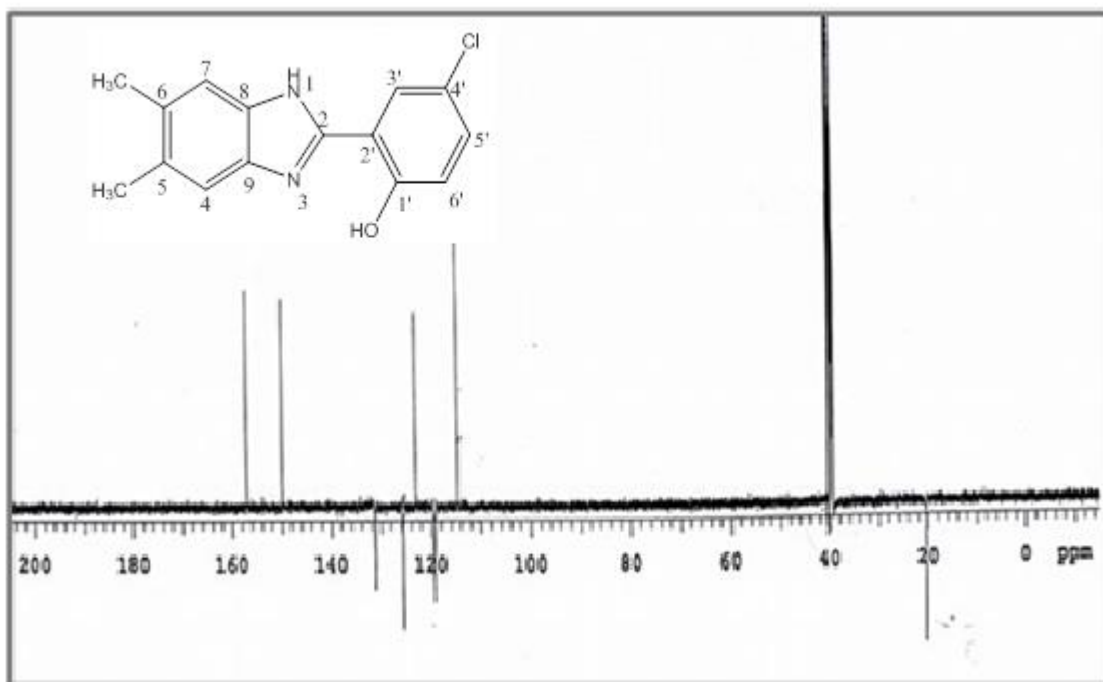


Figure 3.35:  $^{13}\text{C}$ -NMR spectrum of **HL<sub>9</sub>**.

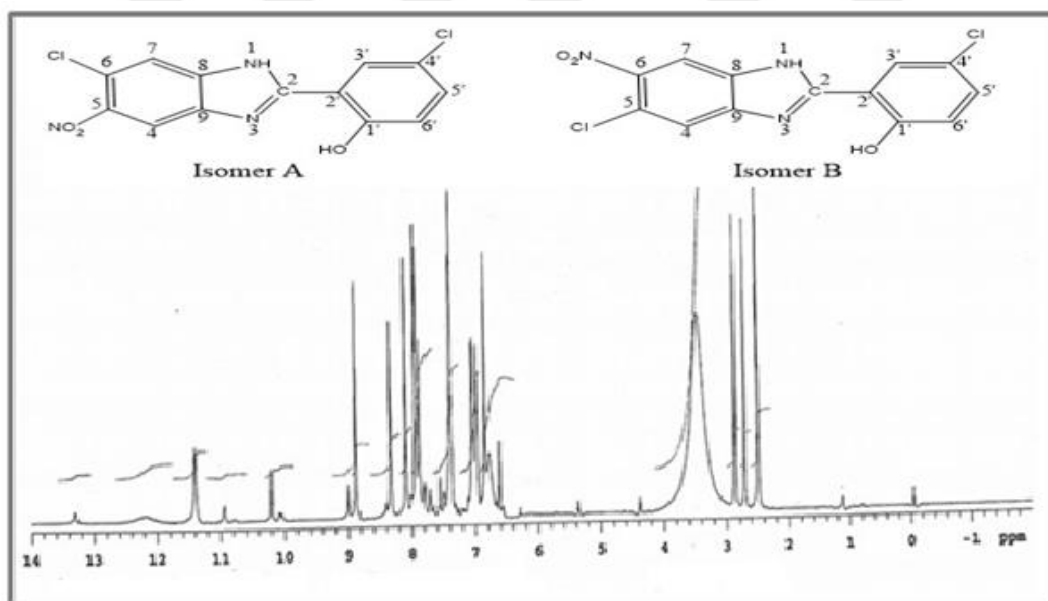
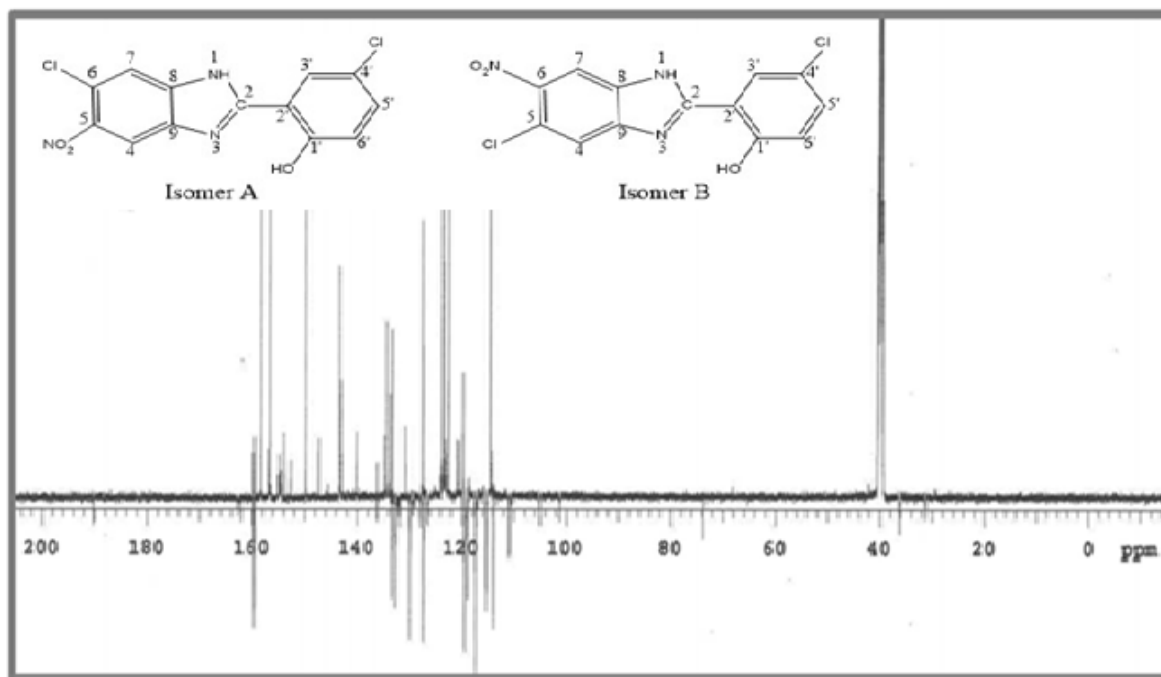


Figure 3.36:  $^1\text{H}$ -NMR spectrum of **HL<sub>10</sub>**.



**Figure 3.37:**  $^{13}\text{C}$ -NMR spectrum of **HL**<sub>10</sub>.

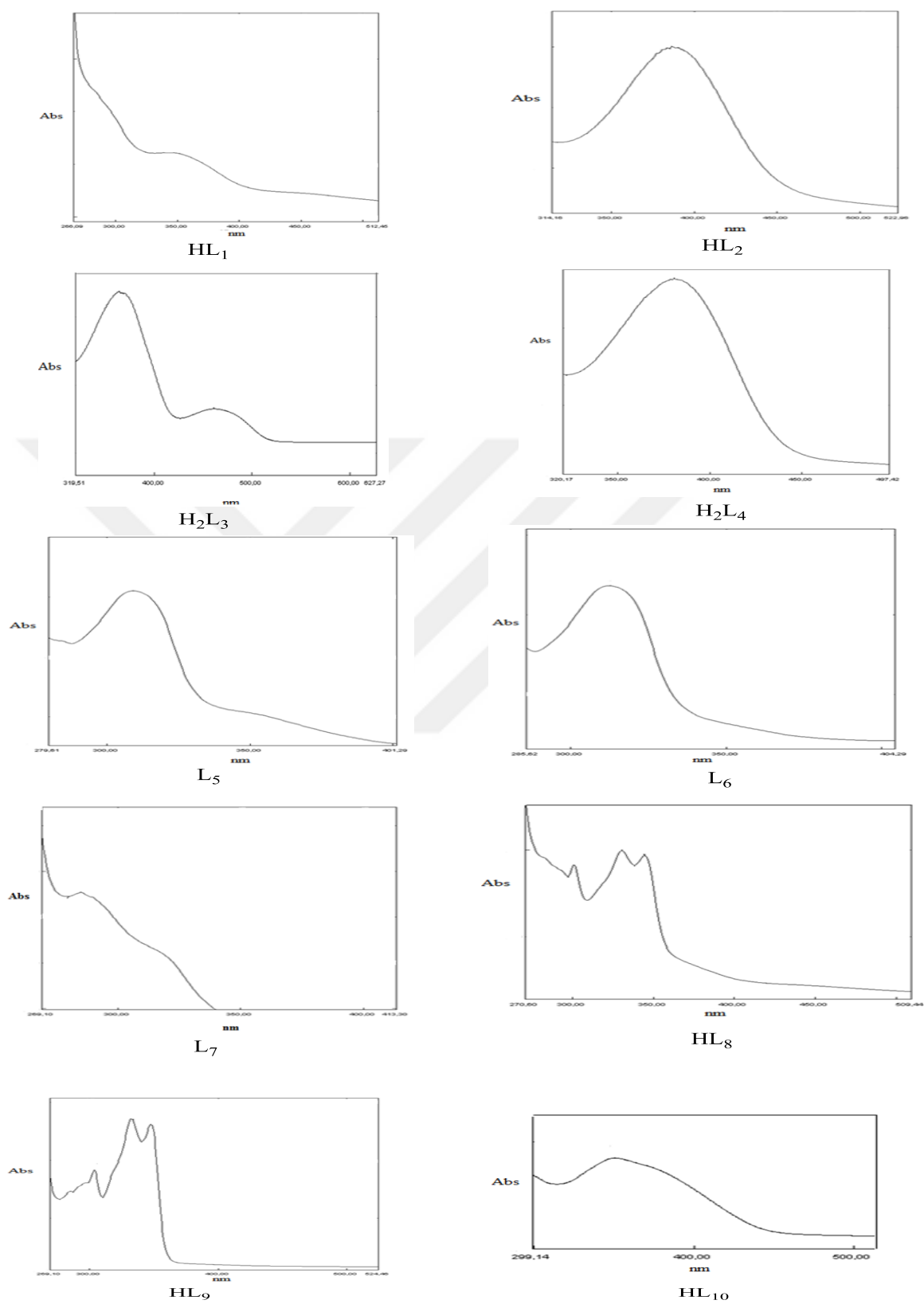
### 3.1.5. UV-Visible Spectroscopy

The electronic (UV-Visible) spectral data were recorded in methanol and given in Table 3.5 and Figure 3.38.

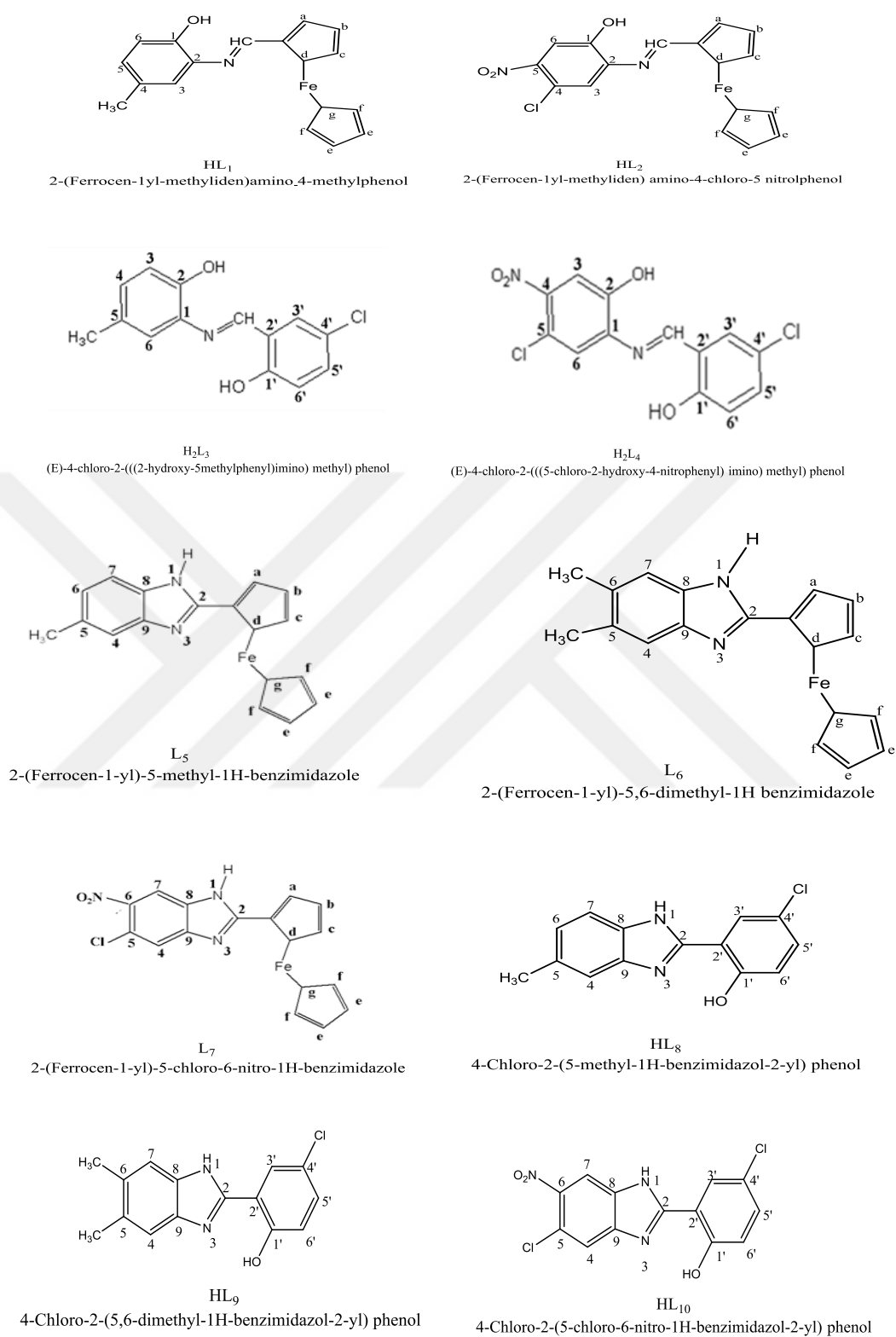
**Table 3.5:** Electronic spectral data of the ligands.

| Compounds (ID)                | Wavelength ( $\lambda_{\max}$ , nm) |
|-------------------------------|-------------------------------------|
| HL <sub>1</sub>               | 343.0m,br, 350.5sh                  |
| HL <sub>2</sub>               | 386.0s,br, 400.0sh                  |
| H <sub>2</sub> L <sub>3</sub> | 363.5m,br, 461.0sh, 485.5m,br       |
| H <sub>2</sub> L <sub>4</sub> | 380.0m,br, 403.0sh                  |
| L <sub>5</sub>                | 309.0m,br, 320.0sh                  |
| L <sub>6</sub>                | 312.0m, 319.5sh                     |
| L <sub>7</sub>                | 285.0m, 300.0sh                     |
| HL <sub>8</sub>               | 301.0 m, 330.0sh, 344.5sh           |
| HL <sub>9</sub>               | 285.0sh, 303.5m, 332.0m, 349.5sh    |
| HL <sub>10</sub>              | 336.5m,br, 372.5sh                  |

s = strong, m = medium, br = broad, sh = shoulder.



**Figure 3.38:** Electronic spectra of the ligands.



**Figure 3.39:** Structure of the ligands.

### 3.2. CHARACTERIZATIONS OF THE METAL COMPLEXES

The analytical data of the  $\text{Co}^{2+}$ ,  $\text{Cu}^{2+}$ ,  $\text{Pd}^{2+}$ ,  $\text{Zn}^{2+}$  and  $\text{Pt}^{2+}$  complexes of the ligands are presented in Table 3.6, 3.7, 3.8, 3.9 and 3.10, respectively. The analytical information of these complexes is in contract good with the calculated values and thus confirming the proposed composition for all the complexes.

#### 3.2.1. Elemental analysis

**Table 3.6:** Analytical data and physical properties of the Co(II) complexes.

| Complex ID   | Formula weight  | Color, yield % | M.P* °C | Element analysis Found (calc)% |                |                 |
|--|---|----------------|---------|--------------------------------|----------------|-----------------|
|  |   |                |         | C                              | H              | N               |
| <b>HL<sub>1</sub></b><br>[Co( <b>HL</b> <sub>1</sub> )Cl <sub>2</sub> (H <sub>2</sub> O) <sub>2</sub> ]·H <sub>2</sub> O             | C <sub>18</sub> H <sub>22</sub> Cl <sub>2</sub> CoFeNO <sub>4</sub>                             | Black<br>75    | 320     | 42.20<br>(43.06)               | 3.46<br>(4.42) | 2.93<br>(2.79)  |
| <b>HL<sub>2</sub></b><br>[Co( <b>HL</b> <sub>2</sub> ) <sub>2</sub> Cl <sub>2</sub> ]·H <sub>2</sub> O                               | C <sub>34</sub> H <sub>28</sub> Cl <sub>4</sub> CoFe <sub>2</sub> N <sub>4</sub> O <sub>7</sub> | Black<br>56    | 300     | 45.01<br>(44.53)               | 3.41<br>(3.08) | 5.81<br>(6.11)  |
| <b>H<sub>2</sub>L<sub>3</sub></b><br>[Co( <b>HL</b> <sub>3</sub> ) <sub>2</sub> ]·3H <sub>2</sub> O                                  | C <sub>28</sub> H <sub>22</sub> Cl <sub>2</sub> CoN <sub>2</sub> O <sub>4</sub>                 | Brownish<br>69 | 300     | 52.16<br>(53.01)               | 3.26<br>(4.45) | 4.00<br>(4.42)  |
| <b>H<sub>2</sub>L<sub>4</sub></b><br>[Co( <b>H<sub>2</sub>L</b> <sub>4</sub> )Cl <sub>2</sub> (H <sub>2</sub> O)]·2H <sub>2</sub> O  | C <sub>13</sub> H <sub>14</sub> Cl <sub>4</sub> CoN <sub>2</sub> O <sub>7</sub>                 | Reddish,<br>82 | 221     | 30.77<br>(30.56)               | 3.12<br>(2.76) | 5.58<br>(5.48)  |
| <b>L<sub>5</sub></b><br>[Co( <b>L</b> <sub>5</sub> )Cl <sub>2</sub> (H <sub>2</sub> O) <sub>3</sub> ]                                | C <sub>18</sub> H <sub>22</sub> Cl <sub>2</sub> CoFeN <sub>2</sub> O <sub>3</sub>               | Brownish<br>75 | 320     | 41.20<br>(43.23)               | 3.46<br>(4.43) | 6.93<br>(5.60)  |
| <b>L<sub>6</sub></b><br>[Co( <b>L</b> <sub>6</sub> )Cl <sub>2</sub> (H <sub>2</sub> O) <sub>3</sub> ]·3H <sub>2</sub> O              | C <sub>19</sub> H <sub>30</sub> Cl <sub>2</sub> CoFeN <sub>2</sub> O <sub>6</sub>               | Brownish<br>70 | 300     | 37.86<br>(40.17)               | 4.65<br>(5.32) | 3.92<br>(4.93)  |
| <b>L<sub>7</sub></b><br>[Co( <b>L</b> <sub>7</sub> ) <sub>2</sub> Cl <sub>2</sub> (H <sub>2</sub> O) <sub>2</sub> ]·H <sub>2</sub> O | C <sub>34</sub> H <sub>30</sub> Cl <sub>4</sub> CoFe <sub>2</sub> N <sub>6</sub> O <sub>7</sub> | Brownish<br>80 | 321     | 43.56<br>(43.12)               | 4.02<br>(3.19) | 6.41<br>(8.87)  |
| <b>HL<sub>8</sub></b><br>[Co( <b>HL</b> <sub>8</sub> )Cl <sub>2</sub> (H <sub>2</sub> O) <sub>2</sub> ]·2H <sub>2</sub> O            | C <sub>14</sub> H <sub>19</sub> Cl <sub>3</sub> CoN <sub>2</sub> O <sub>5</sub>                 | Black<br>87    | 232     | 35.31<br>(36.51)               | 3.66<br>(4.16) | 5.99<br>(6.08)  |
| <b>HL<sub>9</sub></b><br>[Co( <b>HL</b> <sub>9</sub> )( <b>L</b> <sub>9</sub> )Cl(H <sub>2</sub> O)]·2H <sub>2</sub> O               | C <sub>30</sub> H <sub>32</sub> Cl <sub>3</sub> CoN <sub>4</sub> O <sub>5</sub>                 | Blue<br>64     | 337     | 51.55<br>(51.93)               | 4.29<br>(4.65) | 7.56<br>(8.07)  |
| <b>HL<sub>10</sub></b><br>[Co( <b>HL</b> <sub>10</sub> ) <sub>2</sub> Cl <sub>2</sub> ]·2H <sub>2</sub> O                            | C <sub>26</sub> H <sub>18</sub> Cl <sub>6</sub> CoN <sub>6</sub> O <sub>8</sub>                 | Brownish<br>62 | 289     | 38.57<br>(38.36)               | 2.32<br>(2.23) | 9.85<br>(10.32) |

\*M.p (decomposition)

**Table 3.7:** Analytical data and physical properties of the Cu(II) complexes.

| Complex ID   | Formula weight  | Color ,<br>yield % | M.P.*<br>°C | Element analysis<br>Found (calc)% |                |                |
|--|---|--------------------|-------------|-----------------------------------|----------------|----------------|
|  |   |                    |             | C                                 | H              | N              |
| <b>HL<sub>1</sub></b><br>[Cu( <b>HL</b> <sub>1</sub> )Cl <sub>2</sub> ]·H <sub>2</sub> O                                   | C <sub>18</sub> H <sub>21</sub> Cl <sub>2</sub> CuFeNO <sub>3</sub>               | Black<br>77        | 231         | 44.68<br>(44.66)                  | 3.60<br>(3.78) | 1.37<br>(2.86) |
| <b>HL<sub>2</sub></b><br>[Cu( <b>L</b> <sub>2</sub> )Cl(H <sub>2</sub> O)]   | C <sub>17</sub> H <sub>14</sub> Cl <sub>2</sub> CuFeN <sub>2</sub> O <sub>4</sub> | Black<br>80        | 247         | 40.38<br>(40.79)                  | 2.73<br>(2.82) | 5.82<br>(5.60) |
| <b>H<sub>2</sub>L<sub>3</sub></b><br>[Cu( <b>H<sub>2</sub>L</b> <sub>3</sub> )Cl]Cl·3H <sub>2</sub> O                      | C <sub>14</sub> H <sub>16</sub> Cl <sub>3</sub> CuNO <sub>4</sub>                 | Black<br>88        | 235         | 39.72<br>(38.91)                  | 3.37<br>(3.73) | 2.40<br>(3.24) |
| <b>H<sub>2</sub>L<sub>4</sub></b><br>[Cu( <b>H<sub>2</sub>L</b> <sub>4</sub> )Cl <sub>2</sub> (H <sub>2</sub> O)]          | C <sub>13</sub> H <sub>10</sub> Cl <sub>4</sub> CuN <sub>2</sub> O <sub>5</sub>   | Reddish<br>84      | 220         | 32.98<br>(32.56)                  | 2.13<br>(2.10) | 5.73<br>(5.84) |
| <b>L<sub>5</sub></b><br>[Cu( <b>L</b> <sub>5</sub> )Cl <sub>2</sub> (H <sub>2</sub> O)]·H <sub>2</sub> O                   | C <sub>18</sub> H <sub>20</sub> Cl <sub>2</sub> CuFeN <sub>2</sub> O <sub>2</sub> | Brownish<br>73     | 310         | 44.68<br>(44.42)                  | 3.45<br>(4.14) | 6.93<br>(5.76) |
| <b>L<sub>6</sub></b><br>[Cu( <b>L</b> <sub>6</sub> )Cl <sub>2</sub> (H <sub>2</sub> O)]·2H <sub>2</sub> O                  | C <sub>19</sub> H <sub>24</sub> Cl <sub>2</sub> CuFeN <sub>2</sub> O <sub>3</sub> | Brownish<br>83     | 251         | 43.01<br>(44.00)                  | 3.75<br>(4.66) | 5.48<br>(5.40) |
| <b>L<sub>7</sub></b><br>[Cu( <b>L</b> <sub>7</sub> )Cl <sub>2</sub> (EtOH)]  | C <sub>19</sub> H <sub>18</sub> Cl <sub>3</sub> CuFeN <sub>3</sub> O <sub>3</sub> | Brownish<br>84     | 231         | 40.90<br>(40.60)                  | 2.35<br>(3.23) | 7.53<br>(7.48) |
| <b>HL<sub>8</sub></b><br>[Cu( <b>L</b> <sub>8</sub> )Cl(H <sub>2</sub> O)]   | C <sub>14</sub> H <sub>12</sub> Cl <sub>2</sub> CuN <sub>2</sub> O <sub>2</sub>   | Black<br>86        | 286         | 44.96<br>(44.87)                  | 2.85<br>(3.23) | 7.24<br>(7.48) |
| <b>HL<sub>9</sub></b><br>[Cu( <b>L</b> <sub>9</sub> )Cl(H <sub>2</sub> O)]   | C <sub>15</sub> H <sub>14</sub> Cl <sub>2</sub> CuN <sub>2</sub> O <sub>2</sub>   | Brownish<br>57     | 313         | 48.80<br>(48.68)                  | 3.17<br>(4.09) | 7.02<br>(7.10) |
| <b>HL<sub>10</sub></b><br>[Cu( <b>HL</b> <sub>10</sub> )Cl <sub>2</sub> (H <sub>2</sub> O) <sub>2</sub> ]·H <sub>2</sub> O | C <sub>13</sub> H <sub>13</sub> Cl <sub>4</sub> CuN <sub>3</sub> O <sub>6</sub>   | Brownish<br>85     | 320         | 30.58<br>(30.46)                  | 2.63<br>(2.56) | 7.85<br>(8.20) |

\*M.p (decomposition)



**Table 3.8:** Analytical data and physical properties of the Pd(II) complexes.

| Complex ID  | Formula weight   | Color,<br>yield % | M.P °C | Element analysis<br>Found (calc)% |                |                |
|---|--|-------------------|--------|-----------------------------------|----------------|----------------|
|   |  |                   |        | C                                 | H              | N              |
| <b>HL<sub>1</sub></b><br>[Pd( <b>L<sub>1</sub></b> )Cl(H <sub>2</sub> O)]                             | C <sub>18</sub> H <sub>18</sub> ClFeNO <sub>2</sub> Pd                             | Black<br>60       | 225    | 44.01<br>(45.22)                  | 3.16<br>(3.80) | 3.03<br>(2.93) |
| <b>HL<sub>2</sub></b><br>[Pd( <b>L<sub>2</sub></b> )Cl(H <sub>2</sub> O)]                             | C <sub>17</sub> H <sub>14</sub> Cl <sub>2</sub> FeN <sub>2</sub> O <sub>4</sub> Pd | Black<br>55       | 234    | 36.40<br>(37.57)                  | 2.16<br>(2.60) | 4.99<br>(5.15) |
| <b>H<sub>2</sub>L<sub>3</sub></b><br>[Pd( <b>L<sub>3</sub></b> )(H <sub>2</sub> O)]·3H <sub>2</sub> O | C <sub>14</sub> H <sub>18</sub> ClNO <sub>6</sub> Pd                               | Reddish<br>83     | 230    | 36.61<br>(38.86)                  | 3.76<br>(4.42) | 2.72<br>(3.20) |
| <b>H<sub>2</sub>L<sub>4</sub></b><br>[Pd( <b>H<sub>2</sub>L<sub>4</sub></b> )Cl]Cl·H <sub>2</sub> O   | C <sub>13</sub> H <sub>14</sub> Cl <sub>2</sub> N <sub>2</sub> O <sub>8</sub> Pd   | Reddish<br>80     | 260    | 29.99<br>(29.89)                  | 1.49<br>(1.93) | 4.87<br>(5.36) |
| <b>L<sub>5</sub></b><br>[Pd( <b>L<sub>5</sub></b> )Cl <sub>2</sub> (EtOH)]                            | C <sub>20</sub> H <sub>22</sub> Cl <sub>2</sub> FeN <sub>2</sub> OPd               | Brownish<br>69    | 300    | 44.01<br>(44.52)                  | 3.16<br>(4.11) | 6.65<br>(5.19) |
| <b>L<sub>6</sub></b><br>[Pd( <b>L<sub>6</sub></b> )Cl <sub>2</sub> (H <sub>2</sub> O)]                | C <sub>19</sub> H <sub>20</sub> Cl <sub>2</sub> FeN <sub>2</sub> OPd               | Brownish<br>84    | 240    | 43.40<br>(43.42)                  | 3.61<br>(3.84) | 5.05<br>(5.33) |
| <b>L<sub>7</sub></b><br>[Pd( <b>L<sub>7</sub></b> )Cl <sub>2</sub> (H <sub>2</sub> O)]                | C <sub>17</sub> H <sub>14</sub> Cl <sub>3</sub> FeN <sub>3</sub> O <sub>3</sub> Pd | Brownish<br>74    | 229    | 35.36<br>(35.39)                  | 2.33<br>(2.45) | 6.11<br>(7.28) |
| <b>HL<sub>8</sub></b><br>[Pd( <b>L<sub>8</sub></b> )Cl(EtOH)]   | C <sub>16</sub> H <sub>16</sub> Cl <sub>2</sub> N <sub>2</sub> O <sub>2</sub> Pd   | Brownish<br>77    | 260    | 42.37<br>(43.12)                  | 3.01<br>(3.62) | 6.38<br>(6.29) |
| <b>HL<sub>9</sub></b><br>[Pd( <b>HL<sub>9</sub></b> )Cl <sub>2</sub> ]                                | C <sub>15</sub> H <sub>14</sub> Cl <sub>2</sub> N <sub>2</sub> O <sub>2</sub> Pd   | Brownish<br>73    | 274    | 42.26<br>(41.74)                  | 3.06<br>(3.27) | 6.25<br>(6.49) |
| <b>HL<sub>10</sub></b><br>[Pd( <b>HL<sub>10</sub></b> )Cl <sub>2</sub> ]·H <sub>2</sub> O             | C <sub>13</sub> H <sub>9</sub> Cl <sub>4</sub> N <sub>3</sub> O <sub>4</sub> Pd    | Brownish<br>83    | 280    | 30.71<br>(30.06)                  | 1.17<br>(1.75) | 8.10<br>(8.09) |

\* M.p (decomposition)

**Table 3.9:** Analytical data and physical properties of the Zn(II) complexes.

| Complex ID  | Formula weight   | Color,<br>yield % | M.P.<br>* °C | Element analysis<br>Found (calc)% |                |                  |
|---|--|-------------------|--------------|-----------------------------------|----------------|------------------|
|   |  |                   |              | C                                 | H              | N                |
| <b>HL<sub>1</sub></b><br>[Zn(L <sub>1</sub> ) <sub>2</sub> ]·2H <sub>2</sub> O  | C <sub>36</sub> H <sub>36</sub> Fe <sub>2</sub> N <sub>2</sub> O <sub>4</sub> Zn                 | Black<br>65       | 221          | 58.23<br>(58.61)                  | 3.78<br>(4.92) | 1.43<br>(3.80)   |
| <b>HL<sub>2</sub></b><br>[Zn(L <sub>2</sub> ) <sub>2</sub> ]·2H <sub>2</sub> O  | C <sub>34</sub> H <sub>28</sub> Cl <sub>2</sub> Fe <sub>2</sub> N <sub>4</sub> O <sub>8</sub> Zn | Black<br>55       | 234          | 47.60<br>(47.01)                  | 3.96<br>(3.25) | 7.10<br>(6.45)   |
| <b>H<sub>2</sub>L<sub>3</sub></b><br>[Zn(HL <sub>3</sub> ) <sub>2</sub> ]·2H <sub>2</sub> O   | C <sub>28</sub> H <sub>26</sub> Cl <sub>2</sub> N <sub>2</sub> O <sub>6</sub> Zn                 | Yellowish<br>61   | 310          | 54.64<br>(54.00)                  | 4.97<br>(4.21) | 4.27<br>(4.50)   |
| <b>H<sub>2</sub>L<sub>4</sub></b><br>[Zn(H <sub>2</sub> L <sub>4</sub> )Cl <sub>2</sub> (H <sub>2</sub> O) <sub>2</sub> ]·3H <sub>2</sub> O | C <sub>13</sub> H <sub>18</sub> Cl <sub>4</sub> N <sub>2</sub> O <sub>9</sub> Zn                 | Orange<br>55      | 222          | 27.29<br>(28.21)                  | 3.47<br>(3.28) | 4.62<br>(5.06)   |
| <b>L<sub>5</sub></b><br>[Zn(L <sub>5</sub> )Cl <sub>2</sub> (H <sub>2</sub> O)]·H <sub>2</sub> O  | C <sub>18</sub> H <sub>20</sub> Cl <sub>2</sub> FeN <sub>2</sub> O <sub>2</sub> Zn               | Black<br>79       | 323          | 43.53<br>(44.26)                  | 3.85<br>(4.13) | 6.83<br>(5.73)   |
| <b>L<sub>6</sub></b><br>[Zn(L <sub>6</sub> ) <sub>2</sub> Cl <sub>2</sub> ]·H <sub>2</sub> O  | C <sub>38</sub> H <sub>38</sub> Cl <sub>2</sub> Fe <sub>2</sub> N <sub>4</sub> OZn               | Brownish<br>60    | 232          | 55.74<br>(56.02)                  | 4.83<br>(4.70) | 6.32<br>(6.88)   |
| <b>L<sub>7</sub></b><br>[Zn(L <sub>7</sub> ) <sub>2</sub> Cl <sub>2</sub> ]·H <sub>2</sub> O  | C <sub>34</sub> H <sub>26</sub> Cl <sub>4</sub> Fe <sub>2</sub> N <sub>6</sub> O <sub>5</sub> Zn | Brownish<br>51    | 240          | 45.32<br>(44.51)                  | 3.63<br>(2.86) | 11.06<br>(9.16)  |
| <b>HL<sub>8</sub></b><br>[Zn(HL <sub>8</sub> )Cl <sub>2</sub> ]·2H <sub>2</sub> O   | C <sub>14</sub> H <sub>15</sub> Cl <sub>3</sub> N <sub>2</sub> O <sub>3</sub> Zn                 | Black<br>88       | 210          | 39.61<br>(39.01)                  | 4.93<br>(3.51) | 6.64<br>(6.50)   |
| <b>HL<sub>9</sub></b><br>[Zn(L <sub>9</sub> ) <sub>2</sub> (H <sub>2</sub> O) <sub>2</sub> ]·2H <sub>2</sub> O                              | C <sub>30</sub> H <sub>32</sub> Cl <sub>2</sub> N <sub>4</sub> O <sub>6</sub> Zn                 | Brownish<br>63    | 290          | 52.91<br>(52.92)                  | 4.56<br>(4.74) | 7.60<br>(8.23)   |
| <b>HL<sub>10</sub></b><br>[Zn(L <sub>10</sub> ) <sub>2</sub> ]·3H <sub>2</sub> O  | C <sub>26</sub> H <sub>18</sub> Cl <sub>4</sub> N <sub>6</sub> O <sub>9</sub> Zn                 | Brownish<br>63    | 240          | 40.77<br>(40.79)                  | 2.76<br>(2.37) | 10.94<br>(10.98) |

\*M.p (decomposition)

**Table 3.10:** Analytical data and physical properties of the Pt(II) complexes.

| Complex ID  | Formula weight   | Color,<br>yield % | M.P.* °C | Element analysis<br>Found (calc)% |                |                |
|---|--|-------------------|----------|-----------------------------------|----------------|----------------|
|   |  |                   |          | C                                 | H              | N              |
| <b>H<sub>2</sub>L<sub>3</sub></b><br>[Pt(HL <sub>3</sub> )(EtOH)]·Cl                  | C <sub>16</sub> H <sub>17</sub> Cl <sub>2</sub> NO <sub>3</sub> Pt                 | Brownish<br>60    | 232      | 38.01<br>(35.77)                  | 2.87<br>(3.19) | 2.90<br>(2.61) |
| <b>L<sub>5</sub></b><br>[Pt(L <sub>5</sub> )Cl <sub>2</sub> (MeOH)]·2H <sub>2</sub> O | C <sub>19</sub> H <sub>24</sub> Cl <sub>2</sub> FeN <sub>2</sub> O <sub>3</sub> Pt | Brownish<br>51    | 300      | 35.23<br>(35.10)                  | 4.29<br>(3.72) | 4.84<br>(4.31) |
| <b>L<sub>6</sub></b><br>[Pt(L <sub>6</sub> )Cl <sub>2</sub> (MeOH)]·H <sub>2</sub> O  | C <sub>20</sub> H <sub>24</sub> Cl <sub>2</sub> FeN <sub>2</sub> O <sub>2</sub> Pt | Brownish<br>50    | 240      | 38.76<br>(37.17)                  | 4.74<br>(3.74) | 4.96<br>(4.33) |

\*M.p (decomposition)

### 3.2.2. Magnetic moment, conductivity measurements and electronic spectra

**Table 3.11:** Magnetic moment, molar conductivity measurements and electronic spectra data of the Co(II) complexes.

| Complex ID   | $\mu_{\text{eff}}$<br>BM | Molar conductance<br>$\text{Scm}^2\text{mol}^{-1}$ | Wavelength ( $\lambda$ max, nm) |
|--|--------------------------|--|---------------------------------|
| <b>HL<sub>1</sub></b><br>[Co( <b>HL</b> <sub>1</sub> )Cl <sub>2</sub> (H <sub>2</sub> O) <sub>2</sub> ].H <sub>2</sub> O             | 5.24                     | 10.21  | 256.2m,br, 262.1sh, 307.1m      |
| <b>HL<sub>2</sub></b><br>[Co( <b>HL</b> <sub>2</sub> ) <sub>2</sub> Cl <sub>2</sub> ].H <sub>2</sub> O                               | 5.82                     | 18.37  | 262.0m,br, 266.0sh, 307.2m      |
| <b>H<sub>2</sub>L<sub>3</sub></b><br>[Co( <b>HL</b> <sub>3</sub> ) <sub>2</sub> ].3H <sub>2</sub> O                                  | 4.72                     | 29.47  | 430.5m,br, 450.0sh              |
| <b>H<sub>2</sub>L<sub>4</sub></b><br>[Co(H <sub>2</sub> L <sub>4</sub> )Cl <sub>2</sub> (H <sub>2</sub> O)].2H <sub>2</sub> O        | 4.31                     | 28.52  | 365.0sh, 382.0m,br, 412.0sh     |
| <b>L<sub>5</sub></b><br>[Co( <b>L</b> <sub>5</sub> )Cl <sub>2</sub> (H <sub>2</sub> O) <sub>3</sub> ]                                | 4.75                     | 12.36  | 254.0m,br, 260.0sh, 310.0sh     |
| <b>L<sub>6</sub></b><br>[Co( <b>L</b> <sub>6</sub> )Cl <sub>2</sub> (H <sub>2</sub> O) <sub>3</sub> ].3H <sub>2</sub> O              | 4.80                     | 20.10  | 255.2m,br, 261.2sh, 307.7m      |
| <b>L<sub>7</sub></b><br>[Co( <b>L</b> <sub>7</sub> ) <sub>2</sub> Cl <sub>2</sub> (H <sub>2</sub> O) <sub>2</sub> ].H <sub>2</sub> O | 4.64                     | 20.12  | 266.0m,br, 307.2sh, 338.1m      |
| <b>HL<sub>8</sub></b><br>[Co( <b>HL</b> <sub>8</sub> )Cl <sub>2</sub> (H <sub>2</sub> O) <sub>2</sub> ].2H <sub>2</sub> O            | 4.87                     | 21.34  | 256.1s,br, 260.0sh              |
| <b>HL<sub>9</sub></b><br>[Co( <b>HL</b> <sub>9</sub> )( <b>L</b> <sub>9</sub> )Cl(H <sub>2</sub> O)].2H <sub>2</sub> O               | 4.31                     | 35.45  | 260.2m,br, 270.0sh              |
| <b>HL<sub>10</sub></b><br>[Co( <b>HL</b> <sub>10</sub> ) <sub>2</sub> Cl <sub>2</sub> ].2H <sub>2</sub> O                            | 5.57                     | 58.01  | 265.5m,br, 279.0sh              |

s = strong, m = medium, br = broad, sh = shoulder.

**Table 3.12:** Magnetic moment, molar conductivity measurements and electronic spectra data of the Cu(II) complexes.

| Complex ID  | $\mu_{\text{eff}}$<br>BM | Molar conductance<br>$\text{Scm}^2\text{mol}^{-1}$ | Wavelength ( $\lambda_{\text{max}}$ , nm) |
|---|--------------------------|--|---|
| <b>HL<sub>1</sub></b><br>[Cu( <b>HL<sub>1</sub></b> )Cl <sub>2</sub> ] $\cdot$ H <sub>2</sub> O                                   | 3.24                     | 14.53  | 256.1m,br, 261.4sh, 307.0m                |
| <b>HL<sub>2</sub></b><br>[Cu( <b>L<sub>2</sub></b> )Cl(H <sub>2</sub> O)]   | 3.15                     | 19.68  | 259.0m,br, 262.1sh, 307.1m                |
| <b>H<sub>2</sub>L<sub>3</sub></b><br>[Cu( <b>H<sub>2</sub>L<sub>3</sub></b> )Cl]Cl $\cdot$ 3H <sub>2</sub> O                      | 1.77                     | 42.62  | 378.0m,br, 401.5sh, 428.5sh               |
| <b>H<sub>2</sub>L<sub>4</sub></b><br>[Cu( <b>H<sub>2</sub>L<sub>4</sub></b> )Cl <sub>2</sub> (H <sub>2</sub> O)]                  | 1.72                     | 7.55   | 391.0m,br, 450.5sh, 476.5br               |
| <b>L<sub>5</sub></b><br>[Cu( <b>L<sub>5</sub></b> )Cl <sub>2</sub> (H <sub>2</sub> O)] $\cdot$ H <sub>2</sub> O                   | 2.32                     | 10.29  | 255.1m,br, 260.2sh, 307.0m                |
| <b>L<sub>6</sub></b><br>[Cu( <b>L<sub>6</sub></b> )Cl <sub>2</sub> (H <sub>2</sub> O)] $\cdot$ 2H <sub>2</sub> O                  | 4.35                     | 15.83  | 254.2m,br, 260.2sh, 310.0m                |
| <b>L<sub>7</sub></b><br>[Cu( <b>L<sub>7</sub></b> )Cl <sub>2</sub> (EtOH)]  | 2.66                     | 50.02  | 260.8m,br, 307.0m, 338.0sh                |
| <b>HL<sub>8</sub></b><br>[Cu( <b>L<sub>8</sub></b> )Cl(H <sub>2</sub> O)]   | 1.73                     | 27.40  | 290.0m, 300.0sh, 350.0br, 362.5sh         |
| <b>HL<sub>9</sub></b><br>[Cu( <b>L<sub>9</sub></b> )Cl(H <sub>2</sub> O)]   | 1.75                     | 48.01  | 256.1m,br, 260.6sh, 308.0m                |
| <b>HL<sub>10</sub></b><br>[Cu( <b>HL<sub>10</sub></b> )Cl <sub>2</sub> (H <sub>2</sub> O) <sub>2</sub> ] $\cdot$ H <sub>2</sub> O | 1.72                     | 38.70  | 254.3m,br, 270.0m,br, 280.0sh             |

s = strong, m = medium, br = broad, sh = shoulder.

**Table 3.13:** Magnetic moment, molar conductivity measurements and electronic spectral data of the Pd(II) complexes.

| Complex ID   | $\mu_{\text{eff}}$<br>BM | Molar conductance<br>$\text{Scm}^2\text{mol}^{-1}$ | Wavelength ( $\lambda_{\text{max}}$ , nm) |
|--|--------------------------|--|---|
| <b>HL<sub>1</sub></b><br>[Pd(L <sub>1</sub> )Cl(H <sub>2</sub> O)]                             | 2.01                     | 15.08  | 255.1m,br, 260.8sh, 307.2m                |
| <b>HL<sub>2</sub></b><br>[Pd(L <sub>2</sub> )Cl(H <sub>2</sub> O)]                             | 2.00                     | 13.13  | 261.2m,br, 255.2sh, 307.2m                |
| <b>H<sub>2</sub>L<sub>3</sub></b><br>[Pd(L <sub>3</sub> )(H <sub>2</sub> O)]·3H <sub>2</sub> O | -                        | 45.07  | 373.0m,br, 424.0sh, 431.5sh               |
| <b>H<sub>2</sub>L<sub>4</sub></b><br>[Pd(H <sub>2</sub> L <sub>4</sub> )Cl]Cl·H <sub>2</sub> O | -                        | 59.32  | 307.0m,br, 442.0sh, 464.5sh               |
| <b>L<sub>5</sub></b><br>[Pd(L <sub>5</sub> )Cl <sub>2</sub> (EtOH)]                            | 2.20                     | 8.70   | 255.2m,br, 261.8br, 296.2sh, 307.2m       |
| <b>L<sub>6</sub></b><br>[Pd(L <sub>6</sub> )Cl <sub>2</sub> (H <sub>2</sub> O)]                | -                        | 40.00  | 280.2m,br, 289.8sh, 307.0m                |
| <b>L<sub>7</sub></b><br>[Pd(L <sub>7</sub> )Cl <sub>2</sub> (H <sub>2</sub> O)]                | 2.01                     | 58.40  | 225.1m,br, 261.2sh, 307.1m                |
| <b>HL<sub>8</sub></b><br>[Pd(L <sub>8</sub> )Cl(EtOH)]   | -                        | 26.96  | 292.0m, 338.5m, 350.0sh                   |
| <b>HL<sub>9</sub></b><br>[Pd(HL <sub>9</sub> )Cl <sub>2</sub> ]                                | -                        | 26.00  | 255.5m,br, 263.0sh, 307.6m                |
| <b>HL<sub>10</sub></b><br>[Pd(HL <sub>10</sub> )Cl <sub>2</sub> ]·H <sub>2</sub> O             | -                        | 58.49  | 259.5m,br, 270.0sh, 279.0sh               |

s = strong, m = medium, br = broad, sh = shoulder.

**Table 3.14:** Magnetic moment, molar conductivity measurements and electronic spectra data of the Zn(II) complexes.

| Complex ID  | $\mu_{\text{eff}}$<br>BM | Molar conductance<br>$\text{Scm}^2\text{mol}^{-1}$ | Wavelength ( $\lambda_{\text{max}}$ , nm) |
|---|--------------------------|--|---|
| <b>HL<sub>1</sub></b><br>[Zn(L <sub>1</sub> ) <sub>2</sub> ].2H <sub>2</sub> O  | 2.12                     | 16.32  | 262.7m,br, 267.9sh, 307.1m                |
| <b>HL<sub>2</sub></b><br>[Zn(L <sub>2</sub> ) <sub>2</sub> ].2H <sub>2</sub> O  | 2.33                     | 13.13  | 264.8m,br, 270.7sh, 307.3m                |
| <b>H<sub>2</sub>L<sub>3</sub></b><br>[Zn(HL <sub>3</sub> ) <sub>2</sub> ].2H <sub>2</sub> O   | -                        | 14.83  | 435.0m,br, 460.0sh, 470.0sh               |
| <b>H<sub>2</sub>L<sub>4</sub></b><br>[Zn(H <sub>2</sub> L <sub>4</sub> )Cl <sub>2</sub> (H <sub>2</sub> O) <sub>2</sub> ].3H <sub>2</sub> O | -                        | 9.07   | 362.0m,br, 379.0sh                        |
| <b>L<sub>5</sub></b><br>[Zn(L <sub>5</sub> )Cl <sub>2</sub> (H <sub>2</sub> O)].H <sub>2</sub> O  | 2.00                     | 5.98   | 260.1m,br, 297.3sh, 307.9m                |
| <b>L<sub>6</sub></b><br>[Zn(L <sub>6</sub> ) <sub>2</sub> Cl <sub>2</sub> ].H <sub>2</sub> O  | 2.39                     | 15.00  | 254.3m,br, 260.8br, 265.0sh               |
| <b>L<sub>7</sub></b><br>[Zn(L <sub>7</sub> ) <sub>2</sub> Cl <sub>2</sub> ].H <sub>2</sub> O  | 2.98                     | 20.00  | 255.1m,br, 262.4sh,307.0m                 |
| <b>HL<sub>8</sub></b><br>[Zn(HL <sub>8</sub> )Cl <sub>2</sub> ].2H <sub>2</sub> O   | -                        | 8.88   | 298.0m, 329.5sh, 346.5m                   |
| <b>HL<sub>9</sub></b><br>[Zn(L <sub>9</sub> ) <sub>2</sub> (H <sub>2</sub> O) <sub>2</sub> ].2H <sub>2</sub> O                              | -                        | 14.89  | 301.0m, 330.0sh, 345.5m                   |
| <b>HL<sub>10</sub></b><br>[Zn(L <sub>10</sub> ) <sub>2</sub> ].3H <sub>2</sub> O  | -                        | 16.09  | 255.0m,br, 266.5sh, 279.0sh               |

s = strong, m = medium, br = broad, sh = shoulder.

**Table 3.15:** Magnetic moment, molar conductivity measurements and electronic spectra data of the Pt(II) complexes.

| Complex ID  | $\mu_{\text{eff}}$<br>BM | Molar conductance<br>$\text{Scm}^2\text{mol}^{-1}$ | Wavelength ( $\lambda_{\text{max}}$ , nm) |
|---|--------------------------|--|---|
| <b>H<sub>2</sub>L<sub>3</sub></b><br>[Pt(HL <sub>3</sub> )(EtOH)].Cl                  | -                        | 40.32  | 466.0m,br, 487.0sh                        |
| <b>L<sub>5</sub></b><br>[Pt(L <sub>5</sub> )Cl <sub>2</sub> (MeOH)].2H <sub>2</sub> O | 2.04                     | 46.90  | 275.9m,br, 285.1sh, 307.2m                |
| <b>L<sub>6</sub></b><br>[Pt(L <sub>6</sub> )Cl <sub>2</sub> (MeOH)].H <sub>2</sub> O  | 2.13                     | 50.01  | 255.0m,br, 262.0sh, 307.5m                |

s = strong, m = medium, br = broad, sh = shoulder.

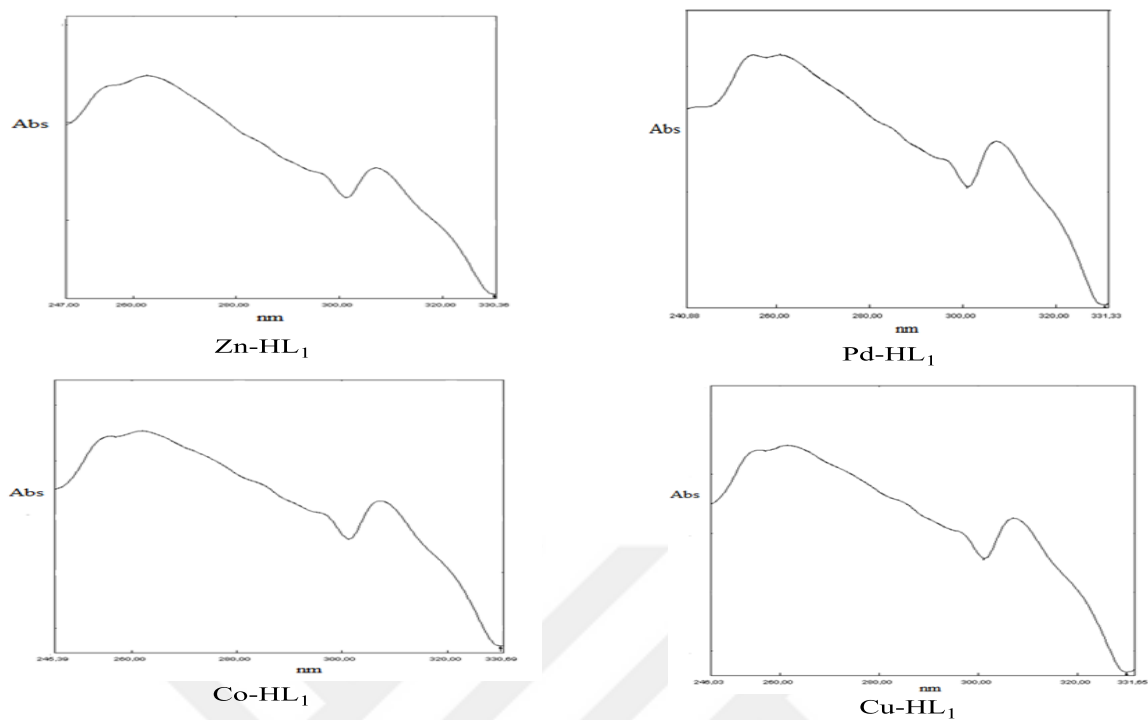


Figure 3.40: Electronic spectra of the  $\text{HL}_1$  complexes.

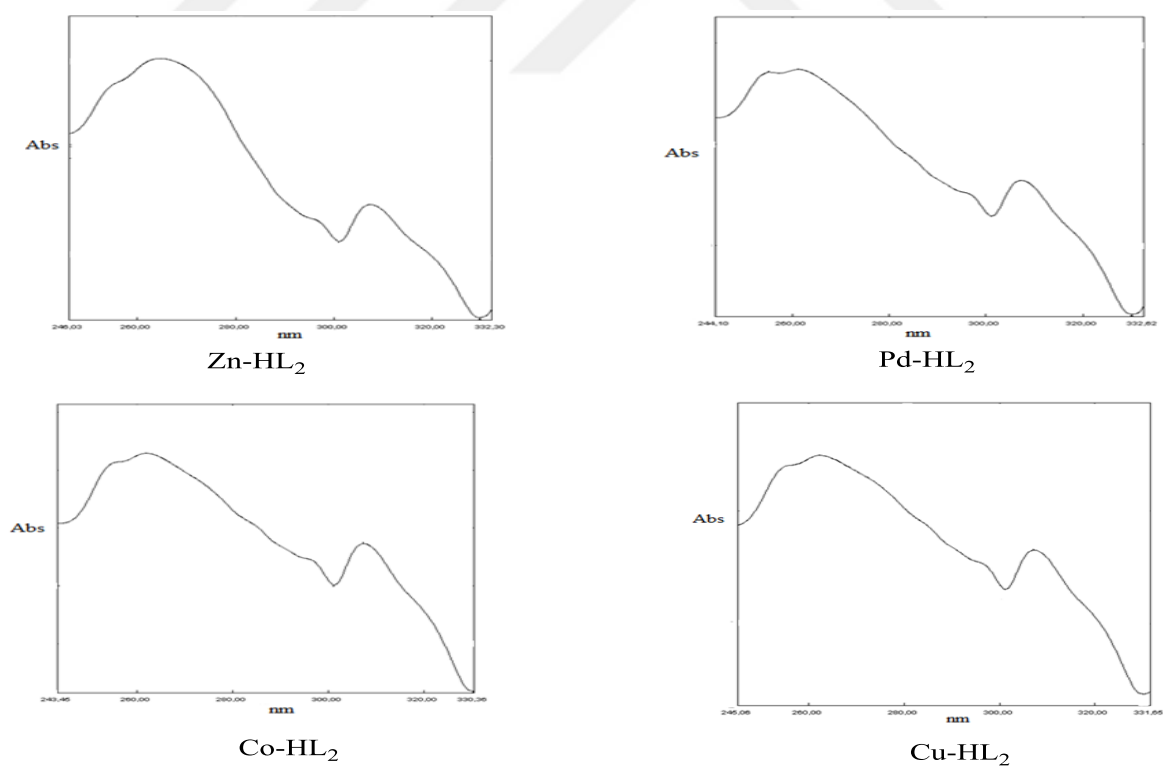


Figure 3.41: Electronic spectra of the  $\text{HL}_2$  complexes.

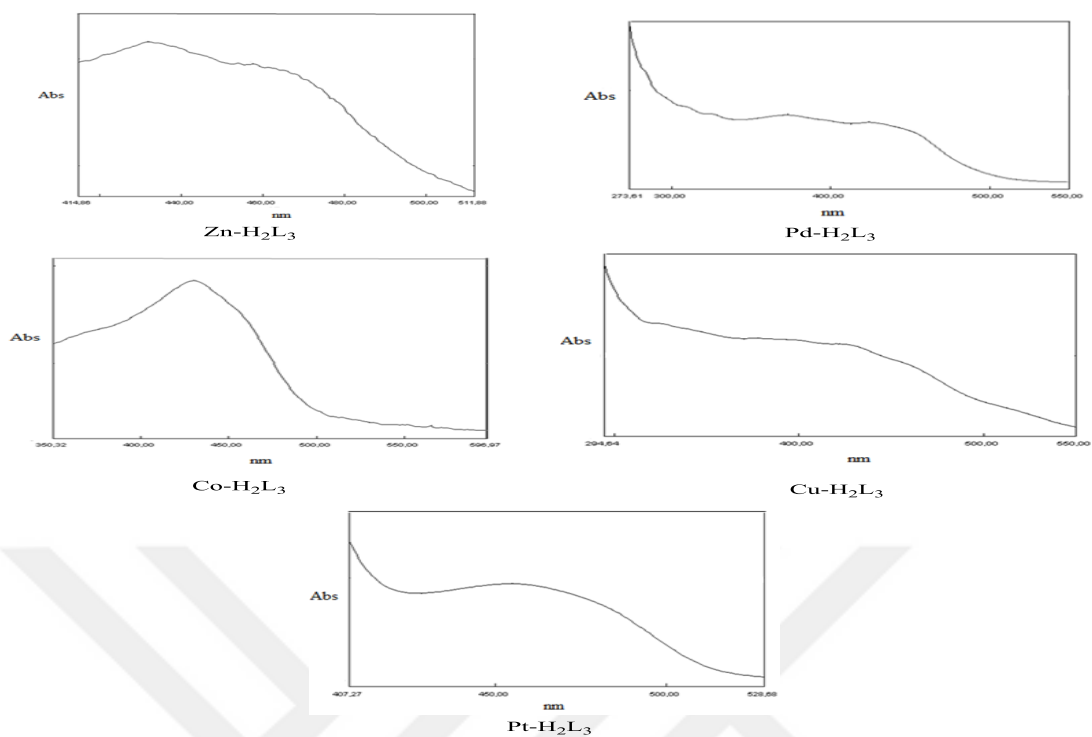


Figure 3.42: Electronic spectra of the  $H_2L_3$  complexes.

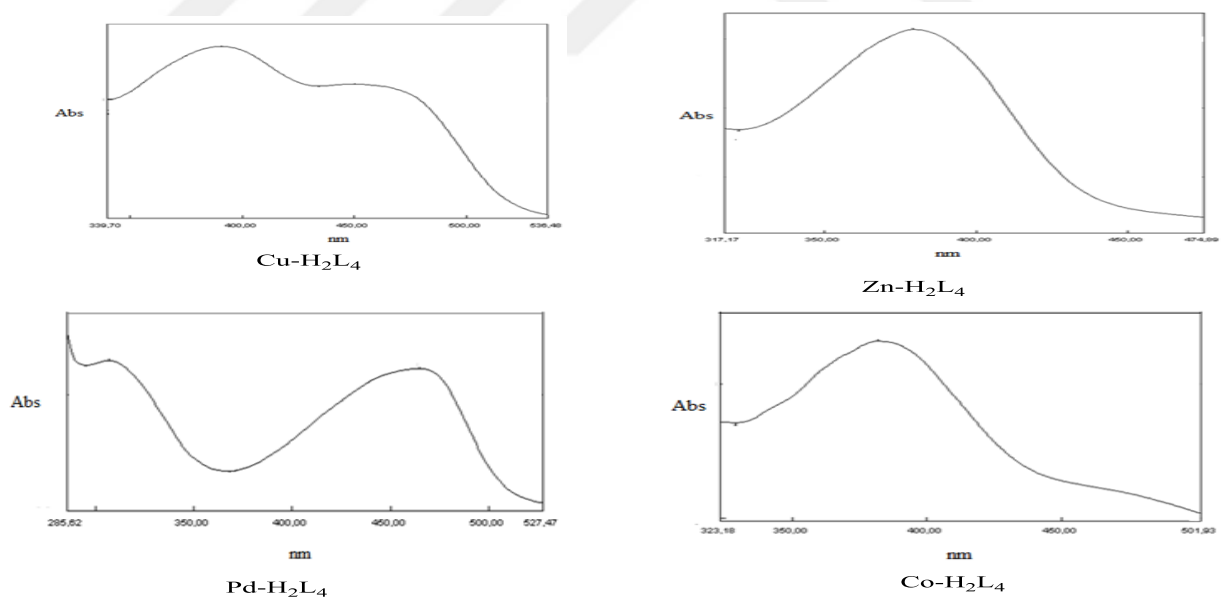
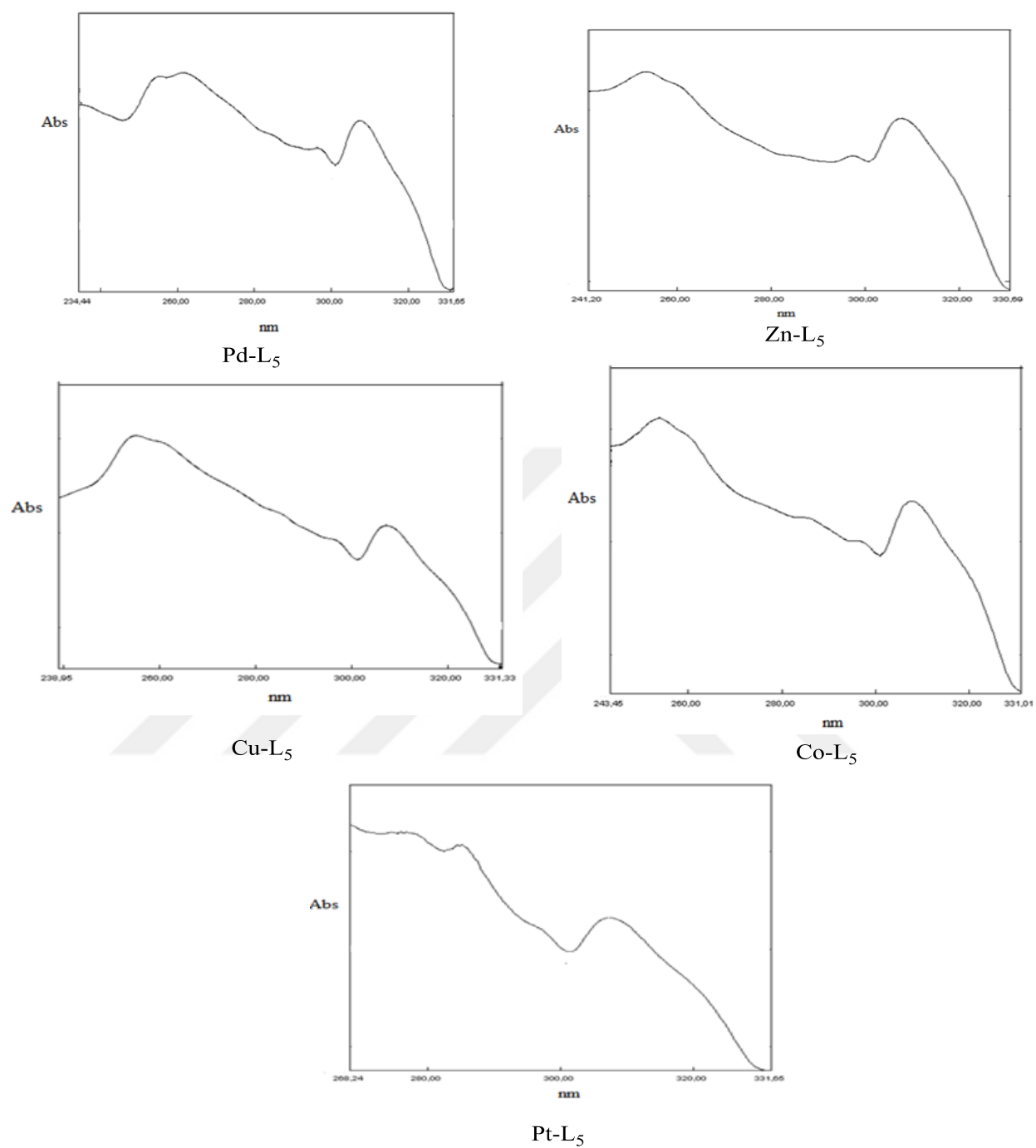
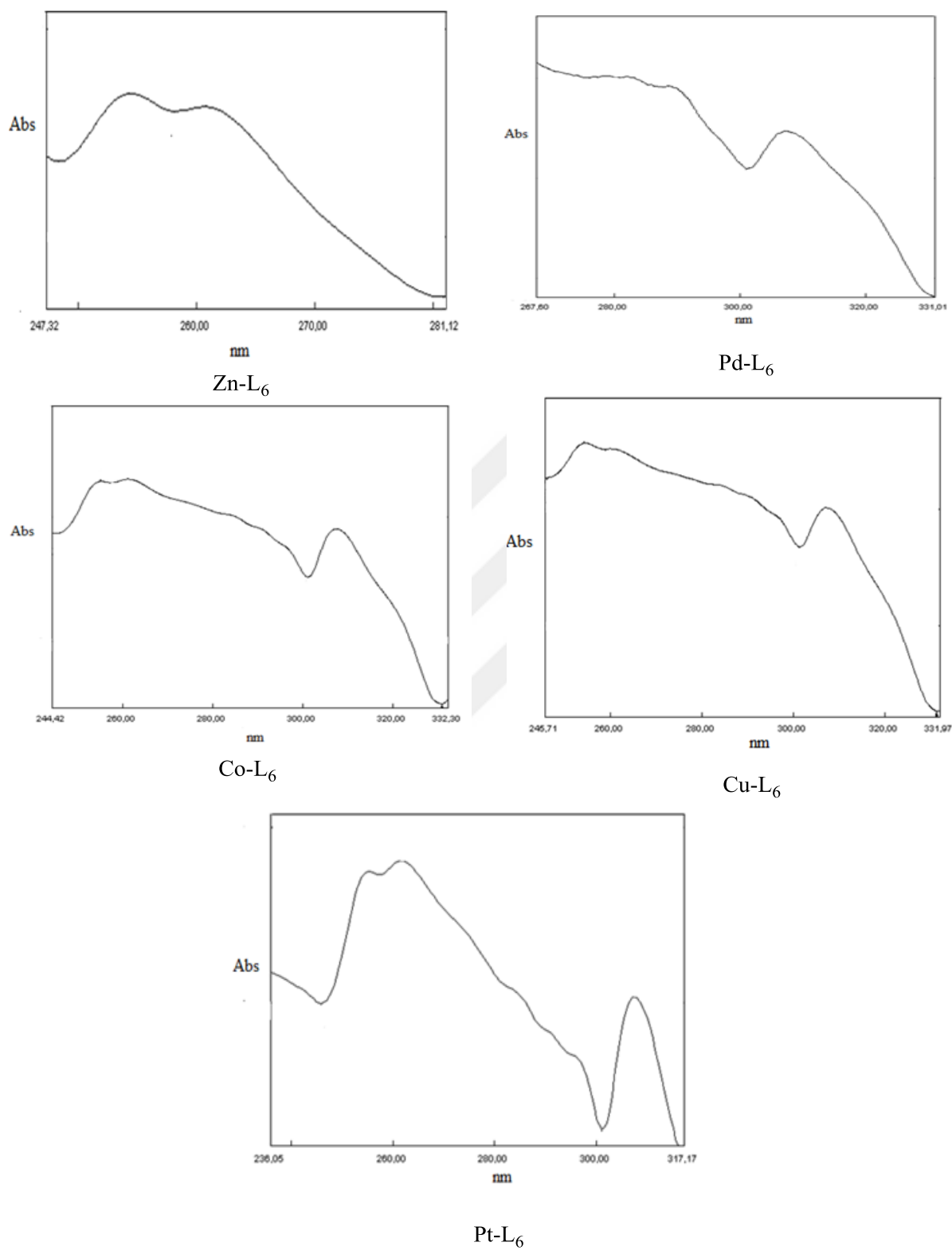


Figure 3.43: Electronic spectra of the  $H_2L_4$  complexes.

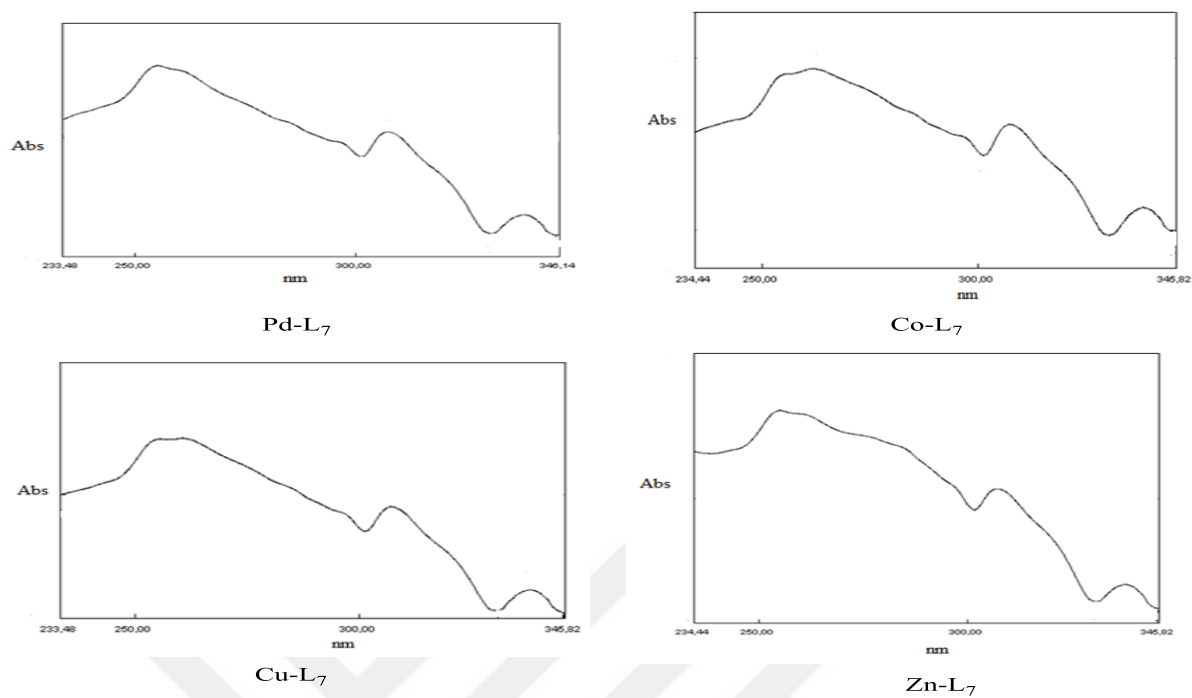




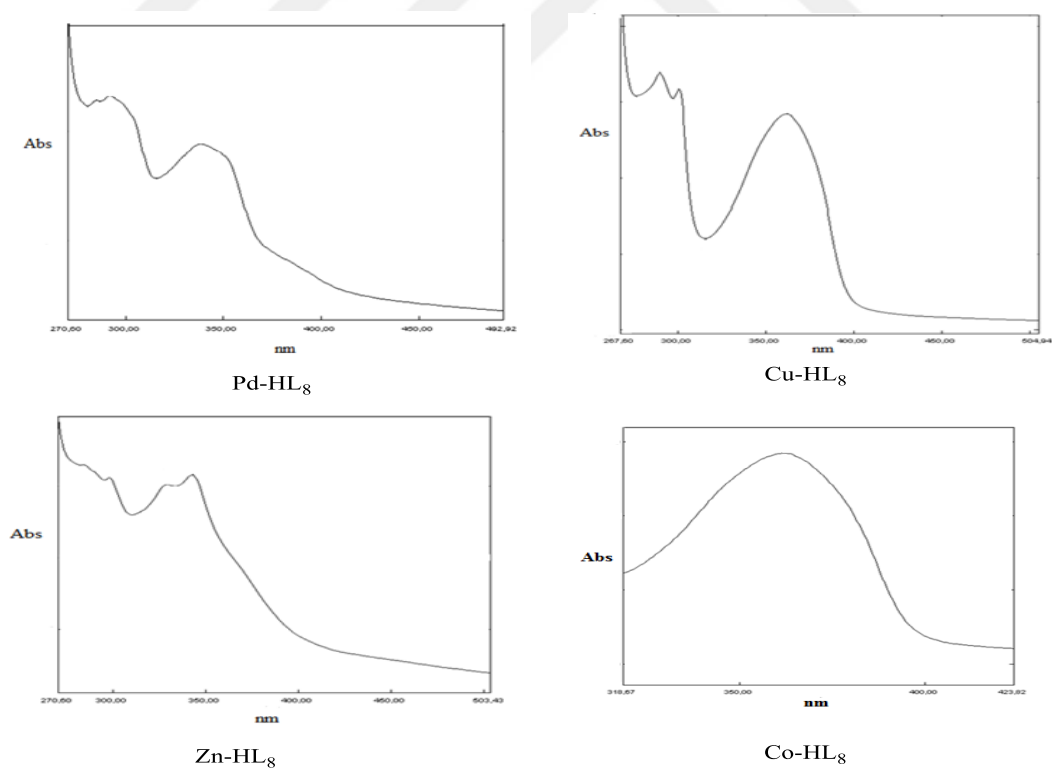
**Figure 3.44:** Electronic spectra of the  $L_5$  complexes.



**Figure 3.45:** Electronic spectra of the L<sub>6</sub> complexes.



**Figure 3.46:** Electronic spectra of the **L<sub>7</sub>** complexes.



**Figure 3.47:** Electronic spectra of the **HL<sub>8</sub>** complexes.

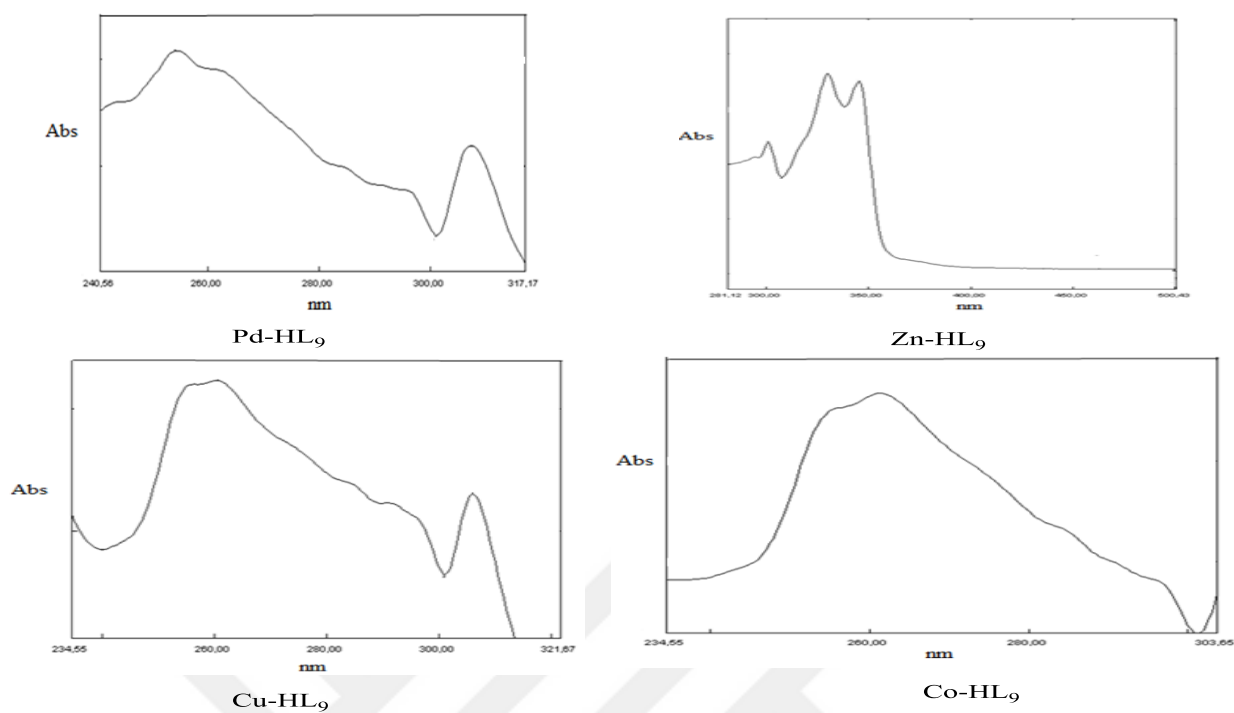


Figure 3.48: Electronic spectra of the  $\text{HL}_9$  complexes.

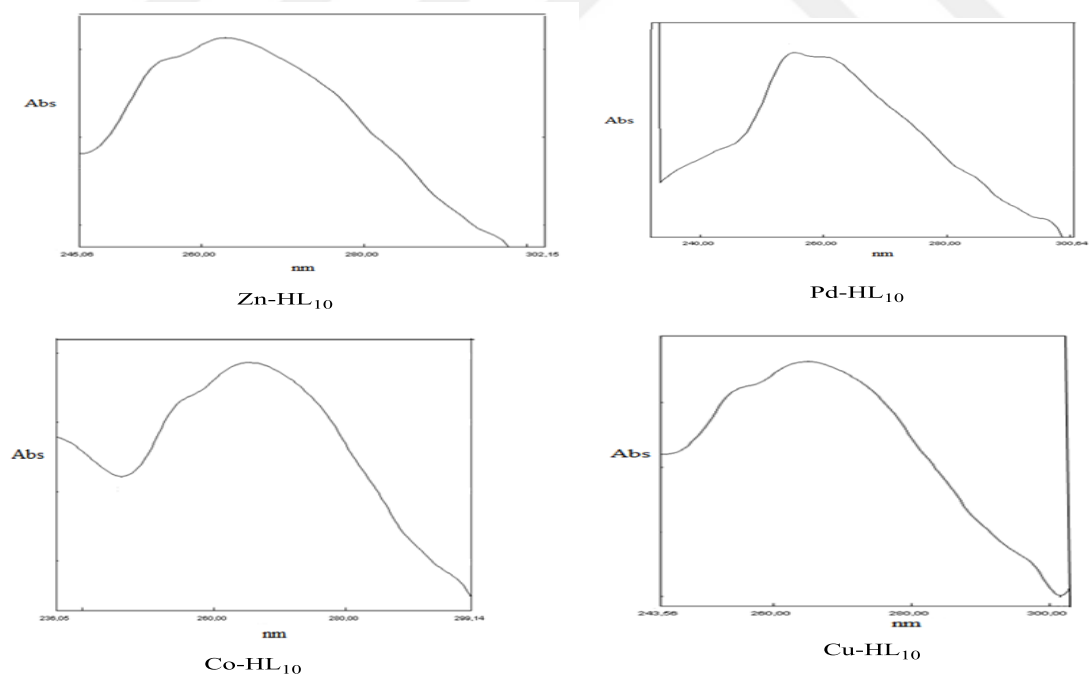
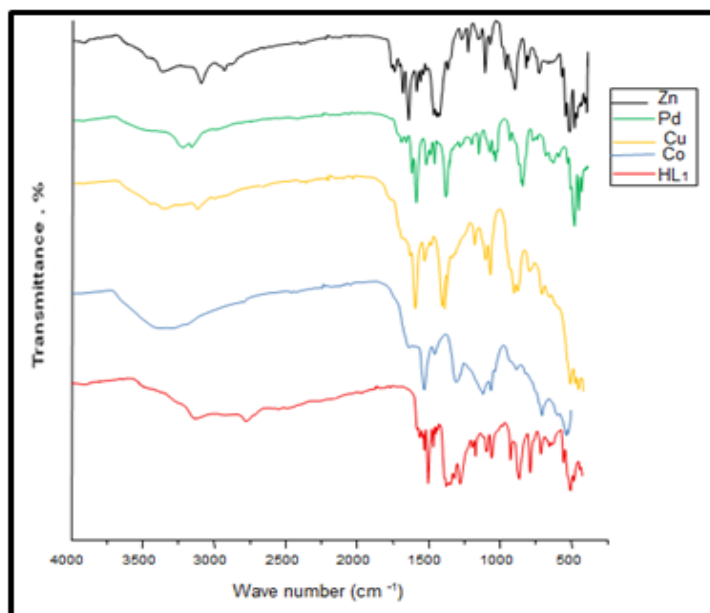


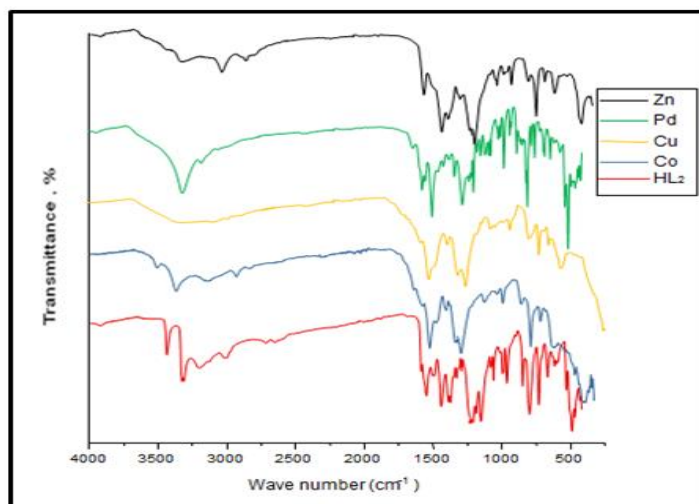
Figure 3.49: Electronic spectra of the  $\text{HL}_{10}$  complexes.

### 3.2.3. Infrared spectra of ligands and the metal complexes

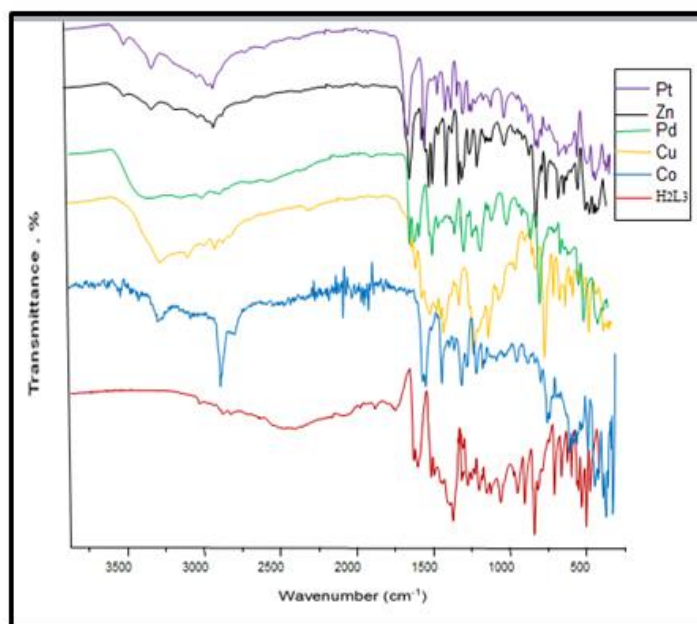
FT-IR spectra of the ligands and the complexes are given in Figure 3.50-3.59.



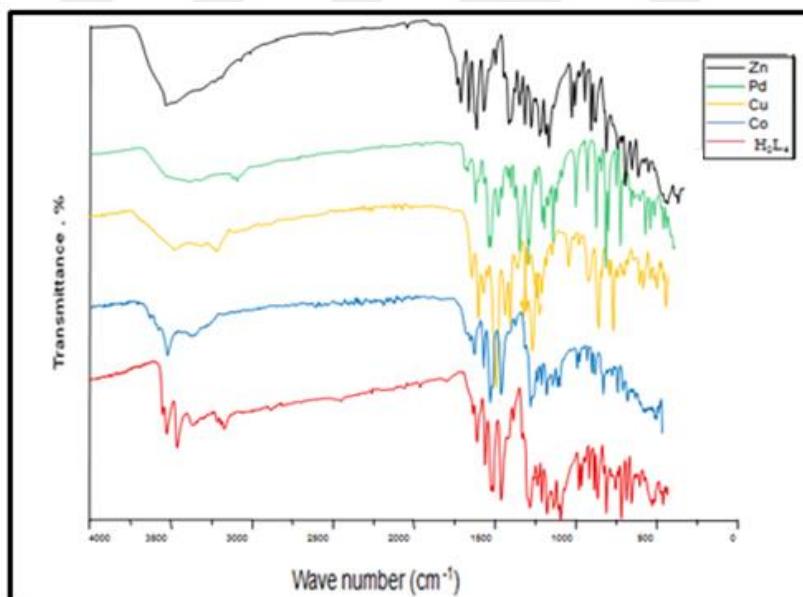
**Figure 3.50:** Comparison of the IR spectra of **HL<sub>1</sub>** and its complexes.



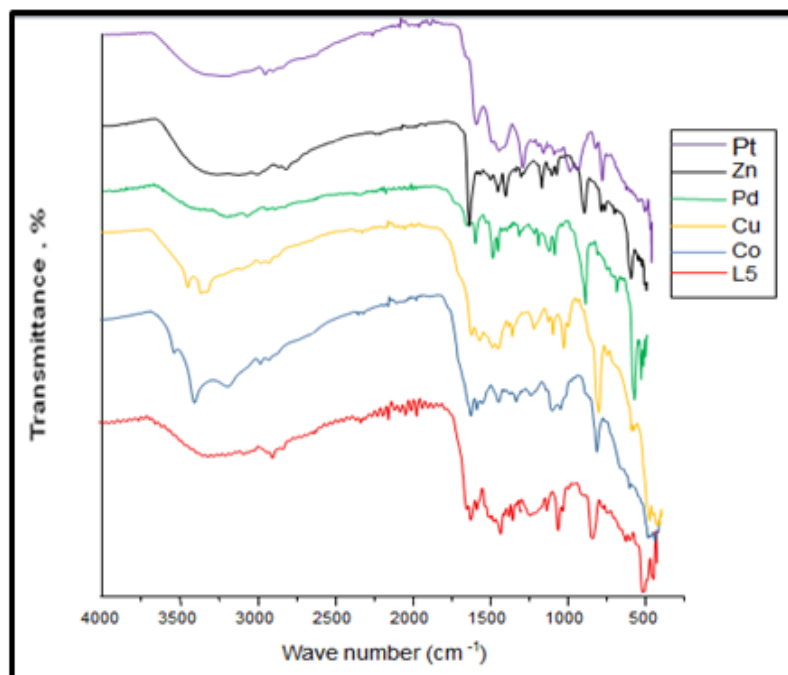
**Figure 3.51:** Comparison of the IR spectra of **HL<sub>2</sub>** and its complexes.



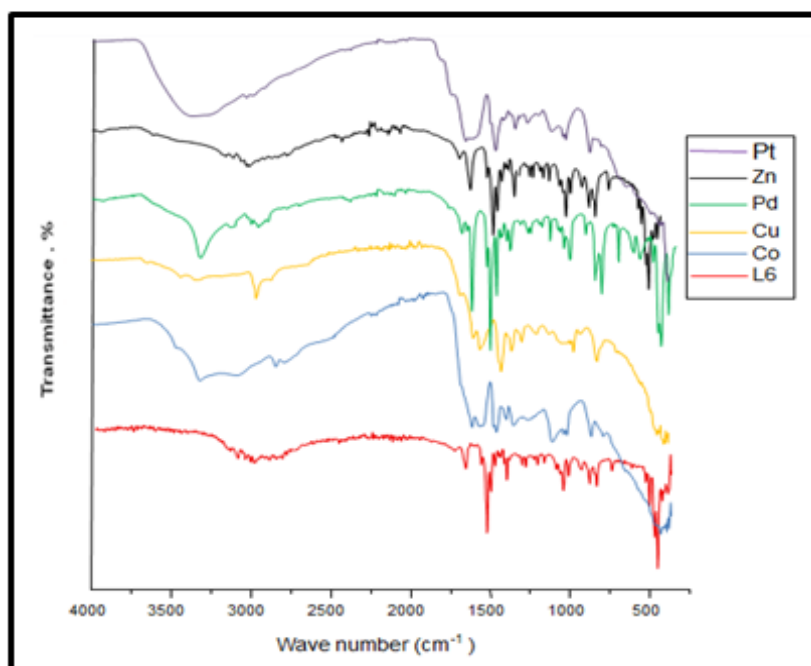
**Figure 3.52:** Comparison of the IR spectra of  $\text{H}_2\text{L}_3$  and its complexes.



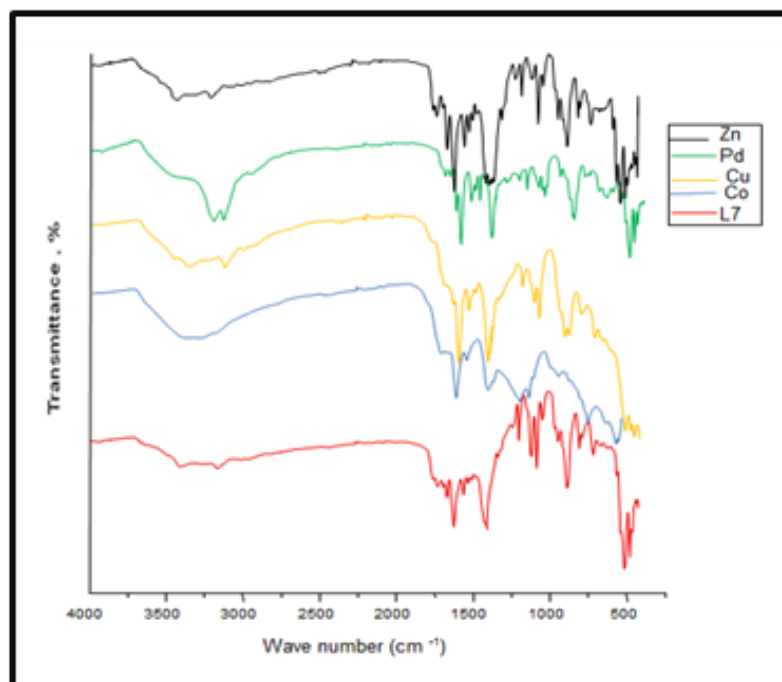
**Figure 3.53:** Comparison of the IR spectra of  $\text{H}_2\text{L}_4$  and its complexes.



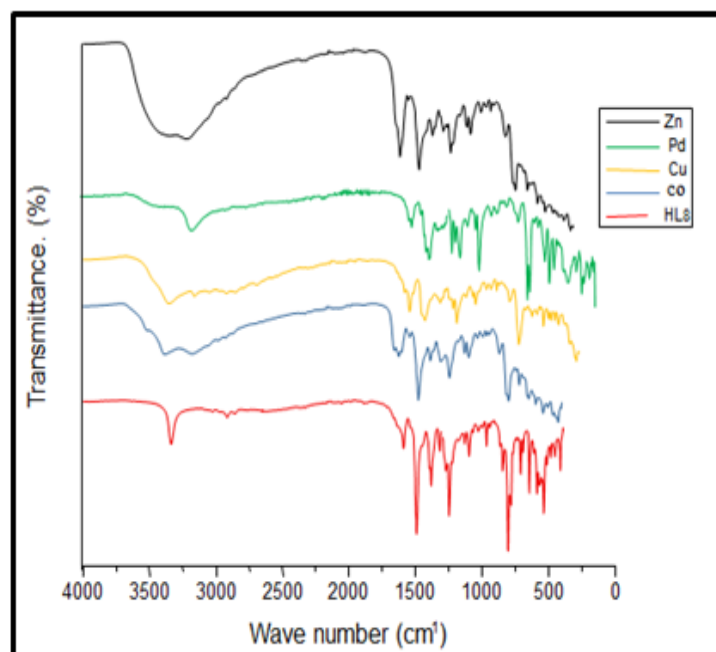
**Figure 3.54:** Comparison of the IR spectra of **L<sub>5</sub>** and its complexes.



**Figure 3.55:** Comparison of the IR spectra of **L<sub>6</sub>** and its complexes.



**Figure 3.56:** Comparison of the IR spectra of **L<sub>7</sub>** and its complexes.



**Figure 3.57:** Comparison of the IR spectra of **HL<sub>8</sub>** and its complexes.



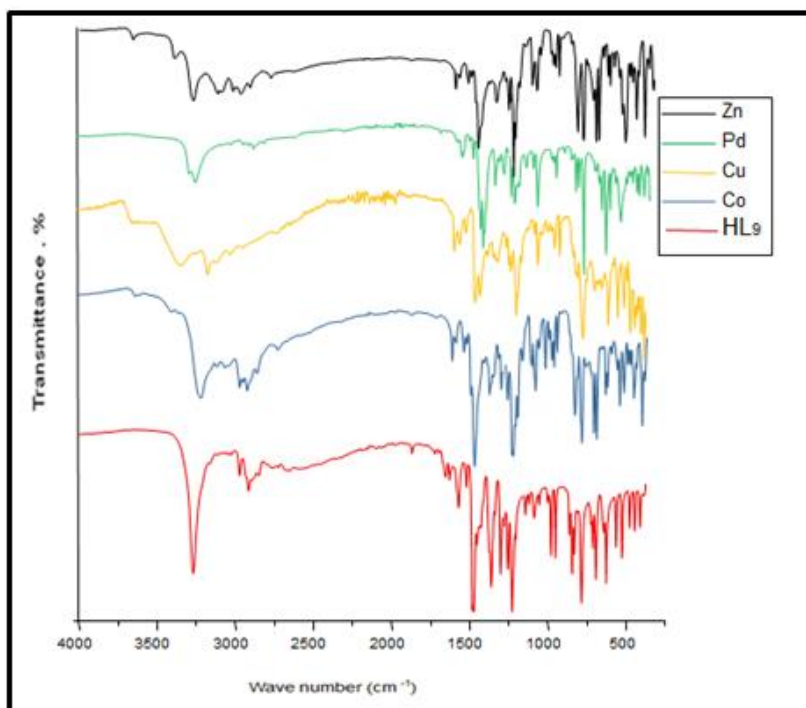


Figure 3.58: Comparison of the IR spectra of **HL<sub>9</sub>** and its complexes.

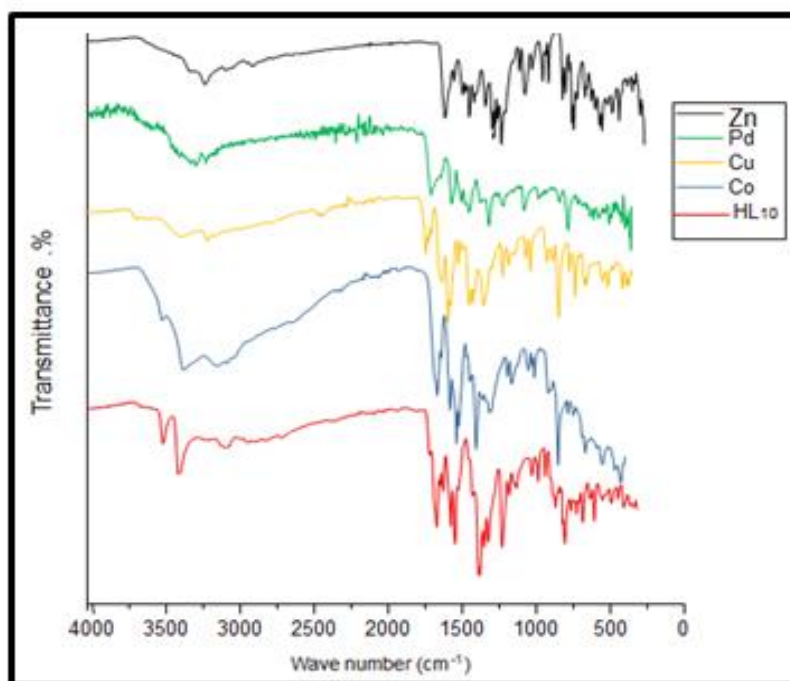


Figure 3.59: Comparison of the IR spectra of **HL<sub>10</sub>** and its complexes.

### 3.2.4. NMR data of diamagnetic metal complex ( $Zn^{2+}$ , $Pd^{2+}$ and $Pt^{2+}$ )

NMR spectra of the diamagnetic metal complexes are given in Table 3.16 and Figures 3.60-3.104.

**Table 3.16:**  $^1H$ -NMR and  $^{13}C$ -NMR spectral data of the diamagnetic metal complex.

| Compounds ID   | Assignments  |
|--|--|
| <b>HL<sub>1</sub></b><br>[Zn(L <sub>1</sub> ) <sub>2</sub> ].2H <sub>2</sub> O                 | <b><math>^1H</math>-NMR:</b> 9.87 (s, 1H, N=CH), 6-8 (m, aromatic), 4.65 (s, br, 2H, 2xH <sub>a</sub> ), 4.28 (s, br, 6H, 2xH <sub>c</sub> +2x H <sub>b</sub> +2xH <sub>d</sub> ), 3.43 (s, 10H, 4xH <sub>f</sub> +4xH <sub>e</sub> +2x H <sub>g</sub> ) 2.49(s, 6H, 2xCH <sub>3</sub> ).<br><b><math>^{13}C</math>-NMR:</b> 69.87 (2xC <sub>g</sub> +4xC <sub>e</sub> +4xC <sub>f</sub> ), 73.55 (2xC <sub>d</sub> +2xC <sub>c</sub> ), 79.86 (2xC <sub>a</sub> +2xC <sub>b</sub> ).<br>There is paramagnetic effect of ferrocen moiety.  |
| <b>HL<sub>1</sub></b><br>[Pd(L <sub>1</sub> )Cl(H <sub>2</sub> O)]                             | <b><math>^1H</math>-NMR:</b> 6-8 (m, Aromatic), 4.25 (s, br, 1H, H <sub>a</sub> ), 4.13 (s, br, 3H, H <sub>c</sub> +H <sub>b</sub> +H <sub>d</sub> ), 3.46 (s, br, 5H, 2xH <sub>f</sub> +2xH <sub>e</sub> +H <sub>g</sub> ) 2.49 (s, 3H, CH <sub>3</sub> ).<br><b><math>^{13}C</math>-NMR:</b> There is no signal due to paramagnetic effect of ferrocene moiety.  |
| <b>HL<sub>2</sub></b><br>[Zn(L <sub>2</sub> ) <sub>2</sub> ].2H <sub>2</sub> O                 | <b><math>^1H</math>-NMR:</b> 6-8 (m, Aromatic), 4.07 (s, br, 2H, 2xH <sub>a</sub> ), 3.28(s, br, 6H, 2xH <sub>c</sub> +2xH <sub>b</sub> + 2xH <sub>d</sub> ), 3.63 (s, 10H, 4xH <sub>f</sub> +4xH <sub>e</sub> +2x H <sub>g</sub> ).<br><b><math>^{13}C</math>-NMR:</b> There is no signal due to paramagnetic effect ferrocene moiety.<br>There is paramagnetic effect ferrocene moiety.  |
| <b>HL<sub>2</sub></b><br>[Pd(L <sub>2</sub> )Cl(H <sub>2</sub> O)]                             | No signal because of the paramagnetic effect ferrocene moiety.   |
| <b>H<sub>2</sub>L<sub>3</sub></b><br>[Zn(HL <sub>3</sub> ) <sub>2</sub> ].2H <sub>2</sub> O    | <b><math>^1H</math>-NMR:</b> 9.00 (s, 1H, N=CH), 7.71 (d, 2H, J=2.93, 2xH <sub>6</sub> ), 7.39 (dd, 2H, J=8.78, 2.93, 2xH <sub>6'</sub> ), 7.19 (d, 2H, J=1.96, 2xH <sub>3'</sub> ), 6.95 (dd, J= 8.79, 1.96, 4H, 2xH <sub>4</sub> +2xH <sub>5'</sub> ), 6.86 (d, J=8.3, 2H, 2xH <sub>3</sub> ) 2.20 (s, 6H, 2xCH <sub>3</sub> ).<br><b><math>^{13}C</math>-NMR:</b> 20.62 (2xCH <sub>3</sub> ), 116.45 (2xC <sub>5</sub> ), 119. 91 (2xC <sub>4</sub> ), 119.91 (2xC <sub>3</sub> ), 120.05 (2xC <sub>6</sub> ), 120.19 (C <sub>1</sub> ), 120.96 (C <sub>1</sub> ), 123.76 (C <sub>2</sub> ), 123.91 (C <sub>2</sub> ) 128.82 (C <sub>5'</sub> ), 128.88 (C <sub>5'</sub> ), 129.64 (C <sub>3'</sub> ), 131.48 (C <sub>3'</sub> ), 133.95 (C <sub>6'</sub> ), 136.10 (C <sub>4'</sub> ), 136.19(C <sub>4'</sub> ), 148.82 (C <sub>2'</sub> ), 149.47 (C <sub>2'</sub> ), 160.06 (2xC <sub>1'</sub> ), 190.00 (N=CH). |
| <b>H<sub>2</sub>L<sub>3</sub></b><br>[Pd(L <sub>3</sub> )(H <sub>2</sub> O)]·3H <sub>2</sub> O | <b><math>^1H</math>-NMR:</b> 8.97 (s, 1H, N=CH), 7.71 (d, J=2.44, 1H, H <sub>6</sub> ), 7.18 (s, 1H, H <sub>3'</sub> ), 7.04 (d, J=8.79, 1H, H <sub>6'</sub> ), 6.94 (d , 2H, J=8.29 , H <sub>5'</sub> +H <sub>4</sub> ), 6.84 (d, J= 8.29, 1H, H <sub>3</sub> ), 2.26 (s, 3H, CH <sub>3</sub> ).<br><b><math>^{13}C</math>-NMR:</b> 20.62 (CH <sub>3</sub> ), 116.85 (C <sub>5</sub> ), 119. 90 (C <sub>4</sub> ), 120.04 (C <sub>3</sub> ), 120.57 (C <sub>6</sub> ), 122.70 (C <sub>1</sub> ), 124.62 (C <sub>2</sub> ), 128.97 (C <sub>5'</sub> ), 129.58 (C <sub>3'</sub> ), 132.77 (C <sub>6'</sub> ), 134.18 (C <sub>4'</sub> ), 149.47 (C <sub>2'</sub> ), 160.10 (C <sub>1'</sub> ), 190.20 (N=CH).   |
| <b>H<sub>2</sub>L<sub>3</sub></b><br>[Pt(HL <sub>3</sub> )(EtOH)].Cl                           | <b><math>^1H</math>-NMR:</b> 11.09 (s, br, 1H, OH ), 9.06 (s, 1H, N=CH), 7.57 (d, J=2.93, 1H, H <sub>3</sub> ), 7.52 (dd, J= 8.79, 2.44, 1H, H <sub>5'</sub> ), 7.43 (dd, J=8.79, 2.93, 1H, H <sub>5</sub> ), 7.11 (d , 1H, J=8.79, H <sub>6'</sub> ), 7.01 (s, 1H, H <sub>3'</sub> ), 6.92 (d, J= 7.8, 1H, H <sub>6</sub> ), 2.26 (s, 3H, CH <sub>3</sub> ).<br><b><math>^{13}C</math>-NMR:</b> 20.62 (CH <sub>3</sub> ), 118.94 (C <sub>5</sub> ), 119.96 (C <sub>4</sub> ), 120.05 (C <sub>3</sub> ), 120.48 (C <sub>6</sub> ), 122.71 (C <sub>1</sub> ), 124.86(C <sub>2</sub> ), 128.87(C <sub>5'</sub> ), 129.61 (C <sub>3'</sub> ), 132.86 (C <sub>6'</sub> ), 136.16 (C <sub>4'</sub> ), 149.37 (C <sub>2'</sub> ), 160.11 (C <sub>1'</sub> ), 190.11(N=CH).   |

|   |  |
|---|--|
| <b>H<sub>2</sub>L<sub>4</sub></b><br>[Zn(H <sub>2</sub> L <sub>4</sub> )Cl <sub>2</sub> (H <sub>2</sub> O) <sub>2</sub> ].3H <sub>2</sub> O | <sup>1</sup> H-NMR: 10.95 (s, br, 1H, OH), 10.31 (s, br, 1H, OH), 10.19 (s, 1H, N=CH), 7.56 (d, J=2.93, 1H, H3'), 7.50 (dd, J= 8.78, 2.93, 1H, H5'), 7.47 (s, 1H, H3), 7.01 (d, 1H, J=8.78, H6'), 6.67 (s, 1H, H6).<br><sup>13</sup> C-NMR: 111.59 (C5), 111.70 (C4), 113.70 (C3), 119.83 (C6), 120.78 (C1), 123.78 (C2), 127.97 (C5)', 133.21 (C3'), 136.14 (C6'), 142.05 (C4'), 145.37 (C2'), 159.87 (C1'), 190.29 (N=CH).   |
| <b>H<sub>2</sub>L<sub>4</sub></b><br>[Pd(H <sub>2</sub> L <sub>4</sub> )Cl].H <sub>2</sub> O.Cl   | <sup>1</sup> H-NMR: 8.86 (s, 1H, N=CH), 8.24 (s, 1H, H3), 7.71 (d, J=2.93, 1H, H3'), 7.32 (dd, J=9.28, 2.92, 2H, H6+H5'), 6.93 (d, J= 8.8, 1H, H6').<br><sup>13</sup> C-NMR: 109.13 (C5), 113.86 (C4), 118.52 (C3), 122.17 (C6), 123.05 (C1), 133.21 (C2), 133.25 (C6)', 134.34 (C3'), 142.10 (C6'), 144.03 (C4'), 150.04 (C2'), 162.69 (C1'), 166.15 (N=CH).  |
| <b>L<sub>5</sub></b><br>[Zn(L <sub>5</sub> )Cl <sub>2</sub> (H <sub>2</sub> O)].H <sub>2</sub> O  | <sup>1</sup> H-NMR: 7.94 (s, br 1H, H4), 7.42 (s, br, 1H, H7), 7.00 (s, br, 1H, H6), 5.05 (s, br, 1H, H <sub>a</sub> ), 4.46 (s, br, 3H, H <sub>c</sub> +H <sub>b</sub> + H <sub>d</sub> ), 4.10 (s, 5H, 2xH <sub>f</sub> +2xH <sub>e</sub> +H <sub>g</sub> ), 2.49 (s, 3H, CH <sub>3</sub> ).<br><sup>13</sup> C-NMR: 21.65 (CH <sub>3</sub> ), 67.86 (C <sub>g</sub> ), 68.88 (C <sub>d</sub> ), 69.87 (2xC <sub>e</sub> +2xC <sub>f</sub> ), 70.00 (C <sub>c</sub> ), 70.24 (C <sub>a</sub> +C <sub>b</sub> ), 132.43 (C5), 133.00 (C6+C7), 139.55 (C4), 153.16 (C8+C9), 162.80 (C2).<br>There is paramagnetic effect ferrocene moiety. |
| <b>L<sub>5</sub></b><br>[Pd(L <sub>5</sub> )Cl <sub>2</sub> (EtOH)]   | <sup>1</sup> H-NMR: 13.04 (s, br, 1H, NH), 8.62 (s, br, 1H, H4), 7.33 (s, br, 2H, H7+H4), 6.44 (s, br, 1H, H6), 4.76 (s, br, 1H, H <sub>a</sub> ), 4.26 (s, br, 3H, H <sub>c</sub> +H <sub>b</sub> +H <sub>d</sub> ), 3.46 (s, 5H, 2xH <sub>f</sub> +2xH <sub>e</sub> +H <sub>g</sub> ), 2.58 (s, 3H, CH <sub>3</sub> ).<br><sup>13</sup> C-NMR: 21.65 (CH <sub>3</sub> ), 70.07 (C <sub>g</sub> ), 71.14 (C <sub>d</sub> ), 110 (2xC <sub>e</sub> +2xC <sub>f</sub> ), 111.62 (C <sub>c</sub> ), 131.37 (C <sub>a</sub> +C <sub>b</sub> ), 132.28 (C5), 133.55 (C6+C7), 139.55 (C4), 141.73 (C8), 153.61 (C9), 153.99 (C2).               |
| <b>L<sub>5</sub></b><br>[Pt(L <sub>5</sub> )Cl <sub>2</sub> (MeOH)].2H <sub>2</sub> O   | No signal because of the paramagnetic effect ferrocene moiety.   |
| <b>L<sub>6</sub></b><br>[Zn(L <sub>6</sub> ) <sub>2</sub> Cl <sub>2</sub> ].H <sub>2</sub> O  | <sup>1</sup> H-NMR: 12.05 (s, br, 1H, NH), 7.0-7.6 (s, br 4H, 2xH4+2xH7), 4.95 (s, 4H, 2xH <sub>a</sub> +2xH <sub>c</sub> ), 4.10 (s, br, 4H, 2xH <sub>b</sub> +2xH <sub>d</sub> ), 3.25 (s, br, 10H, 4xH <sub>e</sub> +4xH <sub>f</sub> +2xH <sub>g</sub> ), 2.30 (s, br, 12H, 4xCH <sub>3</sub> ).<br>There is paramagnetic effect ferrocene moiety.   |
| <b>L<sub>6</sub></b><br>[Pd(L <sub>6</sub> )Cl <sub>2</sub> (H <sub>2</sub> O)]   | <sup>1</sup> H-NMR: 13.02 (s, br, 1H, NH), 6.49 (s, 2H, H4+H7), 4.79 (s, 2H, H <sub>a</sub> +H <sub>c</sub> ), 4.30 (s, 4H, 2xH <sub>f</sub> +2xH <sub>e</sub> ), 3.38 (s, 3H, H <sub>b</sub> +H <sub>d</sub> +H <sub>g</sub> ), 2.38 (s, 3H, CH <sub>3</sub> ).<br><sup>13</sup> C-NMR: 20.76 (CH <sub>3</sub> ), 70.15 (C <sub>g</sub> ), 70.54 (C <sub>d</sub> ), 111.92 (2xC <sub>e</sub> ), 112.06 (2xC <sub>f</sub> ), 131.29 (C <sub>b</sub> ), 131.59 (C <sub>c</sub> ), 131.77 (C <sub>a</sub> +C <sub>b</sub> ), 132.76 (C5), 132.94 (C6+C7), 140.03 (C4), 140.67 (C9+ C8), 153.01 (C2).   |
| <b>L<sub>6</sub></b><br>[Pt(L <sub>6</sub> )Cl <sub>2</sub> (MeOH)].H <sub>2</sub> O  | No signal because of the paramagnetic effect ferrocene moiety.   |

|  |   |
|--|---|
| <b>L<sub>7</sub></b><br>[Zn(L <sub>7</sub> ) <sub>2</sub> Cl <sub>2</sub> ]·H <sub>2</sub> O                   | <sup>1</sup> H-NMR: 13.05 (s, br, 1H, NH), 8.4-6.6 (s, br, 2H, H <sub>4</sub> +H <sub>7</sub> ), 5.08 (s, br, 2H, H <sub>a</sub> +H <sub>c</sub> ), 4.12 (s, br, 2H, H <sub>b</sub> +H <sub>d</sub> ), 3.39 (s, br, 5H, 2xH <sub>e</sub> +2xH <sub>f</sub> +H <sub>g</sub> ).<br>There is paramagnetic effect ferrocen moiety.  |
| <b>L<sub>7</sub></b><br>[Pd(L <sub>7</sub> )Cl <sub>2</sub> (H <sub>2</sub> O)]                                | <sup>1</sup> H-NMR: 12.49 (s, br, 1H, NH), 8.4-6.0 (s, br, 2H, H <sub>4</sub> +H <sub>7</sub> ), 4.81 (s, br, 2H, H <sub>a</sub> +H <sub>c</sub> ), 4.29 (s, br, 2H, H <sub>b</sub> +H <sub>d</sub> ), 3.62 (s, br, 5H, 2xH <sub>e</sub> +2xH <sub>f</sub> +H <sub>g</sub> ).<br><sup>13</sup> C-NMR: 70.28 (C <sub>g</sub> ), 70.89 (C <sub>d</sub> ), 114.48 (2xC <sub>e</sub> ), 115.31(2xC <sub>f</sub> ), 119.86 (C <sub>b</sub> ), 119.87 (C <sub>c</sub> ), 120.64 (C <sub>a</sub> ), 131.47 (C <sub>h</sub> ), 135.98 (C <sub>5</sub> ), 143.18 (C <sub>6</sub> +C <sub>7</sub> ), 143.83 (C <sub>4</sub> ), 143.94 (C <sub>9</sub> +C <sub>8</sub> ), 160.32 (C <sub>2</sub> ).<br>There is paramagnetic effect ferrocen moiety. |
| <b>HL<sub>8</sub></b><br>[Zn(HL <sub>8</sub> )Cl <sub>2</sub> ]·2H <sub>2</sub> O                              | <sup>1</sup> H-NMR: 10.20(s, 1H, NH), 8.05( s, br, 1H,H <sub>3</sub> '), 7.5(d, J=8.3,1H, H <sub>5</sub> '), 7.40(s, 1H, H <sub>4</sub> ), 7.31 (d, 1H, J=8.3, H <sub>6</sub> '), 7.08(d, 1H, J=8.3, H <sub>6</sub> ), 6.97(m,br, 1H, H <sub>7</sub> ), 2.46(s, 3H, CH <sub>3</sub> ).<br><sup>13</sup> C-NMR: 21.63 (CH <sub>3</sub> ), 114.20 (C <sub>5</sub> ) 116. 42 (C <sub>4</sub> ), 119.87 (C <sub>3</sub> ), 123.78 (C <sub>6</sub> ), 123.87 (C <sub>1</sub> ), 133.23 (C <sub>5</sub> '), 136.21 (C <sub>3</sub> '), 141.27 (C <sub>6</sub> '), 150.46 (C <sub>4</sub> '), 157.21 (C <sub>2</sub> '), 159.91 (C <sub>1</sub> ') 162.77 (C <sub>2</sub> ).   |
| <b>HL<sub>8</sub></b><br>[Pd(L <sub>8</sub> )Cl(EtOH)]   | <sup>1</sup> H-NMR: 13.19(s, 1H, NH), 8.13(s, 1H, H <sub>3</sub> '), 8.0(s, br, 1H, H <sub>5</sub> '), 7.60(d, 1H, J=7.8, H <sub>6</sub> '), 7.45(s, 1H, H <sub>4</sub> ), 7.21 (s, br, 1H, H <sub>6</sub> ), 7.02(s,br, 1H, H <sub>7</sub> ), 2.46(s, 3H, CH <sub>3</sub> ).   |
| <b>HL<sub>9</sub></b><br>[Zn(L <sub>9</sub> ) <sub>2</sub> (H <sub>2</sub> O) <sub>2</sub> ]·2H <sub>2</sub> O | <sup>1</sup> H-NMR: 13.34 (s, br, 1H, NH), 8.13 (s, br, 2H, H <sub>4</sub> ), 7.37 (s, br, 4H, 2xH <sub>3</sub> '+2xH <sub>7</sub> ), 7.00 (s, br, 4H, 2xH <sub>6</sub> '+2xH <sub>5</sub> '), 2.44 (s, 12H, 4xCH <sub>3</sub> ).<br><sup>13</sup> C-NMR: 20.47 (2xCH <sub>3</sub> ), 114.70 (C <sub>5</sub> ), 119.41 (C <sub>6</sub> ), 119.43 (C <sub>5</sub> '), 123.15 (C <sub>6</sub> '), 123.16 (C <sub>4</sub> '), 125.22 (C <sub>3</sub> '), 125.72 (C <sub>7</sub> ), 130.85 (C <sub>1</sub> '), 130.67 (C <sub>2</sub> '), 131.32 (C <sub>8</sub> ), 131.40 (C <sub>9</sub> ), 149.89 (C <sub>4</sub> ), 157.03 (C <sub>2</sub> ).   |
| <b>HL<sub>9</sub></b><br>[Pd(HL <sub>9</sub> )Cl <sub>2</sub> ]  | <sup>1</sup> H-NMR: 13.02 (s, br, 1H, NH), 11.14 (s, br, 1H, OH), 9.51 (s, br, 1H, H <sub>4</sub> ), 8.03 (s, br, 1H, H <sub>3</sub> '), 7.60 (s, br, 1H, H <sub>7</sub> ), 7.36 (s, br, 2H, H <sub>6</sub> '+H <sub>5</sub> '), 2.39 (s, 6H, 2xCH <sub>3</sub> ).<br><sup>13</sup> C-NMR: 20.39 (2xCH <sub>3</sub> ), 112.62 (C <sub>5</sub> ), 119.55 (C <sub>6</sub> ), 123.16 (C <sub>5</sub> '), 123.76 (C <sub>6</sub> '), 131.70 (C <sub>4</sub> '), 131.75 (C <sub>3</sub> '), 131.81(C <sub>7</sub> ), 131.85 (C <sub>1</sub> '), 133.41 (C <sub>2</sub> '), 139.18 (C <sub>8</sub> ), 147.49 (C <sub>9</sub> ), 155.50 (C <sub>4</sub> ), 156.36 (C <sub>2</sub> ).   |
| <b>HL<sub>10</sub></b><br>[Zn(L <sub>10</sub> ) <sub>2</sub> ]·3H <sub>2</sub> O                               | <sup>1</sup> H-NMR: 13.41 (s, br, 1H, NH), 8.55 (s, 2H, H <sub>7</sub> ), 8.17 (s, 2H, H <sub>4</sub> ), 7.96 (s, 2H, H <sub>3</sub> '), 7.45 (dd, J=8.78, J= 2.44, 2H, H <sub>5</sub> '), 7.08 (d, J= 8.38, 2H, H <sub>6</sub> ').<br><sup>13</sup> C-NMR: 110.00 (C <sub>7</sub> ), 114.76 (C <sub>4</sub> ), 119.51 (C <sub>5</sub> '+C <sub>6</sub> '), 132.65 (C <sub>4</sub> '), 127.49 (C <sub>6</sub> ), 127.57 (C <sub>5</sub> ), 132.70 (C <sub>1</sub> '), 132.81 (C <sub>2</sub> '), 143.51 (C <sub>8</sub> ), 154.47 (C <sub>9</sub> ), 156.62 (C <sub>3</sub> '), 162.74 (C <sub>2</sub> ).   |
| <b>HL<sub>10</sub></b><br>[Pd(HL <sub>10</sub> )Cl <sub>2</sub> ]·H <sub>2</sub> O                             | <sup>1</sup> H-NMR: 8.37 (s, 1H, H <sub>7</sub> ), 8.13 (s, 1H, H <sub>4</sub> ), 7.93 (s, 1H, H <sub>3</sub> '), 7.43 (dd, J=8.78, J=1.95, 1H, H <sub>5</sub> '), 7.08 (d, J= 8.78, 1H, H <sub>6</sub> '). <sup>13</sup> C-NMR: 114.38 (C <sub>7</sub> ), 119.43 (C <sub>4</sub> ), 119.57 (C <sub>5</sub> '), 123.46 (C <sub>6</sub> '), 123.93 (C <sub>4</sub> '), 127.47 (C <sub>6</sub> ), 127.55 (C <sub>5</sub> ), 132.80 (C <sub>1</sub> '), 132.92 (C <sub>2</sub> '), 143.51 (C <sub>8</sub> ), 154.47 (C <sub>9</sub> ), 155.99 (C <sub>3</sub> '), 162.78 (C <sub>2</sub> ).  |

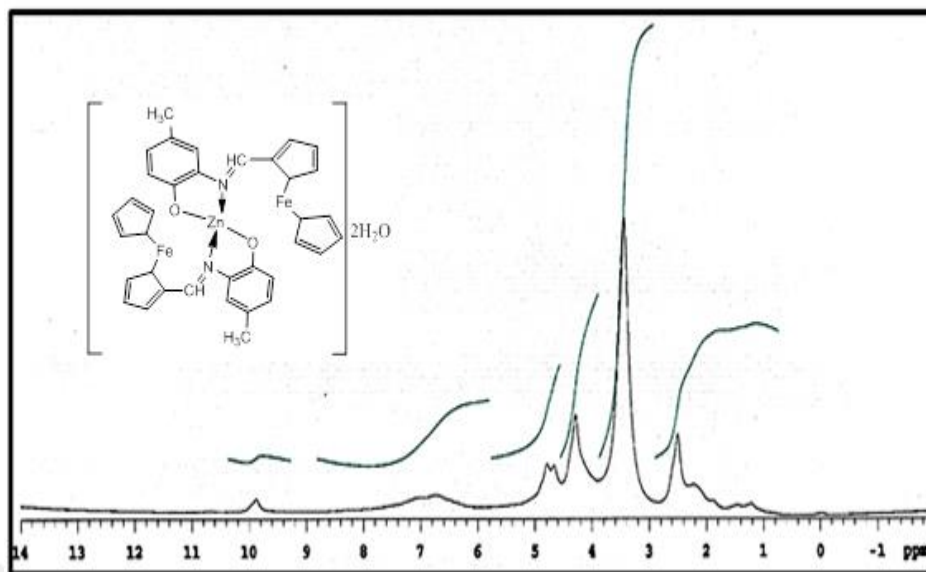


Figure 3.60:  $^1\text{H-NMR}$  spectrum of  $\text{HL}_1+\text{Zn}$  complex.

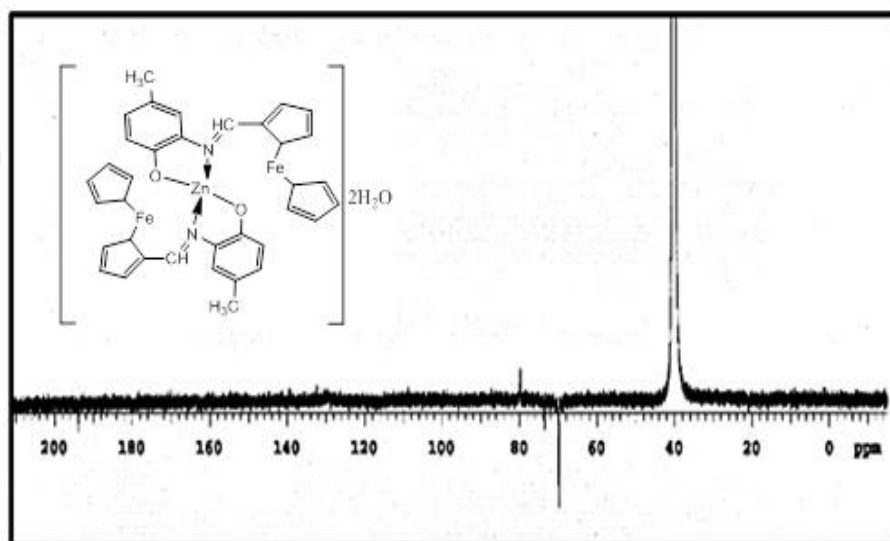
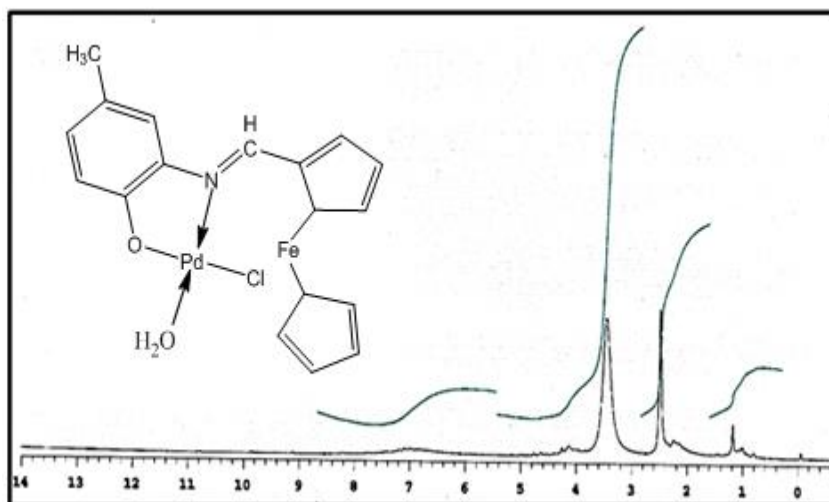
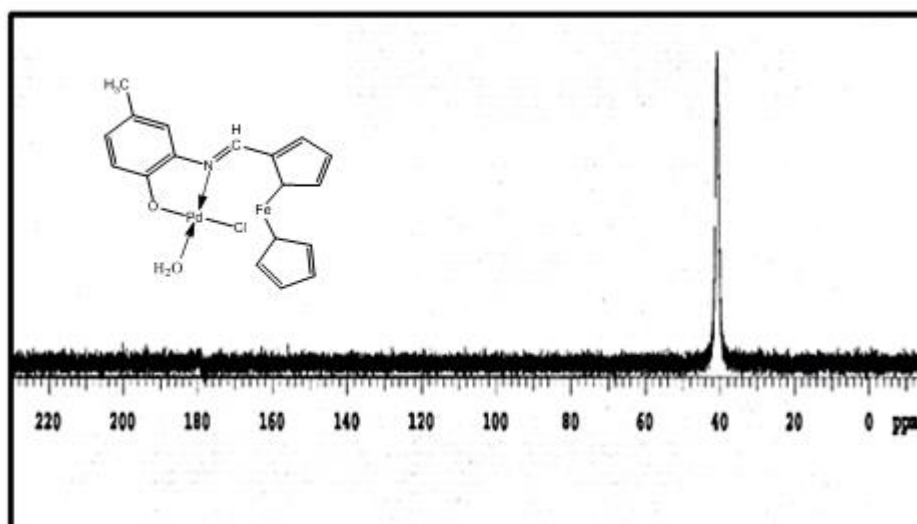


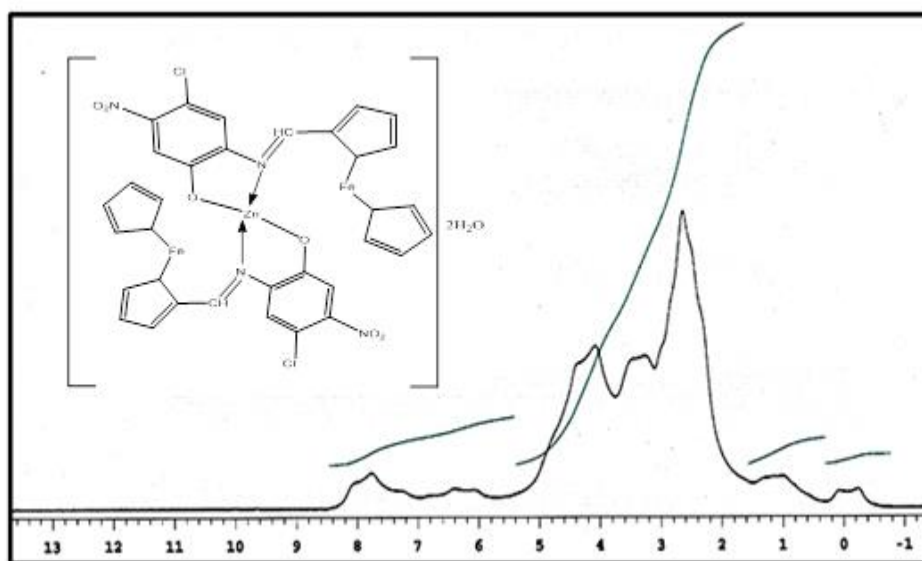
Figure 3.61:  $^{13}\text{C-NMR}$  spectrum of  $\text{HL}_1+\text{Zn}$  complex.



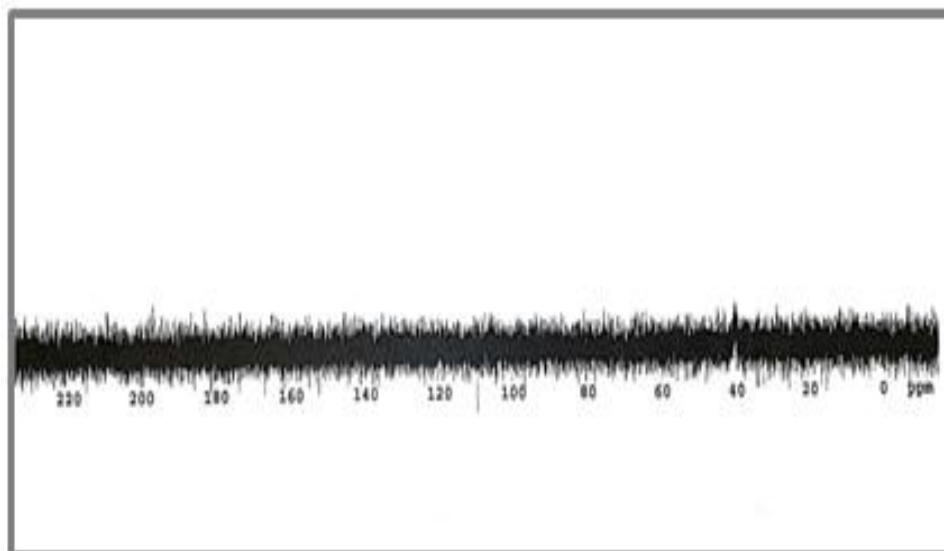
**Figure 3.62:**  $^1\text{H-NMR}$  spectrum of  $\text{HL}_1 + \text{Pd}$  Complex.



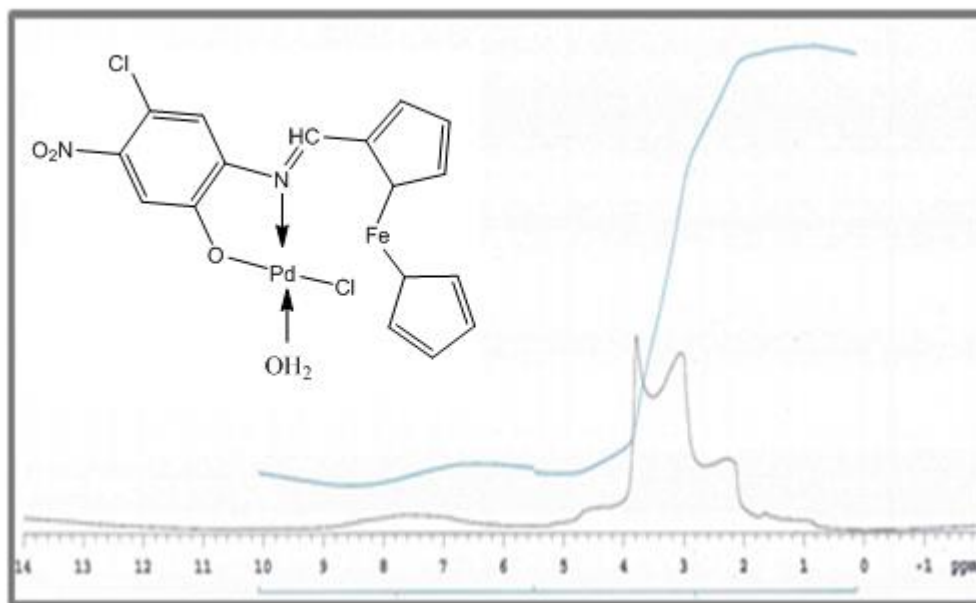
**Figure 3.63:**  $^{13}\text{C-NMR}$  spectrum of  $\text{HL}_1 + \text{Pd}$  Complex.



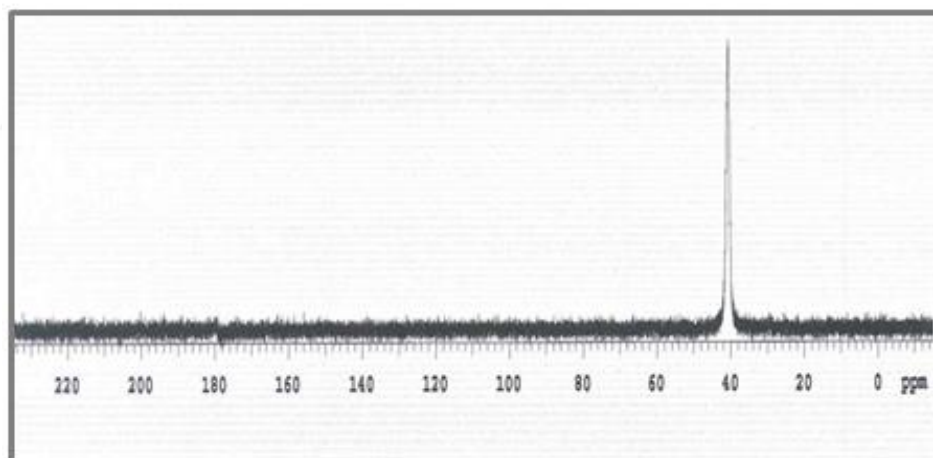
**Figure 3.64:**  $^1\text{H-NMR}$  spectrum of  $\text{HL}_2+\text{Zn}$  complex.



**Figure 3.65:**  $^{13}\text{C-NMR}$  spectrum of  $\text{HL}_2+\text{Zn}$  complex.



**Figure 3.66:**  $^1\text{H-NMR}$  spectrum of  $\text{HL}_2+\text{Pd}$  complex.



**Figure 3.67:**  $^{13}\text{C-NMR}$  spectrum of  $\text{HL}_2+\text{Pd}$  complex.



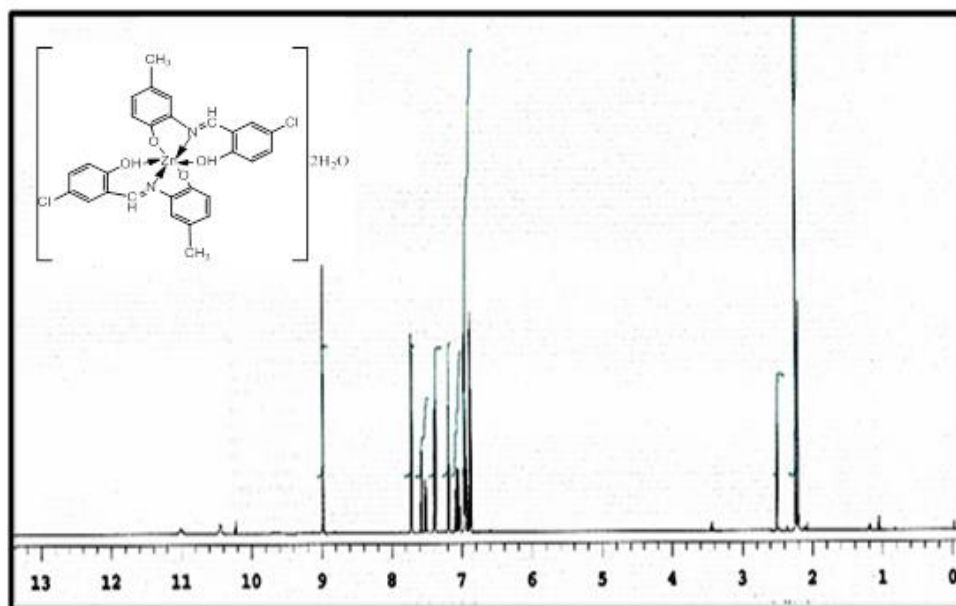


Figure 3.68:  $^1\text{H-NMR}$  spectrum of  $\text{H}_2\text{L}_3 + \text{Zn}$  complex.

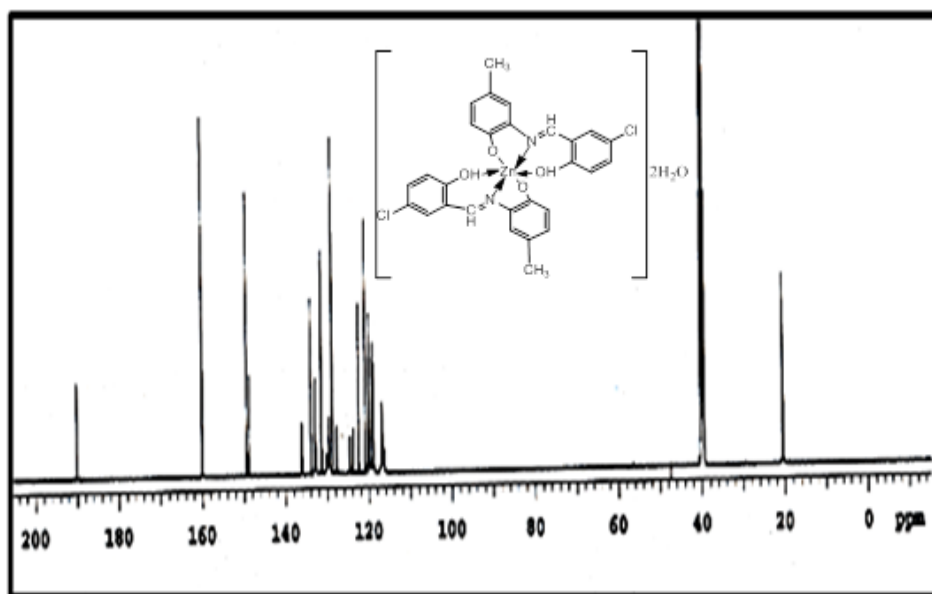


Figure 3.69:  $^{13}\text{C-NMR}$  spectrum of  $\text{H}_2\text{L}_3 + \text{Zn}$  complex.

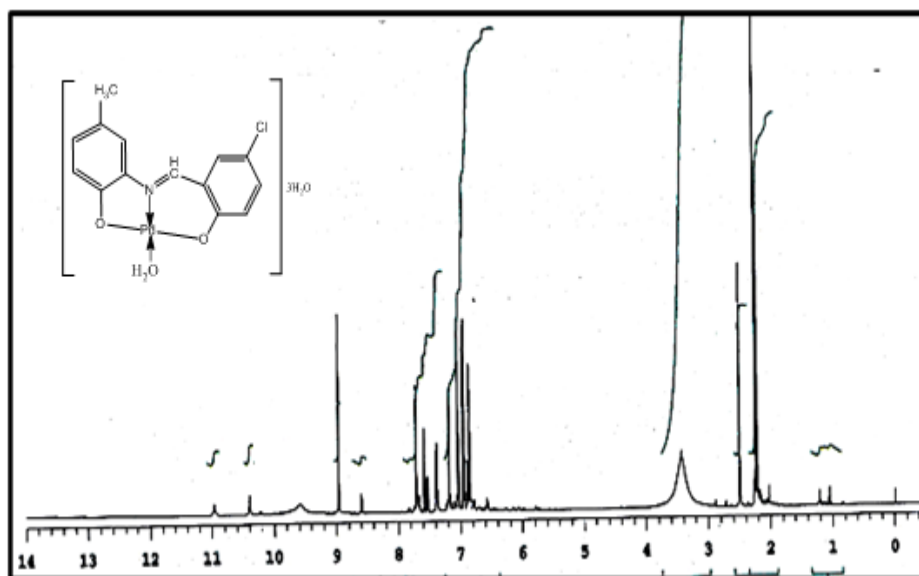


Figure 3.70:  $^1\text{H-NMR}$  spectrum of  $\text{H}_2\text{L}_3+\text{Pd}$  complex.

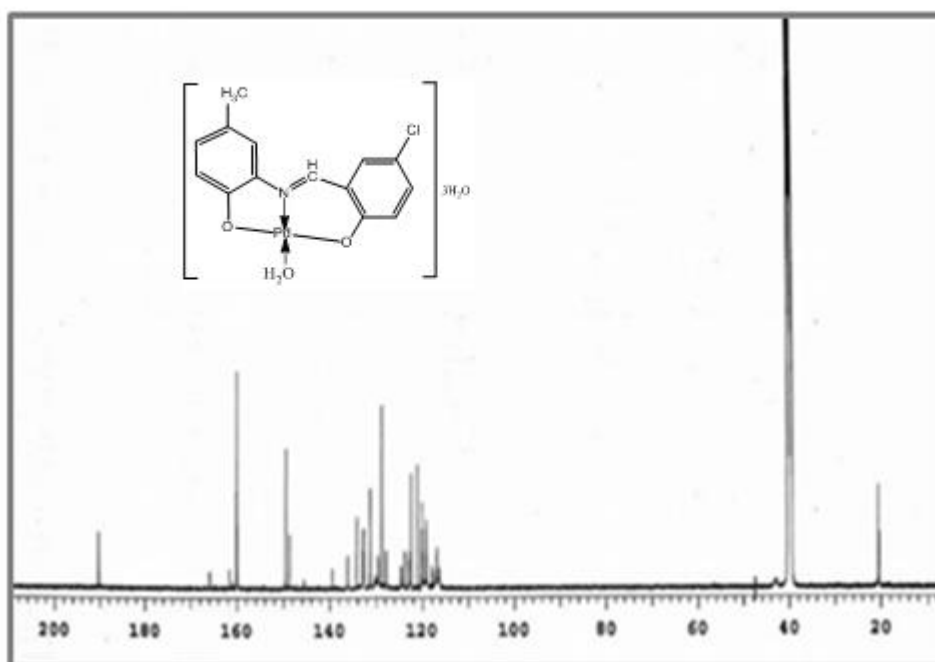


Figure 3.71:  $^{13}\text{C-NMR}$  spectrum of  $\text{H}_2\text{L}_3+\text{Pd}$  complex.

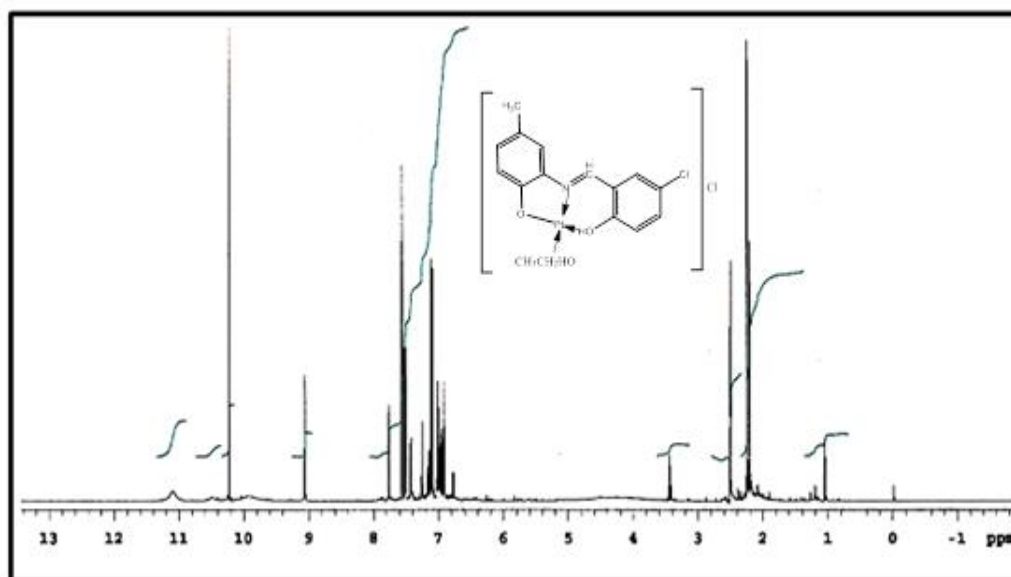


Figure 3.72:  $^1\text{H-NMR}$  spectrum of  $\text{H}_2\text{L}_3+\text{Pt}$  complex.

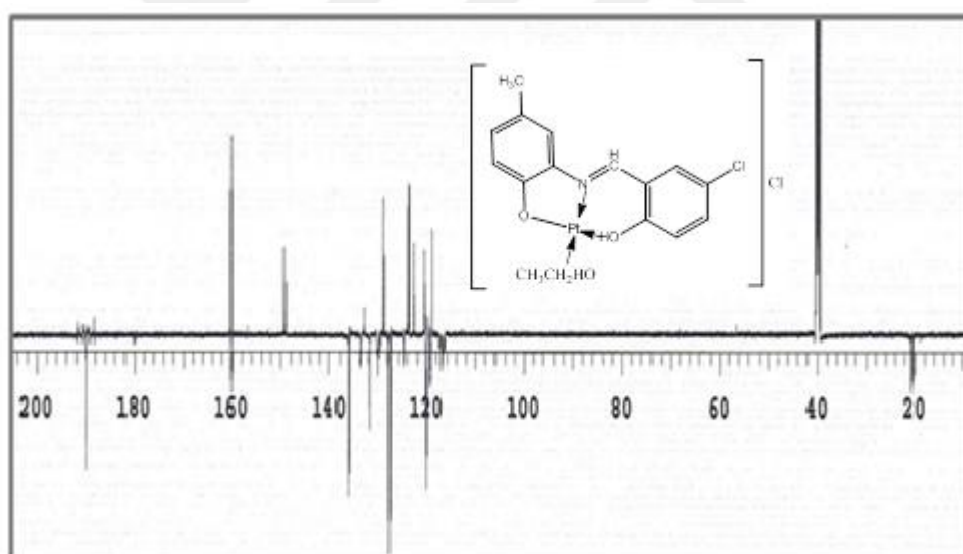


Figure 3.73:  $^{13}\text{C-NMR}$  spectrum of  $\text{H}_2\text{L}_3+\text{Pt}$  complex.

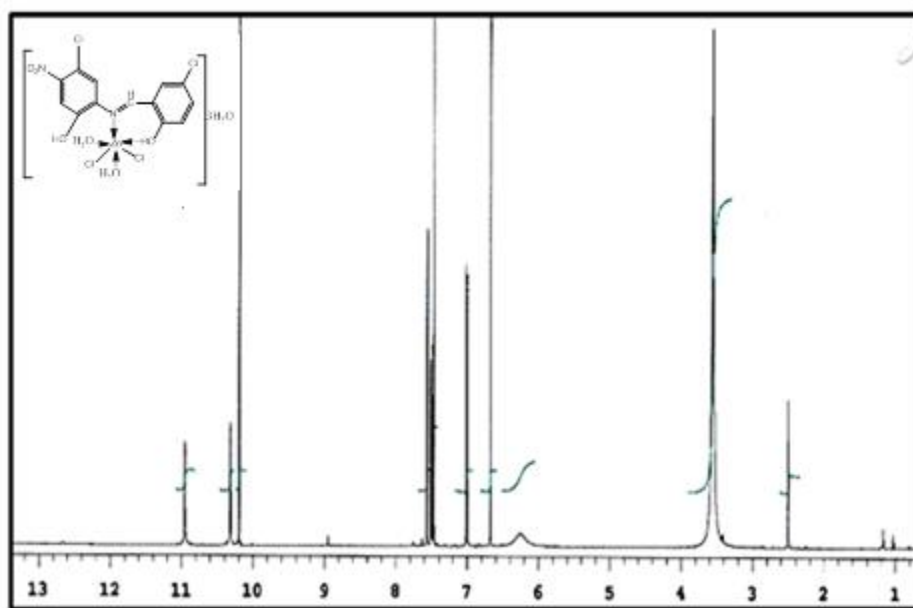


Figure 3.74:  $^1\text{H-NMR}$  spectrum of  $\text{H}_2\text{L}_4+\text{Zn}$  complex.

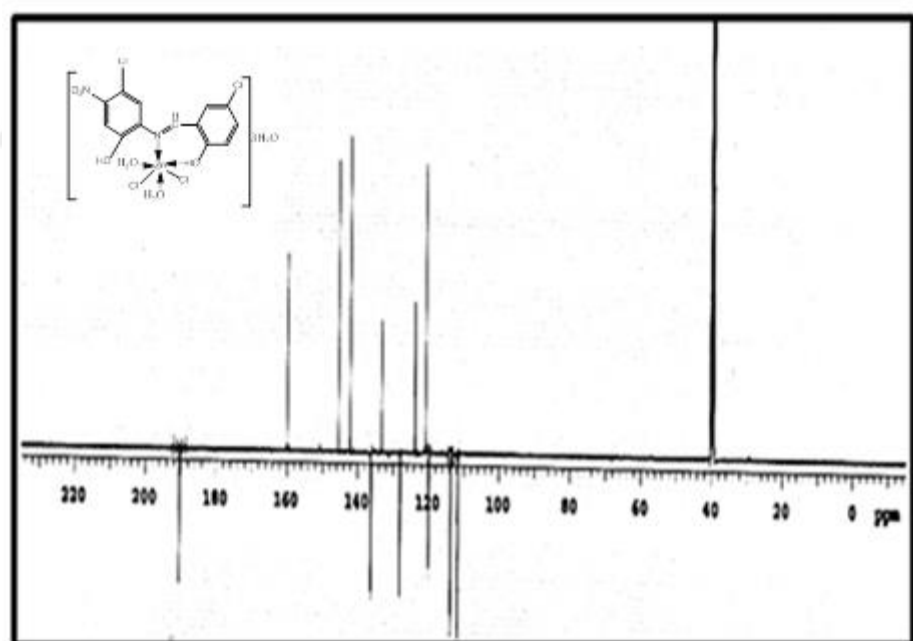


Figure 3.75:  $^{13}\text{C-NMR}$  spectrum of  $\text{H}_2\text{L}_4+\text{Zn}$  complex.

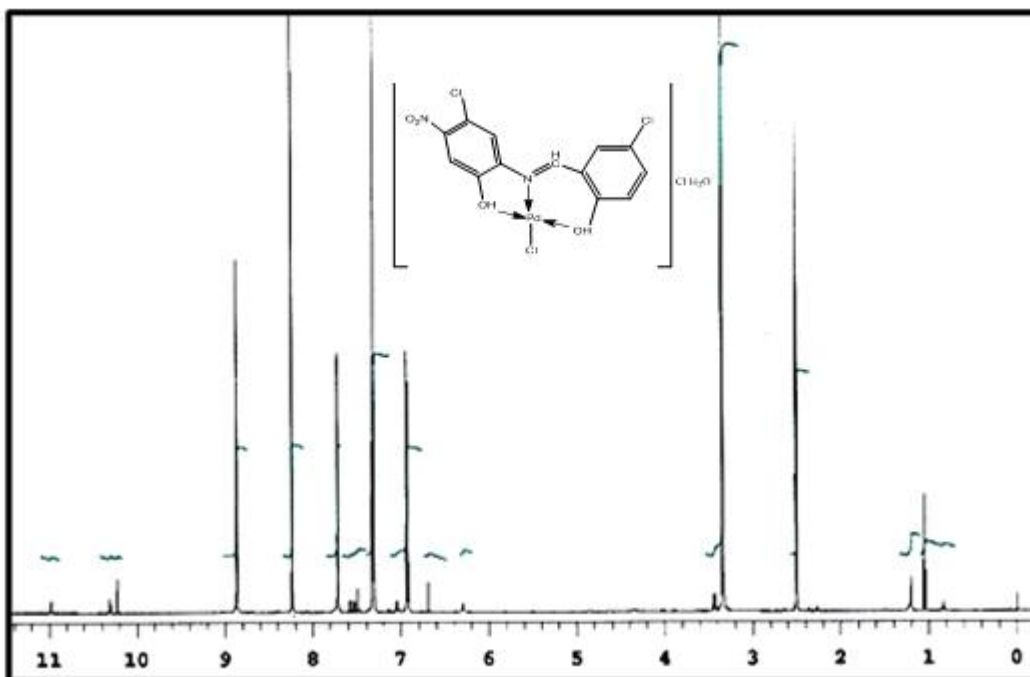


Figure 3.76:  $^1\text{H-NMR}$  spectrum of  $\text{H}_2\text{L}_4+\text{Pd}$  complex.

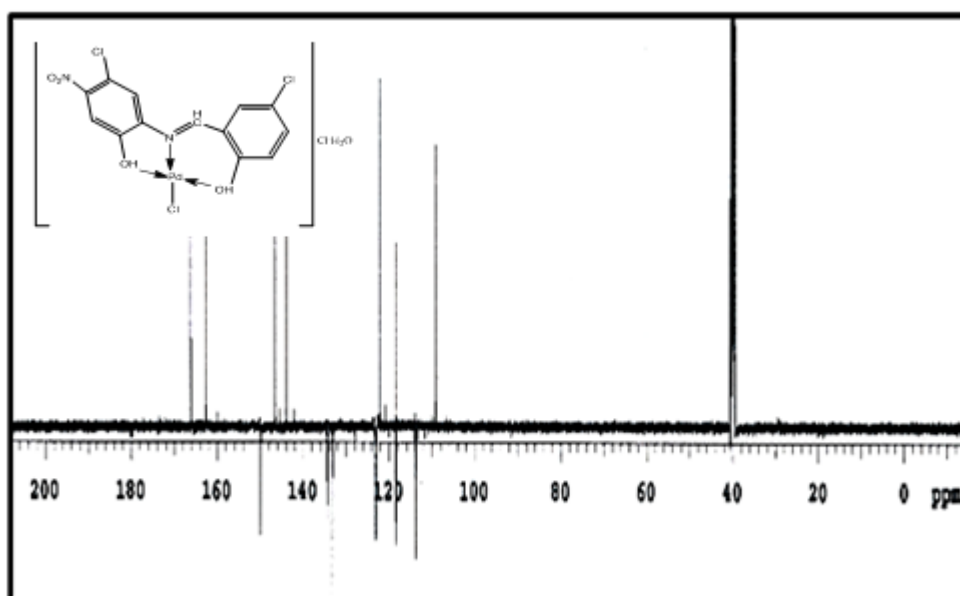
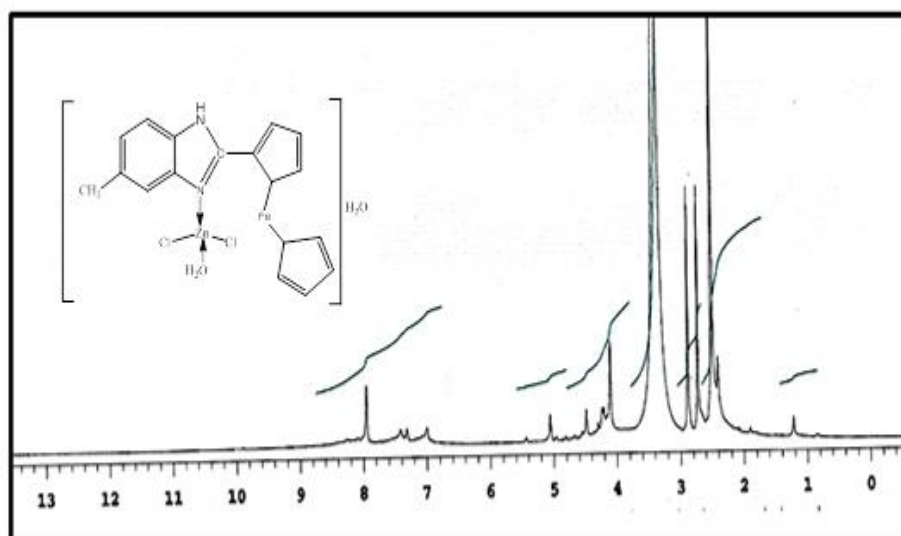
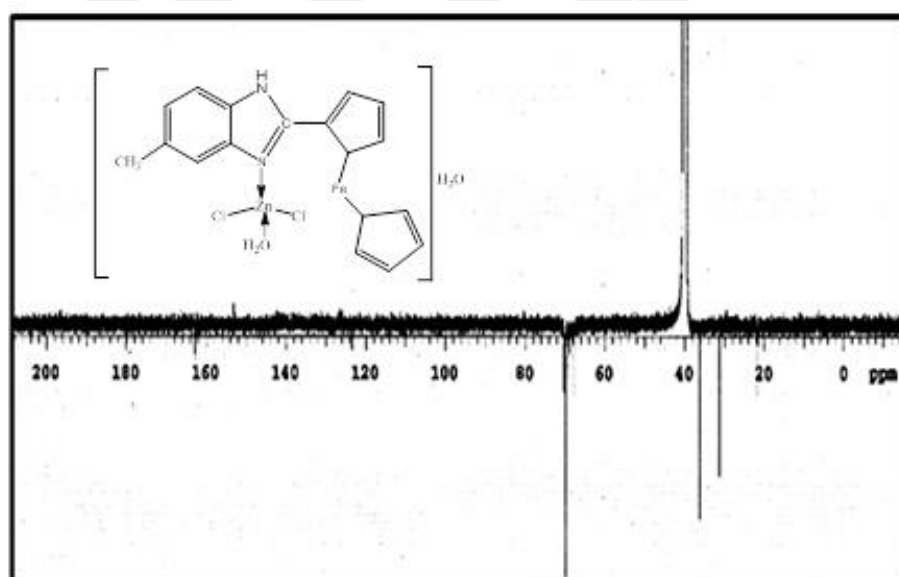


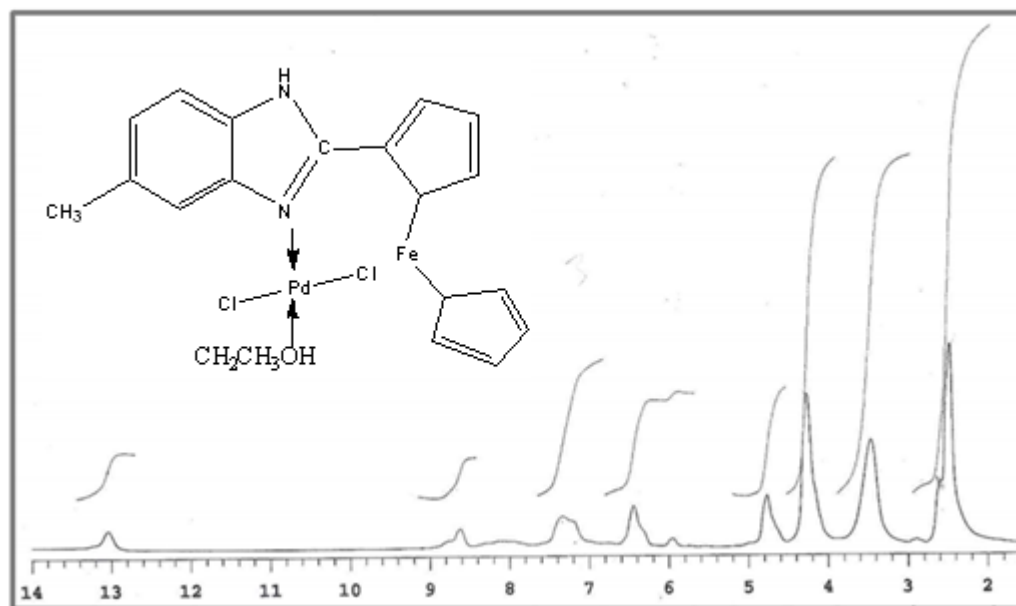
Figure 3.77:  $^{13}\text{C-NMR}$  spectrum of  $\text{H}_2\text{L}_4+\text{Pd}$  complex.



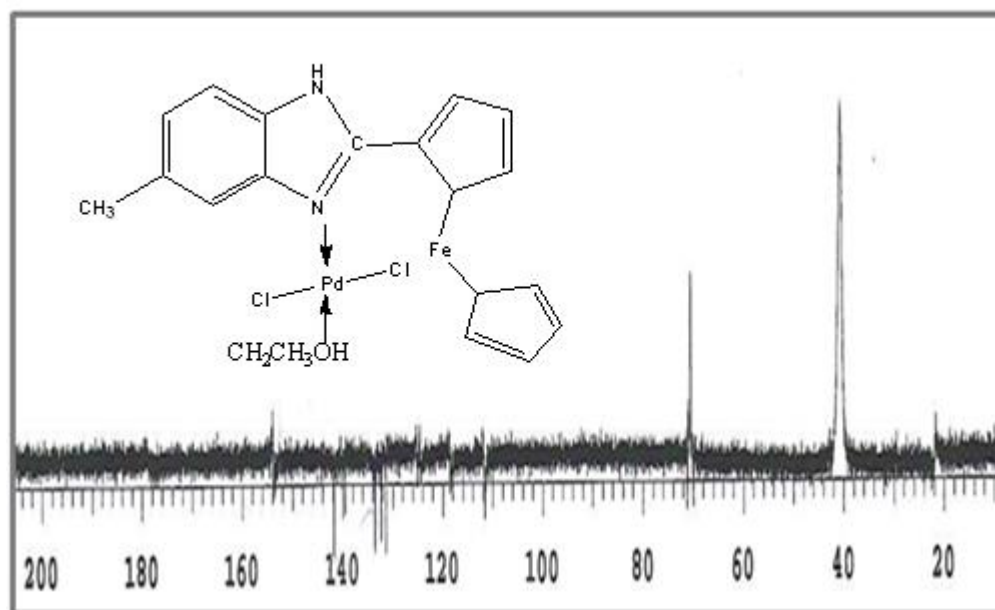
**Figure 3.78:**  $^1\text{H-NMR}$  spectrum of  $\text{L}_5+\text{Zn}$  complex.



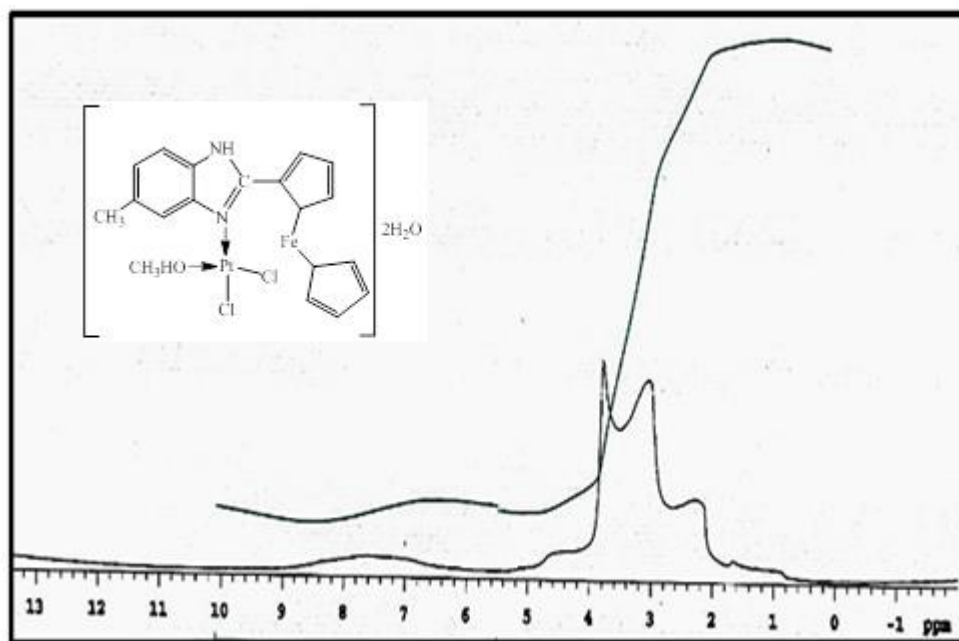
**Figure 3.79:**  $^{13}\text{C-NMR}$  spectrum of  $\text{L}_5+\text{Zn}$  complex.



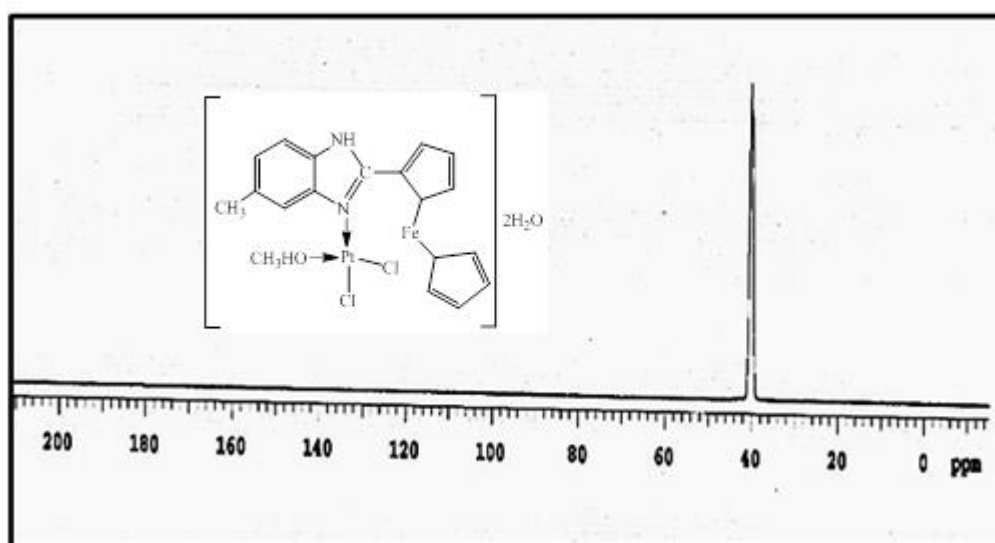
**Figure 3.80:**  $^1H$ -NMR spectrum of  $L_5 + Pd$  complex.



**Figure 3.81:**  $^{13}C$ -NMR spectrum of  $L_5 + Pd$  complex.

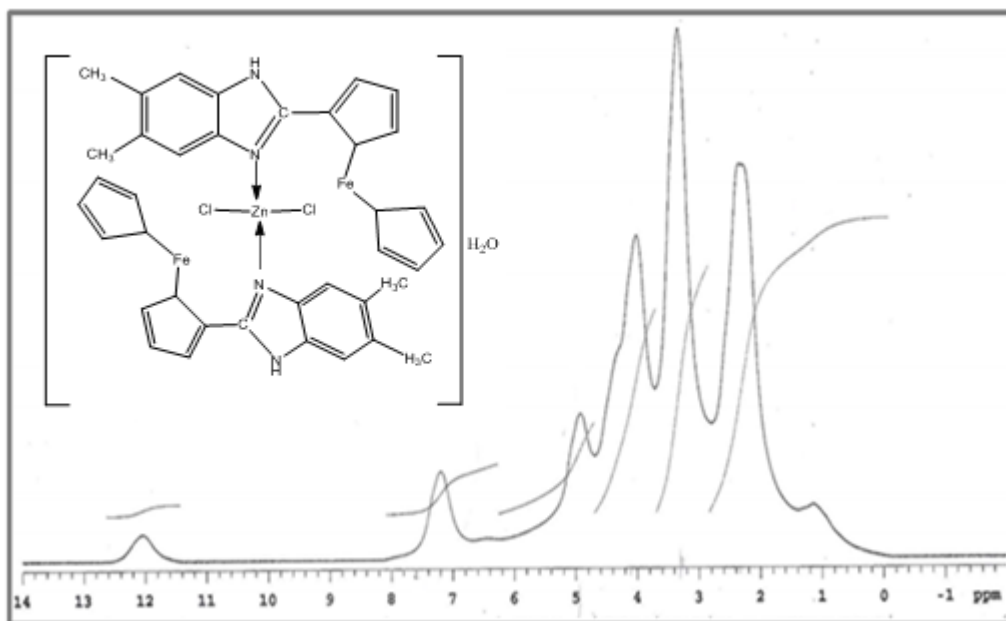


**Figure 3.82:**  $^1\text{H-NMR}$  spectrum of  $\text{L}_5 + \text{Pt}$  complex.

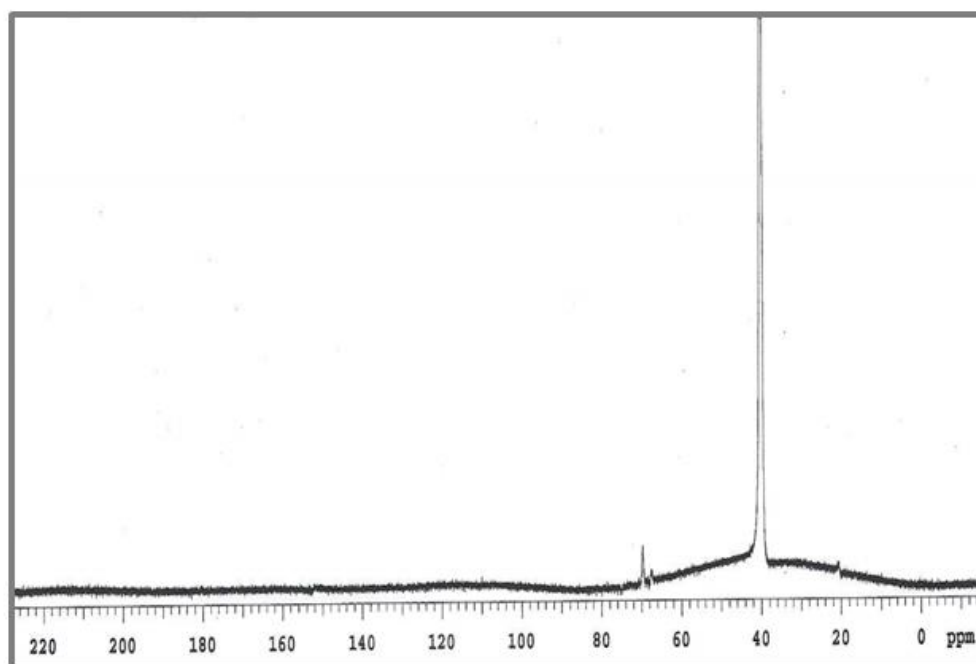


**Figure 3.83:**  $^{13}\text{C-NMR}$  spectrum of  $\text{L}_5 + \text{Pt}$  complex.

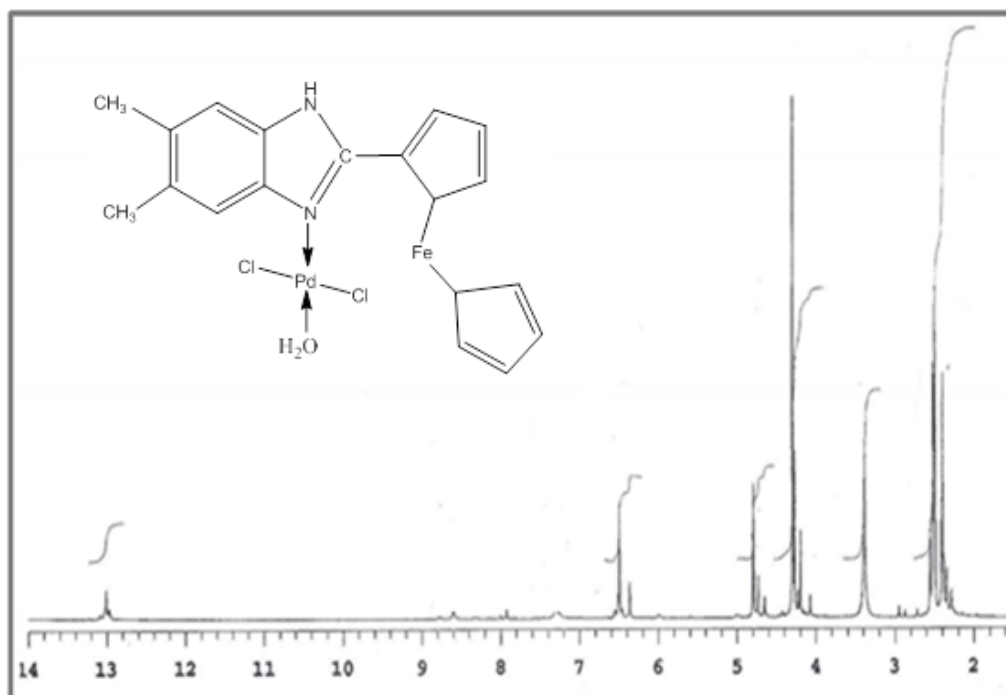




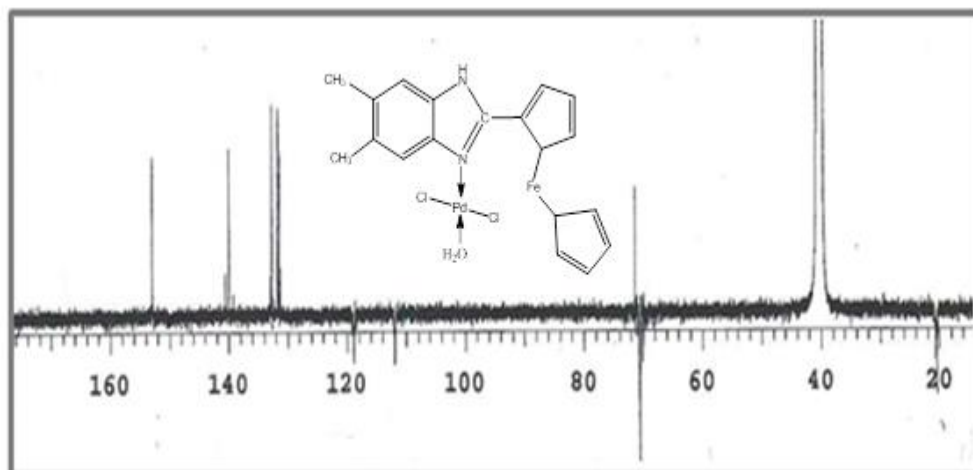
**Figure 3.84:**  $^1H$ -NMR spectrum of  $L_6+Zn$  complex.



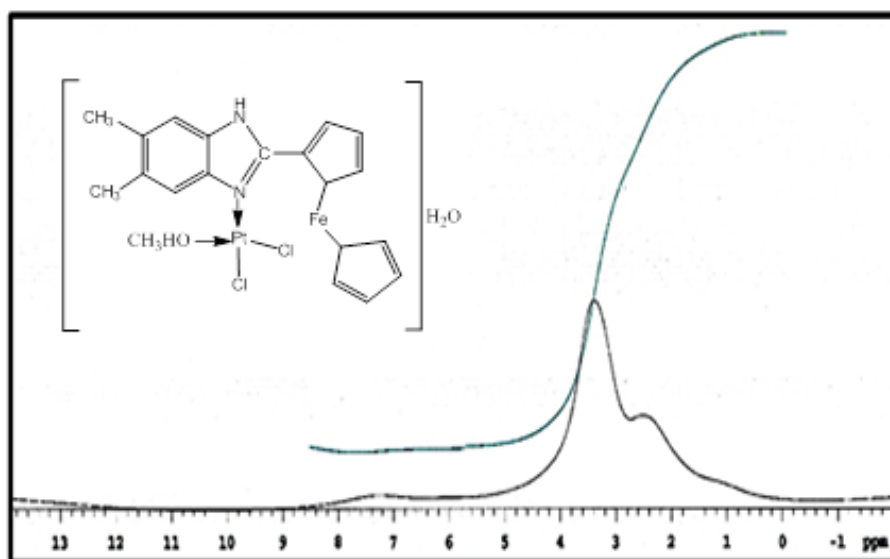
**Figure 3.85:**  $^{13}C$ -NMR spectrum of  $L_6+Zn$  complex.



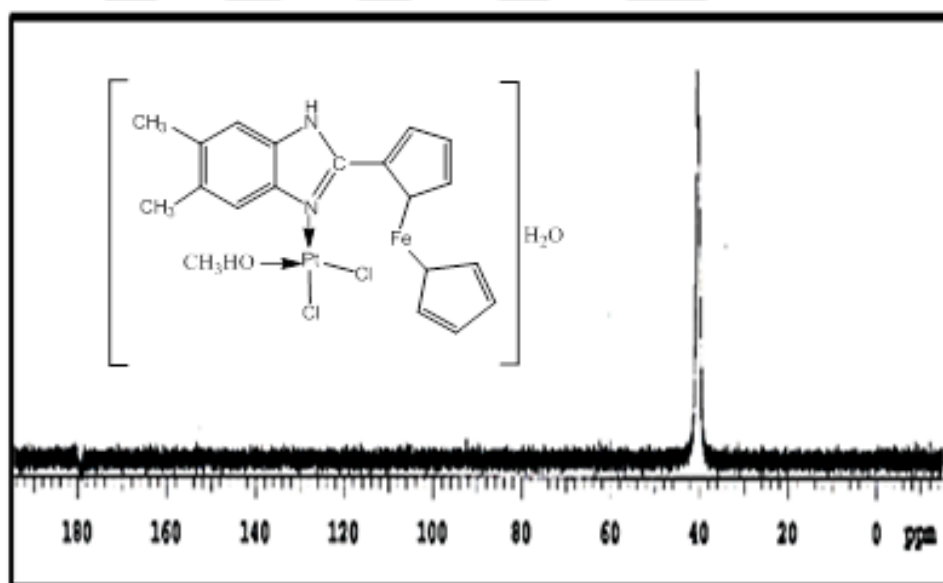
**Figure 3.86:**  $^1H$ -NMR spectrum of  $L_6 + Pd$  complex.



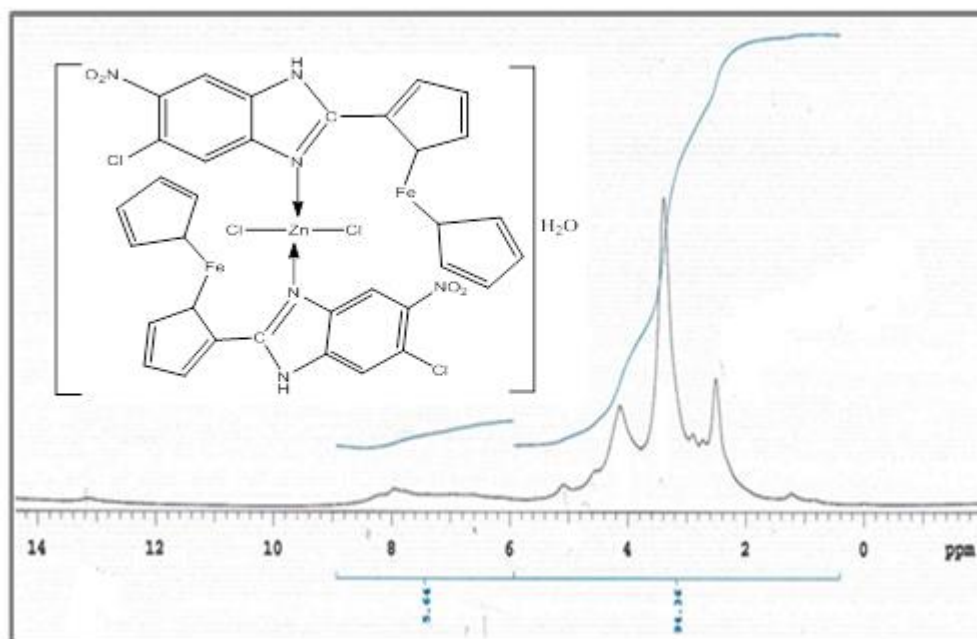
**Figure 3.87:**  $^{13}C$ -NMR spectrum of  $L_6 + Pd$  complex.



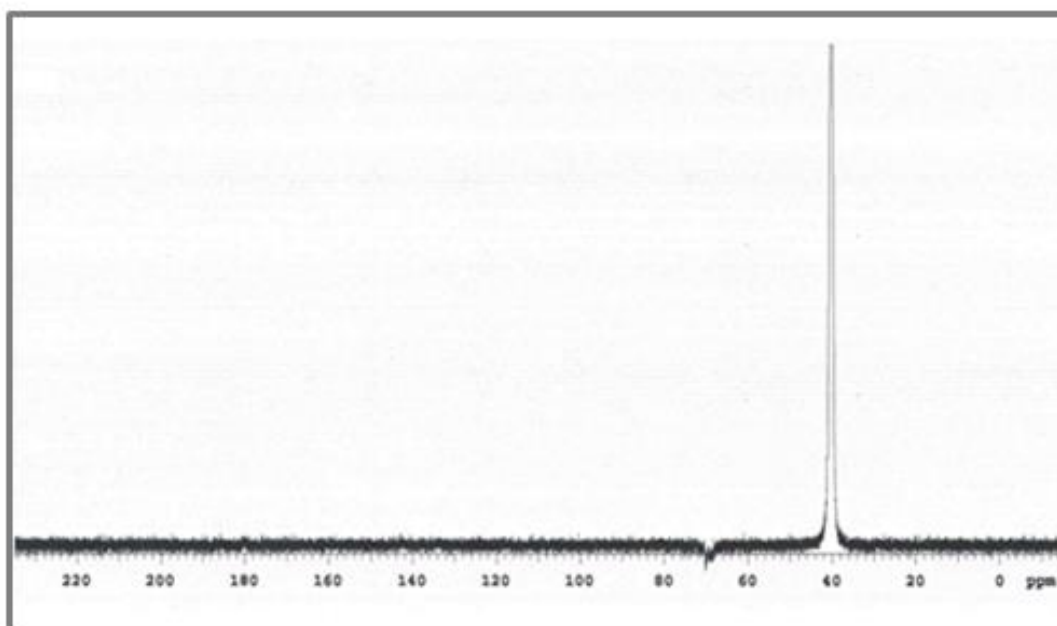
**Figure 3.88:**  $^1H$ -NMR spectrum of  $L_6+Pt$  complex.



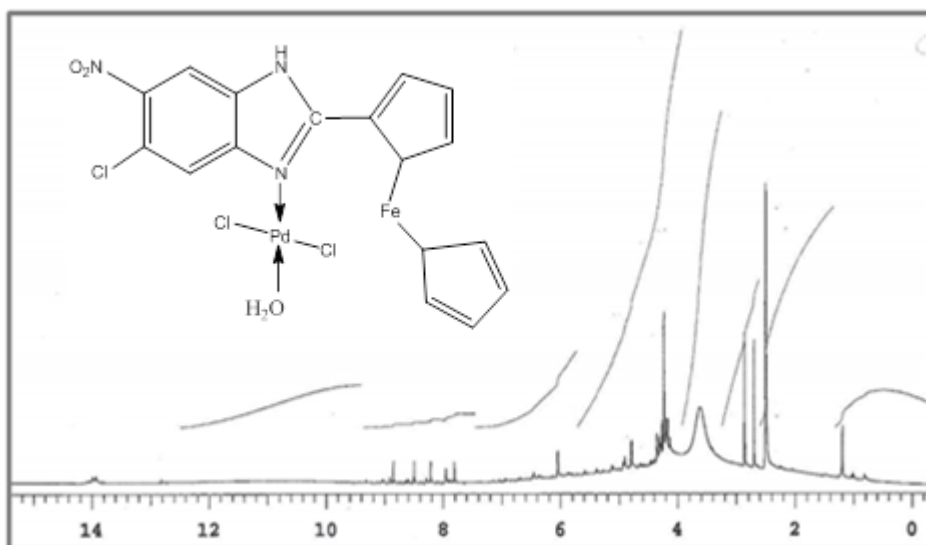
**Figure 3.89:**  $^{13}C$ -NMR spectrum of  $L_6+Pt$  complex.



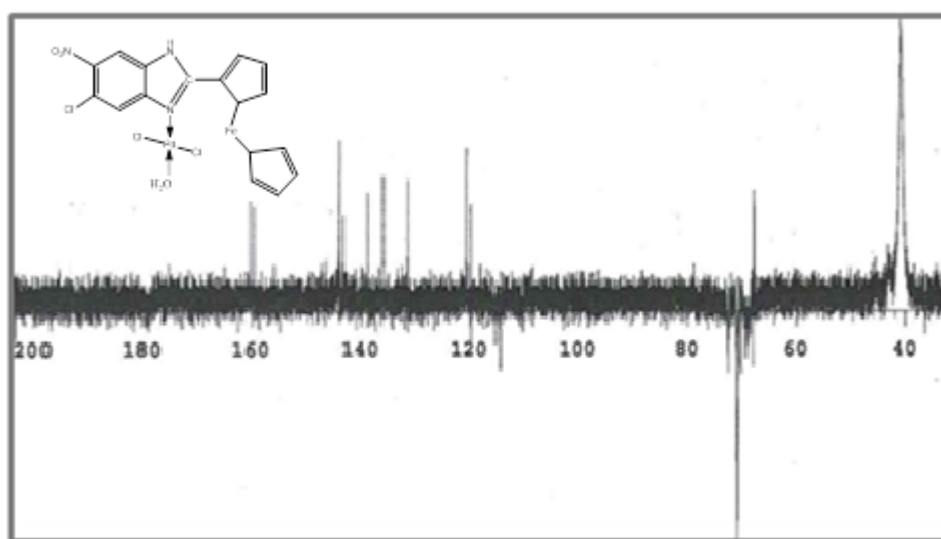
**Figure 3.90:**  $^1H$ -NMR spectrum of  $L_7+Zn$  complex.



**Figure 3.91:**  $^{13}C$ -NMR spectrum of  $L_7+Zn$  complex.



**Figure 3.92:**  $^1H$ -NMR spectrum of  $L_7+Pd$  complex.



**Figure 3.93:**  $^{13}C$ -NMR spectrum of  $L_7+Pd$  complex.

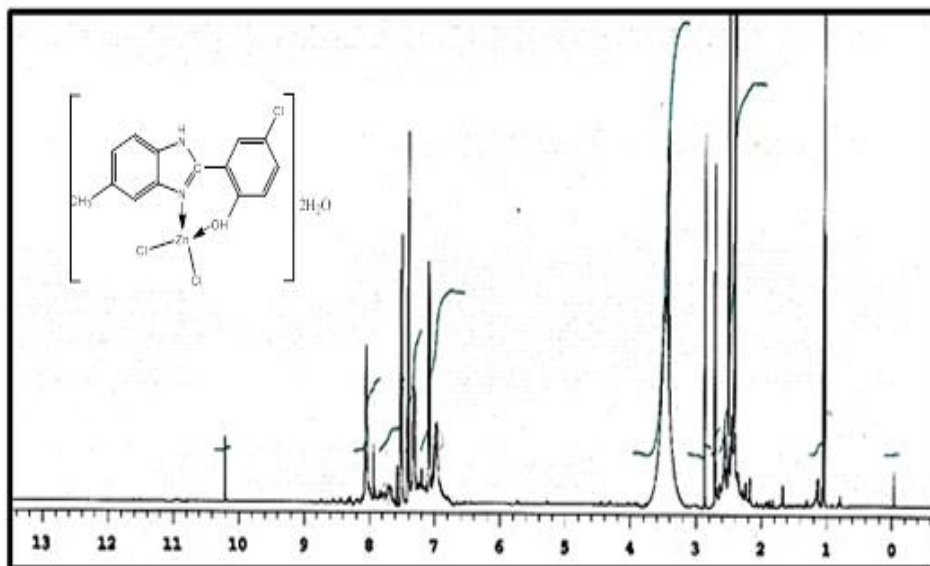


Figure 3.94:  $^1\text{H-NMR}$  spectrum of  $\text{HL}_8+\text{Zn}$  complex.

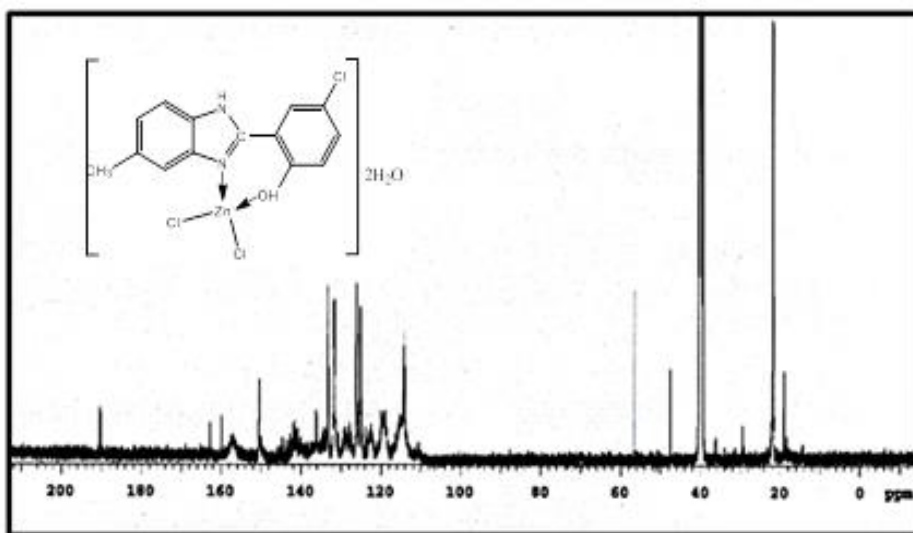


Figure 3.95:  $^{13}\text{C-NMR}$  spectrum of  $\text{HL}_8+\text{Zn}$  complex.

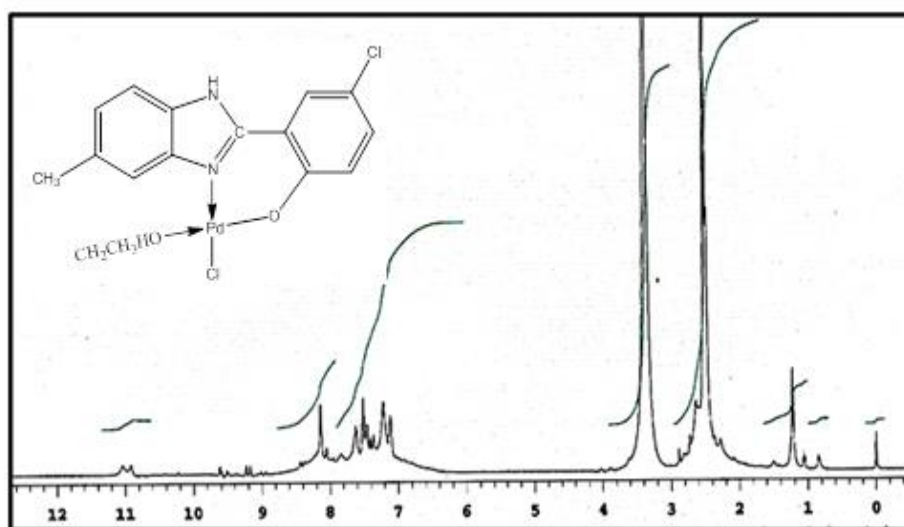


Figure 3.96:  $^1\text{H-NMR}$  spectrum of  $\text{HL}_8 + \text{Pd}$  complex.

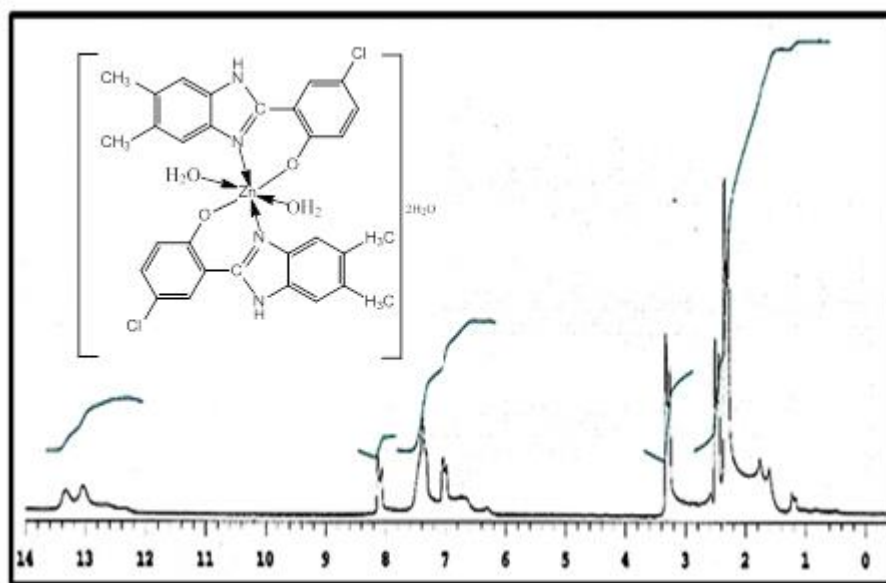
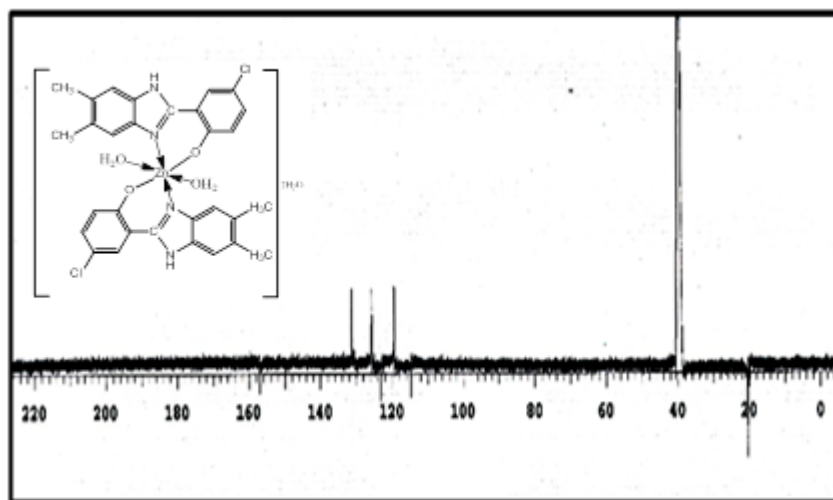
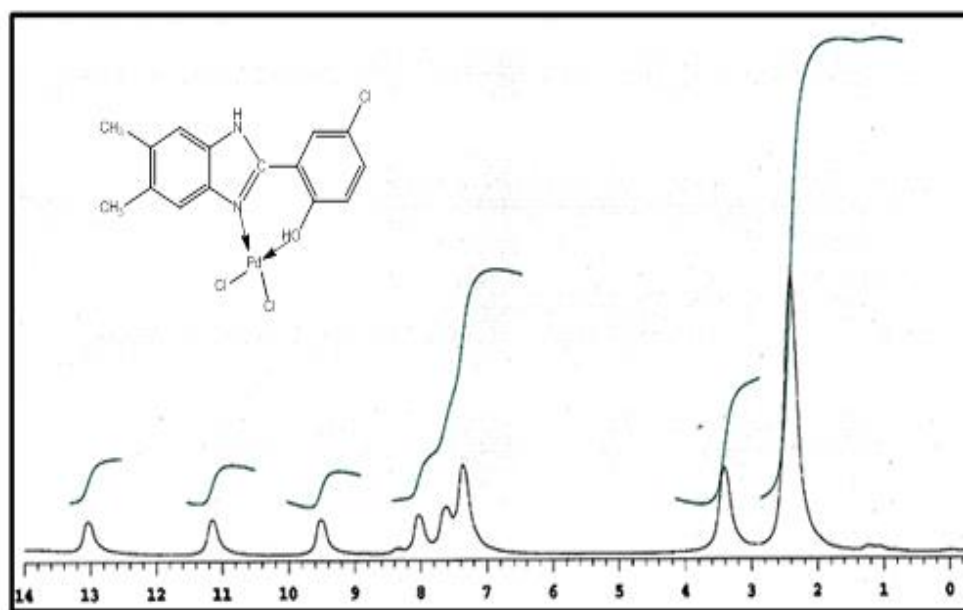


Figure 3.97:  $^1\text{H-NMR}$  spectrum of  $\text{HL}_9 + \text{Zn}$  complex.



**Figure 3.98:**  $^{13}\text{C}$ -NMR spectrum of  $\text{HL}_9+\text{Zn}$  complex.



**Figure 3.99:**  $^1\text{H}$ -NMR spectrum of  $\text{HL}_9+\text{Pd}$  complex.



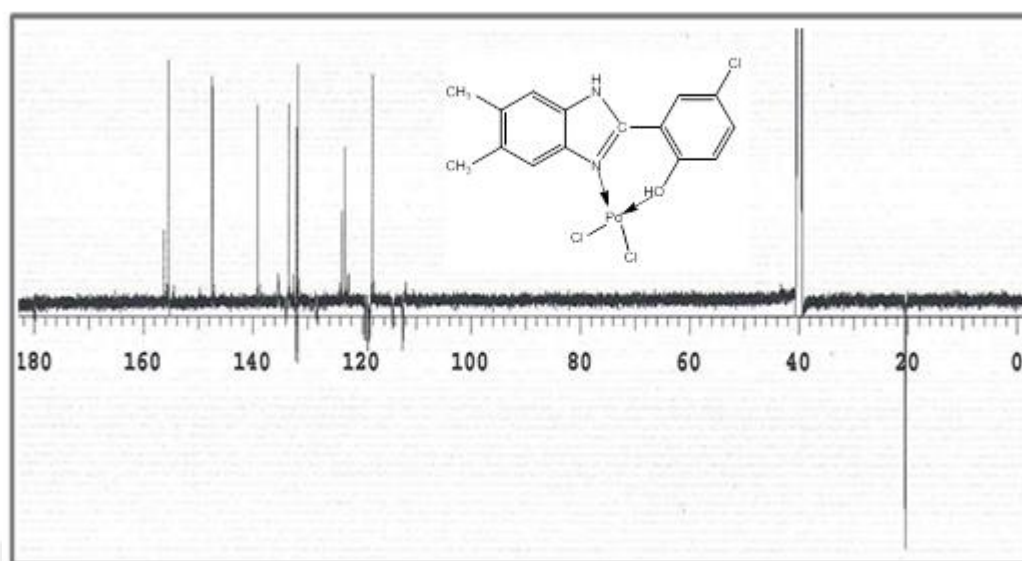


Figure 3.100:  $^{13}\text{C}$ -NMR spectrum of  $\text{HL}_9 + \text{Pd}$  complex.

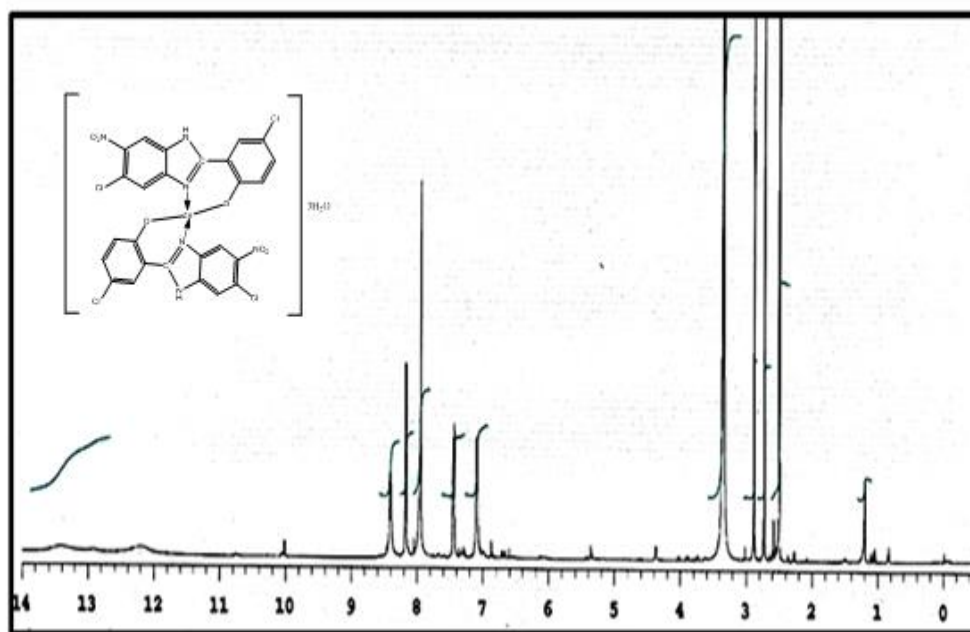


Figure 3.101:  $^1\text{H}$ -NMR spectrum of  $\text{HL}_{10} + \text{Zn}$  complex.

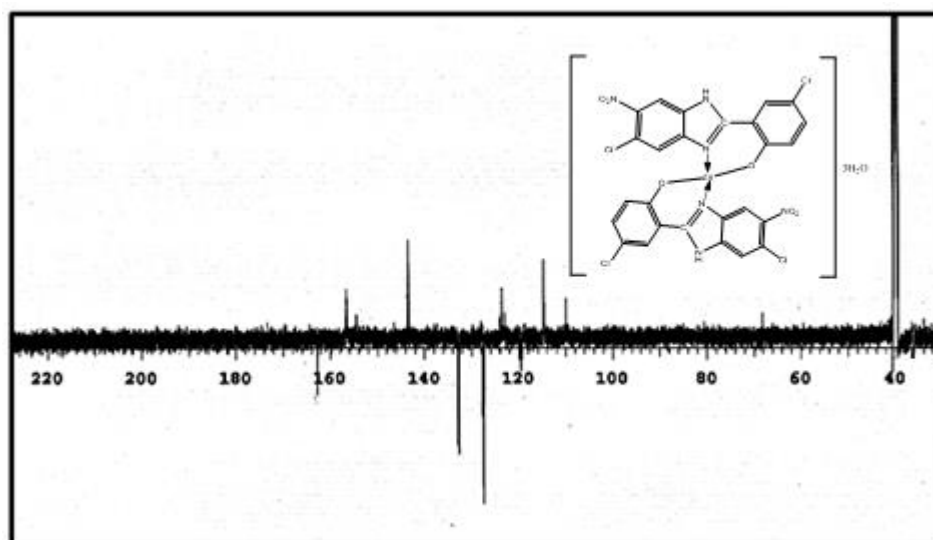


Figure 3.102:  $^{13}\text{C}$ -NMR spectrum of  $\text{HL}_{10}+\text{Zn}$  complex.

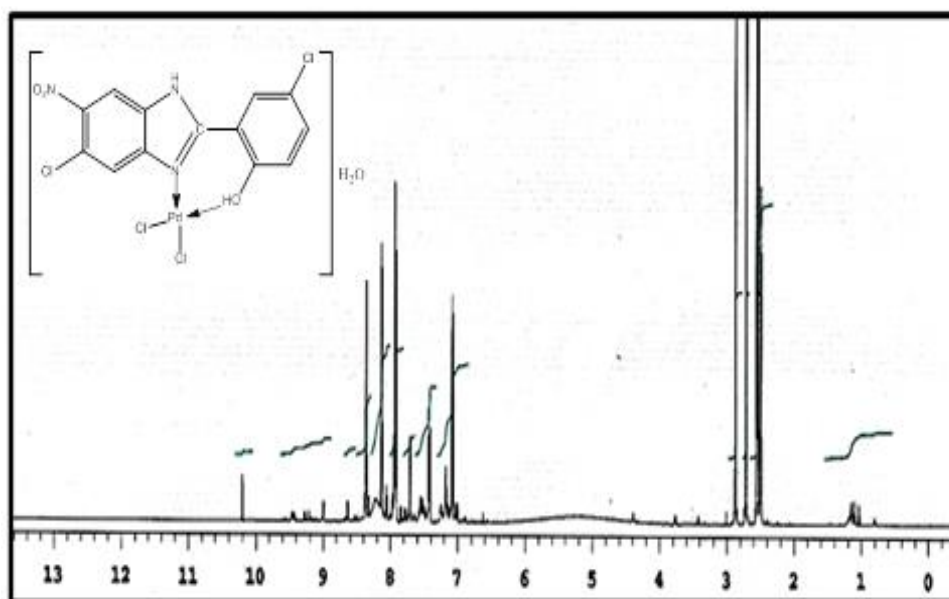
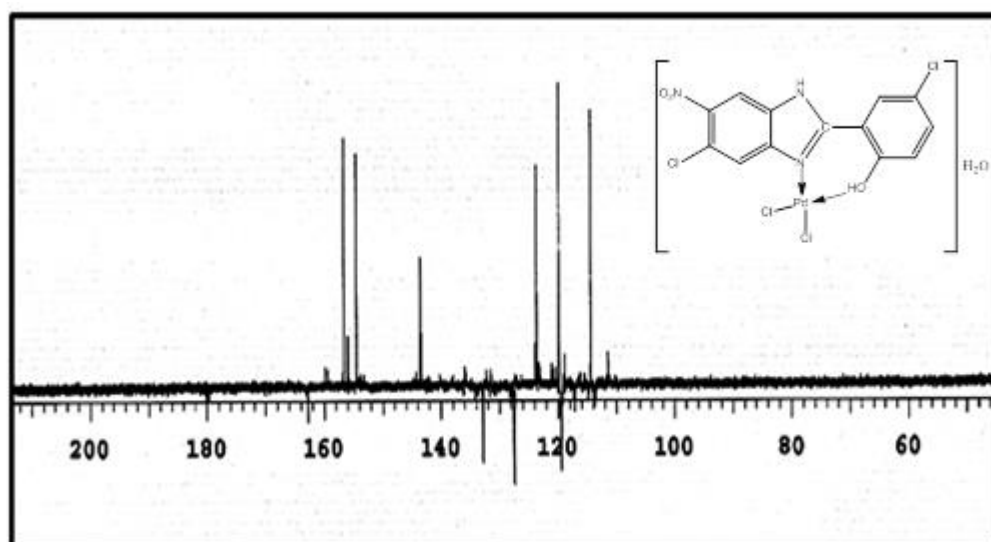


Figure 3.103:  $^1\text{H}$ -NMR spectrum of  $\text{HL}_{10}+\text{Pd}$  complex.



**Figure 3.104:**  $^{13}\text{C}$ -NMR spectrum of  $\text{HL}_{10}+\text{Pd}$  complex.

### 3.3. CRYSTAL STRUCTURE DETERMINATION

Single crystal X-ray diffraction data of  $\mathbf{H}_2\mathbf{L}_3$  and  $[\text{Pd}(\mathbf{L}_3)\text{CH}_3\text{CN}]\cdot\text{H}_2\text{O}$  complex are given at Tables 3.17 and 3.21, respectively. Also, the selected bond distance and angles, hydrogen bond parameters and selected torsion angles are given in Tables 3.18-3.24. Crystal structure of  $\mathbf{H}_2\mathbf{L}_3$  and  $[\text{Pd}(\mathbf{L}_3)\text{CH}_3\text{CN}]\cdot\text{H}_2\text{O}$  complex are given in Figures 3.105 and 3.107, respectively. Unit cell packing diagrams for  $\mathbf{H}_2\mathbf{L}_3$  and  $[\text{Pd}(\mathbf{L}_3)\text{CH}_3\text{CN}]\cdot\text{H}_2\text{O}$  complex are given in Figures 3.106 and 3.108.

**Table 3.17:** X-Ray crystallographic data for  $\mathbf{H}_2\mathbf{L}_3$ .

|   |   |
|---|---|
| Empirical formula   | $\text{C}_{14}\text{H}_{12}\text{ClNO}_2$ |
| Molecular weight, $\text{g mol}^{-1}$                                       | 261.70                                    |
| Color, habit  | Orange, prism                             |
| Crystal system  | Orthorhombic                              |
| Space group   | $\text{P}2_12_12_1$                       |
| $a / \text{\AA}$  | 8.2117(5)                                 |
| $b / \text{\AA}$  | 8.4637(7)                                 |
| $c / \text{\AA}$  | 18.4614(14)                               |
| $V / \text{\AA}^3$  | 1283.09(16)                               |
| Z value   | 4   |
| $d_{\text{calc}} / \text{g cm}^{-3}$  | 1.355                                     |
| $\mu(\text{Mo-K}\alpha) / \text{mm}^{-1}$                                   | 0.290                                     |
| $\theta$ range, $^\circ$  | 3.26 – 26.44                              |
| Measured refls.   | 29512                                     |
| Independent refls.  | 2639                                      |
| $R_{\text{int}}$  | 0.0565                                    |
| $R_1/wR_2$  | 0.0725/0.1324                             |
| Goodness of fit indicator, S  | 1.330                                     |
| $\Delta\rho_{\text{max}}/\Delta\rho_{\text{min}} (\text{e}\text{\AA}^{-3})$ | 0.22 / -0.261                             |

**Table 3.18:** Selected bond distances and angles for  $\mathbf{H}_2\mathbf{L}_3$  (Å, °).

|          |          |           |          |
|----------|----------|-----------|----------|
| C1–C7    | 1.409(6) | C1–C2     | 1.409(6) |
| C1–C6    | 1.433(6) | C6–O1     | 1.290(6) |
| C7–N1    | 1.293(6) | N1–C8     | 1.409(6) |
| C8–C13   | 1.388(6) | C2–C3     | 1.352(7) |
| C8–C9    | 1.393(6) | C9–O2     | 1.353(6) |
| C12–C14  | 1.513(7) | C11–C3    | 1.748(5) |
| C9–C8–N1 | 115.8(4) | C13–C8–N1 | 123.6(4) |
| C8–N1–C7 | 129.6(4) | O2–C9–C8  | 116.3(4) |
| O1–C6–C1 | 117.0(4) | O1–C6–C5  | 122.6(4) |
| C6–C1–C7 | 120.4(4) | C2–C1–C7  | 120.1(4) |
| C1–C7–N1 | 123.0(4) |           |          |

**Table 3.19:** Hydrogen bond parameters for  $\mathbf{H}_2\mathbf{L}_3$  (Å, °).

| D–H...A                  | D–H      | H...A    | D...A     | D–H...A |
|--------------------------|----------|----------|-----------|---------|
| N1–H1...O1               | 0.88 (5) | 1.78 (5) | 2.552 (5) | 146(4)  |
| O2–H2A...O1 <sup>i</sup> | 0.80 (3) | 1.77 (3) | 2.572 (5) | 175(4)  |

(i)  $x+1/2, -y+3/2, -z+1$ **Table 3.20:** Selected torsion angles for  $\mathbf{H}_2\mathbf{L}_3$  (°).

|               |           |              |           |
|---------------|-----------|--------------|-----------|
| C1–C7–N1–C8   | 178.8(4)  | C9–C8–N1–C7  | 173.2(5)  |
| C13–C8–N1–C7  | -7.7(8)   | N1–C8–C9–C10 | 178.2(4)  |
| O2–C9–C8–N1   | -1.7(6)   | O2–C9–C8–C13 | 179.2(4)  |
| O1–C6–C1–C7   | 1.5(7)    | C6–C1–C7–N1  | -0.4(7)   |
| O1–C6–C1–C2   | -179.1(4) | C2–C1–C7–N1  | -179.8(5) |
| C7–C1–C2–C3   | -177.3(5) | C1–C2–C3–C11 | -178.3(4) |
| O2–C9–C10–C11 | -178.7(5) |              |           |

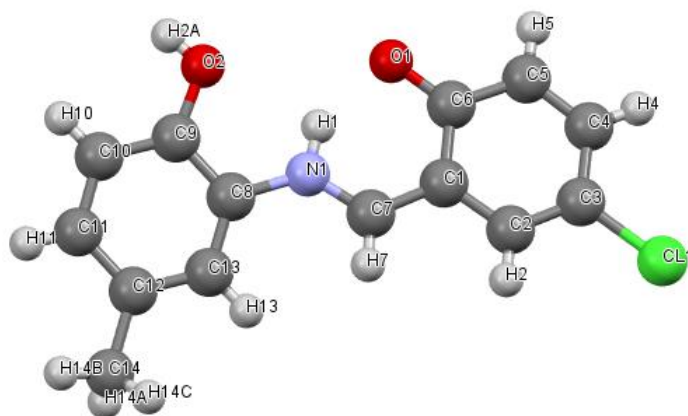


Figure 3.105: The molecular structure of  $\text{H}_2\text{L}_3$  showing the atom numbering scheme.

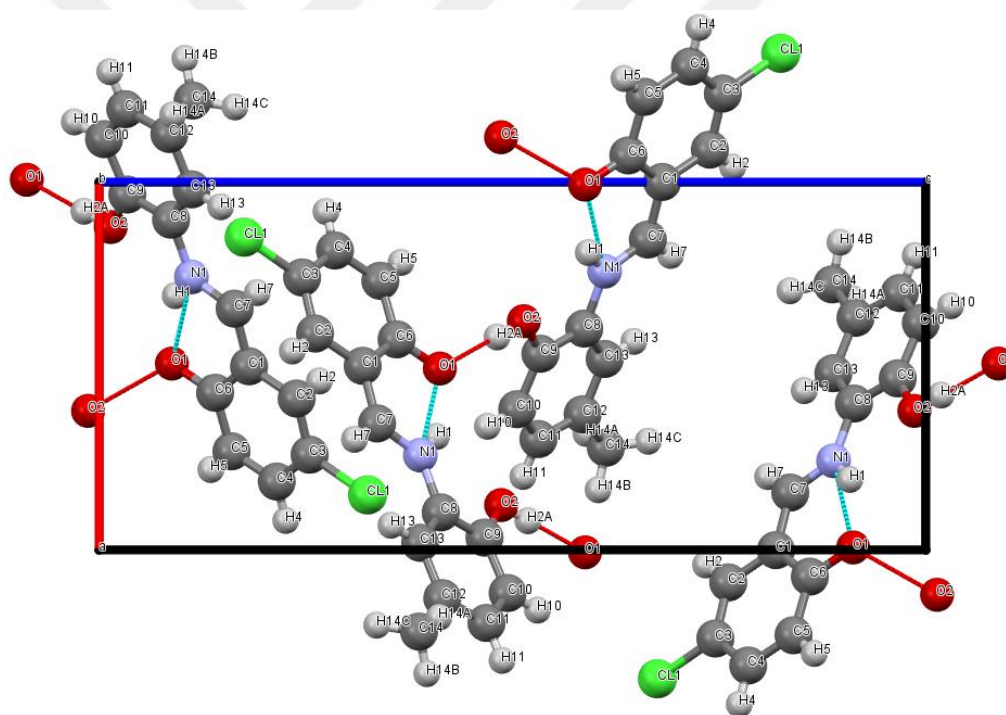
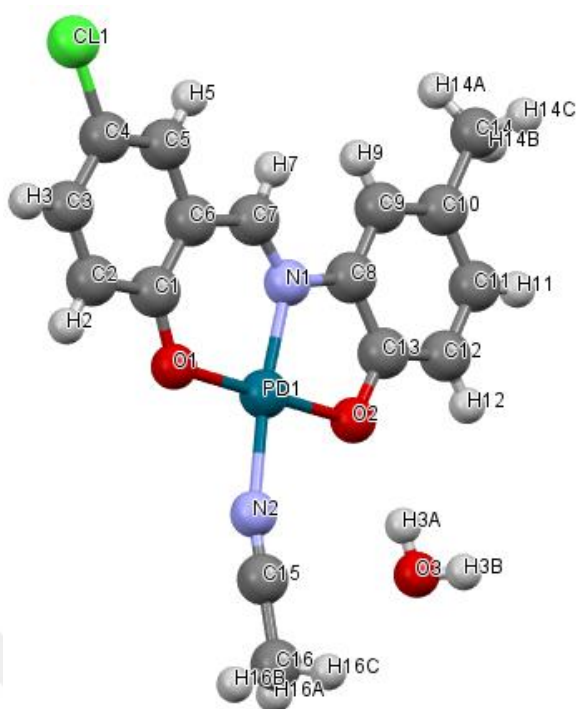


Figure 3.106: Unit cell packing diagram for  $\text{H}_2\text{L}_3$ ; molecular overlap view from the b-axis.

**Table 3.21:** X-Ray crystallographic data for [Pd(L<sub>3</sub>)CH<sub>3</sub>CN]·H<sub>2</sub>O complex.

|  |  |
|--|--|
| Empirical formula  | C <sub>16</sub> H <sub>15</sub> ClN <sub>2</sub> O <sub>3</sub> Pd |
| Molecular weight, g mol <sup>-1</sup>                    | 425.15   |
| Color, habit   | Bronze, block  |
| Crystal system   | Monoclinic   |
| Space group  | C2/c   |
| <i>a</i> / Å   | 37.335(4)  |
| <i>b</i> / Å   | 4.5608(4)  |
| <i>c</i> / Å   | 19.156(2)  |
| <i>V</i> / Å <sup>3</sup>                                | 3260.2(6)  |
| Z value  | 8  |
| <i>d</i> <sub>calc</sub> / g cm <sup>-3</sup>            | 1.732  |
| μ(Mo-Kα) / mm <sup>-1</sup>                              | 1.317  |
| θ range, °   | 3.10 – 26.44   |
| Measured refls.  | 35153  |
| Independent refls.                                       | 3368   |
| <i>R</i> <sub>int</sub>                                  | 0.0851   |
| <i>R</i> <sub>1</sub> / <i>wR</i> <sub>2</sub>           | 0.0847 / 0.1830  |
| Goodness of fit indicator, S                             | 1.169  |
| Δρ <sub>max</sub> /Δρ <sub>min</sub> (eÅ <sup>-3</sup> ) | 0.632 / -1.311   |



**Figure 3.107:** The molecular structure of  $[\text{Pd}(\text{L}_3)\text{CH}_3\text{CN}] \cdot \text{H}_2\text{O}$  complex showing the atom numbering scheme.

**Table 3.22:** Hydrogen bond parameters for  $[\text{Pd}(\text{L}_3)\text{CH}_3\text{CN}] \cdot \text{H}_2\text{O}$  complex ( $\text{\AA}$ ,  $^\circ$ ).

| D–H $\cdots$ A                    | D–H     | H $\cdots$ A | D $\cdots$ A | D–H $\cdots$ A |
|-----------------------------------|---------|--------------|--------------|----------------|
| C16–H16B $\cdots$ O1 <sup>i</sup> | 0.96    | 2.46         | 3.315 (14)   | 148.7          |
| O3–H3A $\cdots$ O2 <sup>ii</sup>  | 0.83(2) | 1.94(4)      | 2.758(10)    | 168(17)        |

(i)  $-x, -y, -z$ ; (ii)  $-x+1/2, -y-1/2, -z$

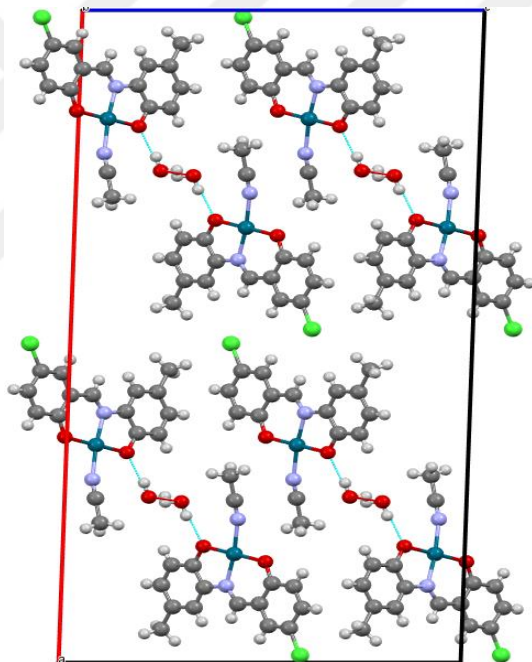


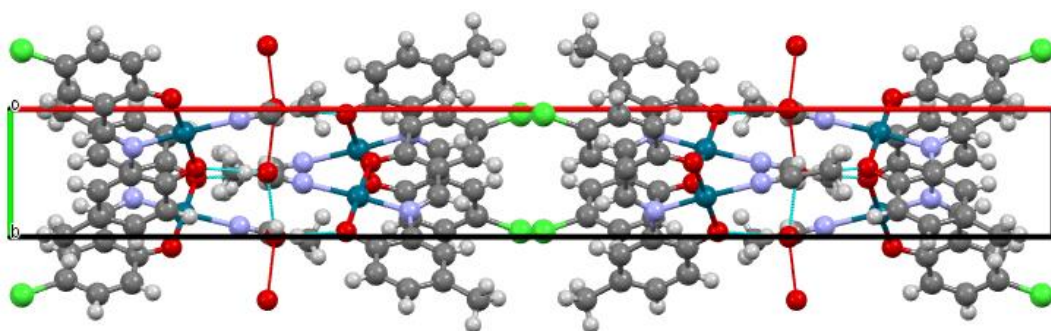
**Table 3.23:** Selected bond distances and angles for [Pd(L<sub>3</sub>)CH<sub>3</sub>CN]·H<sub>2</sub>O complex (Å, °).

|            |           |            |           |
|------------|-----------|------------|-----------|
| C6–C7      | 1.425(12) | C4–C11     | 1.744(8)  |
| C6–C1      | 1.409(11) | C1–O1      | 1.308(10) |
| C13–O2     | 1.334(11) | C7–N1      | 1.293(11) |
| N1–C8      | 1.430(11) | N2–C15     | 1.108(12) |
| C8–C9      | 1.376(12) | C8–C13     | 1.393(12) |
| Pd1–N2     | 2.042(7)  | O2–Pd1     | 1.982(6)  |
| O1–Pd1     | 1.969(6)  | N1–Pd1     | 1.947(7)  |
| C6–C7–N1   | 124.5(7)  | C6–C1–O1   | 126.7(8)  |
| C1–O1–Pd1  | 122.5(5)  | O1–Pd1–N1  | 95.8(3)   |
| Pd1–N2–C15 | 167.3(8)  | N2–C15–C16 | 178.8(13) |
| C7–N1–C8   | 123.6(7)  | N1–Pd1–N2  | 172.9(3)  |
| C9–C8–N1   | 126.2(7)  | C9–C8–C13  | 121.2(8)  |
| C13–C8–N1  | 112.5(7)  | C11–C4–C5  | 120.6(7)  |
| O1–C1–C2   | 116.7(7)  | C11–C4–C3  | 119.4(7)  |
| O1–Pd1–N2  | 90.9(3)   | O2–Pd1–N2  | 89.9(3)   |
| N1–Pd1–O2  | 83.5(3)   |            |           |

**Table 3.24:** Selected torsion angles for  $[\text{Pd}(\text{L}_3)\text{CH}_3\text{CN}]\cdot\text{H}_2\text{O}$  complex (°).

|                |           |               |           |
|----------------|-----------|---------------|-----------|
| O1–C1–C2–C3    | 178.6(8)  | O1–C1–C6–C5   | -178.1(8) |
| O1–C1–C6–C7    | 1.4(14)   | C5–C6–C7–N1   | 179.1(8)  |
| C1–C6–C7–N1    | -0.5(14)  | N1–C8–C9–C10  | 180.0(8)  |
| C9–C8–C13–O2   | -179.2(8) | N1–C8–C13–O2  | 1.4(11)   |
| C6–C7–N1–C8    | -179.3(8) | C6–C7–N1–Pd1  | -5.3(12)  |
| C9–C8–N1–C7    | -6.4(13)  | C13–C8–N1–C7  | 173.0(8)  |
| C9–C8–N1–Pd1   | 179.1(7)  | C13–C8–N1–Pd1 | -1.6(9)   |
| C6–C1–O1–Pd1   | 3.5(12)   | C2–C1–O1–Pd1  | -175.8(6) |
| C12–C13–O2–Pd1 | -178.6(7) | C8–C13–O2–Pd1 | -0.6(10)  |

**Figure 3.108:** Unit cell packing diagram for  $[\text{Pd}(\text{L}_3)\text{CH}_3\text{CN}]\cdot\text{H}_2\text{O}$  complex; molecular overlap view from the b-axis.

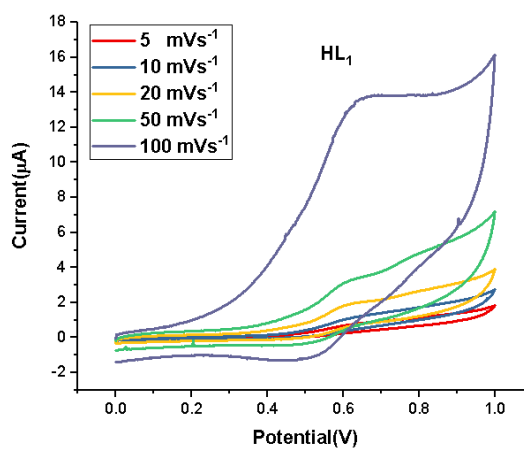


**Figure 3.109:** Unit cell packing diagram for  $[\text{Pd}(\text{L}_3)\text{CH}_3\text{CN}] \cdot \text{H}_2\text{O}$  complex; molecular overlap view from the c-axis.

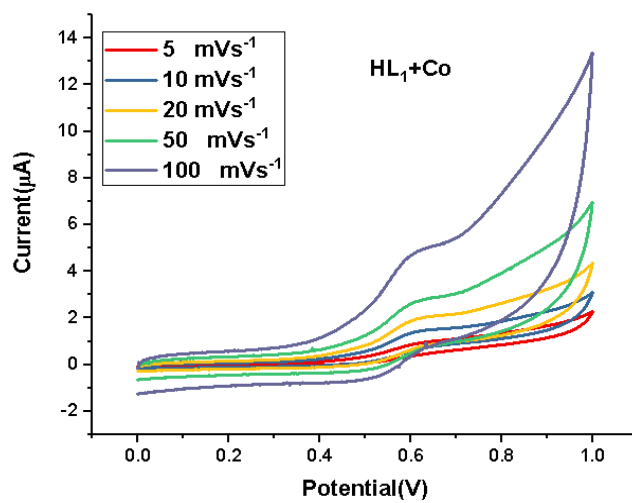
### 3.4. CYCLIC VOLTAMMETRY

**Table 3.25:** Electrochemical parameter of the ligands including ferrocene groups (**HL<sub>1</sub>**, **HL<sub>2</sub>**, **L<sub>5</sub>**, **L<sub>6</sub>** and **L<sub>7</sub>**) and their  $\text{Co}^{2+}$  complexes on GCE electrode vs. Ag/AgCl in methanol solution inclosing 0.1M TBAP as supporting electrolyte at 100 m Vs<sup>-1</sup> scan rate at 25°C.

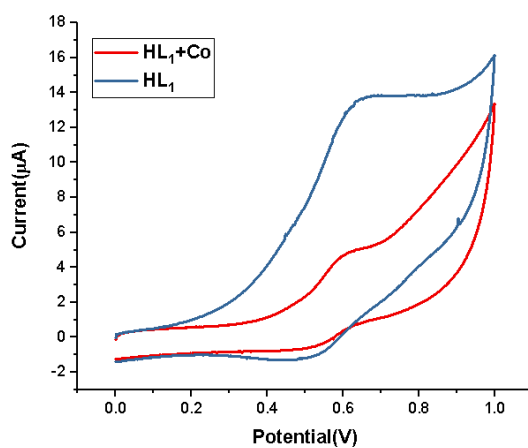
| Compound ID   | E <sub>pa</sub> (V) | E <sub>pc</sub> (V) | ΔE <sub>p</sub> (V) | E° (V) | I <sub>pc</sub> /I <sub>pa</sub> |
|---|---------------------|---------------------|---------------------|--------|----------------------------------|
| <b>HL<sub>1</sub></b>   | 0.64                | 0.51                | 0.13                | 0.57   | 0.8                              |
| [Co( <b>HL<sub>1</sub></b> )Cl <sub>2</sub> (H <sub>2</sub> O) <sub>2</sub> ]·H <sub>2</sub> O              | 0.61                | 0.52                | 0.09                | 0.56   | 0.9                              |
| <b>HL<sub>2</sub></b>   | 0.28, 0.79          | 0.52, 0.72          | 0.07                | 0.75   | 0.9                              |
| [Co( <b>HL<sub>2</sub></b> ) <sub>2</sub> Cl <sub>2</sub> ]·H <sub>2</sub> O                                | 0.61                | 0.54                | 0.07                | 0.57   | 0.9                              |
| <b>L<sub>5</sub></b>  | 0.64                | 0.48                | 0.16                | 0.56   | 0.8                              |
| [Co( <b>L<sub>5</sub></b> )Cl <sub>2</sub> (H <sub>2</sub> O) <sub>3</sub> ]                                | 0.61                | 0.49                | 0.12                | 0.55   | 0.8                              |
| <b>L<sub>6</sub></b>  | 0.67                | 0.54                | 0.13                | 0.6    | 0.8                              |
| [Co( <b>L<sub>6</sub></b> )Cl <sub>2</sub> (H <sub>2</sub> O) <sub>3</sub> ]·3H <sub>2</sub> O              | 0.59                | 0.48                | 0.11                | 0.53   | 0.8                              |
| <b>L<sub>7</sub></b>  | 0.60                | 0.49                | 0.11                | 0.54   | 0.8                              |
| [Co( <b>L<sub>7</sub></b> ) <sub>2</sub> Cl <sub>2</sub> (H <sub>2</sub> O) <sub>2</sub> ]·H <sub>2</sub> O | 0.61                | 0.54                | 0.07                | 0.57   | 0.9                              |



**Figure 3.110:** Cyclic voltammograms of **HL<sub>1</sub>** at GCE at different scan rates.



**Figure 3.111:** Cyclic voltammograms of Co(II) + **HL<sub>1</sub>** at GCE at different scan rates .



**Figure 3.112:** Cyclic voltammograms of **HL<sub>1</sub>** and Co(II) + **HL<sub>1</sub>** at GCE at scan rates 100mVs<sup>-1</sup>.

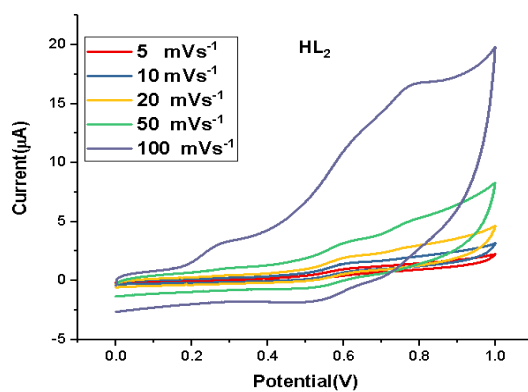


Figure 3.113: Cyclic voltammograms of HL<sub>2</sub> at GCE at different scan rates.

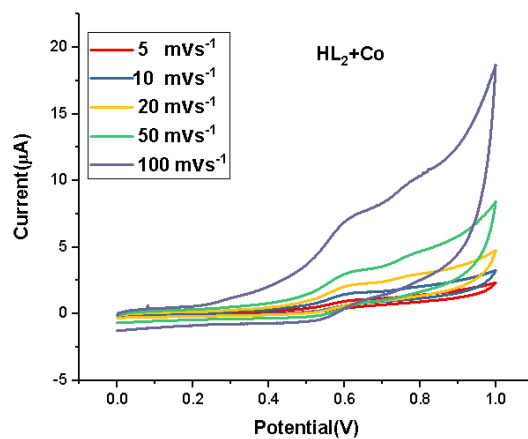
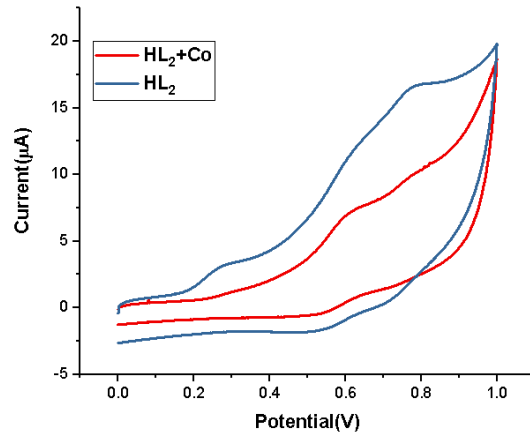
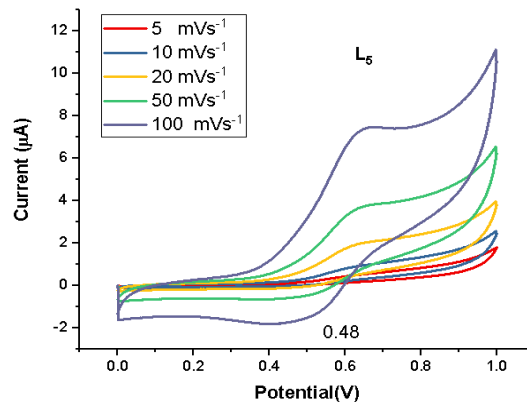


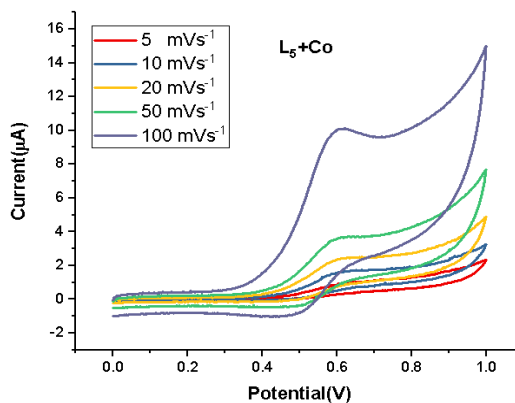
Figure 3.114: Cyclic voltammograms of Co(II)+HL<sub>2</sub> at GCE at different scan rates.



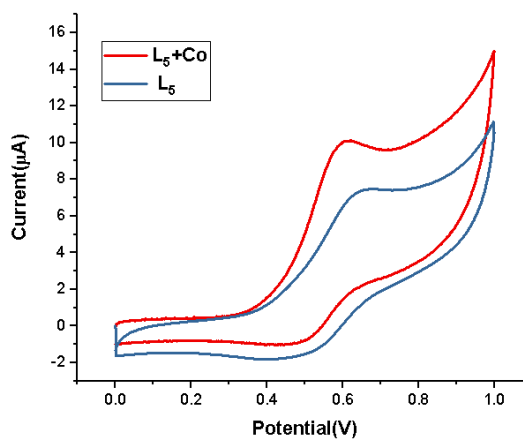
**Figure 3.115:** Cyclic voltammograms of **HL<sub>2</sub>** and **Co(II) +HL<sub>2</sub>** at GCE at scan rates 100 mVs<sup>-1</sup>.



**Figure 3.116:** Cyclic voltammograms of **L<sub>5</sub>** at GCE at different scan rates.

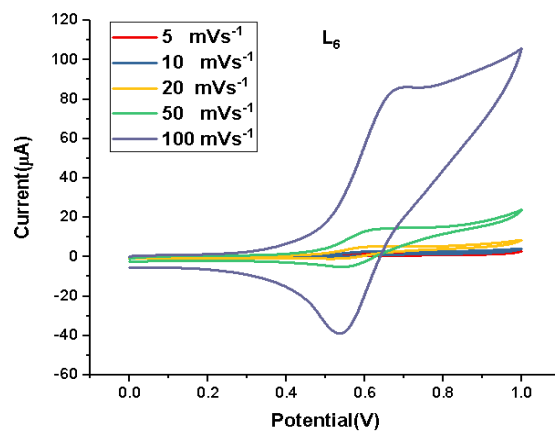


**Figure 3.117:** Cyclic voltammograms of  $\text{Co(II)} + \text{L}_5$  at GCE at different scan rates.

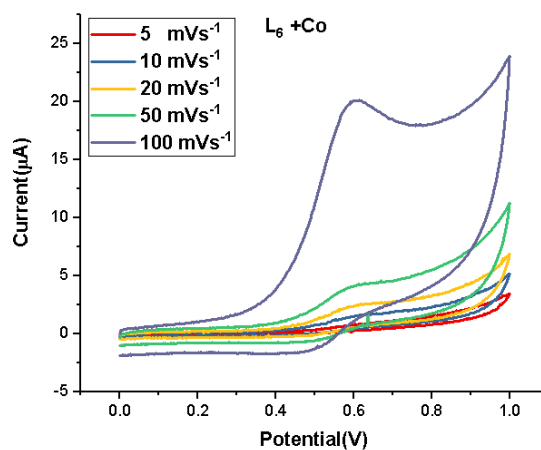


**Figure 3.118:** Cyclic voltammograms of  $\text{L}_5$  and  $\text{Co(II)} + \text{L}_5$  at GCE at scan rates 100  $\text{mVs}^{-1}$ .

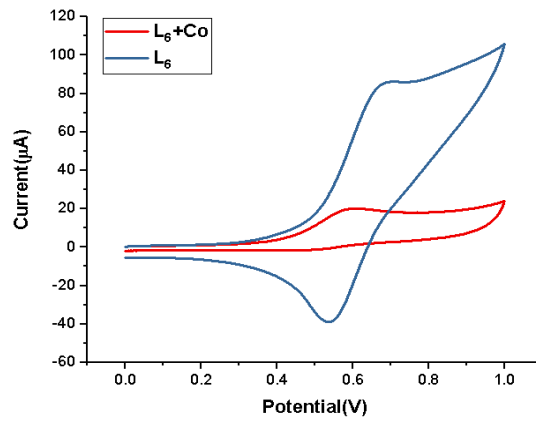




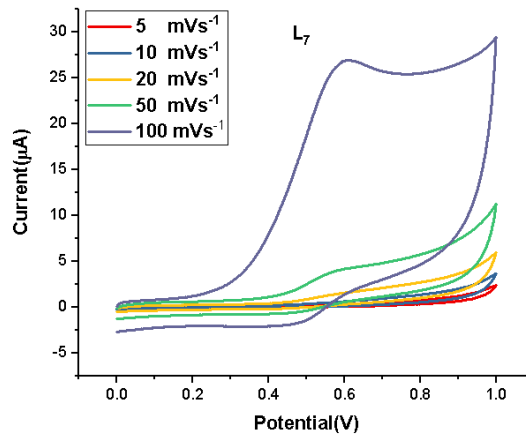
**Figure 3.119:** Cyclic voltammograms of  $L_6$  at GCE at different scan rates.



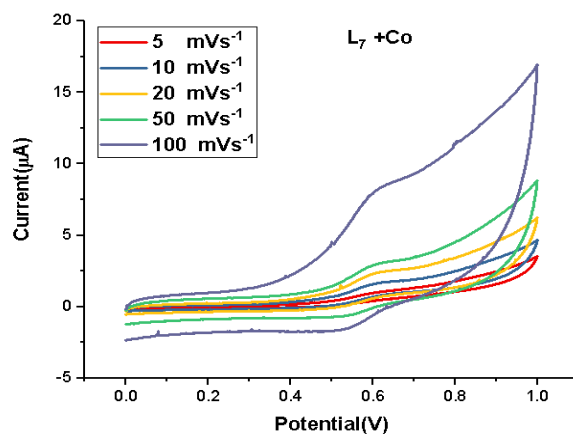
**Figure 3.120:** Cyclic voltammograms of  $Co(II) + L_6$  at GCE at different scan rates.



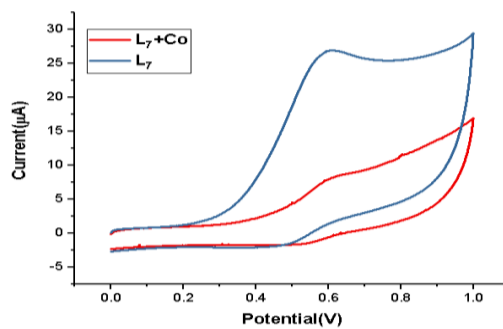
**Figure 3.121:** Cyclic voltammograms of  $L_6$  and  $Co(II) + L_6$  at GCE at scan rates  $100 \text{ mVs}^{-1}$ .



**Figure 3.122:** Cyclic voltammograms of  $L_7$  at GCE at different scan rates.



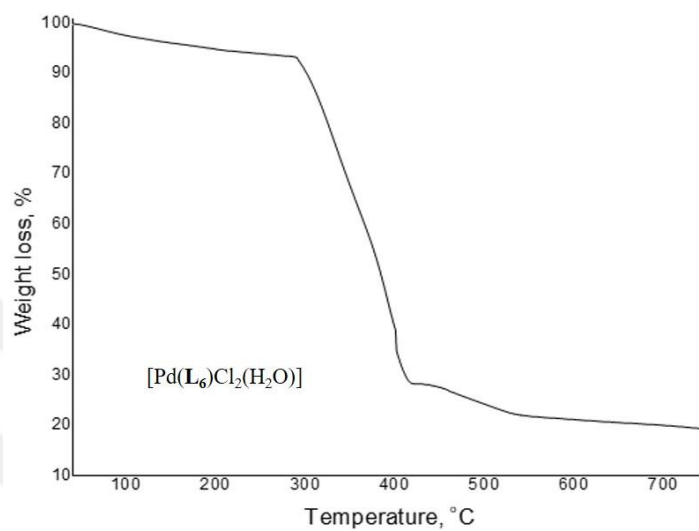
**Figure 3.123:** Cyclic voltammograms of  $Co(II) + L_7$  at GCE at different scan rates.



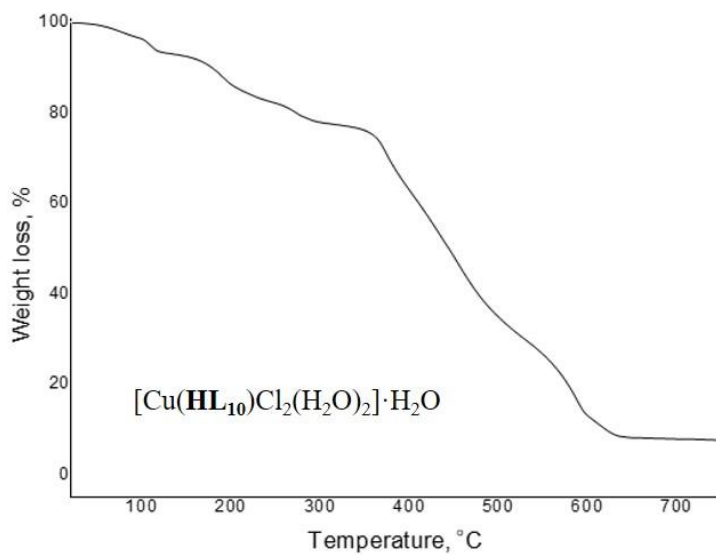
**Figure 3.124:** Cyclic voltammograms of  $L_7$  and  $Co(II) + L_7$  at GCE at scan rates 100  $mVs^{-1}$ .

### 3.5. THERMO GRAVIMETRIC ANALYSIS (TGA)

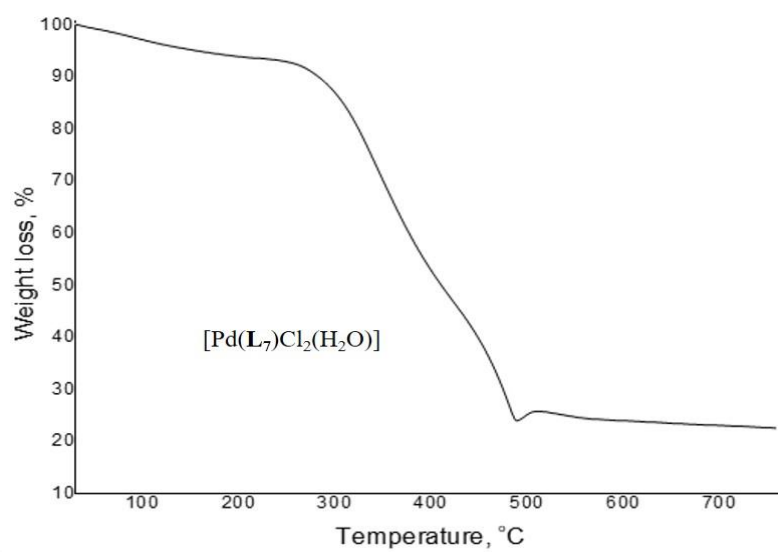
The TGA spectra corresponding spectra are given in Figures 3.125 - 3.129.



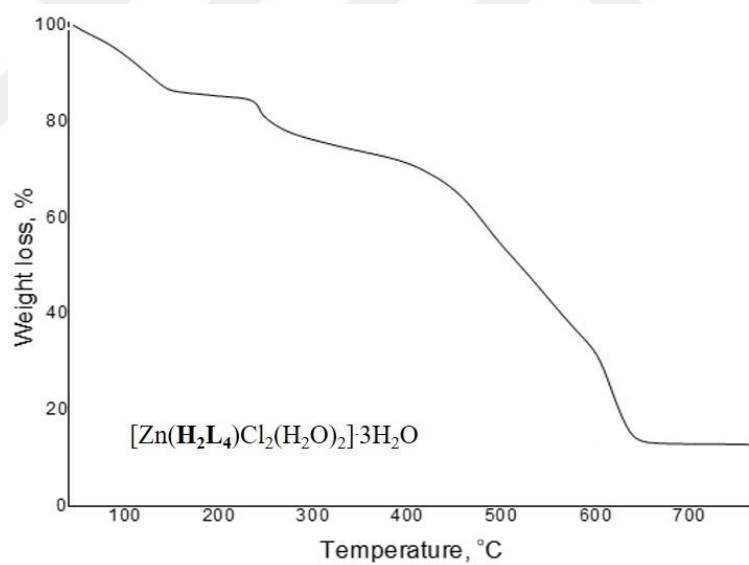
**Figure 3.125:** TGA spectrum of Pd +  $\text{L}_6$



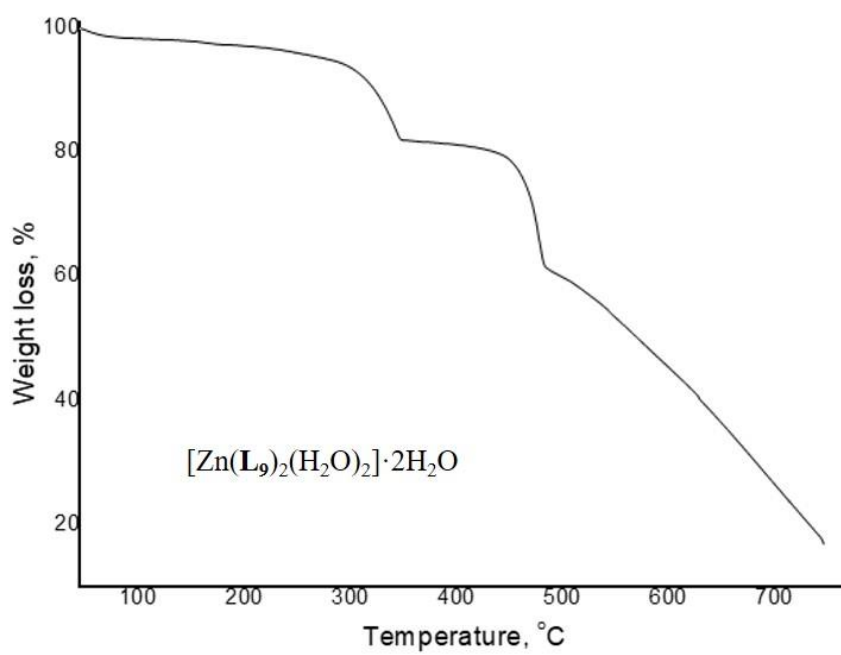
**Figure 3.126:** TGA spectrum of Cu+  $\text{HL}_{10}$



**Figure 3.127:** TGA spectrum of Pd +  $\text{L}_7$



**Figure 3.128:** TGA spectrum of Zn +  $\text{H}_2\text{L}_4$



**Figure 3.129:** TGA spectrum of Zn + L<sub>9</sub>

### 3.6. SUGGESTED STRUCTURES FOR THE METAL COMPLEXES

Based on the above results, following structures are assigned for the metal complexes.

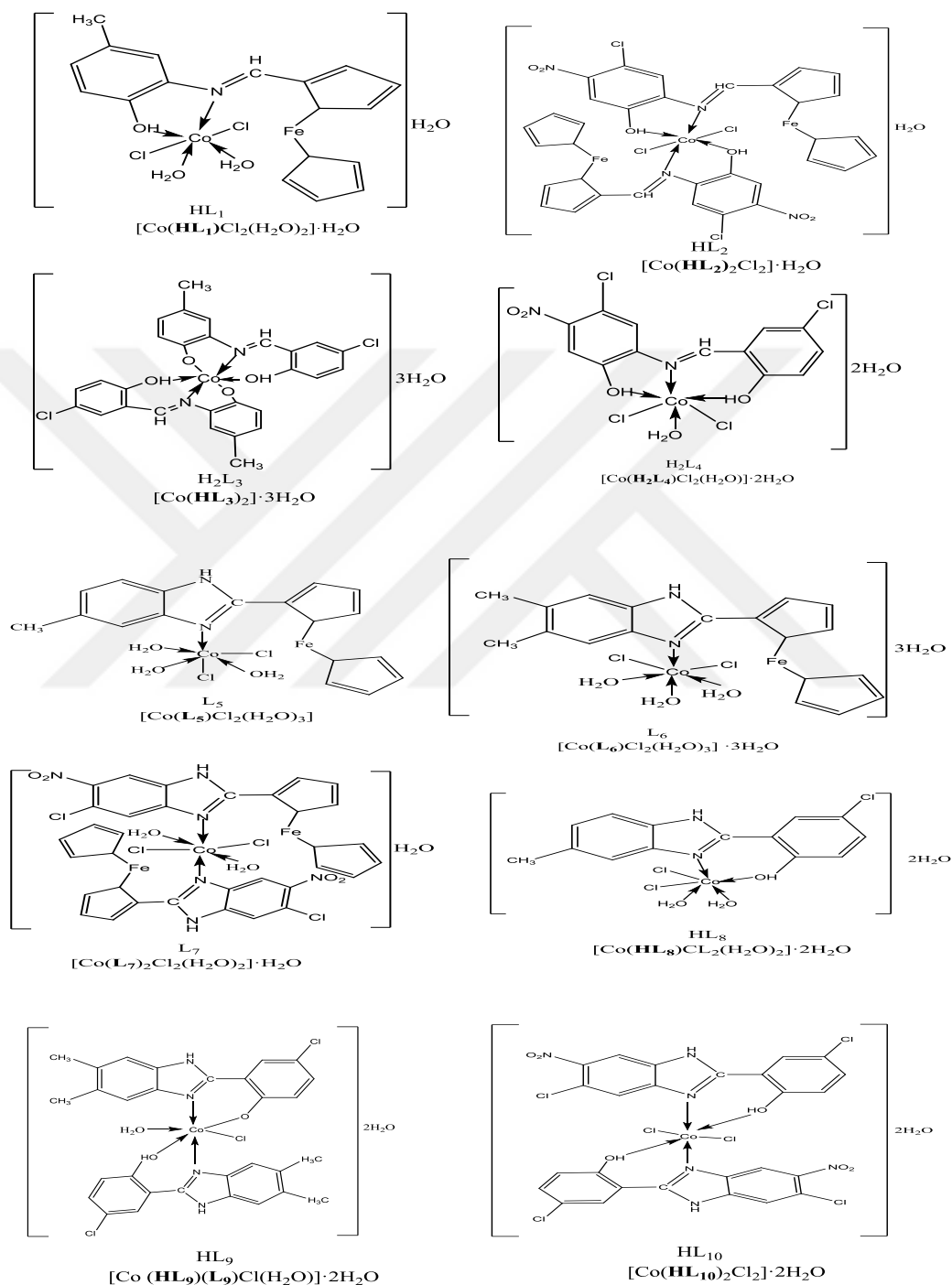
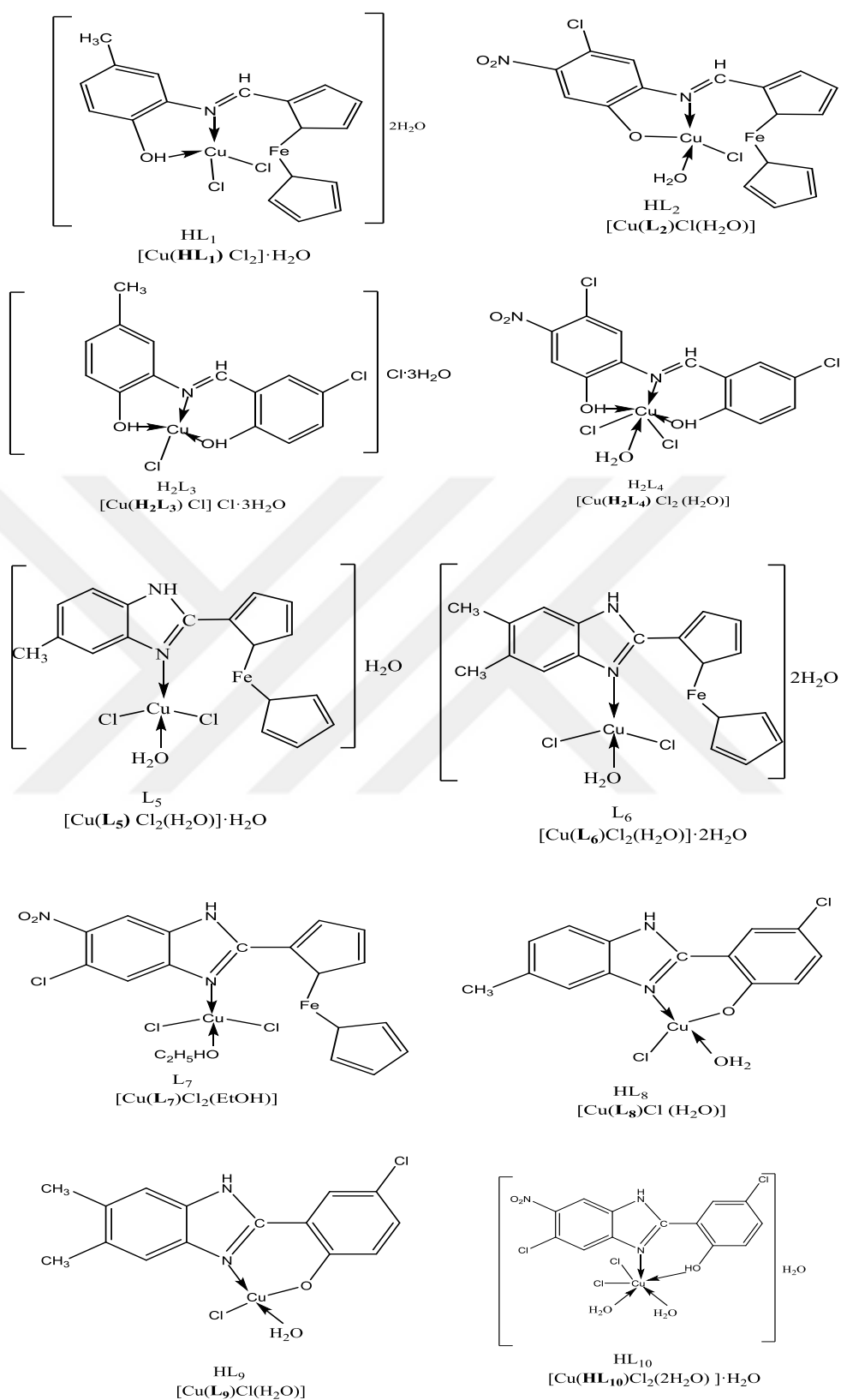
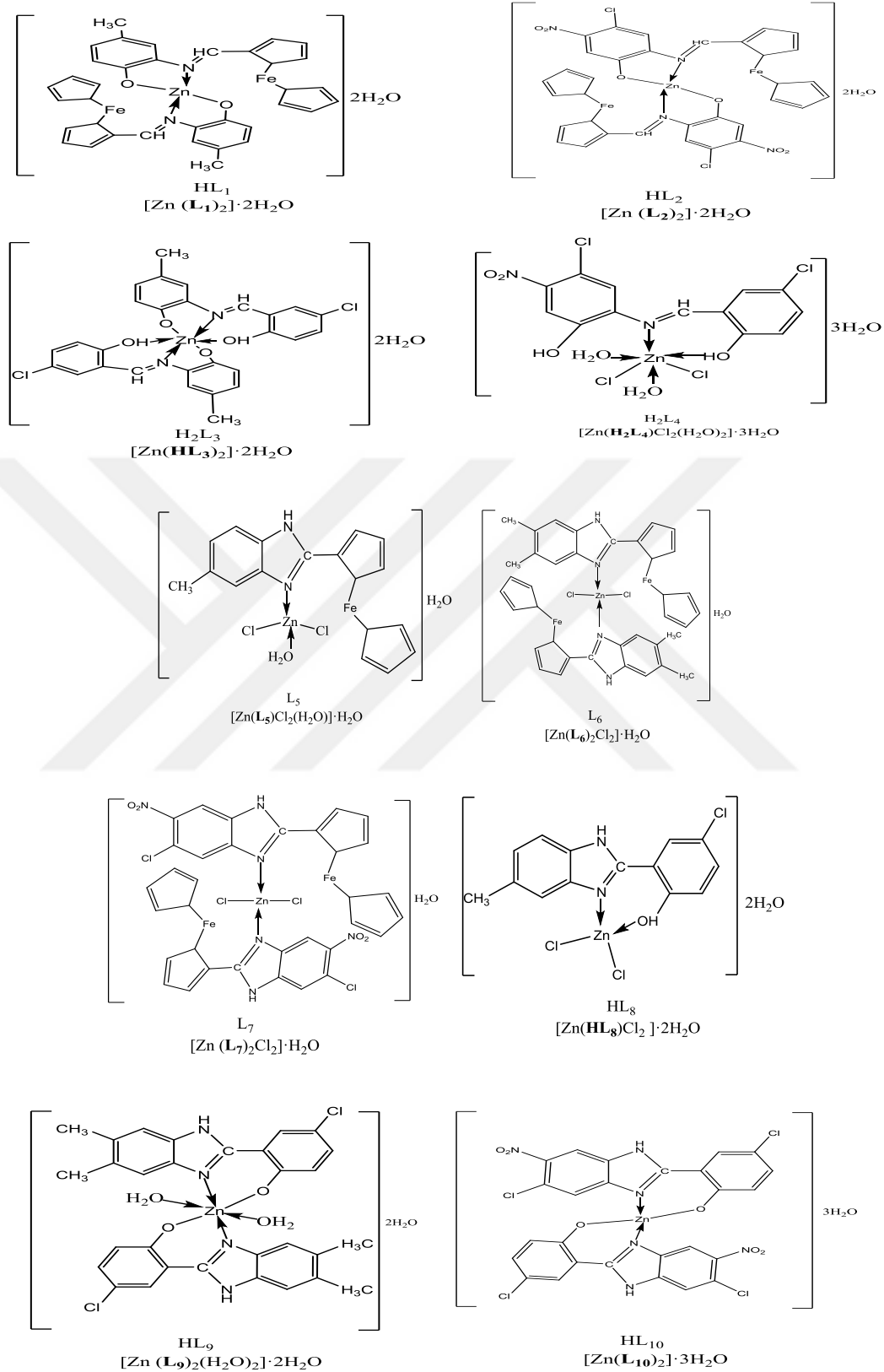


Figure 3.130: Proposed structures for the Co(II) complexes.

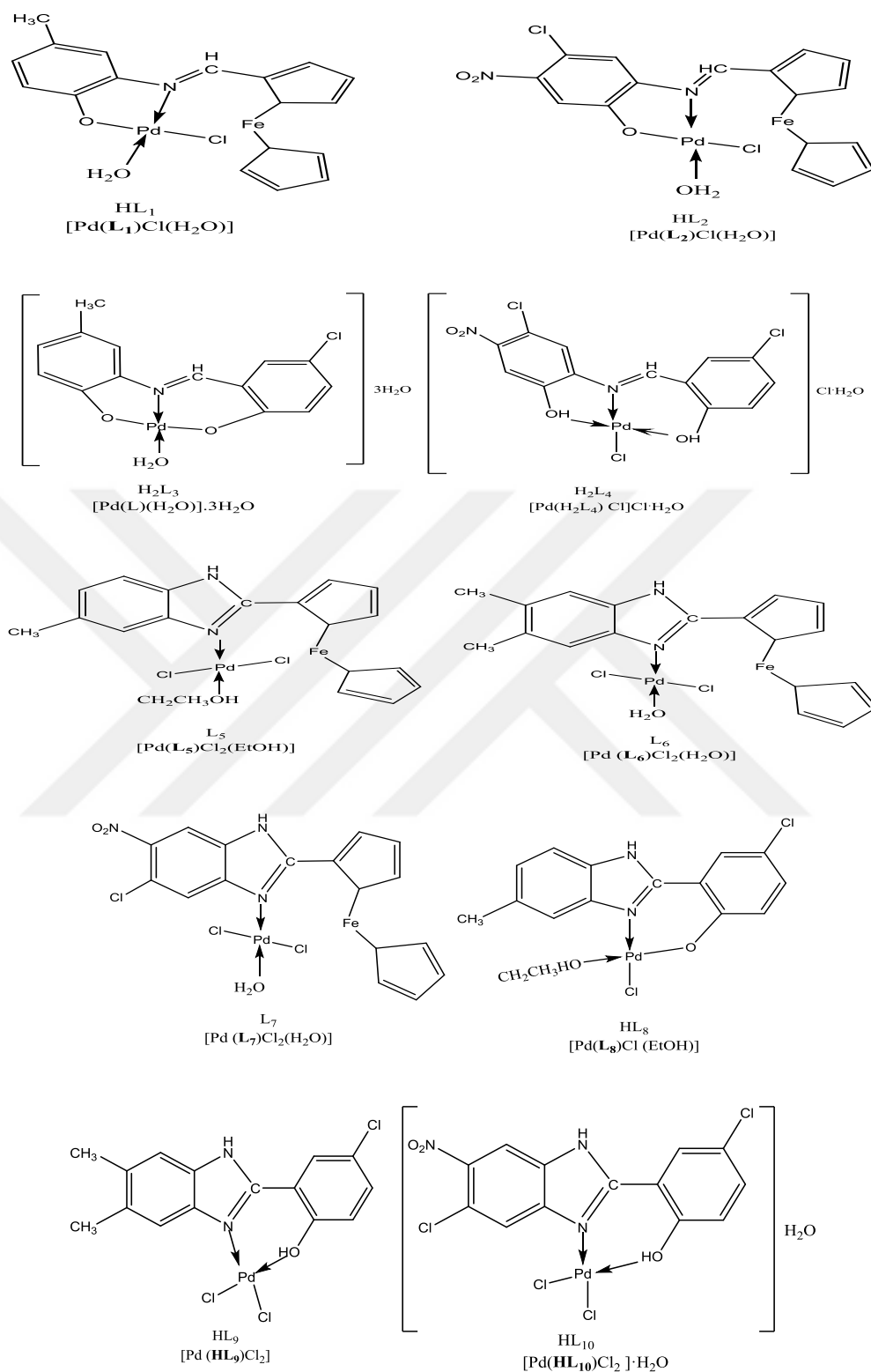


**Figure 3.131:** Proposed structures for the Cu(II) complexes.

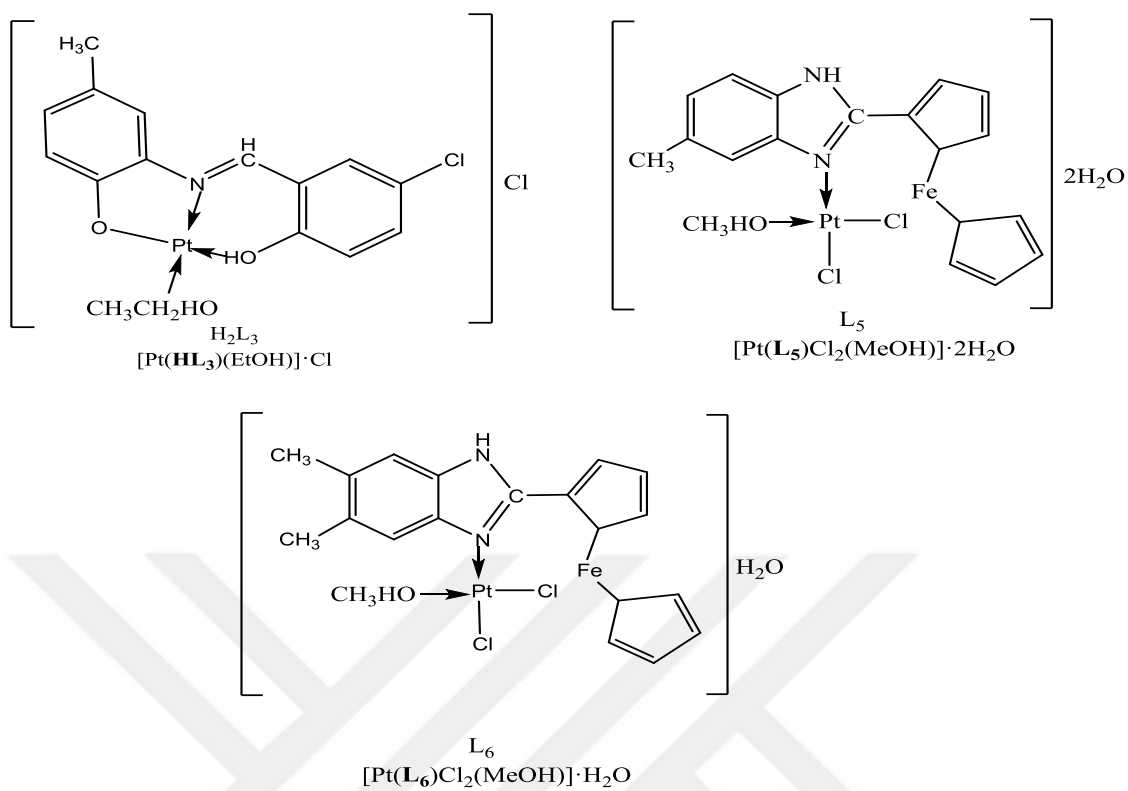




**Figure 3.132:** Proposed structures for the Zn(II) complexes.



**Figure 3.133:** Proposed structures for the Pd(II) complexes.



**Figure 3.134:** Proposed structures for the Pt(II) complexes.

### 3.7. ANTIMICROBIAL ACTIVITY OF THE COMPOUNDS

**Table 3.26:** *In vitro* antimicrobial activity of the compounds and the standard reagents (MIC,  $\mu\text{g mL}^{-1}$ ).

| Microorganisms   |      |      |   |       |     |       |     |     |      |
|--|------|------|---|-------|-----|-------|-----|-----|------|
| Compound   | 1    | 2    | 3 | 4     | 5   | 6     | 7   | 8   | 9    |
| <b>L<sub>5</sub></b>   | 312  | 1250 | - | -     | -   | -     | -   | -   | 312  |
| [Co( <b>L<sub>5</sub></b> )Cl <sub>2</sub> (H <sub>2</sub> O) <sub>3</sub> ]     | 312  | 1250 | - | -     | -   | 625   | 39  | 78  | 156  |
| [Pd( <b>L<sub>5</sub></b> )Cl <sub>2</sub> (EtOH)]                               | 312  | 625  | - | -     | -   | -     | -   | -   | 312  |
| [Cu( <b>L<sub>5</sub></b> )Cl <sub>2</sub> (H <sub>2</sub> O)]·H <sub>2</sub> O  | 312  | 1250 | - | -     | 625 | -     | -   | -   | 625  |
| <b>L<sub>6</sub></b>   | 625  | 625  | - | -     | -   | -     | -   | -   | 1250 |
| [Pd( <b>L<sub>6</sub></b> )Cl <sub>2</sub> (H <sub>2</sub> O)]                   | 625  | 625  | - | -     | -   | -     | -   | 625 | 1250 |
| [Cu( <b>L<sub>6</sub></b> )Cl <sub>2</sub> (H <sub>2</sub> O)]·2H <sub>2</sub> O | 312  | 625  | - | 1250  | -   | -     | -   | -   | 625  |
| <b>L<sub>7</sub></b>   | 312  | 1250 | - | -     | -   | -     | 312 | -   | 312  |
| [Cu( <b>L<sub>7</sub></b> )Cl <sub>2</sub> (EtOH)]                               | 625  | 625  | - | -     | -   | -     | -   | 625 | 625  |
| <b>HL<sub>1</sub></b>  | 156  | 1250 | - | 625   | -   | -     | 312 | -   | 625  |
| <b>HL<sub>2</sub></b>  | 1250 | 625  | - | 312   | 312 | 312   | -   | 625 | 625  |
| [Co( <b>HL<sub>2</sub></b> ) <sub>2</sub> Cl <sub>2</sub> ]·H <sub>2</sub> O     | 312  | 1250 | - | 625   | -   | -     | 312 | 312 | 625  |
| Ciprofloxacin  | 0.25 | -    | - | 0.625 | 0.5 | 0.312 | -   | -   | -    |
| Amphotericin B   | -    | -    | - | -     | -   | -     | 0.5 | 1.0 | 1.0  |

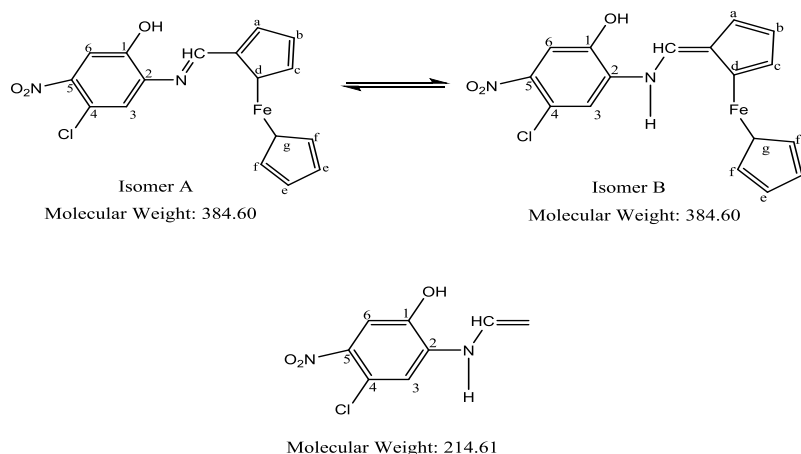
1= *S. aureus* ATCC 29213, 2 = *S. epidermidis* ATCC 12228, 3 = *E. coli* ATCC 25922, 4 = *K. pneumoniae* ATCC 4352, 5= *P. aeruginosa* ATCC 27853, 6=*P. mirabilis* ATCC 14153, 7= *C. albicans* ATCC 1023, 8=*C. parapsilosis* ATCC 22019, 9= *C. tropicalis* ATCC 750.

## 4. DISCUSSION

This chapter explanation around the physical properties and structural details of Schiff bases, benzimidazole derivatives and their metal complexes with  $\text{Cu}^{2+}$ ,  $\text{Zn}^{2+}$ ,  $\text{Co}^{2+}$ ,  $\text{Pt}^{2+}$  and  $\text{Pd}^{2+}$  ions. the synthesized compounds characterized by melting point, elemental analysis, IR, UV-Vis, mass spectra,  $^{13}\text{C}$ -NMR and  $^1\text{H}$ -NMR spectra, cyclic voltammetry, molar conductivity, magnetic moment and single crystal XRD.

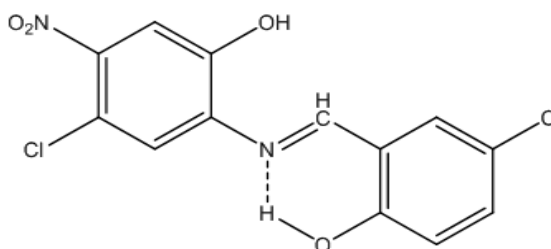
### 4.1. GENERAL PROPERTIES

All the above mentioned synthesized compounds the physical appearance was distinguished through visual observation, all the synthesized compounds are soluble in common organic solvents as DMF and DMSO. The compounds obtained are stable in air, non-hygroscopic, crystalline or precipitate form and obtained in a good yield. The color, melting point, molecular weights and yield of the ligands are summarized in Table 3.1 and for metal complexes in Tables 3.6-3.10. The mass spectra of ligands having peaks at MS (m/z)  $[\text{M}^+]$ : 320.1, 385.0, 262.2, 327.2, 317.2, 331.2, 382.1, 259.3, 273.3, 324.4 for **HL<sub>1</sub>**, **HL<sub>2</sub>**, **H<sub>2</sub>L<sub>3</sub>**, **H<sub>2</sub>L<sub>4</sub>**, **L<sub>5</sub>**, **L<sub>6</sub>**, **L<sub>7</sub>**, **HL<sub>8</sub>**, **HL<sub>9</sub>**, and **HL<sub>10</sub>** respectively are confirming to molecular weights of ligands (Table 3.2, Figures 3.1-3.10). Also some of peaks large than molecular peak due to fragmentation as **HL<sub>2</sub>** molecular peak is 385.0 but fragmentation is 214.9 (Figure 4.1). In the ligand **L<sub>5</sub>**, some fragmentations bigger than the molecular weight is due to the dimeric structures of the ligand or reactions between the fragments or fragments and the ligand.



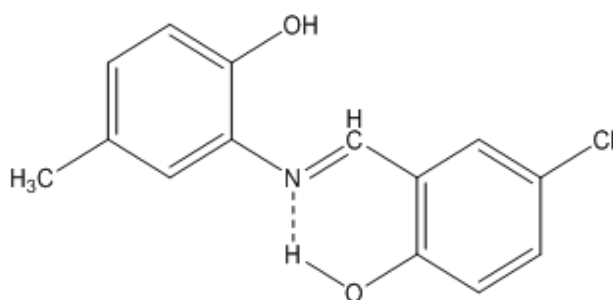
**Figure 4.1:**  $\text{HL}_2$  isomeric structure.

The melting point of metal complexes is higher than the free ligands, most of the metal complexes decompose above  $300^\circ\text{C}$ . It is known that the inter-molecular hydrogen bonding enhances melting point, so melting point of  $\text{H}_2\text{L}_4$ ,  $219^\circ\text{C}$ , is higher than other Schiff bases due to containing inter-and intra- molecular hydrogen bonding (Figure 4.2). Also  $\text{H}_2\text{L}_4$ ,  $\text{L}_7$  and  $\text{HL}_{10}$  contain nitro group and chlorine atom lead to increases melting points [148,149].

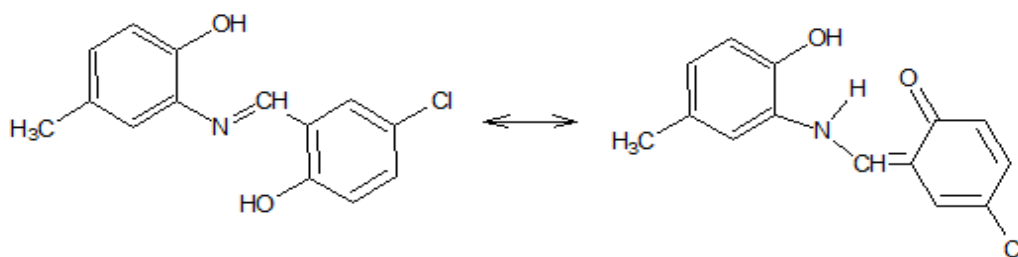


**Figure 4.2:** Intra-molecular hydrogen bonding in  $\text{H}_2\text{L}_4$ .

However, the compound  $\text{H}_2\text{L}_3$  the melting point is lower than that of other Schiff base  $\text{H}_2\text{L}_4$ ,  $\text{HL}_1$  and  $\text{HL}_2$ . So,  $\text{H}_2\text{L}_3$  have intra-molecular hydrogen bonding Figure 4.3, but the phenolic hydroxyl group produced a keto-enol tautomerism and a methyl group at para-position cause decrease melting point (Figure 4.4) [149]. The XRD data of single crystal  $\text{H}_2\text{L}_3$  support this explanation (Table 3.17, Figure 3.105).

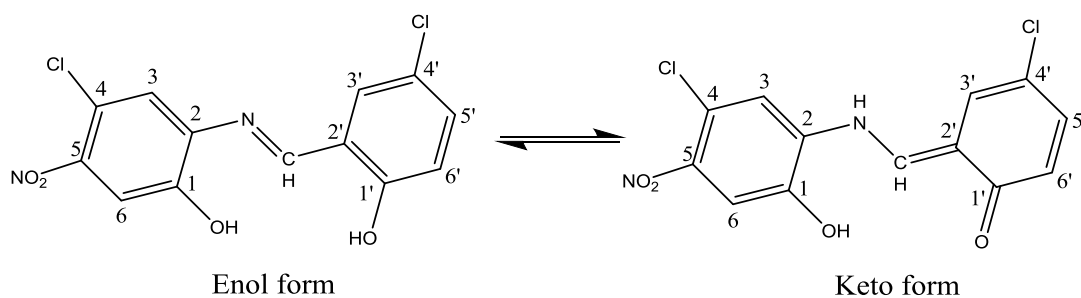


**Figure 4.3:** Intra-molecular hydrogen bonding in  $\mathbf{H}_2\mathbf{L}_3$ .



**Figure 4.4:** Tautomer structure (keto-enol) of the compound  $\mathbf{H}_2\mathbf{L}_3$ .

A several of Schiff bases ligands was effected by  $\text{O}-\text{H}\cdots\text{N}$  (enol-imino) and  $\text{N}-\text{H}\cdots\text{O}$  (keto) tautomer forms. It is reported that the tautomer forms are affected by intermolecular hydrogen bonding such as in  $\mathbf{H}_2\mathbf{L}_3$  and  $\mathbf{H}_2\mathbf{L}_4$  (Figures 4.4-4.5) [138].



**Figure 4.5:** Keto-enol tautomerism of the compound  $\mathbf{H}_2\mathbf{L}_4$ .

Ligands **L**<sub>5</sub>, **L**<sub>6</sub> and **L**<sub>7</sub> are monodentate, **HL**<sub>1</sub>, **HL**<sub>2</sub>, **HL**<sub>8</sub>, **HL**<sub>9</sub> and **HL**<sub>10</sub> are bidentate, **H**<sub>2</sub>**L**<sub>3</sub> and **H**<sub>2</sub>**L**<sub>4</sub> was observed to act as tridentate.

In elemental analysis the analytical information of metal complexes is in contract good with the calculated values and thus confirming the proposed composition for all the complexes the information summarized in Table 3.6-3.10.

#### 4.2. FTIR SPECTROSCOPY

The important IR frequencies of the ligands are summarized in Table 3.3 and Figures 3.11 - 3.20 and IR spectra of the metal complexes are given in Figures 3.50 - 3.59. The medium intensity absorptions at the 1615 - 1666 cm<sup>-1</sup> range are assigned to the C=N stretching mode in the spectra of ligands. In all spectra of the compounds, aromatic rings are observed by specific ring vibrations at  $\nu(\text{C}=\text{C})$  at 1580 - 1450 cm<sup>-1</sup>,  $\nu(\text{C}-\text{H})$  3038 - 3110 cm<sup>-1</sup> and  $\delta(\text{C}-\text{H})$  843 - 731 cm<sup>-1</sup>. The broad bands between 3400 - 2500 cm<sup>-1</sup> demonstrates formation of the OH...N intra-molecular hydrogen bond between the nitrogen atoms and OH proton in the ligands **HL**<sub>1</sub>, **HL**<sub>2</sub>, **H**<sub>2</sub>**L**<sub>3</sub> and **H**<sub>2</sub>**L**<sub>4</sub> [138]. In the IR spectra of the benzimidazole ligands for **L**<sub>5</sub>, **L**<sub>6</sub>, **L**<sub>7</sub>, **HL**<sub>8</sub>, **HL**<sub>9</sub> and **HL**<sub>10</sub> broad bands between 3200 - 3500 cm<sup>-1</sup> are represented to  $\nu(\text{NH})$  stretching vibrations and  $\delta(\text{NH})$  at around 800 - 900 cm<sup>-1</sup>. Also, the bands at the 1000 - 1281 cm<sup>-1</sup> range are specified for  $\nu(\text{C}-\text{N})$  groups. In the IR spectra of the ferrocenyl-benzimidazole derivatives (**L**<sub>5</sub>, **L**<sub>6</sub> and **L**<sub>7</sub>) not including OH groups aromatic and aliphatic CHs are seen clearly at around 3050 cm<sup>-1</sup> and 2920 cm<sup>-1</sup>, respectively, and weak broad bands at the 3100 - 2700 cm<sup>-1</sup> range is due to the intermolecular hydrogen bonding (NH...N=C). Weak or medium stretching vibrations bands close to 2920 cm<sup>-1</sup> as a result of presented methyl group for the ligands **HL**<sub>1</sub>, **H**<sub>2</sub>**L**<sub>3</sub>, **L**<sub>5</sub>, **L**<sub>6</sub>, **HL**<sub>8</sub> and **HL**<sub>9</sub> and their complexes. However, CH of stretching vibrations of CH=N appear at 3000 - 2800 cm<sup>-1</sup> as in the Schiff base ligands such as **HL**<sub>1</sub>, **HL**<sub>2</sub>, **H**<sub>2</sub>**L**<sub>3</sub> and **H**<sub>2</sub>**L**<sub>4</sub> and their complexes [139,150]. There is a very broad band between 2500 - 2800 cm<sup>-1</sup> in **H**<sub>2</sub>**L**<sub>3</sub> because of the strong intra-molecular hydrogen bonding and consequently, aromatic and aliphatic CHs are seen at the 2900 - 3100 cm<sup>-1</sup> range. In **H**<sub>2</sub>**L**<sub>4</sub> ligand, the medium band at 3387 cm<sup>-1</sup> is probably due to the OH group which does not form hydrogen bonding.



The stretching vibration of OH groups of benzimidazolyl-phenol derivatives **HL<sub>8</sub>**, **HL<sub>9</sub>** and **HL<sub>10</sub>**, is clearly seen at 3354, 3276 and 3383 cm<sup>-1</sup>, respectively. In these ligands, stretching vibrations of the aromatic and aliphatic CHs are identified more clearly compared to the other ligands. In addition, in benzimidazolyl-phenol derivatives **HL<sub>8</sub>**, **HL<sub>9</sub>** and **HL<sub>10</sub>**  $\nu(\text{NH})$  is disappeared because of the intra-molecular hydrogen bonding, however in the complexes, it is seen clearly because of the coordination of C=N nitrogen atom and consequently removing the hydrogen bonding. For example, in the Cu(II) complex of **HL<sub>8</sub>**,  $\nu(\text{NH})$  is seen at 3163 cm<sup>-1</sup> as medium band. On the other hand, the C=N group appears weakly or cannot be detected in the benzimidazole derivatives (**L<sub>5</sub>**, **L<sub>6</sub>**, **L<sub>7</sub>**, **HL<sub>8</sub>**, **HL<sub>9</sub>** and **HL<sub>10</sub>**) probably due to the hydrogen bonding ( $-\text{C}=\text{N}\cdots\text{HN}-$ ). However, in the complexes, it is seen more clearly according to the ligand because of removing of the hydrogen bonding on complexation. For example,  $\nu(\text{C}=\text{N})$  of **HL<sub>8</sub>** could be detected as shoulder at 1632 cm<sup>-1</sup>, however it appears at the range of 1626 - 1653 cm<sup>-1</sup> as medium band in the complexes.

The strong bands between 1250 and 1300 cm<sup>-1</sup> are signified for stretching vibrations of C–O, and medium or weak stretching vibration bands of C–Cl are seen at 600 - 650 cm<sup>-1</sup>. The medium bands at 1480 - 1549 cm<sup>-1</sup> and 1350 - 1332 cm<sup>-1</sup> are assigned for symmetric and asymmetric  $\nu(\text{NO}_2)$ , respectively [3].

The characteristic frequencies at around 500 cm<sup>-1</sup> as medium or strong bands are attributed to the stretching vibration of (Fe–Cp) in the ligands including ferrocenyl group (**HL<sub>1</sub>**, **HL<sub>2</sub>**, **L<sub>5</sub>**, **L<sub>6</sub>** and **L<sub>7</sub>**). The medium bands at the 1500 - 1580 cm<sup>-1</sup> range are assigned to the stretching vibration  $\nu(\text{C}=\text{C})$  of Cp group [10].

After complex formation, considerable changes are observed especially in frequencies of the C=N and OH groups or shifting (to higher or lower wavenumbers) compared with the free ligands [139] as expected due to the coordination occur through the C=N nitrogen and OH oxygen atoms. For example, the  $\nu(\text{C}=\text{N})$  band at 1638 cm<sup>-1</sup> in **L<sub>6</sub>** appearing as weak is detected as medium at 1634, 1624 and 1631 cm<sup>-1</sup> in the Zn(II), Cu(II) and Pd(II) complexes, respectively. Similarly,  $\nu(\text{C}=\text{N})$  band shifted to wavenumbers of 1630 and 1624 cm<sup>-1</sup> in the Co(II) and Cu(II) complexes of **L<sub>5</sub>**, which appears at 1658 cm<sup>-1</sup> as medium in the ligand. It is observed that the  $\nu(\text{C}=\text{N})$  band of the complexes of **HL<sub>2</sub>** shifted to the higher wavenumbers, e.g. in the Cu(II) complex at 1704 cm<sup>-1</sup>, whereas it gives absorption at 1655 cm<sup>-1</sup> in the ligand.

The ligands and metal complexes not removed OH protons such as  $[\text{Co}(\mathbf{HL}_2)_2\text{Cl}_2]\cdot\text{H}_2\text{O}$ ,  $[\text{Co}(\mathbf{HL}_{10})_2\text{Cl}_2]\cdot 2\text{H}_2\text{O}$ ,  $[\text{Cu}(\mathbf{H}_2\mathbf{L}_3)\text{Cl}]\text{Cl}\cdot 3\text{H}_2\text{O}$ ,  $[\text{Cu}(\mathbf{H}_2\mathbf{L}_4)\text{Cl}_2(\text{H}_2\text{O})]$ ,  $[\text{Pd}(\mathbf{L}_2)\text{Cl}(\text{H}_2\text{O})]$ ,  $[\text{Pd}(\mathbf{HL}_9)\text{Cl}_2]$ ,  $[\text{Pt}(\mathbf{HL}_3)(\text{EtOH})]\cdot\text{Cl}$  show strong or medium bands for  $\nu(\text{OH})$  at ranging  $3428 - 3325 \text{ cm}^{-1}$  [139,150]. Also, the absorptions for uncoordinated and coordinated water molecules are detected at the  $3500 - 3100 \text{ cm}^{-1}$  (broad),  $1700 - 1600 \text{ cm}^{-1}$  (weak) and  $500 - 600 \text{ cm}^{-1}$  (broad) ranges in the IR spectra of most of the complexes especially in  $\text{Co}(\mathbf{HL}_1)\text{Cl}_2(\text{H}_2\text{O})_2\cdot\text{H}_2\text{O}$ ,  $[\text{Co}(\mathbf{L}_6)\text{Cl}_2(\text{H}_2\text{O})_3]\cdot 3\text{H}_2\text{O}$ ,  $[\text{Co}(\mathbf{L}_7)_2\text{Cl}_2(\text{H}_2\text{O})_2]\cdot\text{H}_2\text{O}$ ,  $[\text{Cu}(\mathbf{L}_6)\text{Cl}_2(\text{H}_2\text{O})]\cdot 2\text{H}_2\text{O}$ ,  $[\text{Pd}(\mathbf{L}_3)(\text{H}_2\text{O})]\cdot 3\text{H}_2\text{O}$ ,  $[\text{Zn}(\mathbf{H}_2\mathbf{L}_4)\text{Cl}_2(\text{H}_2\text{O})_2]\cdot 3\text{H}_2\text{O}$ ,  $[\text{Zn}(\mathbf{L}_5)\text{Cl}_2(\text{H}_2\text{O})]\cdot\text{H}_2\text{O}$ ,  $[\text{Zn}(\mathbf{L}_9)_2(\text{H}_2\text{O})_2]\cdot 2\text{H}_2\text{O}$  and  $[\text{Pt}(\mathbf{L}_5)\text{Cl}_2(\text{MeOH})]\cdot 2\text{H}_2\text{O}$  complexes.

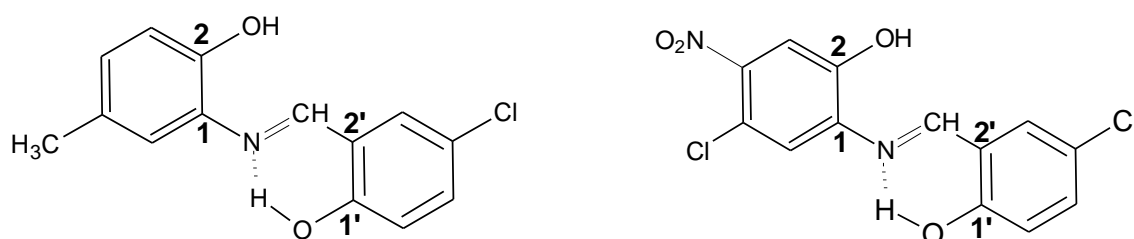
### 4.3. NMR SPECTROSCOPY

The  $^1\text{H}$ -NMR and  $^{13}\text{C}$ -NMR of the ligands summarized in Table 3.4, Figures 3.21 - 3.37, for diamagnetic metal complexes are given in Table 3.16 and Figures 3.60 - 3.104. In the  $^1\text{H}$ -NMR spectra of Schiff bases supported by the existence of a singlet at  $\delta$  (ppm) 8.47, 7.47, 9.0 and 9.0 ( $\mathbf{HL}_1$ ,  $\mathbf{HL}_2$ ,  $\mathbf{H}_2\mathbf{L}_3$  and  $\mathbf{H}_2\mathbf{L}_4$  respectively) confirming the azomethine proton ( $-\text{CH}=\text{N}-$ ). The signals at 9.5 - 11.0 ppm were recognized into the hydroxyl protons, but if strong hydrogen bonding between hydroxyl protons and imine nitrogen atom represented broadness signals or disappeared. Aromatic protons are identified between 6.2 - 8.0 ppm for all the ligands and the complexes. The methyl protons of the ligands  $\mathbf{HL}_1$ ,  $\mathbf{H}_2\mathbf{L}_3$ ,  $\mathbf{L}_5$ ,  $\mathbf{L}_6$ ,  $\mathbf{HL}_8$  and  $\mathbf{HL}_9$  and their complexes show singlet at the 2.23 - 2.49 ppm range [138, 139, 151, 152, 155].

$^1\text{H}$ -NMR spectra of the Schiff bases including ferrocene group, show signals caused by  $-\text{OH}$  proton at 9.90 and 10.27 ppm of  $\mathbf{HL}_1$  and  $\mathbf{HL}_2$ , respectively, and also shows a  $-\text{CH}=\text{N}-$  proton signal at 8.47 and 7.47 ppm for  $\mathbf{HL}_1$  and  $\mathbf{HL}_2$ , respectively [153,154]. Multiplet signals of ferrocene protons are observed at the 4.0 - 5.0 ppm range.

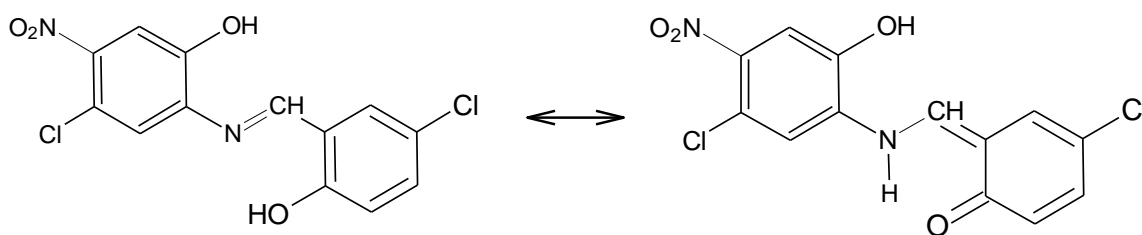
The compound  $\mathbf{H}_2\mathbf{L}_4$  has two isomeric structures (Figure 4.4) depending on  $^1\text{H}$ -NMR spectra (Table 3.4, Figures 3.27-3.29). There is exciting information in the  $^1\text{H}$ -NMR of the  $\mathbf{H}_2\mathbf{L}_3$  and  $\mathbf{H}_2\mathbf{L}_4$  Schiff base ligands having two hydroxyl groups (salicylic and phenolic OH). It is recognized that the resonance signal of one of the salicylic OH proton shifts to the lower field (higher frequency) due to hydrogen bonding. Comparing the  $^1\text{H}$ -NMR data of salicyl part OH protons of the  $\mathbf{H}_2\mathbf{L}_3$  and  $\mathbf{H}_2\mathbf{L}_4$  compounds it can be said that the intra-molecular hydrogen

bond ( $\text{OH}\cdots\text{N}$ ) is formed at 13.9 ppm ( $\text{OH1}'$ ) of  $\text{H}_2\text{L}_3$  and other phenolic proton ( $\text{OH2}$ ) 9.6 ppm. In  $\text{H}_2\text{L}_4$  (enol), the signal at 12.62 ppm ( $\text{OH1}'$ ) is due to the intra-molecular hydrogen bonding ( $\text{OH}\cdots\text{N}$ ) and other phenolic proton appears at 10.28 ppm ( $\text{OH1}$ ) (Figure 4.6) [138,139].



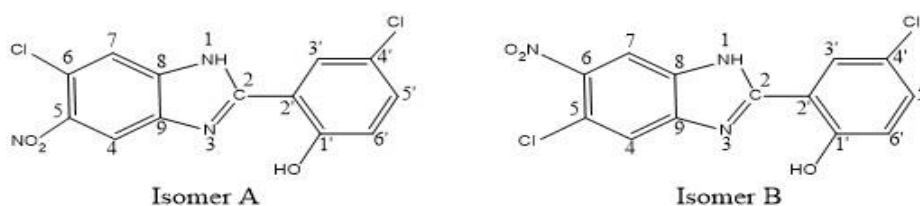
**Figure 4.6:** Intramolecular hydrogen bonding in  $\text{H}_2\text{L}_3$  (left) and  $\text{H}_2\text{L}_4$  ligands (right).

$\text{D}_2\text{O}$  exchange  $^1\text{H-NMR}$  spectra for  $\text{H}_2\text{L}_4$  shows that both OH protons are exchangeable as expected. After  $\text{D}_2\text{O}$  exchange, the signals at 12.62 ( $\text{OH1}'$ ), 10.89 ( $\text{OH1}$ -keto form), and 10.28 ppm ( $\text{OH1}$ -enol form) are removed and the signals at 9.85 s,br ( $\text{NH}$ , keto form) and at 8.61 s,br ( $\text{CH}$ , enol form) were detected (Figure 4.7). The characteristics of the aromatic protons change to broad signals (Table 3.4).



**Figure 4.7:** The keto-enol isomeric structures of the  $\text{H}_2\text{L}_4$ .

However, the ligand  $\text{HL}_{10}$  owns two isomeric structures shown in Figure 4.8 depending on  $^1\text{H-NMR}$  spectra is observed the affected protons by isomer forming (Table 3.4, Figures 3.36 and 3.37).



**Figure 4.8:** The isomeric structures of the **HL<sub>10</sub>**.

In the diamagnetic complexes, some phenolic protons of the ligands are removed especially from **HL<sub>1</sub>**, **HL<sub>2</sub>**, **H<sub>2</sub>L<sub>3</sub>**, **H<sub>2</sub>L<sub>4</sub>**, **HL<sub>8</sub>**, **HL<sub>9</sub>** and **HL<sub>10</sub>** complexes (Table 3.16) after complex formation. In addition, the azomethine proton ( $-\text{N}=\text{CH}-$ ) of the Schiff base ligands (**HL<sub>1</sub>**, **HL<sub>2</sub>**, **H<sub>2</sub>L<sub>3</sub>** and **H<sub>2</sub>L<sub>4</sub>**) is shifted to the lower field on complexation, considerably. For example, in  $[\text{Zn}(\text{L}_1)_2] \cdot 2\text{H}_2\text{O}$  complex, it shifts to 9.87 ppm from 8.47 ppm; in  $[\text{Zn}(\text{H}_2\text{L}_4)\text{Cl}_2(\text{H}_2\text{O})_2] \cdot 3\text{H}_2\text{O}$  it shows shifting with 1.21 ppm (from 8.98 ppm to 10.19 ppm). In the benzimidazole derivatives, (**L<sub>5</sub>** - **HL<sub>10</sub>**), it is observed that NH proton appeared at the 11.40 – 13.36 ppm range as broad singlet, and shifted to the 12.05 – 13.90 ppm range (downfield) in the complexes.

In the  $^{13}\text{C}$ -NMR spectra the ligands demonstration signals around 20.42 - 20.74 ppm caused by methyl group, and signals between 68.25 - 131.77 ppm because of the two cyclopentadienyl rings. The signals at 160.38 and 193.85 ppm can be attributed to the azomethine carbon of **HL<sub>1</sub>** and **HL<sub>2</sub>**, respectively. The aromatic ring signals of both ligands and metal complex compounds appeared between 111.73 to 159.91 ppm, generally. The azomethine carbons of **H<sub>2</sub>L<sub>3</sub>** and **H<sub>2</sub>L<sub>4</sub>** (enol form) are seen at 160.11 and 190.15 ppm, respectively [156,157]. The carbon atoms bonded to OH oxygen atom (C2) give signals at the lower ppm value than the carbon atoms that bonded to the salicyl part OH oxygen (C1'): 119.3 ppm and 159.9 ppm (in enol form of **H<sub>2</sub>L<sub>4</sub>**), respectively [158,159]. On complexation, these carbon atom's signals shifted to down field, for example, in the Pd(II) complex of **H<sub>2</sub>L<sub>4</sub>** they are detected at 133.2 and 162.7 ppm, respectively (Table 3.16). It is observed that the C2 is the carbon atom ( $\text{N}=\text{C}<$ ) appears at the highest ppm value in the benzimidazole derivatives, **L<sub>5</sub>** - **HL<sub>10</sub>**. For example, the C2 of **HL<sub>9</sub>** gives a signal at 159.08 ppm. It shifts to 157.03 and 156.36 ppm in the Zn(II) and Pd(II) complexes (upfield shift), respectively.

#### 4.4. MAGNETIC MOMENT AND MOLAR CONDUCTIVITY MEASUREMENTS

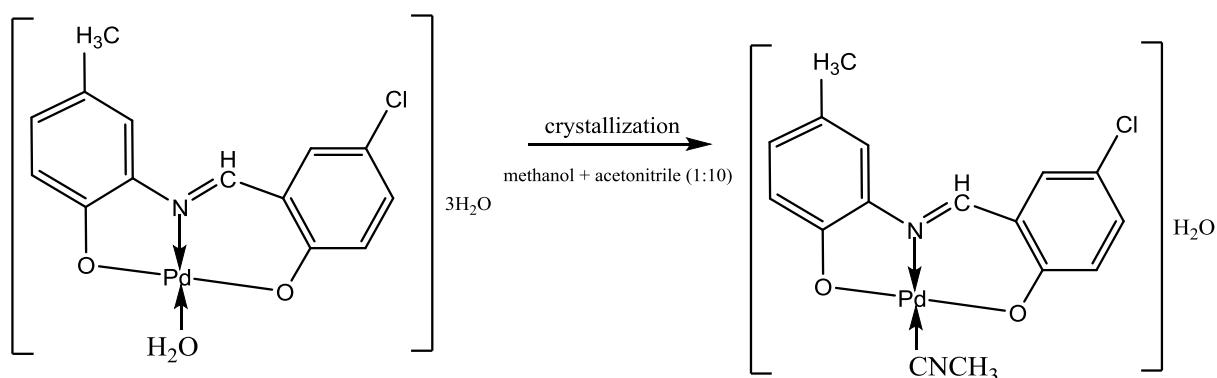
Magnetic moment and molar conductivity measurement values of complex summarized in Tables 3.11-3.15. High spin octahedral of  $\text{Co}^{2+}$  have magnetic moment from 4.31 to 5.82 BM is close to the spin value calculated magnetic moments. As well, tetrahedral and octahedral of  $\text{Cu}^{2+}$  have magnetic moment from 1.72 to 2.20 close to the spin value calculated magnetic moments [138,139]. The magnetic moments for ferrocenyl based complexes was measured, values for these compounds which are higher than the value of the theoretical magnetic moment. Also the diamagnetic nature of Pd(II), Zn(II) and Pt(II) the reported values for the magnetic susceptibility are higher than zero that implying some paramagnetism in the complexes containing ferrocene group due to the diamagnetic system of ferrocene is removed and Fe(II) ion give two paired electron. So, the complex/organometallic compound show paramagnetic character [159, 160].

Molar conductivity measurement carried out in DMF, the value in the range of 7.55-59.32  $\text{Scm}^2\text{mol}^{-1}$ . All the complexes are non-ionic except  $[\text{Cu}(\text{H}_2\text{L}_3)\text{Cl}]\text{Cl}\cdot 3\text{H}_2\text{O}$ ,  $[\text{Pd}(\text{H}_2\text{L}_4)\text{Cl}]\text{Cl}\cdot \text{H}_2\text{O}$  and  $[\text{Pt}(\text{HL}_3)(\text{EtOH})]\cdot \text{Cl}$  complexes 1:1 electrolyte character with molar conductivity values are 42.6, 59.3 and 40.3  $\text{Scm}^2\text{mol}^{-1}$  respectively. Some of the complexes are non-ionic but have higher molar conductivity in DMF due to molecular ion liberates in solution [161].

#### 4.5. X-RAY CRYSTAL STRUCTURE

Single crystal X-ray diffraction data of  $\text{H}_2\text{L}_3$  and  $[\text{Pd}(\text{L}_3)\text{CH}_3\text{CN}]\cdot \text{H}_2\text{O}$  complex are given at Tables 3.17 and 3.21, respectively. Also, the selected bond distance and angles, hydrogen bond parameters and selected torsion angles are given in Tables 3.18-3.24. Crystal structure of  $\text{H}_2\text{L}_3$  and  $[\text{Pd}(\text{L}_3)\text{CH}_3\text{CN}]\cdot \text{H}_2\text{O}$  complex are given in Figures 3.105 and 3.107, respectively. Unit cell packing diagrams for  $\text{H}_2\text{L}_3$  and  $[\text{Pd}(\text{L}_3)\text{CH}_3\text{CN}]\cdot \text{H}_2\text{O}$  complex are given in Figures 3.106 and 3.108.

Single crystal X-ray diffraction data of  $[\text{Pd}(\text{L}_3)\text{CH}_3\text{CN}]\cdot \text{H}_2\text{O}$  after recrystallization in methanol+acetonitrile (1:10), the single crystals were formed the water molecule removed outside of coordination and acetonitrile coordinate Figure 4.9.



**Figure 4.9:** The structure of the Pd+H<sub>2</sub>L<sub>3</sub>.

X-ray crystal structure data of H<sub>2</sub>L<sub>3</sub> clearly exhibit that the keto form is dominant (Fig. 3.105, Table 3.18): C6–O1: 1.290 Å (C=O), C9–O2: 1.353 Å (C–OH), C7–N1: 1.293 Å (CH=N). Also, there are intra- and inter-molecular hydrogen bonds in H<sub>2</sub>L<sub>3</sub>: N1–H1···O1: 1.78 Å, O2–H2A···O1: 1.77 Å (Table 3.19), respectively. The crystal structure is stabilized by intermolecular hydrogen bonds.

X-ray crystal structure data of [Pd(L<sub>3</sub>)CH<sub>3</sub>CN]·H<sub>2</sub>O complex show that the ligand acted as tridentate through two phenolic OH and C=N nitrogen atoms deprotonating the phenolic OH protons and giving a chelate complex. The distances between Pd(II) ion and the donor atoms of H<sub>2</sub>L<sub>3</sub> are the following (Table 3.23): O1–Pd: 1.969 Å, N1–Pd: 1.947 Å, O2–Pd: 1.982 Å, N2–Pd: 2.042 Å (N2 is belonging to solvent molecule, here is an acetonitrile molecule). The fourth coordination is provided by a solvent molecule or ion. The bond angles, O1–Pd–N1: 95.8°, O2–Pd–N1: 83.5°, O1–Pd–N2: 90.0°, O2–Pd–N2: 89.9°, indicate that Pd(II) ion is in a distorted square planar environment (Table 3.23). Some torsion angles are also supports this inference such as C2–C1–O1–Pd: -175.8°, C6–C1–O1–Pd: 3.5°, C9–C8–N1–Pd: 1719.1° etc (Table 3.24). Inter-molecular hydrogen bonds in [Pd(L<sub>3</sub>)CH<sub>3</sub>CN]·H<sub>2</sub>O are detected: C16–H16B···O1: 2.46 Å, O3–H3A···O2: 1.94 Å (Table 3.19) between water molecules and Pd(L<sub>3</sub>)CH<sub>3</sub>CN moiety.

Considering the spectroscopic and physicochemical data, it can be concluded that geometry of the Pd(II) and Pt(II) complexes is almost square planar, Co(II) complexes are generally octahedral. Zn(II) and Cu(II) complexes have tetrahedral (four coordinations) or octahedral (six coordinations) geometries.

#### 4.6. UV-VISIBLE SPECTROSCOPY

The electronic absorption (UV-visible) spectra of ligands along with the complexes in the wavelength from 200 to 800 nm range in methanol were recorded and the results are shown in Table 3.5, 3.11 – 3.15 and Figures 3.38, 3.40 – 3.49. The absorptions at 200–300 nm range in the electronic spectra of the ligand and the complexes correspond to  $\pi \rightarrow \pi^*$  transitions of the aromatic rings. The medium or weak bands at the range of 300 – 350 nm can be assigned to  $n \rightarrow \pi^*$  transitions. The absorptions around 400 nm are due to the intramolecular charge transfer transitions in the ligands. The ligands are dark colored generally, except **H<sub>2</sub>L<sub>3</sub>** and **H<sub>2</sub>L<sub>4</sub>**. The colors of **H<sub>2</sub>L<sub>3</sub>** and **H<sub>2</sub>L<sub>4</sub>** are orange and yellow. The other ligands are brown and black colored. So, the intramolecular charge transfer transitions in these dark colored compounds are expected and observed intensely. All of the complexes are dark colored (brown, dark brown and reddish black etc) and hence intense charge transfer transitions are expected in the UV-visible spectra of the complexes. Likewise, the absorptions above 400 nm should belong to the ligand to metal charge transfer transitions (LMCT). These transitions (absorptions) cover the d-d transitions in the complexes and prevent to detect them. In addition, it was observed that the bands are slightly blue shifted on complexation because of the complexation effect and ligand to metal charge transfer transitions (LMCT). There are no considerable changes in the complexes UV-visible spectral data except the complexes of **H<sub>2</sub>L<sub>4</sub>**. Absorptions are observed between 450–476 nm assigned to the LMCT in the Co(II), Pd(II) and Cu(II) complexes of **H<sub>2</sub>L<sub>4</sub>** (Figures 3.38 and 3.43). These charge transfers are originated from phenolic oxygen atom to the metal ions transitions ( $O \rightarrow M^{2+}$ ) [162-164].

#### 4.7. CYCLIC VOLTAMMETRY

Electrochemical parameter of the selected ligands including ferrocene groups (**HL**<sub>1</sub>, **HL**<sub>2</sub>, **L**<sub>5</sub>, **L**<sub>6</sub> and **L**<sub>7</sub>) and their Co<sup>2+</sup> complexes, the CV parameters are given in Table 3.25 and presented in Figures 3.110 - 3.124. Cyclic voltammograms illustrate that working electrode polarity come to be higher positive, the sign oxidation is detected at anodic peak potential (E<sub>pa</sub>), due to ferrocene moiety is changed into oxidized form. As well reverse scan working electrode polarity converts into less positive (reversed process), following reduction of the oxidized product happening as cathodic signal is detected at cathodic peak potential (E<sub>pc</sub>). All the above mentioned compounds appearance reversed process. Anodic and cathodic peak separation ( $\Delta E_p$ ) was establishing is 0.07 V **HL**<sub>2</sub> best significance suggestive of one-electron oxidation and 0.13, 0.16, 0.13, 0.11 V **HL**<sub>1</sub>, **L**<sub>5</sub>, **L**<sub>6</sub> and **L**<sub>7</sub> respectively, it is a little higher showing slow electron transfer. General, the great value  $\Delta E_p$  recognized to the resistance influence. The Co<sup>2+</sup> complexes decrease the  $\Delta E_p$  values (0.09, 0.07, 0.12, 0.11 and 0.07) in [Co(**HL**<sub>1</sub>)Cl<sub>2</sub>(H<sub>2</sub>O)<sub>2</sub>] $\cdot$ H<sub>2</sub>O, [Co(**HL**<sub>2</sub>)<sub>2</sub>Cl<sub>2</sub>] $\cdot$ H<sub>2</sub>O, [Co(**L**<sub>5</sub>)Cl<sub>2</sub>(H<sub>2</sub>O)<sub>3</sub>], [Co(**L**<sub>6</sub>)Cl<sub>2</sub>(H<sub>2</sub>O)<sub>3</sub>] $\cdot$ 3H<sub>2</sub>O and [Co(**L**<sub>7</sub>)<sub>2</sub>Cl<sub>2</sub>(H<sub>2</sub>O)<sub>2</sub>] $\cdot$ H<sub>2</sub>O respectively, which lead to increase electron transfer. The strong electron-withdrawing nitro group in **HL**<sub>2</sub> makes the oxidation of the iron (of the ferrocenyl group) difficult by shifting the oxidation potential in more positive direction by increasing E<sub>pa</sub> 0.79. General for all complexes the electrochemical process remains one electron reversible [165].

#### 4.8. THERMO GRAVIMETRIC ANALYSIS (TGA)

The crystal and coordinated water molecules for [Cu(**HL**<sub>10</sub>)Cl<sub>2</sub>(H<sub>2</sub>O)<sub>2</sub>] $\cdot$ H<sub>2</sub>O, [Pd(**L**<sub>6</sub>)Cl<sub>2</sub>(H<sub>2</sub>O)], [Pd(**L**<sub>7</sub>)Cl<sub>2</sub>(H<sub>2</sub>O)], [Zn(**H**<sub>2</sub>**L**<sub>4</sub>)Cl<sub>2</sub>(H<sub>2</sub>O)<sub>2</sub>] $\cdot$ 3H<sub>2</sub>O and [Zn(**L**<sub>9</sub>)<sub>2</sub>(H<sub>2</sub>O)<sub>2</sub>] $\cdot$ 2H<sub>2</sub>O complexes were investigated by means of thermogravimetric analysis (TGA). The water contains of these complexes were quantified by analysing the TGA curves. As known the crystal water molecules remove below 100°C, the coordinated water molecules remove above 100°C. There is no considerable weight loss under 100°C in [Pd(**L**<sub>6</sub>)Cl<sub>2</sub>(H<sub>2</sub>O)] and [Pd(**L**<sub>7</sub>)Cl<sub>2</sub>(H<sub>2</sub>O)] complexes whereas [Cu(**HL**<sub>10</sub>)Cl<sub>2</sub>(H<sub>2</sub>O)<sub>2</sub>] $\cdot$ H<sub>2</sub>O, [Zn(**H**<sub>2</sub>**L**<sub>4</sub>)Cl<sub>2</sub>(H<sub>2</sub>O)<sub>2</sub>] $\cdot$ 3H<sub>2</sub>O and [Zn(**L**<sub>9</sub>)<sub>2</sub>(H<sub>2</sub>O)<sub>2</sub>] $\cdot$ 2H<sub>2</sub>O complexes have both lattice (uncoordinated) and coordinated water molecules in different amounts (Figures 3.125 - 3.129. ). For example, weight loss in [Cu(**HL**<sub>10</sub>)Cl<sub>2</sub>(H<sub>2</sub>O)<sub>2</sub>] $\cdot$ H<sub>2</sub>O complex is 3.2% up to 85°C that corresponds to one mole of uncoordinated lattice water (theoretical value is 35.% for one mole of water). The weight loss



with 8% at 150°C representing approximately amount of two moles of H<sub>2</sub>O may be accepted as evidence for two mole of coordinated water (theoretical value: 7.02%). In the other complexes, the status of the water molecules is determined by means of TGA data.

The TGA results also gave supporting information about the metal contains of the complexes. For instance, theoretical metal oxide (CuO) percentage in [Cu(HL<sub>10</sub>)Cl<sub>2</sub>(H<sub>2</sub>O)<sub>2</sub>]·H<sub>2</sub>O complex is 15.5% and TGA supports this with a residue of 14.2% at around 700°C (Fig. 3.126).

#### 4.9. ANTIMICROBIAL ACTIVITY

Selected some synthesized ligands including ferrocene group and their complexes were screened against species bacteria and fungi are summarized in Table 3.26. It is detected that all selected compounds exhibit weak to moderate activity toward *Staphylococcus aureus* and *Staphylococcus epidermidis* and *Candida tropicalis*. Only four compounds [Cu(L<sub>6</sub>)Cl<sub>2</sub>(H<sub>2</sub>O)]·2H<sub>2</sub>O, HL<sub>1</sub>, HL<sub>2</sub> and [Co(HL<sub>2</sub>)<sub>2</sub>Cl<sub>2</sub>]·H<sub>2</sub>O show weak to moderate antibacterial activity against *Klebsiella pneumoniae*. The two compounds [Cu(L<sub>5</sub>)Cl<sub>2</sub>(H<sub>2</sub>O)]·H<sub>2</sub>O and HL<sub>2</sub> are moderate effective against *Pseudomonas aeruginosa*. In addition the [Co(L<sub>5</sub>)Cl<sub>2</sub>(H<sub>2</sub>O)<sub>3</sub>] and HL<sub>2</sub> are moderate effective against *Proteus mirabilis*. But [Co(L<sub>5</sub>)Cl<sub>2</sub>(H<sub>2</sub>O)<sub>3</sub>] exhibit a broader spectrum as compared to the other compounds agonist *Candida albicans*, *Candida parapsilosis* and *Candida tropicalis*, Other hand, [Pd(L<sub>6</sub>)Cl<sub>2</sub>(H<sub>2</sub>O)], [Cu(L<sub>7</sub>)Cl<sub>2</sub>(EtOH)], HL<sub>2</sub> and [Co(HL<sub>2</sub>)<sub>2</sub>Cl<sub>2</sub>]·H<sub>2</sub>O moderate activity on *Candida parapsilosis*. No above compounds have any activity toward the *Escherichia Coli* (not reported).

The results of these studies exhibited significant to moderate antifungal and anti-bacterial properties. Conversely, the metal salts used did not show any effect on the microorganisms. The compounds have higher antifungal activity then antibacterial activity.

## 5. CONCLUSION AND RECOMMENDATIONS

Schiff bases and benzimidazole derivatives are groups of compounds which can be applied in many fields, particularly in medical chemistry and drug applications. Ferrocene group-containing compounds are of interest because of their stability, their use in organic synthesis studies and their biological activities. In this dissertation two different ligand groups were prepared: four Schiff base compounds (**HL**<sub>1</sub>, **HL**<sub>2</sub>, **H**<sub>2</sub>**L**<sub>3</sub> and **H**<sub>2</sub>**L**<sub>4</sub>) and six benzimidazole derivatives (**L**<sub>5</sub>, **L**<sub>6</sub>, **L**<sub>7</sub>, **HL**<sub>8</sub>, **HL**<sub>9</sub> and **HL**<sub>10</sub>) including ferrocene and phenol groups in this study; totally ten ligands were synthesized. Five of these ligands e.g. **HL**<sub>1</sub>, **HL**<sub>2</sub>, **L**<sub>5</sub>, **L**<sub>6</sub> and **L**<sub>7</sub>, contain ferrocene groups whereas the other five, **H**<sub>2</sub>**L**<sub>3</sub>, **H**<sub>2</sub>**L**<sub>4</sub>, **HL**<sub>8</sub>, **HL**<sub>9</sub> and **HL**<sub>10</sub>, have phenol group. The metal complexes with Cu<sup>2+</sup>, Zn<sup>2+</sup>, Co<sup>2+</sup>, Pt<sup>2+</sup> and Pd<sup>2+</sup> of the ligands have been synthesized in good yield. Some analytical and spectral techniques such as elemental analysis, FTIR, <sup>1</sup>H- and <sup>13</sup>C-NMR, UV-visible, mass spectrometry (MS) and cyclic voltammetry analysis were performed for the characterization of the compounds. The ligands were monitored by thin layer chromatography (TLC) and their molecular weights were confirmed by MS analyses. Molar conductivity and magnetic moment were also measured for complex compounds. Furthermore, X-ray single crystal analysis of the **H**<sub>2</sub>**L**<sub>3</sub> ligand and ([Pd(**L**<sub>3</sub>)CH<sub>3</sub>CN]·H<sub>2</sub>O) were also performed. The ligands **L**<sub>5</sub>, **L**<sub>6</sub> and **L**<sub>7</sub> have monodentate characteristic, **HL**<sub>1</sub>, **HL**<sub>2</sub>, **HL**<sub>8</sub>, **HL**<sub>9</sub> and **HL**<sub>10</sub> bidentate, **H**<sub>2</sub>**L**<sub>3</sub> and **H**<sub>2</sub>**L**<sub>4</sub> were observed to act as tridentate. The presence of two different metal ions in the complexes of the ferrocene-containing ligands brought heterobinuclear characteristic to these compounds and thus these compounds have become more interesting.

In the infrared spectra, appearance of absorption bands at 1600–1650 cm<sup>-1</sup> assigned to C=N stretching mode of both Schiff bases and benzimidazole derivatives. The broad bands at around the 3200–3500 cm<sup>-1</sup> are assigned to ν(NH) stretching vibrations and δ(NH) at around 800–900 cm<sup>-1</sup>. The ferrocenyl moiety the (Fe-Cp) stretching vibration is seen at 500–450 cm<sup>-1</sup> as a medium band and stretching vibrations of C=C bonds belonging to the aromatic structures and the cyclopentadienyl (Cp) group of the ferrocene section were determined between 1550–1600 cm<sup>-1</sup> as a medium band. Stretching vibrations of phenolic C–O bonds were observed in 1200 - 1300 cm<sup>-1</sup> region. Significant changes were observed in these bands

with complex formation. For example, complex formation was verified by shifting of CH=N bands towards higher frequency along.

NMR spectroscopy also supported the proposed structures of synthesized compounds.  $^1\text{H}$  NMR spectra displayed signals for all the protons in their characteristic regions, aromatic protons were observed in the region 6.2-8.0 ppm, formation of Schiff base linkage was established by the appearance of signal for azomethine proton and absence of  $\text{NH}_2$  peaks as 8.47, 7.47, 9.0 and 9.0 ( $\text{HL}_1$ ,  $\text{HL}_2$ ,  $\text{H}_2\text{L}_3$  and  $\text{H}_2\text{L}_4$  respectively). In the NMR spectra of the diamagnetic compounds, significant changes were observed in phenolic OH protons and carbon atoms in all ligands as expected, with the formation of complex. In the Schiff base complexes, significant shifts were observed in protons of azomethine groups (N=CH) and in carbon atoms signals in diamagnetic Schiff base complexes. X-ray analysis of  $\text{H}_2\text{L}_3$  shows that the ligand in solid state keto form is dominant. In the  $^1\text{H}$ -NMR spectrum of  $\text{H}_2\text{L}_4$ , a mixture of keto-enol tautomeric structure appears. According to the molar conductivity measurements, all the complexes have non-ionic character except  $[\text{Cu}(\text{H}_2\text{L}_3)\text{Cl}]\text{Cl}\cdot 3\text{H}_2\text{O}$ ,  $[\text{Pd}(\text{H}_2\text{L}_4)\text{Cl}]\text{Cl}\cdot \text{H}_2\text{O}$  and  $[\text{Pt}(\text{HL}_3)(\text{EtOH})]\cdot \text{Cl}$  (these three complexes have 1:1 electrolyte character and their molar conductivity values are 42.6, 59.3 and 40.3  $\text{Scm}^2\text{mol}^{-1}$  respectively). The magnetic moment measurement results also contributed to the geometry and structural properties of complex compounds. For example, in the  $\text{Co}^{2+}$  compounds, the magnetic moment values between 4.31-5.82 BM indicate that the  $\text{Co}^{2+}$  ion in these complexes has a high spin structure and the complex geometry is tetrahedral or octahedral. Also, in some  $\text{Cu}^{2+}$  complexes, the magnetic moment values between 1.70-2.20 BM are also in the expectation and give clues about the complexes being octahedral or tetrahedral. In addition, in many paramagnetic complex compounds containing ferrocene group, the magnetic moment value is higher than expected also in some complexes expected to be diamagnetic ( $\text{Zn}^{2+}$ ,  $\text{Pd}^{2+}$ ,  $\text{Pt}^{2+}$  complexes) the paramagnetic character is detected. This abnormality shows that the diamagnetic properties of the  $\text{Fe}^{2+}$  ion in the ferrocene group are eliminated and the magnetic moment value of the molecule is contributed by approximately two non-paired electrons. UV-visible data shows that there are intense intramolecular charge transfers in the ligands and ligand to metal charge transfer (LMCT) transitions in the complexes. Because of the intense LMCT transitions in the complexes, adequate information about the d-d transitions in the metal ions could not be obtained.

Crystal structures of some compounds  $\mathbf{H}_2\mathbf{L}_3$  and  $[\text{Pd}(\mathbf{L}_3)\text{CH}_3\text{CN}]\cdot\text{H}_2\text{O}$  are studied. Single crystal analysis  $\mathbf{H}_2\mathbf{L}_3$  revealed the structure presence of keto-enol tautomerization. The X-ray analysis data approve a square planar geometry for  $[\text{Pd}(\mathbf{L}_3)\text{CH}_3\text{CN}]\cdot\text{H}_2\text{O}$ . It can be suggested the square-planar geometry for the other Pt(II) and Pd(II) complexes. Crystal structure data are supported by elemental analysis and other characterizations.

Redox behavior of the selected ligands including ferrocene groups ( $\mathbf{HL}_1$ ,  $\mathbf{HL}_2$ ,  $\mathbf{L}_5$ ,  $\mathbf{L}_6$  and  $\mathbf{L}_7$ ) and their  $\text{Co}^{2+}$  complex was examined by advanced electrochemical techniques a cyclic voltammetry. Electrochemical results revealed that ferrocene based synthesized compounds and Co(II) complexes undergo reversible diffusion controlled electron transfer process and might be employed in those systems where stable redox systems. The anodic and cathodic peak separation ( $\Delta E_p$ ) was establishing is 0.07 V  $\mathbf{HL}_2$  is best significance suggestive of one-electron oxidation and 0.13, 0.16, 0.13 and 0.11 V  $\mathbf{HL}_1$ ,  $\mathbf{L}_5$ ,  $\mathbf{L}_6$  and  $\mathbf{L}_7$  respectively, it is a little higher showing slow electron transfer. General, the great value of the  $\Delta E_p$  recognized to the resistance influence. The  $\text{Co}^{2+}$  complexes decrease the  $\Delta E_p$  value (0.09, 0.07, 0.12, 0.11 and 0.07) in  $[\text{Co}(\mathbf{HL}_1)\text{Cl}_2(\text{H}_2\text{O})_2]\cdot\text{H}_2\text{O}$ ,  $[\text{Co}(\mathbf{HL}_2)_2\text{Cl}_2]\cdot\text{H}_2\text{O}$ ,  $[\text{Co}(\mathbf{L}_5)\text{Cl}_2(\text{H}_2\text{O})_3]$ ,  $[\text{Co}(\mathbf{L}_6)\text{Cl}_2(\text{H}_2\text{O})_3]\cdot 3\text{H}_2\text{O}$  and  $[\text{Co}(\mathbf{L}_7)_2\text{Cl}_2(\text{H}_2\text{O})_2]\cdot\text{H}_2\text{O}$  respectively, which lead to increase electron transfer. Electrochemical process of the complexes remains one electron reversible. The strong electron-withdrawing nitro group in  $\mathbf{HL}_2$  makes the oxidation of the iron (of the ferrocenyl group) difficult by shifting the oxidation potential in more positive direction by increasing  $E_{pa}$  0.79. In addition, some selected ligands containing ferrocene moiety and their complexes were screened against species of Gram-positive and Gram-negative bacteria and fungi using the disk diffusion method. It was observed that many compounds exhibited antifungal and antibacterial effects from weak to medium.  $[\text{Co}(\mathbf{L}_5)\text{Cl}_2(\text{H}_2\text{O})_3]$  complex, *C. albicans*, *C. parapsilosis* and *C. tropicalis* fungi, compared to other compounds showed a broader range of activity.

In this Ph.D thesis the interesting ligands synthesized especially including ferrocene and phenol groups and their complexes because of cheap, easy and direct synthetic and higher stability. In my work just Schiff bases, benzimidazole derivatives are synthesized, in the future better prepared benzoxazole derivatives. Future investigations should be directed towards the development of new applications as catalytic application.

## REFERENCES

- [1]. Garnovskii, A.D., Sennikova, E.V. and Kharisov, B.I., 2009, Coordination aspects in modern inorganic chemistry, *Open inorg chem*, 3(1), 1–20.
- [2]. Malik, S., Ghosh, S. and Mitu, L., 2011, Complexes of some 3d-metals with a Schiff base derived from 5-acetamido-1, 3, 4-thiadiazole-2-sulphonamide and their biological activity, *J. serb. chem. soc.*, 76(1), 1387–1394.
- [3]. Hariprasath, K., Deepthi, B., Babu, I.S., Venkatesh, P., Sharfudeen, S. and Soumya, V., 2010, Metal complexes in drug research - a review, *Chem. pharm. res*, 2 (4), 496-499.
- [4]. Mahurpawar, M., 2015, Effects of heavy metals on human health, *Int. j. reseacrh-granthaalayah*, 2350(530), 2394–3629.
- [5]. Banerjea, D., 1980, *Coordination chemistry*, 1st ed., Oxford, ISBN: 9781483151328.
- [6]. Pahontu, E., Fala, V., Gulea, A., Poirier, D., Tapcov, V. and Rosu, T., 2013, Synthesis and characterization of some new Cu(II), Ni(II) and Zn(II) complexes with salicylidene thiosemicarbazones: antibacterial, antifungal and in vitro antileukemia activity, *Molecules*, 18(8), 8812–8836.
- [7]. Pauling, L. and Zelek, S.H., 1984, Valence-bond concepts in coordination chemistry and the nature of metal-metal bonds, *Chem educ*, 61(7), 582.
- [8]. Bethe, H., 1928, Theorie der Beugung von Elektronen an Kristallen, *Ann. Phys*, 392(17), 55–129.
- [9]. Van Vleck, J., 1932, Theory of the variations in paramagnetic anisotropy among different salts of the iron group, *Physical review*, 41(2), 208–215.
- [10]. Garnovskii, A.D., Sennikova, E.V. and Kharisov, B.I., 2009, Coordination aspects in modern inorganic chemistry, *the open inorganic chemistry journal*, 3(1), 1-20.
- [11]. Al Zoubi, W., Al-Hamdani, A.A.S. Ahmed, S.D. and Ko, Y.G., 2017, Synthesis, characterization, and biological activity of Schiff bases metal complexes, *phys org chem*, 14(1), 1-13.

- [12]. Djebbar-Sid, S., Benali-Baitich, O. and Deloume, J.P., 1997, Synthesis, characterization and electrochemical behaviour of some copper(II) complexes with linear and tripodal tetradentate ligands derived from schiff bases, *Polyhedron*, 16 (13), 2175–2182.
- [13]. Ramesh, R., 2004, Spectral and catalytic studies of ruthenium(III) Schiff base complexes, *Inorg chem commun*, 7(2), 274–276.
- [14]. Sreeja, P.B., Sreekanth, A., Nayar, C.R., Kurup, P.M.R., Usman, A., Razak, I.A., Chantrapromma, S. and Fun, H.K., 2003, Synthesis, spectral studies and structure of 2-hydroxyacetophenone nicotinic acid hydrazone, *J. mol. struct.*, 645(2), 221–226.
- [15]. Rakha, T.H., Bekheit, M.M. and Ibrahim, K.M., 1989, Ligational , thermal , corrosion inhibition and antimicrobial properties of salicylidinebenzenesulphonylhydrazone, *Transition metal chemistry*, 14(5), 371–374.
- [16]. Yusnita, J., Puvaneswary, S., Mohd, A.H., Robinson, W.T. and Kwai-Lin, T., 2009, Synthesis, structural characterization and antibacterial activity of 2,6-diacetylpyridine bis(benzenesulfonohydrazone) Schiff bases and their copper(II) complexes, *Polyhedron*, 28(14), 3050–3054.
- [17]. Vicini, P. Geronikaki, A. Incerti, M. Busonera, B. Poni, G. Cabras, C.A. La Colla, P., 2003, Synthesis and biological evaluation of benzo[d]isothiazole, benzothiazole and thiazole Schiff bases, *Bioorganic med chem*, 11(22), 4785–4789.
- [18]. Shanty, A.A., 2017, *Heterocyclic schiff bases of aminophenols and their transition metal complexes: a versatile pharmacophore*. Thesis (PhD), Cochin University.
- [19]. Correa, W. H., Papadopoulos, S., Radnidge, P., Roberts, B.A., and Scott, J.L., 2002, Direct, efficient, solvent-free synthesis of 2-aryl-1,2,3,4-tetrahydroquinazolines, *Green chem*, 4(3), 245–251.
- [20]. Xavier, A. and Srividhya, N., 2014, Synthesis and study of Schiff base ligands, *Appl chem*, 7(11), 6–15.
- [21]. Vanden, A.T.R., Cave Gareth, W.V., Raston, C.L., 2006, Benign approaches for the synthesis of bis-Imine Schiff bases, *Green chem*, 8(3), 50-53.

- [22]. Serbest, K., Özen, A., Ünver, Y., Mustafa, Er., Değirmencioglu, I. and Sancak, K., 2009, Spectroscopic and theoretical study of 1,2,4-triazole-3-one based salicylaldehyde complexes and evaluation of superoxide-scavenging properties, *J. mol. struct.*, 922(3), 1–10.
- [23]. Khalil, S.M.E., 2000, Chromotropic changes of Cu(II) and Ni( II) complexes with chromotropic changes of Cu(II) and Ni( II) complexes with N<sub>2</sub>O<sub>2</sub> and N<sub>3</sub>O<sub>2</sub> Schiff-base ligands in the solid phase, *J. coordination chemistry*, 52 (1), 73-86.
- [24]. Srestha, N., Banerjee, J. and Srivastava, S., 2014, A review on chemistry and biological significance of benzimidazole nucleus, *Pharm*, 4(12), 28–41.
- [25]. Spasov, A.A., Yozhitsa, I.N., Bugaeva, L.I. and Anisimova, V.A., 1999, Benzimidazole derivatives: Spectrum of pharmacological activity and toxicological properties (a review), *Pharm chem*, 33(5), 232–243.
- [26]. Chimirri, A., Grasso, S., Monforte, P., Rao, A., Zappala, M., Monforte, A. Pannecouque, C., Witvrouw, M. Balzarini, J. and De Clercq, E., 1999, Synthesis and biological activity of novel 1H,3H-thiazolo 3,4-a benzimidazoles: non-nucleoside human immunodeficiency virus type 1 reverse transcriptase inhibitors, *Antivir chem chemother*, 10(4), 211–217.
- [27]. Husain, A., Varshney, M.M., Rashid, M., Mishra, R. and Akhter, A., 2011, Available online through benzimidazole: a valuable insight into the recent advances and biological activities, *Pharm. Res*, 4(2), 413–419.
- [28]. Shatha, M.A., 2010, *Synthesis of novel dimeric and oligomeric benzimidazoles targeted to nucleic acid minor groove binding*, Thesis (PhD), University of Manchester.
- [29]. Goudgaon, N.M. and Ummature, S.B., 2015, Synthesis, characterization and biological evaluation of novel C-2 substituted benzimidazole heterocycles, *Pharmacy research*, 9(12), 643–649.
- [30]. Chornous, V.A., Bratenko, M.K. and Vovk, M.V., 2001, Synthesis and antimicrobial activity of pyrazole-4-carboxylic acid hydrazides and N-(4-pyrazolyl) hydrazones of aromatic and heteroaromatic aldehydes, *Pharm. Chem*, 35(4) 26–28.

- [31]. Rollas, S, Gulerman, N., Erdeniz, H., 2002, Synthesis and antimicrobial activity of some new hydrazones 50 - 096 of 4-fluorobenzoic acid hydrazide and 3-acetyl-2,5-disubstituted- 1,3,4-oxadiazolines, *Il Farmaco*,57(2), 171-174.
- [32]. Masunari, A. and Tavares, L.C., 2007, A new class of nifuroxazide analogues: Synthesis of 5-nitrothiophene derivatives with antimicrobial activity against multidrug-resistant staphylococcus aureus, *Bioorganic med chem*, 15(12), 4229–4236.
- [33]. Göker, H., Özden, S., Yildiz, S. and Boykin, D. W., 2005, Synthesis and potent antibacterial activity against MRSA of some novel 1,2-disubstituted-1H-benzimidazole-N-alkylated-5-carboxamidines,*J. med. chem.*, 40(10), 1062–1069.
- [34]. Tunçbilek, M. Kiper, T. and Altanlar, N., 2009 , Synthesis and in vitro antimicrobial activity of some novel substituted benzimidazole derivatives having potent activity against MRSA, *Med chem*, 44(3), 1024–1033.
- [35]. Goldman, L., Franke, E.K., Kindel, D. J., Blaney, D.J. and Richfield, D., 1963, Inhibition of enteroviruses by 2-( $\alpha$ -hydroxybenzyl)-benzimidazole and related compounds, *Nature*, 197(487), 912–914.
- [36]. Sullivan, D.G.O., Pantic D. and Wallis, A.K., 1965, New 1,2-Disubstituted benzimidazoles with high inhibiting effects on poliovirus replication, *Cellular and molecular life sciences*, 23(2), 123–124.
- [37]. Tewari, A.K. and Mishra, A., 2006, Synthesis and antiviral activities of N-substituted-2-substituted-benzimidazole derivatives, *Indian journal of chemistry*, 45(23), 489-493.
- [38]. Walia, R., Hedaitullah, M.D., Naaz, S.F., Iqbal, K. and Lamba, H.S., 2011, Benzimidazole derivatives – an overview, *Int. j. res. pharm chem.*, 1(3), 565- 574.
- [39]. Hernandez-Luis, F., Hernandez-Campos, A., Castillo R., Navarrete-Vazquez, G., Soria-Arteche, O., Hernandez-Hernandez, M., Yopez-Mulia,L., 2010, Synthesis and Biological Activity of 2-(Trifluoromethyl)-1H-benzimidazole Deriv- atives Against Some Protozoa and *Trichinella spiralis*, *Eur j med chem*, 45(7), 3135-3141.
- [40]. Cook, G.C., 1990, Use of benzimidazole chemotherapy in human helminthiasis: indications and efficacy, *Parasitol today*, 6(4), 133–136.



- [41]. Kazimierczuk, Z., Upcroft, J.A., Upcroft, P., Górska, A., Starościak, B. and Laudy, A., 2002, Synthesis, antiprotozoal and antibacterial activity of nitro- and halogeno-substituted benzimidazole derivatives, *Acta Biochim Pol.* 49(1), 185–195.
- [42]. Valdez, J., Cedillo, R., Hernández-Campos, A., Yépez, L., Hernández-Luis, F., Navarrete-Vázquez, G., Tapia, A., Cortés, R., Hernández, M. and Castillo, R., 2002, Synthesis and antiparasitic activity of 1H-benzimidazole derivatives, *Bioorganic and medicinal chemistry letters*, 12(16), 2221–2224.
- [43]. Xiao, L., Saeed, K. and Herd, R.P., 1996, Efficacy of albendazole and fenbendazole against *Giardia* infection in cattle, *Vet. parasitol*, 61(2), 165–170.
- [44]. Katiyar, S.K., Gordon, V.R., McLaughlin, G.L. and Edlind, T.D., 1994, Antiprotozoal activities of benzimidazoles and correlations with  $\beta$ -tubulin sequence, *Antimicrob agents chemother*, 38(9), 2086–2090.
- [45]. Negro-Vilar, A., 1999, Selective androgen receptor modulators (SARMs): a novel approach to androgen therapy for the new millennium, *Clin endocrinol Metab*, 84(10), 0–3.
- [46]. Raymond, A.Ng., Jihua, G., Vernon, C.A.J., James, L., George F.A., Tifanie S., Olivia, L., Scott, G.L., Zhihua, S., 2007, Synthesis and SAR of potent and selective androgen receptor antagonists: 5,6-Dichloro-benzimidazole derivatives, *Bioorganic Med chem lett.*, 17(3), 784–788.
- [47]. Gardiner, J.M., Loyns, C.R., Burke, A., Khan, A. and Mahmood, N., 1995, Synthesis and HIV-1 inhibition of novel benzimidazole derivatives, *Bioorg Med chem lett*, 5(12), 1251–1254.
- [48]. Shah, D.I., Sharma, M., Bansal, Y., Bansal, G. and Singh, M., 2008 Angiotensin II - AT1receptor antagonists: Design, synthesis and evaluation of substituted carboxamido benzimidazole derivatives, *Eur j med chem*, 43(9), 1808–1812.
- [49]. Jat, R.K., Jat, J.L. and Pathak, D.P., 2006, Synthesis of benzimidazole derivatives : as antihypertensive agents, *E-Journal chem*, 3(4), 278–285.
- [50]. Dubey, P.K., Naidu, A., Reddy, P.V.V. P., N. D., Kumar, M. and Vineel, B. G., 2008, Studies on synthesis of unsymmetrical 2,2'-bisbenzimidazole sulphides of

pharmacological interest, *India journal of chemistry*, 47(1),1443–1446.

[51]. Lindberg, P., Brändström, A. and Wallmark, B., 1987, Structure—activity relationships of omeprazole analogues and their mechanism of action, *Trends in pharmacological sciences*, 8(10), 399-402.

[52]. Nawrocka, W., Sztuba, B., Kowalska, M.W., Liszkiewicz, H., Wietrzyk, J., Nasulewicz, A., Pełczyńska, M. and Opolski, A., 2004, Synthesis and antiproliferative activity in vitro of 2-Aminobenzimidazole derivatives, *II farmaco*, 59( 22), 83-91.

[53]. Ramla, M.M., Omar, M.A., El-Khamry, A.M.M. and El-Diwan, H.I., 2006 ,Synthesis and antitumor activity of 1-substituted-2-methyl-5-nitrobenzimidazoles, *Bioorganic med chem*, 14(21), 7324–7332.

[54]. Demirayaka, S., Kayagilb, I. and Yurttasc, L., 2011, Microwave supported synthesis of some novel 1, 3- Diarylpyrazino [1, 2-a] benzimidazole derivatives and investigation of their anticancer activities, *European journal of medicinal chemistry*, 46(1), 411-416.

[55]. Gowda, N.R., Kavitha, C.V., Chiruvella K.K., Joy, O., Rangappa, K.S. and Raghavan, S.C., 2009, Synthesis and biological evaluation of novel 1-(4- methoxyphenethyl)-1Hbenzimidazole-5-carboxylic acid derivatives and their precursors as antileukemic agents, *Bioorg med chem lett*, 19(16), 4594-600.

[56]. Anisimova, V.A., Spasov, A.A., Kosolapov, V.A., Tolpygin, I.E., Porotikov, V.I., Kucheryavenko, A.F., Sysoeva, V.A., Tibir'kova E. V., El'tsova, L.V., 2009, Synthesis and pharmacological activity of 3-(2,2,2-trichloro-1-hydroxyethyl)imidazo[1,2-a]benzimidazole dihydrochlorides, *Pharmaceutical chemistry journal*, 43(9), 2–3.

[57]. Nakano, H., Inoue, T., Kawasaki, N., Miyataka, H., Matsumoto, H., Taguchi T., Inagaki N., Nagai, H. and Satoh, T., 2005, Synthesis of benzimidazole derivatives as antiallergic agents with 5-lipoxygenase inhibiting action, *Genetics*, 5 (2), 352–356.

[58]. Wagner, R.W., Brown, P.A., Johnson, T.E. and Lindsey, J.S., 1991, Self-assembly of molecular devices containing a ferrocene, a porphyrin and a quinone in a triple macrocyclic architecture, *Journal of the chemical society chemical communications*, 1(20), 1463–1466.

[59]. Miller, J.S. and Epstein, A.J., 1994, Organic and Organometallic Molecular Magnetic

Materials—Designer Magnets, *Angew chemie int. ed. english*, 33(4), 385–415.

[60]. Nicot, D.B., Mathieu, R., Montauzon, D.D., Lavigne, G. and Majoral, J.p., 1994, Using phosphohydrazides as building blocks to multiredox polymetallic compounds containing ferrocenyl groups. electrochemical and nmr behaviors in solution, *Inorg chem*, 33(3), 434–443.

[61]. Santis, G.D., Fabbrizzi, L., Licchelli, M. and Pallavicini, P., 1994, Controlling the acidity of the carboxylic group by a ferrocene based redox switch, *Inorganica chim acta*, 225(2), 239–244.

[62]. Liu, W.J., Xiong, G.X. and Wang, W.P., 2007, Research on synthesis and conductivity of ferrocenyl Schiff base and its salt, *Appl organomet chem*, 21(2), 83–88.

[63]. Wilkinson, G., Rosenblum, M., Whiting, M.C. and Woodward, R.B., 1952, The structure of iron bis-cyclopentadienyl, *Am chem soc*, 74(8), 2125–2126.

[64]. Kealy, T.J. and Pauson, P.L., 1951, A new type of organo-iron compound, *Nature*, 2(1), 1039–1040.

[65]. Uno, M., Dixneuf, P.H., 1998, Organometallic Triskelia Novel Tris (vinylideneruthenium(II)), Tris(alkynylruthenium(II)), and Triruthenium–Triferrocenyl Complexes, *Angewandte chemie international edition*, 37(12), 1714–1717.

[66]. Ohsawa, Y., Hanck, K.W. and DeArmond, M.K., 1984, A systematic electrochemical and spectroscopic study of mixed-ligand ruthenium(II) 2,2'-bipyridine complexes  $[\text{Ru}(\text{bpy})_3\text{-nLn}]^{2+}$  (n=0,1,2 and 3), *Electroanal chem*, 175(2), 229–240.

[67]. Pagel, K., Werner, A. and Friedrichsen, W., 1994, Ferrocene und Ferrocenophane mit dipolaren Strukturelementen, *J. organomet chem*, 481(1), 109–123.

[68]. Coe, B.J., Jones, C.J., McCleverty, J.A., Bloor, D. and Cross, G., 1994, An assessment of second harmonic generation by donor acceptor molecules containing stilbenyl or diarylazo bridges between ferrocenyl donor and nitro acceptor groups, *J. organomet chem*, 464(2), 225–232.

[69]. van Staveren D. R. and Metzler-Nolte, N., 2004, Bioorganometallic chemistry of ferrocene, *Pharm mol biotechnol*, 104(1), 5931–5985.

- [70]. Thomas, K.R., Lin, J.T. and Wen, Y.S., 1999, Synthesis, spectroscopy and structure of new push-pull ferrocene complexes containing heteroaromatic rings (thiophene and furan) in the conjugation chain, *Organomet chem*, 575(1), 301-309.
- [71]. Iskander, M.F., El-Sayed, L. and El-Toukhy, A., 1975, Coordination compounds of hydrazine derivatives with transition metals-XIX, *J. inorg. nucl. chem.*, 42(2), 1145–1150.
- [72]. Broene, R.D. and Buchwald, S.L., 1993, Asymmetric Hydrogenation of Unfunctionalized Trisubstituted Olefins with a Chiral Titanocene Catalyst, *J.Am. chem. soc.*, 115(26), 12569–12570.
- [73]. Zaheer, M., Shah, A., Akhter, Z., Qureshi, R., Mirza, B., Tauseef, M. and Bolte, M., 2011, Synthesis, characterization, electrochemistry and evaluation of biological activities of some ferrocenyl Schiff bases, *Appl. organomet. chem.*, 25(1), 61–69.
- [74]. Coates, G. E., Green, M.L.H. and Wade, K., 1967, *Organo-metallic compounds*, 3rd ed. London.
- [75]. Kröhnke, F., 1963 , Heterocyclic Systems with Bridgehead Nitrogen Atoms (in zwei Teilen), *Angewandte chemie*, 76(5), 239.
- [76]. Jonas, K., 1985, Reactive organometallic compounds obtained from metallocenes and related compounds and their synthetic applications, *Angew chemie int ed english*, 24 (4), 295–311.
- [77]. Olivia, R.A., Lorna, C., Andrew, L.G., Richard, J.K. and Patrick, C.M., 2004, Functionalized cyclopentadienyl titanium organometallic compounds as new antitumor drugs, *Organometallics*, 23(2), 288–292.
- [78]. Nlate, S., Ruiz, J., Sartor, V., Navarro, R., Blais, J.C. and Astruc, D., 2000 ,Molecular batteries: Ferrocenylsilylation of dendrons, dendritic cores, and dendrimers: new convergent and divergent routes to ferrocenyl dendrimers with stable redox activity, *Chem. eur. j.*, 6(14), 2544–2553.
- [79]. Stephen, B. and Dermot, O, 1997, Metal-Metal Interactions in Linke Metallocenes, *Chemical reviews* , 97(3), 637-670.

- [80]. Sato, M., Kudo, A. and Saitoh, H., 1996, A structural rearrangement on the oxidation of 1,2-bis(ruthenocenyl) ethylene derivatives leads to unprecedented ( $\mu$ - $\eta^6$ : $\eta^6$ -pentafulvadiene) diruthenium complexes, *Chem. commun.*, 1(1), 25–26.
- [81]. Pannell, K.H., Dementiev, V.V., Cervantes-Lee, H.Li.F., Nguyen, M.T. and Diaz, A.F., 1994, (1,1'-Ferrocenediyl)ferrocenyl(methyl)silane, Its Thermally Ring-Opened Polymer, and Oligomer Models, *Organometallics*, 13(9), 3644–3650.
- [82]. Peacock, A. F. A. and Sadler, P.J., 2008, Medicinal organometallic chemistry: designing metal arene complexes as anticancer agents, *Chem. asian j.*, 3(11), 1890–1899.
- [83]. Chohan, Z.H., 2002, Antibacterial copper(II) complexes of 1,1'-symmetric ferrocene-derived Schiff-base ligands: Studies of the effect of anions on their antibacterial properties, *Appl organomet. chem*, 16(1), 17–20.
- [84]. Igor, S., 2017, Ferrocene and transition metal bis ( dicarbollides ) as platform for design of rotatory molecular switches, *Molecule*, 22(12), 2201.
- [85]. Nesmeyanov, A.N., Perevalova, E.G. and Golovnya, R.V., 1954, Reaction of ferrocene with diazo compounds, *Dokl akad. nauk SSSR*, 99(2), 539-542.
- [86]. Shah, F.U., Akhter, Z., Siddiqi, H.M., Parvez, M., 2007, Synthesis, structure and characterization of some Schiff bases bearing phenylferrocene, *Appl. organomet chem*, 21(1), 758-762.
- [87]. Wilkinson, G., Rosenblum, M., Whiting, M.C. and Woodward, R.B., 1952, The structure of iron bis-cyclopentadienyl, *J. am. chem. soc.*, 74(8), 2125–2126.
- [88]. Bochmann, M., 1995, *Complexes with Transition Metal- Carbon bond*, Chemistry Book Reviews., 1st ed, London, ISBN: 9780198557500.
- [89]. Osella, D., Ferrali, M., Zanello, P., Laschi, F., Fontani, M., Nervi, C. and Cavignoli, G., 2000, On the mechanism of the antitumor activity of ferrocenium derivatives, *Inorg chim acta*, 306(1), 42-48 .

- [90]. Shazia, A., Mahmood, R., Hani, C., Peter N.P., Parkash, J., Abdu, I. H. Maryam, M., Ghufrana, A.S., Azhar, K.M., Sania, B., Ashraf, A. and Sarwar, M. J., 2016, Molecular mechanisms and mode of tamoxifen resistance in breast cancer, *Bioinformation*, 12(3), 135–139.
- [91]. Nguyen, A., Top, S., Vessières, A., Pigeon, P., Huché, M., Hillard, E.A. and Jaouen, G., 2007, Organometallic analogues of tamoxifen: Effect of the amino side-chain replacement by a carbonyl ferrocenyl moiety in hydroxytamoxifen, *Organomet chem*, 692 (6), 1219–1225.
- [92]. Köpf-Maier, P., Köpf, H. and Neuse, E.W., 1984, Ferricenium complexes: a new type of water-soluble antitumor agent, *Cancer res clin oncol*, 108(3), 336–340.
- [93]. Osella, D., Ferrali, M., Zanello, P., Laschi, F., Fontani, M., Nervi, C. and Cavigioli, G., 2000, On the mechanism of the antitumor activity of ferrocenium derivatives, *Inorganica chim acta*, 306(1), 42–48.
- [94]. Jaouen, G., Vessières, A. and I. S. Butler., 1993, Bioorganometallic chemistry: a future direction for transition metal organometallic chemistry, *Acc. chem. res.*, 26(7), 361–369.
- [95]. Williams, G.M., Olmstead, J. and Breksa A.P., 1989, Coordination complexes of cobalt: inorganic synthesis in the general chemistry laboratory, *chem. educ.*, 66(12), 1043–1045.
- [96]. Housecroft, C.E. and Sharpe A.G., 2005, *Inorganic Chemistry*, 2nd ed, England, ISBN: 0130399132.
- [97]. Gupta, K.C. and Sutar, A.K., 2008, Catalytic activities of Schiff base transition metal complexes, *Chem rev*, 252(12), 1420-1450.
- [98]. Saliu, F., Putomatti, B. and Rindone, B., 2012, Applied homogeneous catalysis with organometallic compounds: a comprehensive review, *Tetrahedron lett*, 6(6), 943–944.
- [99]. Anand, P., Patil, V.M., Sharma, V.K., Khosa, R.L. and Masand, N., 2012 Schiff bases: a review on biological insight, *International journal of drug design and discovery*, 3(3), 851-868.
- [100]. Chohan, Z. H. and Praveen, M., 2001, Synthesis, characterization, coordination and antibacterial properties of novel asymmetric 1,1'-disubstituted ferrocene-derived Schiff-base

ligands and their Co(II), Cu(II), Ni(II) and Zn(II) complexes, *Appl organomet chem*, 15(7), 617–625.

[101]. Housecroft, C.E. and Sharpe, A.G., 2012, *Inorganic chemistry*, 4th ed. Prentice Hall, England, ISBN: 978-0-273-74276-0.

[102]. Franks, M., Gadzhieva, A., Ghandhi, L., Murrell, D., Blake, A.J., Davies, E.S., Lewis, W., Moro, F. McMaster, J. and Schroder, M., 2013, Five coordinate M(II)-diphenolate [M = Zn(II), Ni(II), and Cu(II)] Schiff base complexes exhibiting metal- and ligand-based redox chemistry, *Inorg chem*, 52(2), 660-670.

[103]. Anbu, S., Kandaswamy, M. and Varghese, B., 2010, Structural, electrochemical, phosphate-hydrolysis, DNA binding and cleavage studies of new macrocyclic binuclear nickel(II) complexes, *Dalton transactions*, 39(16) 3823.

[104]. Mukherjee, P., Drew, M.G.B. and Ghosh, A., 2008, Anion-directed template synthesis and hydrolysis of mono-condensed Schiff base of 1,3-pentanediamine and *o*-hydroxyacetophenone in Ni(II) and Cu(II) complexes, *Eur j inorg chem*, 1(21), 3372-3381.

[105]. Kumar, S. and Trivedi, A., 2016, A review on role of nickel in the biological system, *Int j curr microbiol apple sci.*, 5 (3), 719–727.

[106]. Piper, T. S., Cotton, F. A. and Wilkinson, G., 1955, Cyclopentadienyl-carbon monoxide and related compounds of some transitional metals, *Inorg nucl. chem*, 1(3), 165–174.

[107]. Zhang, X. and Kanatzidis, M.G. Hogan, T. and Kannewurf, C.R., 1996, NaCu<sub>4</sub>S<sub>4</sub>, a simple new low-dimensional, metallic copper polychalcogenide, structurally related to CuS, *J am chem soc*, 27 (17), 693–694.

[108]. Cotton, F.A. and Wilkinson, G, 1988, *Advanced Inorganic Chemistry*, 5nd ed., New York, ISBN 0-471-02775-8.

[109]. Bal, S., 2016 , A novel azo-Schiff base ligand and its cobalt, copper, nickel complexes: synthesis, characterization, antimicrobial, catalytic and electrochemical features, *Anadolu univ j sci technol appl sci eng*, 17(2), 315–326.

- [110]. Ejidike, I.P. and Ajibade, P.A., 2015, Synthesis, characterization and biological studies of metal(II) complexes of (3E)-3-[(2-[(E)-[1-(2,4-Dihydroxyphenyl) ethylidene]amino)ethyl]imino]-1-phenylbutan-1-one schiff base, *Molecules*, 20 (6), 9788–9802.
- [111]. Franks, M., Gadzhieva, A., Ghandhi, L., Murrell, D., Blake, A.J., Davies, E.S., Lewis, W., Moro, F., McMaster, J. and Schroder, M., 2013, Five coordinate M(II)-diphenolate [M = Zn(II), Ni(II), and Cu(II)] Schiff base complexes exhibiting metal- and ligand-based redox chemistry, *Inorg chem*, 52(2), 660-670.
- [112]. Anuradha, K. and Rajavel, R., 2011, New macrocyclic binuclear Copper(II), Nickel(II) and Oxovanadium(IV) complexes, *International journal of pharmacy and technology*, 3(3), 3175-3185.
- [113]. Kaur, R.H and Kishorekapur, B., 2013, on Application of Copper Schiff base complex A Review, *Sci rev chem commun*, 3 (1), 1–15.
- [114]. Ourari, A., Aggoun, D. and Ouahab, L., 2013, A novel copper(II)-Schiff base complex containing pyrrole ring: Synthesis, characterization and its modified electrodes applied in oxidation of aliphatic alcohols, *Inorganic chemistry communications*, 33 (1), 118-124.
- [115]. Bagchi A.A.R. and Mukherjee, P., 2015, A review on transition metal complex- modern weapon in medicine, *Int. j recent adv pharm res*, 5(3), 171–180.
- [116]. Chisholm, M.H., Gallucci, J.C. and Zhen, H. Huffman, J.C., 2001, Three-coordinate zinc amide and phenoxide complexes supported by a bulky Schiff base ligand, *Inorg chem*, 40 (19), 5051-5054.
- [117]. Yang, J., Yuan, J.W., Zha, R.H. and Zeng, Q.F., 2009, Bis{2-[3-(dimethylamino)propyliminomethyl]-4,6-disulfanylphenolato}cobalt(II), *Acta crystallogr*, 65(1), 1090.
- [118]. Deshmukh, A.P., Akerkar, V.G. and Salunkhe, M.M., 2000, Decomposition of H<sub>2</sub>O<sub>2</sub> using ion exchange resin with a spacer containing  $\alpha$ -nitroso- $\beta$ -naphthol as a functional group, *Molecular catalysis a chemical*, 153(2), 75-82.
- [119]. Tobriya, S. K., 2014, Biological applications of Schiff base and its metal complexes- a review, *Int j sci res*, 3(9), 1254–1256.



- [120]. Kumaran, J.S., Priya, S., Muthukumaran, J., Jayachandramani, N. and Mahalakshmi, S., 2013, Synthesis, characterization and biological activity of salen-mixed ligand complexes with nickel(II), copper(II) and cobalt(III), *Journal of chemical and pharmaceutical research*, 5(10), 206-217.
- [121]. Poewr, C.D and Ritter T., 2011, Palladium(III) in synthesis and catalysis, *Organomet chem*, 35(2), 129–156.
- [122]. Chen, W., Shimada, S. and Tanaka, M., 2002, Synthesis and structure of formally hexavalent palladium complexes, *Science*, 295 (5553), 308–310.
- [123]. Crabtree R.H., 2002, Chemistry: a new oxidation state for Pd, *Science*, 295 (308), 6520.
- [124]. Dodd, D. W., Toews, H.E., Trevail, M.J., Jennings, M. C., Hudson, R.H.E. and Jones, N.D., 2009, Synthesis and evaluation of the in vitro DNA-binding properties of chiral cis-dichloro(pyridyloxazoline)platinum(II) complexes, *Can j chem*, 87(1), 321–327.
- [125]. Tyree, S.Y., 1967, *Inorganic syntheses*, 9th ed , College of William and Mary, ISBN: 9780470132401.
- [126]. Kelland, L., 2007, The resurgence of platinum-based cancer chemotherapy, *Nat rev cancer*, 7(8), 573-584.
- [127]. Todd, R.C. and Lippard, S.J., 2010, Structure of duplex DNA containing the cisplatin 1,2- $\{Pt(NH_3)_2\}^{2+}$ -d(GpG) cross-link at 1.77 Å resolution, *Inorg biochem*, 104 (9), 902-908.
- [128]. Todd, R.C. and Lippard S. J., 2009, Inhibition of transcription by platinum antitumor compounds, *Metallomics*, 1(4), 280.
- [129]. Hall, M.D., Mellor, H.R., Callaghan, R. and Hambley, T.W., 2007, Basis for design and development of platinum(IV) anticancer complexes, *Med chem*, 50(15), 3403-3411.
- [130]. Wheate, N.J., Walker, S., Craig, G.E. and Oun R., 2010, The status of platinum anticancer drugs in the clinic and in clinical trials, *Dalton trans*, 39(35), 8113.
- [131]. Reithofer, M.R., Bytzek, A.K., Valiahd, S.M., Kowo, C.R., Groessl, M., Hartinger, C.G., Jakupec, M.A., Galanski, M. and Keppler, B.K., 2011, Tuning of lipophilicity and

cytotoxic potency by structural variation of anticancer platinum(IV) complexes, *Inorg biochem*, 105(1), 46-51.

[132]. Pasqua, Di., Anthony, J., Kerwood, D.J., Shi, Yi., Jerry, G. and Dabrowiak, J.C., 2011, Stability of carboplatin and oxaliplatin in their infusion solutions is due to self-association, *Dalton transactions*, 40(18), 4821.

[133]. Yee-Ping, H., Steve, C.F.A. and Kenneth K.W. T., 2003, Platinum based anticancer agents: innovative design strategies and biological perspectives, *Medicinal research reviews*, 23(5), 633-655.

[134]. Reedijk, J. and Lohman, P.H.M., 1985, Cisplatin: Synthesis, antitumour activity and mechanism of action, *Pharm weekbl sci ed*, 7(5), 173-180.

[135]. Liu Y.T., Lian G.D., Yin D.W. and Su B.J., 2012, Synthesis and antimicrobial activity of some novel ferrocene-based Schiff bases containing a ferrocene unit, *Research on chemical intermediates*, 38(5), 1043-1053.

[136]. Heydenhauss, D., Kramer, C. R. and Jaenecke, G., 1986, The effect of substituents on the half-wave potential of 2-ferrocenyl substituted imidazole and benzimidazole, *Zeitschrift fuer physikalische chemie (Leipzig)*, 267(1), 33-44.

[137]. Benito, A., Martinez-Manez, R., Paya, J.; Soto, J., Tendero, M. J. L. and Sinn, E., 1995, Reaction of ferrocenecarbaldehyde with o-phenylenediamine. Crystal structure of N-ferrocenylmethyl-2-ferrocenyl-benzimidazole, *J. Organomet chem*, 503(2), 259-263.

[138]. Cinarli, A., Gürbüz, D., Tavman, A. and Birteksöz, S., 2011, synthesis, spectral characterizations and antimicrobial activity of some schiff bases of 4-chloro-2-aminophenol, *Chem soc ethiop*, 25(3), 407-417.

[139]. Tavman, A., 2006, Synthesis, spectral characterisation of 2-(5-methyl-1H-benzimidazol-2-yl)-4-bromo/nitro-phenols and their complexes with zinc(II) ion, and solvent effect on complexation, *Spectrochimica acta*, 63(1), 343-348.

[140]. Zapata, F., Caballero, A., Espinosa, A., Tarraga, A. and Molina, P., 2009, Imidazole-Annulated Ferrocene Derivatives as Highly Selective and Sensitive Multichannel Chemical Probes for Pb(II) Cations, *Org chem*. 74(13), 4787-4796.

- [141]. Tavman, A., Birteksoz, S and Oksuzomer, F., 2012, Spectral and Thermal Characterization and antimicrobial Effect of 3-(5-H/Me/Cl/NO<sub>2</sub>-1H-benzimidazol-2-yl)-benzene-1,2-diols and Some Transition Metal Complexes, *S. Afr. J. Chem*, 65(1), 150–158.
- [142]. Gürbüz, D., Çınarlı, A., Tavman, A. and Birteksöz Tan, S., 2015, Synthesis, characterization and antimicrobial activity of some transition metal complexes of n-(5-chloro-2-hydroxyphenyl)-3-methoxy-salicylalimine, *Bull chem soc ethiop*, 29(1), 63-74.
- [143]. Sheldrick, G.M., 2008, A Short History of SHELX, *Acta crystallographica*, A64, 112-122.
- [144]. Sheldrick, G.M., 2015, Crystal Structure Refinement with SHELXL, *Acta crystallographica*, C71, 3-8.
- [145]. APEX2, Bruker AXS Inc., 2013, Madison Wisconsin USA.
- [146]. Macrae, C.F., Bruno, I.J., Chisholm, J.A., Edgington, P.R., McCabe, P., Pidcock, E., Rodriguez-Monge, L., Taylor, R., van de Streek, J. and Wood, P.A., 2008, New features for the visualization and investigation of crystal structures, *Journal of applied crystallography*, 41, 466-470.
- [147]. Farrugia, L.J., 2012, Wingx and ortep for windows: an update, *J. appl. cryst.* 45, 849–854.
- [148]. Gavranic, M., Kaitner, B., Mestrovic, E. J., 1996, Intramolecular N–H...O hydrogen bonding, quinoid effect, and partial  $\pi$ -electron delocalization in N-aryl Schiff bases of 2-hydroxy-1-naphthaldehyde: the crystal structures of planar N-( $\alpha$ -naphthyl) and N-( $\beta$ -naphthyl)-2-oxy-1-naphthalimine, *Chem crystallogr*, 26(1), 23-28.
- [149]. Ünver, H., Polat, K., Ucar, M., Zengin, D.M ., 2003, Synthesis and keto-enol tautomerism in N-(2-hydroxy-1-naphthylidene)anils, *Spect lett*, 36(4), 287-301.
- [150]. Tavman, A, 2008, Crystal Structure of N-(4-Chloro-2-hydroxyphenyl) methoxy salicylalimine, *Analytical sciences*. 24(1).
- [151]. Xiaoxian, Z., Yongmin, L., Fajun, N, and Yongxiang, M, 1992, Ferrocenyl thiosemicarbazone and its transition metal complexes, *Polyhedron*, 11(4), 447-451.

- [152]. Kopf-Maier, P., Kopf, H., Neuse, E. W. J. 1984, Ferricenium complexes: A new type of water-soluble antitumor agent, *Cancer res clin oncol*, 108(3), 336-340.
- [153]. Hegazy W. H. and Gaafar, A.E.D.M., 2012, Synthesis of organometallic-based biologically active compounds: in vitro antibacterioial and antifungal of asymmetric ferrocene-derived Schiff bases complexes, *Egypt. j. chem.* 55(3), 277-290
- [154]. Mokhles, M.A.E., 2004, Synthesis and spectroscopic characterization of some ferrocenyl schiff bases containing pyridine moiety and their complexation with cobalt, nickel, copper and zinc, *J chinese chemical society*, 51(1),499-504.
- [155]. Kamali, S., Wang, H., Mitra, D., Ogata, H., Lubitz, W., Manor, B.C., Rauchfuss, T.B., Byrne, D., Bonnefoy, V., Jenney, F.E., Adams, M.W.W., Yoda, Y., Alp, E., Zhao, J., Cramer, S., 2013, Observation of the Fe-CN and Fe-CO vibrations in the active site of [NiFe] hydrogenase by nuclear resonance vibrational spectroscopy, *Angewandte Chemie Int. Ed.*, 52(2), 724-728.
- [156]. Harinath, Y., Harikishore, D., Kumar Reddy, B., Kumar, N., Apparao, C. and Seshaiiah, K., 2013, Synthesis, spectral characterization and antioxidant activity studies of a bidentate Schiff base, 5-methyl thiophene-2-carboxaldehyde-carbohydrazone and its Cd(II), Cu(II), Ni(II) and Zn(II) complexes, *Spectrochim. acta mol biomol spectrosc*, 101(1), 264-272.
- [157]. Kovala-Demertzi, D., Domopoulou, A., Demertzis M. A., G. Valle and A. Papageorgiou., 1997, Palladium(II) complexes of 2-acetylpyridine N(4)-methyl, N(4)-ethyl and N(4)-phenyl-thiosemicarbazones. Crystal structure of chloro(2-acetylpyridineN(4) methylthio semicarbazonato) palladium(II) Synthesis, spectral studies, in vitro and in vivo antitumour activity, *J. Inorg. biochem.*, 68(2) 147-155.
- [158]. Kovala-Demertzi, D., Yadav, P. N., M., Demertzis, A. and Coluccia, M., 2000, synthesis, crystal structure, spectral properties and cytotoxic activity of platinum(II) complexes of 2-acetyl pyridine and pyridine-2-carbaldehyde N(4)-ethyl-thiosemicarbazones, *J Inorg biochem*, 78(4), 347-354.

- [159]. Xiuyun Z., Jinlan., Yi G, and Xiao C.Z., 2009, Ab Initio study of structural and magnetic properties of  $TM_n(\text{ferrocene})_{n+1}$  (TM Sc, Ti, V, Mn) sandwich clusters and nanowires, *Acs nano*, 3(3), 537–545.
- [160]. Munyaneza, A., Kumar, G and Morobe I., 2018, Synthesis, characterization and in vitro biological activities of pyrazolylpalladium(II) complexes towards selected strains, *Synthesis and catalysis: open access*, 3(1).
- [161]. Moamen, S., Refat, I.M., El-Deen, M.A., Zein, A. A., Adam, M.I. Kobeasy, 2013, Spectroscopic, Structural and Electrical Conductivity Studies of Co(II), Ni(II) and Cu(II) Complexes derived from 4- Acetylpyridine with Thiosemicarbazide, *Int. J. Electrochem sci.*, 8(1), 9894 - 9917.
- [162]. D.S. Chowdhuri, A. Rana, M. Bera, E. Zangrando, S. Dalai., 2009, 3D zinc(II) coordination polymers built up by triazole and benzene-polycarboxylate anions: Synthesis, crystal structure, thermal and photoluminescence characterization, *Polyhedron*, 28 (1), 2131–2136.
- [163]. G.-X. Liu, K. Zhu, S. Nishihara, R.-Y. Huang, X.-M. Ren., 2009, Syntheses, structures and photoluminescent properties of two zinc(II) coordination polymers based on aromatic polycarboxylate and 1,4-bis(imidazol-1-ylmethyl)benzene, *Inorg. chim acta*, 362 (14), 5103–5108.
- [164].A. Tavman, N.M. Agh-Atabay, A. Neshat, F. Guçin, B. Dulger, D. Hacıu., 2006, Structural characterization and antimicrobial activity of 2-(5-H/methyl-1H-benzimidazol-2-yl)-4-bromo/nitro-phenol ligands and their  $Fe(NO_3)_3$  complexes, *Transition met chem*, 31(2), 194-200.
- [165]. Ranchet, D., Tommasino, J. B., Vittori, O., Fabre, P.L., 1998, Solvent effects on the electrochemical behavior of iron(III) Schiff base complex, *J. Solution chem*, 27, 979–991.
- [166]. Clinical and Laboratory Standards Institute (CLSI)., 2006. Methods for dilution antimicrobial susceptibility tests for bacteria that grow aerobically: Approved Standard M7-A5. Wayne, PA, USA.
- [167]. Clinical and Laboratory Standards Institute (CLSI)., 2002. Reference method for broth dilution antifungal susceptibility testing of yeasts: Approved Standard M27-A2. 2nd Ed., Clinical Laboratory Standards, Wayne, PA, USA.

[168]. Clinical and Laboratory Standards Institute., 2014. Performance standards for antimicrobial susceptibility testing; 24th informational supplement. M 100-S24:CLSI, Wayne, PA, USA.



## CURRICULUM VITAE

| <b>Personal Information</b> |  |
|-----------------------------|--|
| Name Surname                | ELHAM AHMED S. ABDULMALEK<br>ALTERHONI                                   |
| Place of Birth              | Tripoli, Libya   |
| Date of Birth               | 28.07 1984   |
| Nationality                 | <input type="checkbox"/> T.C. <input checked="" type="checkbox"/> Other: |
| Phone Number                | 05511226567  |
| Email                       | elhamabdalmaleek@gmail.com   |
| Web Page                    |  |

| <b>Educational Information</b> |                    |
|--------------------------------|--------------------|
| <b>B. Sc.</b>                  |                    |
| University                     | Tripoli University |
| Faculty                        | Pharmacy           |
| Department                     | Pharmacy           |
| Graduation Year                | 2005-2006          |

| <b>M. Sc.</b> |                        |
|---------------|------------------------|
| University    | Teesside university    |
| Institute     | Science and technology |
| Department    | Chemistry              |
| Programme     | Analytical chemistry   |

| <b>Ph. D.</b> |                                |
|---------------|--------------------------------|
| University    | Istanbul University-Cerrahpasa |
| Institute     | Institute of Graduate Studies  |
| Department    | Department of Chemistry        |
| Programme     | Chemistry Programme            |